METHANOL AMINATION OVER HYDROTHERMALLY TREATED ZEOLITES RHO AND MORDENITE

By

Linda Heather Callanan van Steen

Thesis Presented for the Degree of

DOCTOR OF PHILOSOPHY

in the Department of Chemical Engineering

UNIVERSITY OF CAPE TOWN

August 1999

Revision: January 2000

For Eric

"Then at the balance let's be mute,

We never can adjust it;

What's done we partly may compute,

But know not what's resisted."

- Robert Burns

ACKNOWLEDGEMENTS

There are many people who have contributed in part to the success of this work. Firstly, thanks must go to all the people who have helped in a practical way. The ladies, Pam, Lorna, Suzanna, Shireen and Helen for both admin and analyses. The "guys" for keeping me sane in the face of adversity. Also, thanks to all the project students, Zanele, Zonke, Zandile, Matlou, Janet and Patrick for taking measurements (and for not destroying my rig).

I would also like to thank the NRF, THRIP and the University of Cape Town for financial support and the Du Pont company, especially Stephan Schwarz, for the samples of zeolite Rho.

To my supervisors, Cyril O'Connor and Eric van Steen, thanks for getting me started and for all the help along the way.

And of course to Eric for always being there.

SYNOPSIS

Methylamines are important chemicals in many industrial processes. They have use as intermediates for the production of many compounds containing amino groups as well as being used on their own. The acid catalysed amination of methanol generally yields a thermodynamically controlled product distribution. The equilibrium distribution for mono-, di-, and trimethylamine (MMA, DMA, and TMA), at 325 °C and a molar methanol to ammonia ratio of 1, is 17, 21, and 62 mol % respectively. The market demand, on the other hand, is for about 33, 53, and 14 mol % MMA, DMA and TMA.

Industrially, methylamines are formed by the reaction of methanol or dimethyl ether and ammonia over amorphous silica-alumina. This process involves large separation and recycle units which are both costly and energy intensive as the separation requires azeotropic distillation at 15 bar. Methylamines can be formed over other solid acid catalysts with definite crystal structures, namely zeolites. While being more active than amorphous silica-alumina, most zeolites do not show improved selectivity. Catalysts, which have, however, been reported to show improved selectivity to DMA, include zeolites Rho, ZK-5 and Chabazite. In addition, certain forms of hydrothermally treated Mordenite can produce non-equilibrium product distributions. The performance of Rho can also be improved with hydrothermal treatment.

The objectives of this study were briefly as follows. Firstly, the question was asked as to which of the catalysts studied, *viz.* Rho and Mordenite, was the most suitable for the methanol amination reaction. The second objective was to find the optimal performance achievable from any catalyst using hydrothermal treatment. The third, and possibly most important, objective was to propose reasons for the changes caused to each catalyst by hydrothermal treatment.

Repeated cycles of reaction and regeneration, in air, of Rho and Mordenite caused an increase in activity as well as a shift in the amine product selectivity to the lower substituted amines, MMA and DMA. This is proposed to be due to the presence of hydrogen containing species on the surface of the catalysts, which were not desorbed during normal flushing procedures, but were burnt off the surface with air, yielding water as a product. This water acts as an *in situ* steaming agent and as such causes changes to the reaction behaviour of the catalyst.

From this it was concluded that care should be taken when regenerating catalysts after reaction as inadvertent steaming of the catalyst could occur.

Samples of the two catalysts, Rho and Mordenite were subjected to varying times of hydrothermal treatment. These samples were then analysed for their performance, both in terms of activity and selectivity, in the methanol amination reaction and were fully characterised. Adsorption studies using methanol, ammonia and water were also carried out over the catalysts.

One of the most significant findings of this work was the difference in the manner in which the two zeolites, Rho and Mordenite, were affected by the hydrothermal treatment. The two most important differences, which this treatment caused in the catalysts, were the change in the distribution of the acid sites and the change in the surface area and pore volume. In the case of Rho there was a loss in the total number of acid sites, primarily from the weaker of the two initial acid sites. Hydrothermal treatment of Mordenite caused less of a loss in the total number of acid sites in the catalyst but caused a second type of acid site to be formed at the expense of the original sites. Steaming of Rho caused a large increase in the micropore volume of the catalyst whereas steaming of Mordenite caused a decrease in this value. In both zeolites, steaming caused the generation of extra-framework aluminium species in both catalysts. Neither of the catalysts showed measurable change in the XRD spectra or SEMs.

The hydrothermal treatment caused a contradictory effect in the adsorption behaviour of the two catalysts in that the total adsorption capacity of Rho showed a maximum while that of Mordenite continually decreased. The initial changes in the adsorption capacity were directly related to the changing pore volumes. The decrease in adsorption capacity over Rho at longer steaming times is proposed to be due to the presence of extra-framework aluminium within the pore structure of the catalyst. Over Rho the adsorption affinity for ammonia, as opposed to Methanol, was found to increase while that over Mordenite decreased.

The changes in the performance of the catalysts for the methanol amination reaction were correlated to the changes in acidity, structure and adsorption capacity of the two catalysts. Over Rho it was found that the rate of consumption of ammonia correlated reasonably with the pore volume of the catalyst. The rate of reaction of methanol initially increased due to the overall increase in activity of the catalyst, but decreased later due to the changing selectivity of the system. This correlated with the decreasing total adsorption capacity of the catalyst.

The change in amine selectivity seen over Rho with steaming time correlated with the generation of extra-framework aluminium within the pore structure of the catalyst. The presence of the extra-framework aluminium causes increased diffusional constraints within the pores of the catalyst and may constrain the formation of the larger, TMA, molecule but not effect the overall rate of ammonia consumption. The presence of extra-framework aluminium was also thought to be responsible for the decrease in the total adsorption capacity seen over Rho at longer steaming times.

The generation of larger amounts of dimethyl ether over Mordenite was related to the formation of the second type of acid site. This site, which is probably of a Lewis acidic nature, had a far higher affinity for methanol and hence led to an increase in the chemisorption of methanol at the catalyst surface and hence to the higher rate of formation of dimethyl ether. The large loss of the original acid site type in the Mordenite, which was selective to amines, caused the decrease in the overall formation of amines.

TABLE OF CONTENTS:

Acknowledgements iii

Synopsis iv

Table of Contents: vii

List of Figures xi

List of Tables xiv

Nomenclature xv

1. INTRODUCTION AND LITERATURE REVIEW *1*

1.1 Introduction 1

1.1.1 Processes for the Production of Methylamines 2

1.2 Catalysts for the Amination of Methanol 7

1.2.1 Amorphous Silica-Alumina 7

1.2.2 H-Rho 8

1.2.3 Mordenite 12

1.2.4 H-ZK-5 15

1.2.5 H-ZSM5 17

1.2.6 SAPO Catalysts 17

1.2.7 Chabazite 18

1.3 Catalyst Preparation 20

1.3.1 Ion-Exchange Techniques 20

1.3.2 Calcination Procedures 22

1.4 Post Synthesis Modification 25

1.4.1 Acid Leaching 25

1.4.2 Steaming 26

1.4.3 Extra Framework Alumina 28

1.4.4 Surface Treatment 30

1.5 Reaction Conditions 32

1.5.1 Influence of Methanol: Ammonia Feed Ratio 32

1.5.2 Temperature 34

1.5.3 Methanol Conversion 35

1.5.4 Addition of Water 37

1.6. Kinetics and Thermodynamics 38

1.6.1 Thermodynamics of the Methanol Amination Reaction 38

1.6.2 Reaction Mechanism 39
1.6.3 Experimentally Determined Kinetics 41
1.6.4 Experimentally Determined Reaction Mechanism 42
1.6.5 Reaction Mechanism over Brønsted Acid Catalysts 44

1.7 Objectives of Research 46

2. EXPERIMENTAL PROCEDURE 47

2.1 Catalysts 47
2.1.1 Rho 47
2.1.2 Mordenite 47
2.1.3 Silica-Alumina 47

2.2 Post-Synthesis Modification Techniques 48
2.2.1 Ion Exchange 48
2.2.2 Calcination 48
2.2.3 Hydrothermal Treatment 48

2.3 Catalyst Characterisation 50
2.3.1 Structural Analysis 50
2.3.2 Analysis of Acidity 52

2.4. Reaction of Methanol and Ammonia to Form Methylamines 55
2.4.1 Reaction Apparatus 55
2.4.2 Experimental Procedure 57

2.5 Adsorption Studies 58
2.5.1 Experimental Procedure 58
2.5.2 Thermal Conductivity Analysis 61

3. INITIAL STUDIES 63

3.1 Catalyst Characterisation 63
3.1.1 Rho 63
3.1.2 Mordenite 67

3.2 Reaction Studies 70

3.3 Reaction-Regenration Cycles 74
3.3.1 Zeolite Rho 75
3.3.2 Mordenite 81

3.4 Presence of Water 83

4. HYDROTHERMAL TREATMENT 89

4.1 Characterisation of Acidity 90
4.1.1 Temperature Programmed Desorption 90
4.1.2 NMR 94
4.1.3 Atomic Adsorption Spectroscopy 95
4.2 Structural Characterisation 97
4.2.1 BET 97
4.2.2 SEM 102
4.2.3 XRD 103
4.3 Rho 104
4.4 Mordenite 108
4.4.1 Severe Hydrothermal Treatment 110
4.5 Discussion 113
4.5.1 Contradiction Between Activity and Selectivity 113
4.5.2 Rho 115
4.6.2 Mordenite 117
5. Adsorption Studies 119
5.1 Rho 121
5.1.1 Pure Component Adsorption 121
5.1.2 Binary Adsorption Studies 125
5.2 Mordenite 129
5.2.1 Pure Component Adsorption 129
5.2.2 Binary Adsorption Studies 132
5.3 Discussion 137
5.3.1 Rho 137
5.3.2 Mordenite 140
6. DISCUSSION 143
6.1 Comparison of Catalyst Changes Caused by Hydrothermal Treatment 143
6.1.1 Changes in Reaction Behaviour 143
6.1.2 Structural and Acidic Changes 144
6.1.3 Change in Adsorption Behaviour 146
6.2 Relationship Between Catalyst Changes and Reaction Performance 149
6.2.1 Rho 149
6.2.2 Mordenite 151
7. Conclusions 153

REFERENCES *157*

Appendix I: Thermodynamic Data *165*

Appendix II: Gas Chromatography *167*

Appendix III: X-ray Diffraction and IR Data *171*

Appendix IV: NH_3-Temperature Programmed Desorption *177*

Appendix V: Reaction Data *180*

Appendix VI: Effect of Particle Size *189*

Appendix VII: Identification of Mass Spectra Peaks *192*

Appendix VIII: Dehydroxylation of Zeolite Rho *193*

Appendix X: Adsorption Data *195*

LIST OF FIGURES

Figure 1.1: Framework Topology of Zeolite Rho 8
Figure 1.2: Framework structural changes from (a) dehydrated H-Rho to (b) Ca.D-Rho 9
Figure 1.3: Framework Topology of Mordenite 12
Figure 1.4: Framework Topology of ZK-5 15
Figure 1.5: Framework Topology of Chabazite 18
Figure 1.6: Amine Content in Amines as a function of Calcination Temperature for zeolite Rho 23
Figure 1.7: Activity and selectivity over Rho as a function of Steaming Temperature 27
Figure 1.8: Catalytic activities and selectivities for methylamine synthesis on H-Mordenite (left) and $SiCl_4$ treated H-Mordenite (right) as a function of molar NH_3 to CH_3OH ratio 33
Figure 1.9: Catalytic activity and selectivity for methylamine synthesis on H-Chabazite as a function of molar NH_3 to CH_3OH ratio 33
Figure 1.10: Amine selectivity over H-Mordenite (a) and H-Mordenite treated with TEOS (b) as a function of methanol conversion 35
Figure 1.11: Distribution of N containing species over Na-Mordenite (a) and silica - alumina (b) as a function of methanol conversion 36
Figure 1.12: Molar selectivity vs. fractional methanol conversion over H-Rho 36
Figure 1.13: Equilibrium Methylamines Distribution 38
Figure 1.14: Mechanism of Methylamine Formation over Brønsted acid catalysts 45

Figure 2.1: Temperature Programmed Desorption Rig 52
Figure 2.2: Flow sheet of experimental apparatus 55
Figure 2.3: Reactor used for methanol amination reactions 56
Figure 2.4: Ampoule Sampling System 57
Figure 2.5: Determination of total adsorption capacity 59
Figure 2.6: Determination of Physisorbed Amount 60
Figure 2.7: Effect of dilution on TCD signal response 62

Figure 3.1: XRD patterns of zeolite Na.Cs-Rho (A) 64
Figure 3.2: XRD Pattern of zeolite Na.Cs-Rho B 64
Figure 3.3: SEM photographs of Rho A (a) and Rho B (b) 65
Figure 3.4: Thermal Desorption Spectrum of Rho 66
Figure 3.5: XRD Pattern of Mordenite 67
Figure 3.6: SEM Photograph of the untreated Mordenite used in this work (a) and a highly crystaline Mordenite Sample (b) 68
Figure 3.7: Thermal Desorption Spectrum of Untreated Mordenite 69
Figure 3.8: Activity in the methanol amination reaction over zeolites Rho (A), Mordenite and silica-alumina at 400°C 70
Figure 3.9: Method of Reaction-Regeneration cycles 74

Figure 3.10: Integral Rates of Methanol Consumption and Product formation vs. Number of reaction/regeneration cycles over zeolite Rho A. 75
Figure 3.11: Amine content in the fraction of total amines produced as a function of the number of reaction-regeneration cycles over zeolite Rho (A). 76
Figure 3.12: Integral rate of methanol consumption as a function of the number of reaction-regeneration cycles under variation of the reaction time per cycle over zeolite Rho (A). 77
Figure 3.13: Amine content in amine fraction as a function of the number of reaction-regeneration cycles under variation of the reaction time per cycle over zeolite Rho (A) 78
Figure 3.14: Integral rate of methanol consumption as a function of the number of reaction-regeneration cycles under variation of the calcination time per cycle over zeolite Rho (A) 79
Figure 3.15: Integral Rate of Methanol Consumption and Amine formation as a function of the number of reaction-regeneration cycles over Mordenite. 81
Figure 3.16: Amine content in the fraction of amines as a function of the number of reaction-regeneration cycles over Mordenite. 82
Figure 3.17: Temperature Programmed Desorption of Reaction Products (excluding water) from zeolite Rho after reaction. 83
Figure 3.18: Temperature Programmed Desorption of water after reaction from zeolite Rho after reaction 84
Figure 3.19: Water release during Temperature Programmed desorption of reaction products and following contact with oxygen. 85
Figure 3.20: Schematic representation of the dissociation of Tetramethyl ammonium ions on the surface of an acidic catalyst 86

Figure 4.1: Comparison of Thermal Desorption spectra for increased steaming time of zeolite Rho (A) 90
Figure 4.2: Deconvolution of Thermal Desorption Spectrum using Gaussian approximation to the peak shapes. 91
Figure 4.3: Comparison of Thermal Desorption spectra over Mordenite at 0 and 8 hrs steaming 93
Figure 4.4: ^{27}Al NMR Spectra for increased steaming time of zeolite Rho(A). 95
Figure 4.5: Total Surface Area of Rho (B) as a function of Steaming Time as determined by BET analysis 98
Figure 4.6: Pore volume of Rho (B) as a function of Steaming Time as determined by BET analysis 98
Figure 4.7: BET isotherm for unsteamed H-Mordenite 99
Figure 4.8: Total Surface Area of Mordenite as a function of Steaming Time as determined by BET analysis 100
Figure 4.9: Change in Micro- and Mesopore volume of Mordenite with steaming time 101
Figure 4.10: Scanning Electron Micrographs of zeolite Rho (A) in the untreated form (a) and after 8 hours of steaming (b) 102
Figure 4.11: Scanning Electron Micrographs of Mordenite in the untreated (A) form and after 16 hours of steaming (B) 103
Figure 4.12: Integral rate of methanol and ammonia consumption as a function of steaming time over zeolite Rho (A). 104
Figure 4.13: Amine content in the fraction of amines as a function of steaming time over zeolite Rho (A). 105

Figure 4.14: Integral Rate of Methanol Consumption over Rho (A) and Mordenite as a function of steaming time. 108
Figure 4.15: Amine content in the fraction of amines as a function of steaming time over Mordenite. 109
Figure 4.16: Integral rate of Methanol consumption a function of over Mordenite. 111
Figure 4.17: Amine content in the fraction of amines as a function of steaming time over Mordenite for severe steaming conditions. 111
Figure 4.18: Theoretical Progression of Yield vs. Conversion for a series of three reversible reactions 113

Figure 5.1: Total adsorption capacity of pure compounds as a function of steaming time for zeolite Rho(B). . 121
Figure 5.2: Chemisorption capacity of pure compounds as a function of steaming time for zeolite Rho(B) 123
Figure 5.3: Physisorption capacity of pure compounds as a function of steaming time for zeolite Rho(B) 124
Figure 5.4: Ratio of total Methanol to Water adsorption over zeolite Rho(B) vs. steaming time. 125
Figure 5.5: Ratio of total Methanol to Water adsorption over zeolite Rho(B) vs. steaming time. 126
Figure 5.6: Ratio of ammonia to methanol chemisorption over zeolite Rho(B) vs. steaming time. 127
Figure 5.7: Ratio of ammonia to methanol physisorption over zeolite Rho(B) vs. steaming time. 128
Figure 5.8: Total adsorption capacity of pure compounds as a function of steaming time for Mordenite. 129
Figure 5.9: Chemisorption capacity of pure compounds as a function of steaming time for Mordenite. 131
Figure 5.10: Physisorption capacity of pure compounds as a function of steaming time for Mordenite. 131
Figure 5.11: Ratio of total Methanol to Water adsorption over Mordenite vs. steaming time. 132
Figure 5.12: Ratio of Methanol to Water Chemisorption over Mordenite vs. steaming time. 133
Figure 5.13: Ratio of Methanol to Water Chemisorption over Mordenite vs. steaming time. 134
Figure 5.14: Ratio of ammonia to methanol chemisorption over Mordenite vs. steaming time. 135
Figure 5.15: Ammonia and Methanol physisorption from a binary mixture over Mordenite as a function of steaming time. 136
Figure 5.16: Ratio of Chemisorption to Physisorption vs. steaming time over zeolite Rho for pure Methanol and Ammonia. 138
Figure 5.17: Yield of Dimethyl ether and total Amines over Mordenite as a function of steaming time. 141

Figure 6.1: Comparison of Pore Volume and Rate of Ammonia consumption over Rho 149

LIST OF TABLES

Table 1.1: Manufacture and value of alkylamines 2
Table 1.2: Reported Selectivities in the Methanol Amination Reaction 5
Table 1.3: Relative Selectivity of methylamines in the fraction of methylamines (mol %) for various samples of naturally occurring Chabazite 19
Table 1.4: Reaction Data on H-Mordenite and Na-H-Mordenite with differing Na content before and after steam treatment 21

Table 3.1: Initial Reaction Studies at 400°C 71
Table 3.2: Initial reaction studies at 325°C 73

Table 4.1: Comparison of Thermal Desorption peaks for zeolite Rho (A) at different steaming times 92
Table 4.2. Ammonia desorption from Mordenite steamed for various times 93

Table 5.1: Increase in adsorption capacities of pure compounds over zeolite Rho(B) with steaming time. 122
Table 5.2: Decrease in adsorption capacities of pure compounds over Mordenite with steaming time. 130

NOMENCLATURE

MMA	monomethylamine
DMA	dimethylamine
TMA	trimethylamine
DME	dimethyl ether
MeOH	methanol
Tc	critical temperature
Pc	critical pressure
M	molar mass
λ	thermal conductivity
y_i	mole fraction of compound i in the vapour phase
x_i	mole fraction of compound i in the liquid phase
f	dimensionless friction factor
d_p	particle diameter
L	bed length (m)
Δp	pressure drop
ρ_p	fluid density
ε	bed voidage
v	intersticial velocity
Re	Reynold's Number
D_{ax}	Axial Dispersion coefficient
Sc	Schmidt number
z	bed length
q	concentration in the adsorbed phase
Pe'	Peclet number
R_p	particle radius
EFAl	Extra-framework Aluminium
C/N	Carbon to Nitrogen Ratio
W/F	Residence Time ($min.mg_{cat}.ml^{-1}$)

Introduction and Literature Review

1. INTRODUCTION AND LITERATURE REVIEW

1.1 INTRODUCTION

Other reviews of the methanol amination reaction may be found [Schweizer et al., 1992; Corbin *et al.*, 1997]. This purpose of this review is to critically evaluate the literature on the subject of methanol amination as it pertains to work performed for this thesis.

Amines and their derivatives find applications in a wide variety of chemical processes. Their many uses include pharmaceuticals, antioxidants for fuels and oils, stabilisers for synthetic rubbers, detergents and extractants for rare earth metals as well as being used as intermediates to form chemicals for use in the agricultural, textile, plastics, and explosives industries [Klyuev and Khidekel, 1980; Schweizer *et al.*, 1992; Nekrasova and Shuikin, 1965].

The alkyl amines can be formed from many different starting materials including alcohols, ethers, halogen derivatives aldehydes, ketones and unsaturated hydrocarbons together with ammonia or other nitrogen containing compounds. The number of processes available to produce the alkyl amines is equally varied. Table 1.1 gives the production rate and value of a selection of low carbon number alkylamines (1992 statistics). It can thus be seen that of the series of methylamines, the largest demand is for dimethylamine (DMA).

The aim of studying amine synthesis is firstly, to develop a process that is both efficient and selective. In particular, for methylamine synthesis, a process to produce dimethylamine selectively is desirable. More specifically, the process should give a product spectrum, which closely matches the market demand. Complex engineering of the catalyst and reaction process is required to produce the three methylamines in the desired ratio. Thermodynamically it is the trimethylamine (TMA) that is favoured while the market demand is mostly for dimethylamine and secondly for monomethylamine (MMA) with less trimethylamine being required. The catalyst should in addition have a high activity and a long lifetime. It is also desired to suppress the formation of side products.

Table 1.1: Manufacture and value of alkylamines

Amine	Abbreviation	Manufacture (tons/yr.)	Value ($/kg) 1992 values
Monomethylamine	MMA	32 000	1.04
Dimethylamine	DMA	80 000	1.04
Trimethylamine	TMA	15 000	1.04
Monoethylamine	MEA	20 000	2.68
Diethylamine	DEA	7 000	2.67
Triethylamine	TEA	6 500	2.76
n-Propylamine	MPA	500	2.45
Dipropylamine	DPA	17 000	2.69
Tripropylamine	TPA	Small	3.59
Isopropylamine	IMPA	23 000	2.16
n-Butylamine	MBA	1 900	2.76
Dibutylamine	DBA	3 000	2.89
Tributylamine	TBA	700	3.48
Diisobutylamine	DIBA	18 000	2.76

[Schweizer *et al.*, 1992]

Dimethyl ether (DME) is the most common side product formed over acid catalysts. Although it can be recycled to the reactor and converted to the amines with ammonia, this does put an increased load on the expensive separation step of the manufacturing processes.

Other by-products reported for the amination reaction include saturated and unsaturated hydrocarbons, aldehydes, ketones, hydrogen and ethers. The exact product distribution is a function of the feed alcohol and the catalyst used [Klyuev and Khidekel, 1980].

1.1.1 Processes for the Production of Methylamines

At present in industry, methylamines are formed mainly over unselective acidic catalysts, most commonly amorphous silica-alumina. In these processes, an equilibrium distribution of the amines is obtained. The products are separated and the unwanted excess of TMA and MMA as well as DME are recycled back to the reactor to give the overall desired product distribution. This is however a very expensive and energy intensive process as the separation

step of the process involves azeotropic distillation at 15 to 20 bar. The utility requirements for such a process are 22 - 198 kWh of electricity and 7.5 - 13t steam per ton of methylamine [Ashina *et al.*, 1986]. Currently employed industrial processes include the Leonard process and the process of the Roam and Haas Company [Hydrocarbon Processing, 1965; 1979].

Although methylamine production in industry is limited to the reaction of methanol or dimethyl ether and ammonia over an amorphous silica-alumina catalyst there are many other ways in which these molecules can be produced.

1.1.1.1 Solid Acid Catalysts - The dehydration mechanism

The most commonly used method of producing methylamines is the reaction of methanol or dimethyl ether and ammonia over an acidic catalyst. The catalysts used are typically some form of silica-alumina, alumina, silica or other metal oxides. This includes both the amorphous catalysts and the large number of those with definite crystal structures, for example the zeolites. Currently, in industry, the most common method of production involves reaction over an amorphous silica-alumina catalyst.

The amorphous acid catalysts all produce the methylamines in thermodynamically determined equilibrium ratios [Schweizer *et al.*, 1992; Nekrasova and Shuikin, 1965]. These catalysts also show a rather poor activity. The reaction is carried out adiabatically, at high temperatures, with T_{max} at ca. 400 °C, which results importunately in rapid catalyst deactivation.

Zeolites are crystalline aluminosilicates consisting of cornerlinked tetrahedra of $[SiO_4]^{4-}$ and $[AlO_4]^{5-}$. The Si and Al atoms are located at the centre of these tetrahedra with the O atoms being shared between adjacent tetrahedra. A structure containing only Si in the tetrahedra would be charge neutral but the inclusion of Al results in an overall negative charge to the framework of the catalyst. This overall negative charge is balanced by cations, typically alkali or alkali earth metals that can be substituted with protons. The relation of the cation to acidity in the catalyst will be discussed later in the thesis. The arrangement of these tetrahedra result into regular channels and cavities within the catalyst structure is what gives an individual zeolite its structure. The structure of each zeolite is unique.

Many zeolites have been found to have higher activity for the methanol amination reaction than the amorphous Silica-alumina, even at low temperatures [Abrams *et al.*, 1990; Shannon *et al.*, 1988; Keane *et al.*, 1987; Ashina, 1986; Segawa and Tachibana, 1991; Chen *et al.*, 1994]. This means that they can be used at conditions where the deactivation rate is lower. Although the acidic zeolite catalysts have high activity for the amination reaction, many of them do not show much improvement in selectivity towards dimethylamine (DMA). A number of small pore zeolites (Rho, Chabazite, ZK-5) do however show an improved selectivity as well as high activity [Keane, 1987; Shannon, 1988]. It has been suggested [Keane, 1987] that the improved selectivity is due to the diffusion constraint of the TMA within the pores of these zeolites. As a rough guide, those zeolites with 8-membered rings show good selectivity to DMA. Table 1.2 gives a selection of the results obtained over various acid catalysts for the reaction of methanol and ammonia to form methylamines.

As can be seen below, another zeolitic catalyst that is being successfully used to selectively produce the amines is Mordenite. Although Mordenite has a twelve membered ring structure it can be modified by ion exchange, dealumination and external surface treatment to produce the desired product ratio. It also has the benefit of being a relatively cheap catalyst to produce.

On these solid acid catalysts it is important to have a good knowledge of the nature of the acid sites, i.e., the strength, number and type as well as the mobility of molecules on these sites [Sharma, 1993]. It has been found that the Brønsted acid sites lead to the formation of amines, while Lewis sites can cause an enhancement in the formation of dimethyl ether (DME) and other side products [Fetting, 1991]. It is also suggested however that certain forms of Lewis acidity enhance the performance of the catalyst.

There are a number of ways in which the selectivity of the catalyst to dimethylamine (DMA) can be improved. The most common of these is to prevent the trimethylamine (TMA) from exiting the internal pore structure of the catalyst by narrowing either the pores or the pore mouths. This leads to the TMA being held up within the framework and thus being reconverted into the lower substituted amines. The external surface is also often poisoned or covered with an inert layer to prohibit the unselective reaction on the external surface.

Table 1.2: Reported Selectivities in the Methanol Amination Reaction

Catalyst	Treatment (1)	Temp (K)	C/N (2)	MeOH conv (%)	MMA	DMA (mol%)	TMA (3)	DME	Reference
H-Rho		598	1	90	34	53	13		Keane, 1987
H-Rho		598	1	90	16	54	30		Corbin, 1990b
H-Rho	TMP	598	1	90	14	86	0.4		Corbin, 1990b
H-Mordenite		598	1	90	18	13	69		Keane, 1987
H- Mordenite		653	1	>90	21	20	38	21	Segawa, 1991
H- Mordenite	$SiCl_4$	653	1	>90	33	65	1	1	Segawa, 1991
H- Mordenite		(5)	1	90	18	13	68	1	Abrams, 1989a
H- Mordenite	$SiCl_4$	613	2	52	58	34	2	6	Ilao,1996
H- Mordenite		613	2	68	48	21	24	6	Ilao,1996
H- Mordenite		633	1	90	19	25	57		Gründling, 1996a
H- Mordenite	TEOS	633	1	90	30	65	5		Gründling, 1996a
H- Mordenite	(Zeolon)	673	1	86	34	42	23	1	Mochida, 1983
H- Mord -15		633	1	93	28	25	47		Gründling, 1997
H- Mord -20		633	1	89	20	25	55		Gründling, 1997
H- Mord -10		633	1	89	40	36	24		Gründling, 1997
Na- Mord	$SiCl_4$	653	1	>90	38	57	1	4	Segawa, 1991
Na- Mord		(4)	1	90	40	20	6		Weigert, 1987
silica-alumina	(H)	598	1	90	31	17	52		Keane, 1987
silica-alumina	(H)	653	1	>90	18	11	44	27	Segawa, 1991
silica-alumina		613	2	69	33	15	23	30	Ilao,1996
γ-alumina		613	2	86	25	12	9	55	Ilao,1996
Chabazite		598	1	90	43	43	11		Keane, 1987
Chabazite		(5)	1	90	12-25	22-60	15-63	1-3	Abrams, 1989a
H-Chabazite		613	2	89	56	41	3	1	Ilao,1996
H-ZK-5		600	1	90	22-42	29-72	4-34	4-40	Shannon, 1989
H-ZSM-5		(5)	1	90	3	7	67	22	Abrams, 1989a
H-ZSM-5		673	1	87	21	28	50	1	Mochida, 1983
H-ZSM-5		613	2	80	19	22	56	2	Ilao,1996
Ca-A		(5)	1	90	25	20	50	7	Abrams, 1989a
Ferrierite		(5)	1	90	31	27	36	7	Abrams, 1989a
H-ferrierite		613	2	39	52	31	12	5	Ilao,1996
H-Faujasite		613	2	86	18	11	53	19	Ilao,1996
H-Y		(5)	1	90	12	11	61	16	Abrams, 1989a

Notes: (1) Treatment performed after synthesis, prior to reaction. (2) Molar Feed ratio, carbon to ammonia (3) Selectivities converted to mole % when originally given as C or wt%. (4) Temp. not given (5) Temperature varied to obtain conversion - temp not given

1.1.1.2 Metal Catalysts - Dehydrogenation or Reductive Amination

Another method of producing amines is the use of a metal or supported metal catalyst [Sewell *et al.*, 1995], although this can not be used for the production of methylamines. This is a reductive process in which hydrogen is added to the system. There is however no net consumption of hydrogen. Besides being part of the reaction mechanism, the hydrogen is reported to retard coke formation on the catalyst. [Schweizer *et al.*, 1992; Nekrasova and Shuikin, 1965]

1.1.1.3 Other processes for the formation of alkylamines

There are a number of other processes for the formation of amines, including the reaction of ammonia with aldehydes, ketones or alkyl halides. Another is the reaction of HCN with an olefin. These processes are carried out over various catalysts. A more unusual method of producing methylamines is a modified Fisher-Tropsh synthesis over a promoted iron catalyst using a feed of CO, H_2, and ammonia [Schweizer *et al.*, 1992]. This process is however not very efficient.

1.2 CATALYSTS FOR THE AMINATION OF METHANOL

As was shown in Table 1.2, there are many catalysts that have been tested for their performance in the acid catalysed methanol amination reaction. The success obtained is varies with respect to the DMA selectivity obtained and seems to depend both on the structure of the catalyst and the nature of its acidity. In this section, a number of catalysts used for the methanol amination reaction will be discussed.

1.2.1 Amorphous Silica-Alumina

As the name implies, this catalyst has no definite crystal structure. Although it is the catalyst used most widely in industry, it is not selective, yielding a thermodynamically controlled product distribution. It also produces fairly high levels of DME. It has been shown that there is a sharp decrease in the amount of DME formed over silica-alumina with increasing temperature from 300 to 450°C [Mochida *et al.*, 1983]. This is another reason, besides its low activity, that silica-alumina is not a suitable catalyst at lower reaction temperatures. The selectivity change with temperature may well be due to the stronger dependence of the rate of amine formation than the rate of DME formation on temperature.

The activity of this and all solid acid catalysts arises from the charge imbalance between the Si and Al in the framework. This causes the formation of acid sites. If pure silica is used it is essentially inactive. If pure alumina is used, it produces almost exclusively DME [Ilao *et al.*, 1996].

Although this catalyst is non-shape selective, it provides a good medium on which to study the surface kinetics for this reaction as its large pore diameter means that internal diffusion can be neglected.

1.2.2 H-Rho

Zeolite Rho has been found to be an excellent catalyst for the amination of methanol to form methylamines. It is both highly active and shows a product distribution that is closer to the market demand. Selectivities to DMA obtained over this catalyst of between 50 and 70 mol % have been reported. [Keane *et al.* , 1987; Shannon *et al.*, 1988a; Abrams *et al.*, 1990]. As this catalyst is highly active, it can be operated at lower temperatures, i.e., at conditions under which deactivation is minimal, thereby extending the catalyst life [Shannon *et al.*, 1988a].

Rho consists of a body centred cubic structure of α-cages that are joined by double eight membered rings of 3.6 Å diameter. These rings form a three dimensional pore structure. When in the ammonium form, the NH_4^+ ions are normally found to be located at the centre of the 8-membered rings [McCusker, 1984; Szostak, 1992]. It has also been seen that the ammonium ions can be located at the centre of the double 8-membered rings [McCusker, 1984; Fischer et. al., 1989] and studies using ND_4-Rho have revealed ions located in the α-cages of the catalyst [Fischer et al., 1989]. Figure 1.1 shows the framework topology of Rho.

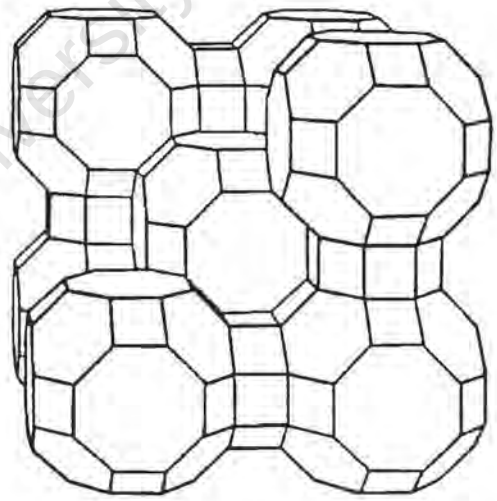

Figure 1.1: Framework Topology of Zeolite Rho

[Szostak, 1992]

Ideally, Rho has a highly symmetrical structure [Im3m] but in reality the catalyst does not conform to this, e.g., the Cs exchanged form has a [I43m] structure [Parise *et al.*, 1984a]. Rho undergoes significant unit cell dimension changes depending on the degree of hydration and ion exchange [Parise *et al.*, 1984a,b; Corbin *et al.*, 1990a; McCusker and Baerlocher, 1983, McCusker, 1984]. Neutron powder diffraction has been used to determine the change in the crystal structure. Dehydrated H-Rho (a = 15.098 Å) is the most symmetric and Ca,D-Rho (a=13.965Å) the most asymmetric. The larger cations and water or other adsorbed molecules cause framework distortion and ring elongation, i.e., constriction of the pores [Corbin *et al.*, 1990a; Szostak, 1992]. Vega and Luz [1988] found that the adsorption of the methylamines, methanol and water onto H-Rho also caused framework distortion. Figure 1.2 shows the framework structural changes from dehydrated H-Rho to Ca,D-Rho.

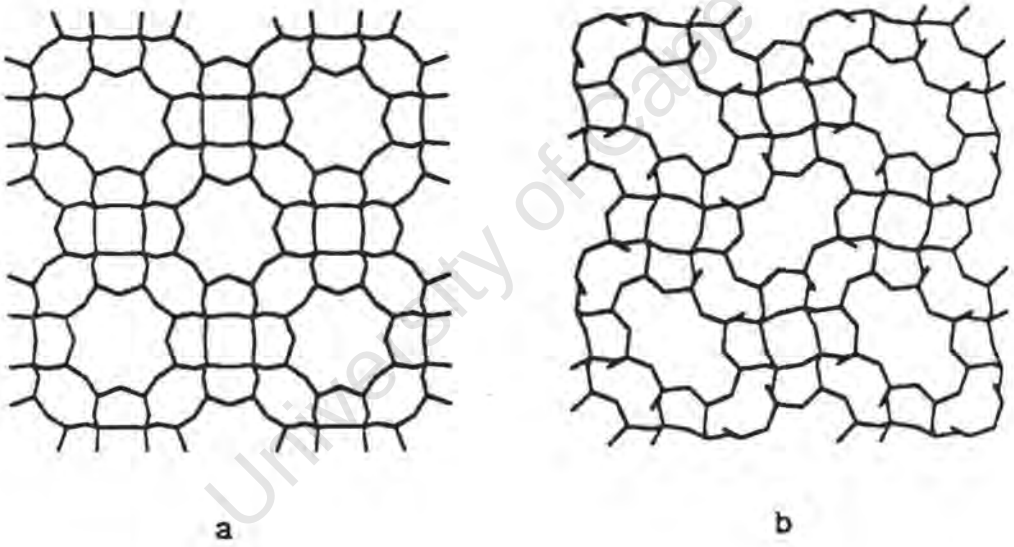

Figure 1.2: Framework structural changes from (a) dehydrated H-Rho to (b) Ca,D-Rho
[Corbin, 1990a]

Also, as with all zeolites, the structure of Rho is a strong function of temperature. For example, H-Rho has a unit cell dimension, a = 15 Å at 30 °C and a = 14.75 Å at 300 °C [Parise *et al.*, 1984b; Abrams *et al.*, 1990]. The flexibility of the framework of this catalyst

might offer an opportunity to manipulate the catalyst for increased selectivity [Corbin *et al.*, 1990a].

The catalyst selectivity can be further improved in a number of ways. Firstly, hydrothermal treatment can be used to improve catalyst selectivity without adversely affecting the activity [Shannon *et al.*, 1988a]. The second way to improve the performance is to apply coatings of either alumina or silica, for example, to the surface of the catalyst [Bergna *et al.*, 1989]. Post-synthesis modification will be discussed in more detail in chapter 1.4.

As with all catalysts, the selectivity obtained is a strong function of the reaction conditions applied. This will also be discussed later, in chapter 1.3.

There is a large variation in the results obtained for Rho due to the change in the concentration and type of impurity phases formed in addition to Rho in the synthesis procedure [Shannon *et al.*, 1988a]. The impurity phases that frequently occur in Rho are gel, Chabazite, Pc and Pollucite [Shannon *et al.*, 1988b].

Gel is formed when the catalyst synthesis is stopped prematurely. It has very low activity and produces a near equilibrium product distribution. It has a low concentration of internal and a high concentration of external Lewis acid sites.

Pc, which is a dimensionally cubic zeolite with the Gismondine structure [Szostak, 1992], is formed irregularly during synthesis. It is essentially inactive below 400 °C and is not selective [Shannon *et al.*, 1988b].

Pollucite is formed in the later stages of crystallisation. It is not very active and is non-selective. This phase is the biggest culprit for non-selectivity of Rho as some forms of Pollucite can be slightly active.

Chabazite can be formed at the same time as Rho and is often present at a concentration of between 5 and 20 wt% concentration. It has a relatively high surface area and is therefore active. It can be highly selective and does not usually pose a problem to the overall catalyst performance. Chabazite has been studied in its own right as a catalyst for the methanol amination reaction [Abrams *et al.*, 1989; Ilao *et al.*, 1996]. It has been found that high silica preparations may be made of zeolite Rho, in which no Chabazite is formed [Chatelain et al., 1995].

Most of the impurity phases can be inertised by calcination or steaming at higher temperatures [Shannon *et al.*, 1988b]. This means that the selectivity is unaffected at lower reaction temperatures but that the apparent activity of the Rho drops due to the dilution of the catalyst with unreactive amorphous material.

It has been suggested that the performance of Rho is also dependant on the degree of hydration of the parent catalyst [Gier et al., 1985]. It seems that while the dehydrated catalyst is more active, the hydrated catalyst is more selective. These results are however not conclusive as they do not indicate the time on stream after which the samples were taken. This is an important point as water is a reaction product and hence, the dehydrated catalyst could be expected to quickly take up the product water. Secondly, the ammonia can be expected to displace any water adsorbed on the surface.

1.2.3 Mordenite

Mordenite is a naturally occurring zeolite which can be synthesised easily [Barrer, 1982]. This catalyst consists of 4- and 5-membered rings joined together to form a 2-dimensional pore structure consisting of 12- and 8-membered rings. In reality, the catalyst can be considered as a 1-dimensional structure of 12-membered ring channels with side pockets [Szostak, 1992]. The pore dimensions of this catalyst are typically 6.5 x 7.0 Å. Figure 1.3 shows the framework topology of Mordenite

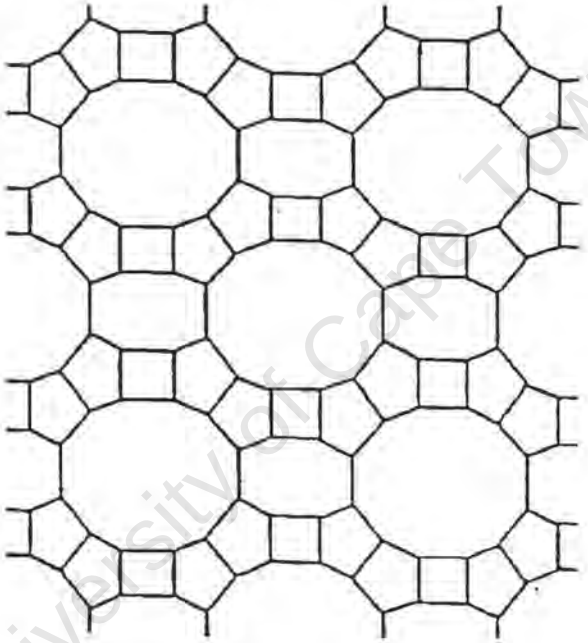

Figure 1.3: Framework Topology of Mordenite

[Szostak, 1992]

As could be seen from Table 1.2, much work has been done on methanol amination over Mordenite. Ashina *et al.* [1986] found that synthetic Mordenite performed better than natural Mordenite and that it gave a slightly better than equilibrium product distribution. Mochida *et al.* [1983] likewise found increased selectivity to DMA over Mordenite. While Mochida *et al.* do show a slight increase in selectivity to DMA, it is only the treated forms of this catalyst that show significant improvements in selectivity. Additionally, both the H- and alkali- or

alkali earth metal- exchanged forms (e.g. Na, Mg) of Mordenite have been proposed as selective catalysts for the formation of lower substituted methylamines [Weigert, 1987; Mochida et. al., 1983; Ashina et. al., 1986]. The activity of H-Mordenite is however higher than that of Na-Mordenite [Ernst and Pfeifer, 1992].

All three methylamines are able to adsorb readily onto the surface of Mordenite [Weigert, 1987]. Segawa and Tachibana [1991] found that MMA and DMA adsorb very rapidly and TMA only slightly slower onto H-Mordenite. Subsequently it was stated that the molar amount of TMA adsorbed onto H-Mordenite is less than MMA or DMA due to size constraints [Ilao *et al.*, 1996].

H-Mordenite has been found to have only Brønsted acid sites with essentially no Lewis acid sites [Maache *et al.*, 1995; Datka *et al.*, 1997]. If ammonia is adsorbed onto H-Mordenite after methanol then the methanol is completely displaced and no amines are formed even up to 523 K [Ilao *et al.*, 1996]. It also has a few very strong sites, possibly associated with extra-framework alumina. This was determined by both pyridine and ammonia microcalorimetry and ammonia TPD [Chen *et al.*, 1992; Sharma *et al.*, 1993; Chen *et al.*, 1994a]. If the catalyst undergoes very high temperature calcination, the number of acid sites decreases, as does the acid strength [Chen *et al.*, 1992].

As with Rho, Mordenite is active at lower temperatures and can therefore be operated at conditions that result in decreased deactivation. The lifetime of the catalyst was found to be approximately 1 year when operated at 300 to 328 °C. With increasing reaction temperatures, the catalyst deactivates much faster [Ashina *et al.*, 1986]. It was observed that when the activity of Mordenite had dropped by half, the selectivity to DMA and TMA had decreased while that to MMA had increased. It was not stated whether this was caused by the changing conversion or by increasing diffusional constraints of the coke layer.

It has been found that the selectivity of H-Mordenite can be greatly improved by treatment with $SiCl_4$. This however only works when the catalyst is treated in the Na form and then ion-exchanged to the H-form. Treatment of the H-form with $SiCl_4$ results in almost complete dealumination of the catalyst. On Mordenite which had been treated with $SiCl_4$ in the Na form and subsequently ion exchanged, the TMA uptake was found to be practically zero which indicates that the pore mouths had been successfully blocked [Segawa and Tachibana, 1991].

The effect of Brønsted and Lewis acidity on the methanol amination reaction will be discussed in detail in chapter 1.6. It is however important, at this point, to note the exclusive Brønsted acidity of fresh H-Mordenite.

The performance of Na and other alkali-exchanged Mordenites is very different to that of H-Mordenite. It has been found by a number of authors that Na-Mordenite is more selective but less active than H-Mordenite [Segawa and Tachibana, 1991; Kogelbauer *et al.*, 1994; Kogelbauer *et al.*, 1996]. Over a number of alkali-exchanged (Li/Na/K/Rb/Cs) Mordenites selectivities of ca. 40 % DMA were obtained. This was further improved, to >60%, with steam treatment [Zhang *et al.*, 1994].

Weigert [1987] postulated that the mechanism over Na-Mordenite was different due to the absence of Brønsted acid sites and that this was responsible for the different selectivities observed. (This will also be discussed in more detail in Chapter 1.6).

As with the H-form of the catalyst, the selectivity of Na-Mordenite can be improved by treatment with $SiCl_4$. The adsorption of TMA onto Na-Mordenite that had been treated with $SiCl_4$ was found to be negligible while MMA and DMA adsorbed readily. This indicates that the treatment of Na-Mordenite with $SiCl_4$ significantly blocks the pores [Segawa and Tachibana, 1991]. The performance of the catalyst can also be further improved by hydrothermal treatment.

The level of ion exchange is important when combined with steam treatment. Over the catalysts that do not undergo steaming, the performance remains constant but when steam treatment is employed then there is a maximum in DMA selectivity with the ion-exchange level [Zhang *et al.*, 1994]. As the number of alkali ions increases, so does the selectivity to MMA and DMA. The activity however drops with increasing alkali content [Ashina *et al.*, 1986]. Mochida *et al.* [1983] has shown the performance of a number of different ion-exchanged Mordenites at various temperatures. It was found that in general these catalysts showed a non-equilibrium product distribution, i.e., high selectivities to MMA and DMA and lower TMA selectivities.

It has also been shown that the Al content of alkali-exchanged zeolites affects the catalytic performance [Kogelbauer *et al.*, 1994, 1996]. At higher Al contents, it was found that more TMA and DME were formed.

1.2.4 H-ZK-5

ZK-5 has been studied as a possible catalyst for the methanol amination reaction [Shannon *et al.*, 1989]. It has a structure very similar to that of Rho. The framework of ZK-5 consists of truncated cuboctahedra joined by double six membered rings [Szostak, 1992]. Figure 1.4 shows the framework topology of ZK-5. It does show shape selective behaviour for this reaction, yielding higher than equilibrium DMA selectivities [Keane *et al.*, 1987]. The selectivity of H-ZK-5 depends on the calcination procedure, whether or not steam treatment is used and on the Cs content of the catalyst. As the Cs content increases, the DMA selectivity increases [Shannon *et al.*, 1989].

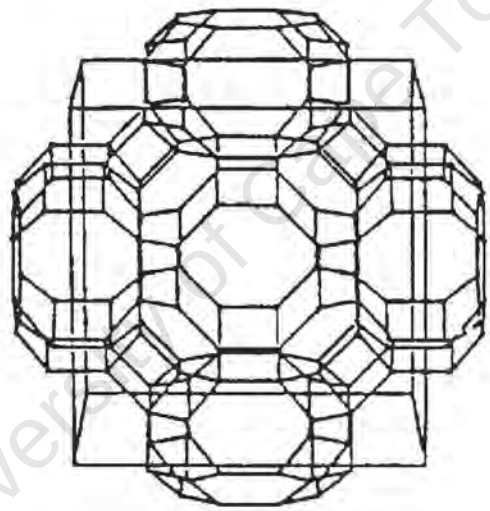

Figure 1.4: Framework Topology of ZK-5

[Szostak, 1992]

A study on the affect of crystal structure was performed on this catalyst [Schwarz et. al., 1998]. In this study it was seen that larger crystals of modified K,Cs-Rho and K,Sr-Rho while being less active than the smaller crystals showed very low TMA selectivity (1 mol% TMA at 70% methanol conversion).

Although it would seem that this would be a good catalyst for this reaction, it undergoes considerable framework damage at even moderately high calcination temperatures. The framework is slightly stabilised in the presence of steam [Shannon *et al.*, 1989]. In general it can be said that ZK-5 is less stable, active and selective than Rho.

1.2.5 H-ZSM5

ZSM-5 consists of intersecting channels, one straight and one sinusoidal. The resulting pore structure has three-dimensional intersecting 10-membered rings of 5.3 x 5.6 Å and 5.1 x 5.5 Å.

A number of studies have been performed over ZSM-5 to determine its performance for the methanol amination reaction. Although it has proved to be a highly active catalyst, it does not show any real shape selective properties. At slightly less than 100% conversion of methanol, at all temperatures there is a slight increase in MMA selectivity but the selectivity to DMA is unchanged [Herrman *et al.*, 1988].

As with all catalysts, the selectivity obtained is a function of the reaction conditions employed, *viz.* temperature, methanol to ammonia (C/N) ratio and conversion. DME is also produced at lower temperatures but decreases with increasing reaction temperature. There has been no evidence shown that either hydrothermal or surface treatment will improve the selectivity of this catalyst.

1.2.6 SAPO Catalysts

Non-zeolitic, molecular sieve, acidic catalysts such as the SAPO catalysts can be used for the formation of methylamines. In particular, SAPO-11 and SAPO-34 have been used to selectively produce MMA at up to 60 % selectivity. This catalyst was improved by the addition of cations, anions and salts of metals [Olson and Kaiser, 1988].

The SAPO catalysts are silicoaluminophosphates, which have structures that are similar to the zeolites but with P atoms incorporated into the structure. For example, SAPO-34 is isomorphous to Chabazite [Szostak, 1992] (see section 1.2.7 for structure of Chabazite). SAPO-11 has a medium size pore structure of unidimensional 10-membered rings and pore openings of 6.7 x 4.4 Å.

1.2.7 Chabazite

Chabazite has been shown to be an exceptionally good natural catalyst for the formation of lower substituted methylamines. The framework of Chabazite consists of ellipsoidal cavities connected by eight membered rings. The pore openings of this catalyst have a dimension of 3.8 x 3.8 Å. The product distribution is strongly dependent on where the sample was obtained, although all samples of Chabazite show similar activity. Figure 1.5 shows the framework topology of Chabazite.

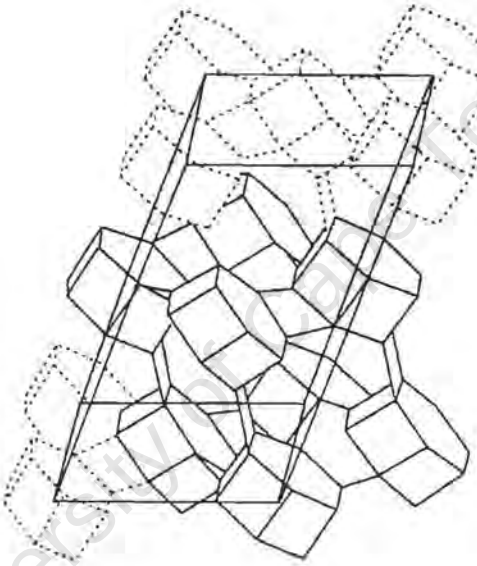

Figure 1.5: Framework Topology of Chabazite

[Szostak, 1992]

There have been a number of studies performed over Chabazite for the methanol Amination reaction [Keane *et al.*, 1987; Abrams *et. al.*, 1989; Ilao *et al.*, 1996; Lobo *et al.*, 1999]. Table 1.3 shows the distribution of amines for a number of different samples of naturally occurring Chabazite. It can be seen that the results obtained with this catalyst depend strongly on the source of the catalyst. In general, synthetic Chabazites perform better, yielding lower TMA selectivities (cf. Table 1.2).

Table 1.3: Relative Selectivity of methylamines in the fraction of methylamines (mol %) for various samples of naturally occurring Chabazite

[Abrams *et al.*, 1989]

MMA	DMA	TMA	CATALYST SOURCE
12	22	63	Bowie/Arizona
20	43	32	Durkee/Oregon
14	26	59	Bear Springs/Arizona
16	29	53	Wikieup/Arizona
15	32	50	Christmas/Arizona
18	33	48	Beaver Divide/Wyoming
18	42	40	Nova Scotia/Canada
25	60	15	Naples/Italy

(selectivities for reaction at 90% methanol conversion)

The selectivity of Chabazite in general can be explained by the adsorption of the amines. Over a synthetic Chabazite, MMA and DMA both readily adsorb into the pore structure but very little TMA adsorbs [Ilao *et al.*, 1996].

As with the other zeolites, it has also been found that the selectivity of Chabazite is dependent on the level of ion exchange. If there is much potassium in the structure, the activity is lower, the selectivity is not as good and more DME is formed [Ilao *et al.*, 1996]. The effect is therefore different from Mordenite where increasing the alkali ion content increases the selectivity to DMA.

There is evidence that the types of acid sites on Chabazite are not exactly the same as that of other zeolites. It has been found that, if ammonia adsorbs onto Chabazite after methanol, not the entire amount of methanol is displaced and some amines are formed [Ilao *et al.*, 1996]. This is again unlike Mordenite, where ammonia completely displaces adsorbed methanol without amine formation [Ilao *et al.*, 1996].

The rate of DME formation over Chabazite, as with other catalysts, was found to be a function of Al content.

1.3 CATALYST PREPARATION

The way in which a catalyst is prepared is extremely consequential to the way in which that catalyst performs. The most obvious influence on catalyst behaviour is the catalyst synthesis or primary preparation phase. This will not be dealt with other than to mention its importance in obtaining the correct catalyst structure. Of more interest here is the effect of secondary preparation procedures, namely ion exchange and calcination.

1.3.1 Ion-Exchange Techniques

Most catalysts are synthesised in their alkali form. To obtain the active protonic form, these catalysts are immersed in an aqueous solution of an ammonium salt e.g., ammonium nitrate. The strength of the solution, the temperature and the time of the exchange all have an effect on the percentage of alkali ions that are exchanged for ammonium ions. Care must also be taken, as too severe a treatment will dealuminate the catalyst thus causing framework damage. The ammonium form of the catalyst is converted to the protonic form by heating the catalyst in flowing gas (either N_2 or air) to drive off the ammonia.

It has already been shown in Chapter 1.2 that the type of cation present on the catalyst has many effects on the process. The Brønsted acidic catalyst, where the catalyst is in the protonic form has a very different reaction mechanism to that of the alkali or rare earth cation exchanged catalyst, which has a primarily Lewis acid function. It is also possible to have a catalyst that is not exclusively one form or the other. This happens when there is a mixture of protons and alkali ions at the surface, i.e., when incomplete ion exchange has taken place.

Table 1.4 shows the change in selectivity and activity of a Mordenite catalyst treated with increasing concentrations of NaCl, i.e., the catalyst is progressively back exchanged from the H- to the Na- form. The more pronounced effect is seen when the exchange is combined with steam treatment, which makes it more shape selective.

Table 1.4: Reaction Data on H-Mordenite and Na-H-Mordenite with differing Na content before and after steam treatment

[Data taken from Zhang *et al.*, 1994]
T=400 °C, ammonia/methanol=1, W/F=6.3 min.mg_{cat}.ml^{-1}. HM=parent catalyst. M1-4 = catalyst treated with increasing concentration of NaCl, W=water treatment at 500°C.

Samples	MeOH	Selectivity C%			
	conv.%	DME	MMA	DMA	TMA
HM	85.9	2.0	18.3	43.0	36.7
M1	84.7	0.8	19.1	43.2	36.9
M2	79.6	0.9	20.4	44.4	34.4
M3	58.4	1.0	20.7	46.8	31.5
M4	48.0	1.1	20.2	49.7	29.0
HMW	81.5	14.5	13.5	41.2	30.8
M1W	95	4.4	17.8	60.9	16.8
M2W	85.3	4.4	21.6	65.8	8.1
M3W	68.5	2.3	35.5	59.6	2.6
M4W	36.5	2.7	55.5	40.2	1.6

1.3.2 Calcination Procedures

Calcination procedures employed vary quite considerably. Calcination essentially involves the heating of the catalyst in a specific atmosphere. For the catalysts considered in this report, calcination is usually carried out between 400 and 600 °C in an atmosphere of either nitrogen or air. The purpose of calcination is twofold, to drive off both water and ammonia from the protonic form and to remove any extraneous organic compounds that might be present on the catalyst.

The way in which the catalyst is contacted with the flowing gas can also be varied. The methods include a plug flow system, shallow bed calcination in which the catalyst is moved on a quartz boat through the hot zone of a belt furnace and deep bed calcination in which the catalyst is heated in a covered crucible [Shannon *et al.*, 1988a].

Catalyst treatment with water at elevated temperatures will be dealt with in Chapter 1.6 as a completely different issue to calcination. Care must however be taken when calcining as there are two possibilities for inadvertently steaming the catalyst. Firstly, if the catalyst is heated too fast in an insufficient flow of gas then the water that was adsorbed onto the framework will not have sufficient time to desorb and will therefore be present at sufficiently high temperatures to steam the catalyst. Also if there are organics present on the catalyst and the flowing gas is air, then these will be burnt to form water. Once again this should not be a problem if the catalyst is heated slowly as the first step in the burning off of these compounds, oxidative dehydrogenation takes place at lower temperatures leaving carbon on the surface which is in turn burnt off at higher temperatures forming CO and CO_2 [Zhao, 1991].

1.3.2.1 Effect of calcination temperature

Upon calcining Rho, over the temperature range 400 to 600 °C no change in crystallinity was observed [Shannon *et al.*, 1988a]. Figure 1.6 shows the effect of calcination temperature on selectivity for Rho. With increasing calcination temperature there was no change in the activity or the rate of DME formation. There was an increase in the number of internal Lewis and a decrease in the internal Brønsted acid sites [Shannon *et al.*, 1988a]. The results for H-

ZK-5 were very similar to those obtained over Rho, as the calcination temperature is increased, the DMA yield increases.

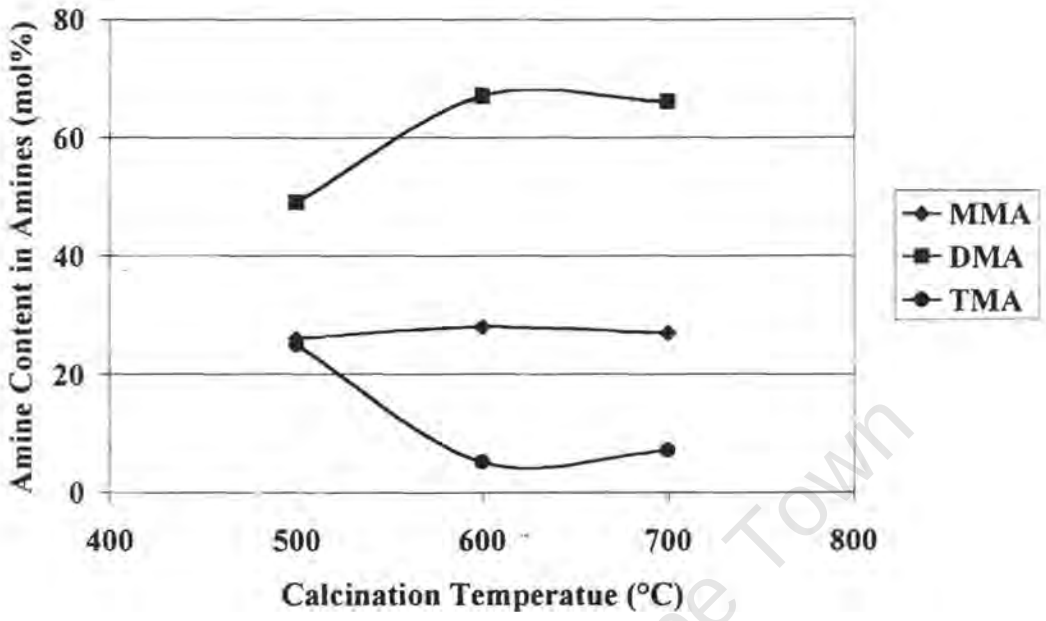

Figure 1.6: Amine Content in Amines as a function of Calcination Temperature for zeolite Rho

[Data taken from Shannon *et al.*, 1988a; $T_{reaction}$ = 325°C, $t_{calcination}$ = 4 hrs, C/N =1, X_{MeOH}=90%, p=1atm]

If the calcination temperature is too high, then the catalysts will undergo framework deterioration. The temperature at which this disintegration starts to occur depends on the individual catalyst. At temperatures higher than 600°C, a slight dealumination of the Rho framework was observed. Rho will withstand temperatures of up to 700°C before complete destruction of its crystal structure can be observed [Shannon *et al.*, 1988a]. ZK-5 is not as robust and deteriorates at much lower temperatures [Shannon *et al.*, 1988b]. Very high calcination temperatures have also been found to damage the structure of H-Mordenite [Chen *et al.*, 1992; O'Donnovan *et al.*, 1995]. A decrease in the number and strength of acid sites on the catalyst and also an increase in the variation of acid site type evidence this. The effect is possibly caused by dealumination and/or dehydroxylation [Chen *et al.*, 1992].

1.3.2.2 Effect of calcination time

Calcination at a given set of conditions for a longer period of time gives an increased probability that the ammonia/organics will be completely removed. There is however for any set of conditions a point beyond which the catalyst can not be altered due to thermodynamic constraints.

No conclusive studies were performed on the effect of calcination time over any of the catalysts.

1.4 POST SYNTHESIS MODIFICATION

Post synthesis modification encompasses a number of techniques by which the structure of a catalyst is changed. These techniques are widely used to modify the behaviour of the catalyst both in terms of activity and selectivity. The most common procedures used on catalysts for the methanol amination reaction can be divided into two categories: dealumination and surface treatment.

Dealumination is a process by which some, or all, of the framework Al is removed from the catalyst's crystal lattice or framework. This can be done by either leaching the Al out with acidic solution or by treating the catalyst with steam at high temperatures (hydrothermal treatment). The aluminium removed from the crystal lattice may take a number of forms [Corma *et al.*, 1989; Martens *et al.*, 1997], these include monomeric, hydrolysed, cationic species which may be fully dislodged from the framework or may still be co-ordinated to between one and three framework oxygen atoms. The aluminium may also form oligomeric or polymeric aluminium oxyhydroxides or oxides. It is also possible for amorphous silica-alumina to be formed, occluded within the zeolite. It is possible for completely dislodged aluminium species to migrate to the surface of the crystal and accumulate as oligomeric or polymeric species on the external surface [Martens *et al.*, 1997]. When discussing dealumination it is normal to distinguish between framework and bulk dealumination. Framework dealumination, as discussed above, is when the aluminium is removed from the crystal lattice but remains in contact with the catalyst crystal. Bulk dealumination is the complete removal of aluminium from the crystal. The amount of aluminium removed from the catalyst structure can be seen on examination of the different reports to be dependent on both the severity of the conditions used and the catalyst in question [Haag, 1987; van Niekerk, 1992; Scherzer, 1984; Corma, 1989,1996; Burgfels, 1995; Englehardt, 1987]. The effect of extra-framework aluminium species occluded in the crystal structure of the catalyst will be discussed further in section 1.4.3.

1.4.1 Acid Leaching

Many compounds can leach Al from the crystal lattice. These include mineral and organic acids, metal halides, oxyhalides and metal alcoholates. It has been found that acid leaching

removes the Al from the framework and then washes it out of the pore structure [O'Donovan *et al.*, 1995].

1.4.2 Steaming

Under steaming conditions, water gives mobility to both Al and Si species in the catalyst. The Al that migrates out of the framework may be replaced by Si [Barrer, 1982; Shannon *et al.*, 1988a]. This is the reason that the framework of Rho was found to be more stable with increasing temperature under steaming than under dry calcination. The structures of many other zeolites such as ZK-5 and USY were also found to be more stable under steaming conditions [Corma *et al.*, 1989; Cotterman *et al.*, 1989; Sherzer *et al.*, 1984; Shannon *et al.*, 1988b].

With increasing steaming temperature there is a drop in the catalyst crystallinity. Figure 1.7 shows the activity as defined by space velocity and selectivity vs. steaming temperature for zeolite Rho. The activity of the catalyst drops substantially after 500 °C but there is a good improvement in selectivity. Above 600 °C the amount of DME produced starts to rise rapidly.

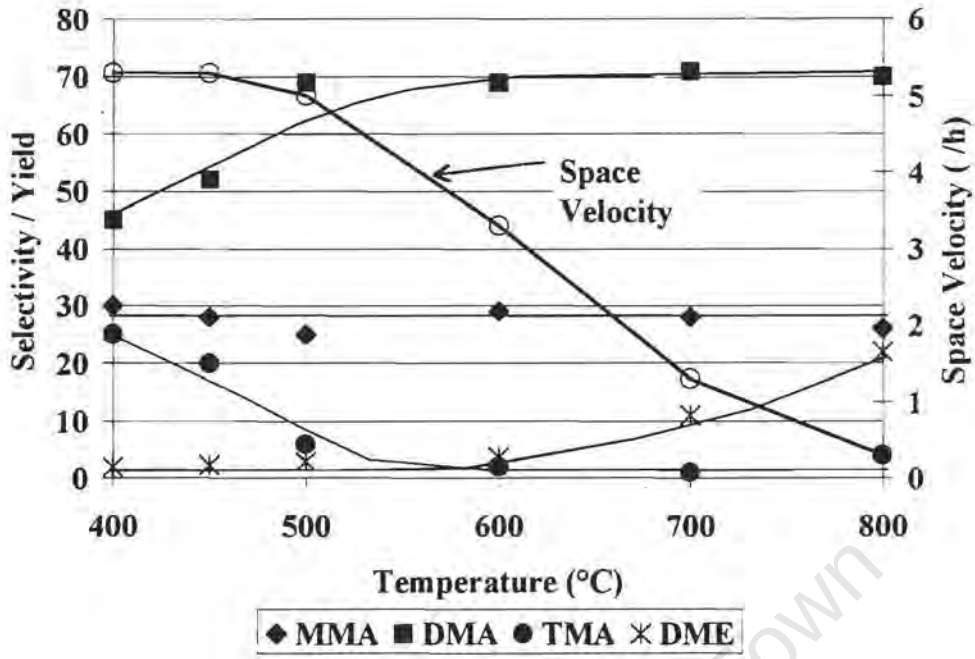

Figure 1.7: Activity and selectivity over Rho as a function of Steaming Temperature

[Data from Shannon *et al.*, 1988a. $T_{reaction}$ = 325°C, C/N = 1, X_{MeOH}=90%, p=1atm]

Ashina *et al.* [1986] found that steaming Mordenite lead to an increase in the selectivity to DMA with very little change in activity. They assumed that the change was due to external site damage but offered no proof of this. Greater then 60 % DMA selectivity was achieved after steam treatment. Similar treatment of T zeolites also results in an increase in the product selectivity to lower amines. T zeolites are a distorted intergrowth of Offretite and Erionite, with the larger portion of the structure consisting of Offretite. The resulting catalyst is three-dimensional with pore openings of 3.6 x 4.8 Å.

The effect of the partial pressure of steam on the behaviour of Rho was also investigated [Shannon *et al.*, 1988a]. The selectivity to DMA as a function of steam partial pressure appears to go through a maximum. A conclusive statement can however not be made since there is a large gap in the data. There is a decrease in acid site concentration with steam partial pressure.

It was found that with increased steaming temperature of Rho, the number of internal Lewis sites initially dropped and then stayed constant [Shannon *et al.*, 1988a]. Under steaming conditions a small number of very strong acid sites are formed.

With steaming of Rho and Mordenite there is evidence of framework dealumination [Shannon *et al.*, 1988a; Ashina *et al.*, 1986]. It has also been found over acidic T zeolites that hydrothermal treatment results in the removal of Al from the framework. Dingerdissen *et al.* [1991] assume that the extra-framework alumina migrates into the interior of the catalyst and thus improves selectivity by increasing diffusion constraints. Zhang *et al.* [1994] found that steaming led to dealumination and crystal shrinkage. The formation of mesopores was not observed.

1.4.3 Extra Framework Alumina

Evidence for the production of extra framework aluminium was offered by Shannon *et al.* [1988a] who observed that under steaming conditions there was a shift in the IR band for the bridging OH groups. This was substantiated using ^{27}Al MAS NMR. The extra framework aluminium causes the frequency shift from 3610 to 3640 cm-1. It is suggested that the EFAl may enhance the acid strength of the catalyst. The decrease in TMA selectivity is related to the increase in the degree of dealumination. There has also been some evidence shown that the presence of EFAl can affect the strength of the bonding of TMA to the framework. It was seen that the TMA bond strength increased with increasing EFAl content [Abrams *et al.*, 1990].

It has been seen over many zeolites, with respect to a different reaction, that there is an optimum degree of dealumination at which the catalyst is most active [Shertukde *et al.*, 1993; Carvajal *et al.*, 1990; Fritz and Lunsford, 1989; Haag and Chen, 1987]. The increased acid strength is often ascribed to the interaction of Lewis acid sites with the Brønsted acid sites [Mirodatos and Barthomeuf, 1981; Lago *et al.*, 1986]. It is suspected that the Lewis acid site withdraws electron density from the neighbouring Brønsted acid sites although this issue is not clear. It is also suspected that large extra-framework aluminium species may be responsible for reduced activity of catalysts due to partial charge balancing of the framework with cationic extra-framework aluminium [Kubelkova *et al.*, 1989]. The extra-framework

aluminium may also reduce the activity by causing pore blockage of the catalyst [Bamwenda *et al.*, 1994, 1995; Miller *et al.*, 1992].

Also with the methanol amination reaction, it is not always thought that EFAl is beneficial. For example, Segawa and Tachibana [1993] state that EFAl is a hindrance to the catalyst performance. It has also been shown that γ-alumina alone produces exclusively DME [Ilao *et al.*, 1996].

It could therefore be supposed that the interaction between the extra-framework Al and the acid sites plays a significant role in the selectivity improvement in the methanol amination reaction rather than the EFAl alone. This does not however rule out the pore blocking effects of the EFAl or the possibility of the Si or Al atoms migrating to the external surface of the catalyst and hence blocking the unselective sites on the surface.

1.4.4 Surface Treatment

Surface coatings and other types of surface treatment can also improve the performance of zeolites. The catalyst selectivity can be increased by either poisoning (or blocking) any unselective external sites or by increasing diffusional constraints and thereby increasing the shape selective properties of the catalyst. This can be achieved by narrowing the pore mouth and thus increasing the diffusion constraints on the larger molecules or by generally causing increased diffusion constraints within the catalyst structure [Bergna *et al.*, 1989; Corbin *et al.*, 1990b; Segawa and Tachibana, 1991,1993; Gründling *et al.*, 1996a; Herrman *et al.*, 1988]. This treatment normally only affects the external sites and maybe the access to the internal pore structure of the catalyst but leaves the interior of the catalyst to behave as normal.

One way to achieve this improvement in selectivity is to apply a coating of either Al_2O_3 or SiO_2 to the catalyst surface. The Al_2O_3 is applied as an excess solution of $Al_2(OH)_5Cl$ followed by calcination. SiO_2 is applied as either TEOS (tetraethoxysilane) in toluene or as MSA (monosilicic acid) [Bergna *et al.*, 1989]. The application of these compounds to Rho was found by Bergna *et al.* [1989] to decrease the TMA selectivity by half. Except for the treatment with MSA they did not observe an effect on the DME selectivity. The exact TMA selectivity was found to be proportional to the thickness of the coating applied. The thickness did not affect the activity of the catalyst, which indicates that the external surface is relatively small and that the coating does not enter the pores.

Gründling *et al.* [1996a] proposed that the treatment of Mordenite with a silicon-containing compound lead to pore mouth narrowing and/or a decrease in acid site concentration at the surface. Much of their study concentrated on treatment with TEOS. Besides a dramatic shift in amine selectivity to the lower substituted amines over Mordenite, treatment with TEOS leads to a decrease in DME formation. At the end of their experiments, they stated that the increase in selectivity could not be due to a restricted transition state as all the amines were seen in the pores. It could also not be due to the external surface being blocked as an increase rather than a decrease in activity was seen. The only possibility left then was that the pore mouths had become narrower thereby restricting the exit of TMA from the internal pore structure.

There are many other compounds that can be used to inertise the surface of catalysts. Some examples of these are TMP (trimethyl phosphite), HMDS (hexamethyldisilizane), silicon

tetrachloride, $(Me)_3SiCl$, $(Me)_2SiCl_2$, TEB (tetraethyl borate), $TiOCl_2$ and PCl_3. All these compounds lead to improved selectivity to the lower substituted methylamines. In particular the phosphorus containing compounds eliminate external surface acidity as seen by IR after pyridine sorption [Corbin *et al.*, 1990b]. Adsorption studies of the three amines onto two catalysts (the Na & H forms of $SiCl_4$ treated Mordenite) showed that $SiCl_4$ treatment narrowed the catalyst pores to an extent where the TMA could no longer diffuse into the framework [Segawa and Tachibana, 1991; 1993]. Some of the smaller of these compounds, $SiCl_4$ in particular, can enter the pores of the catalyst. It is therefore unclear as to what change exactly they are causing to the catalyst.

As with the hydrothermal treatment, care must be taken as incorrect treatment procedures can result in framework damage. An example of this is the treatment of Mordenite with $SiCl_4$. If the Na form is treated and then ion-exchanged to the H-form the result is a catalyst that produces very little TMA and high selectivities of MMA and DMA. If however the H form is treated with $SiCl_4$, the framework collapses due to almost complete dealumination [Segawa and Tachibana, 1991, 1993].

1.5 REACTION CONDITIONS

The conditions under which the methanol amination reaction is carried out, *viz.* temperature, reactant partial pressure, space velocity and reactant feed ratios, all affect the selectivity obtained for the process. Although in reality it is difficult to completely separate these reaction variables from one another, an attempt will be made to discuss the effect of each one individually.

1.5.1 Influence of Methanol: Ammonia Feed Ratio

For the reaction of methanol and ammonia to form methylamines, the ratio of methanol to ammonia in the feed has a strong influence on the product spectrum. This is because changing the ratio of the feed compounds changes the equilibrium distribution and therefore the chemical potential for the different products. Figures 1.8 and 1.9 show the effect of ammonia to methanol ratio on the activity and selectivities obtained over three different catalysts.

In general, as the proportion of ammonia in the feed increases, the proportion of the lower substituted amines (MMA and DMA) increases. It is also observed that in these examples as well as others, the DMA selectivity goes through a maximum at, or near, $NH_3/CH_3OH = 1$.

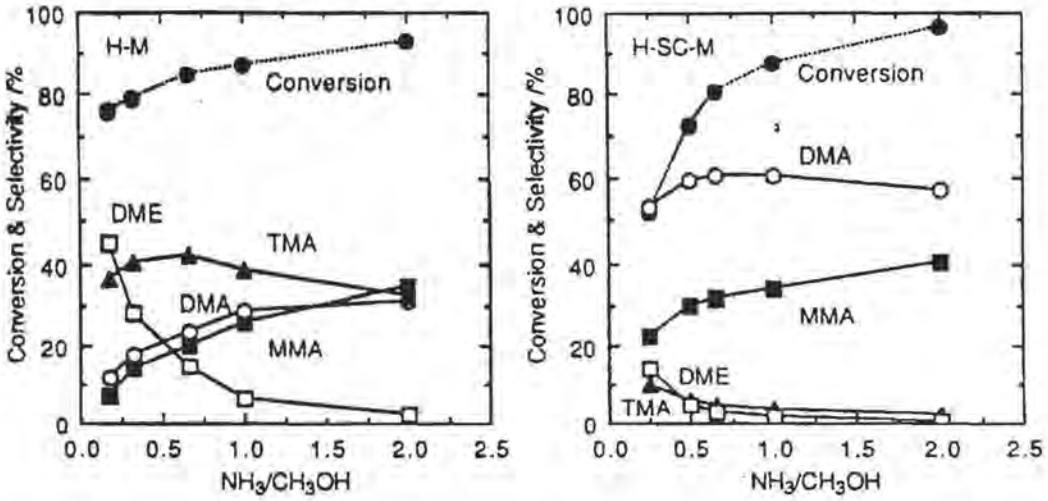

Figure 1.8: Catalytic activities and selectivities for methylamine synthesis on H-Mordenite (left) and $SiCl_4$ treated H-Mordenite (right) as a function of molar NH_3 to CH_3OH ratio

Reaction temperature = 633 K, W/F = 62 gh.mol^{-1}, p_{MeOH} = 2.8 kPa. [Segawa and Tachibana, 1992]

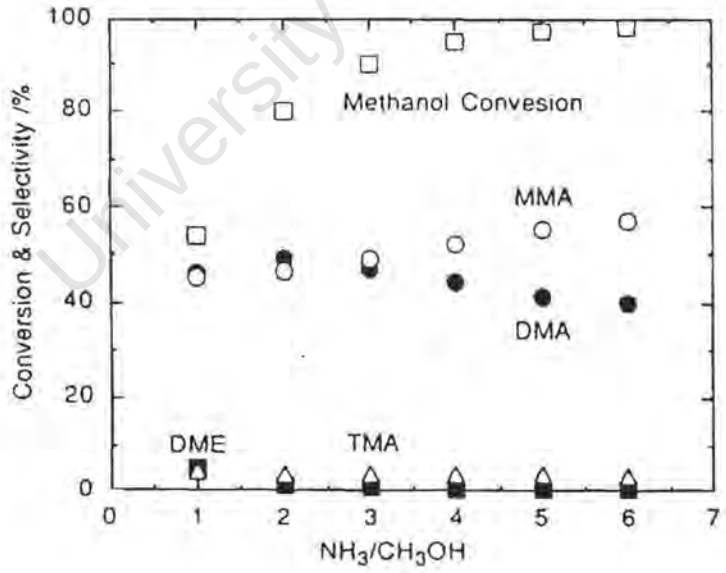

Figure 1.9: Catalytic activity and selectivity for methylamine synthesis on H-Chabazite as a function of molar NH_3 to CH_3OH ratio

Reaction temperature = 613K, W/F = 67 gh.mol^{-1}, p_{MeOH} = 2.8 kPa [Ilao *et al.*, 1996]

1.5.2 Temperature

The temperature at which this reaction is carried out obviously affects both the activity and selectivity observed over any given catalyst. In general, the methanol conversion increases and TMA selectivity decreases with increasing temperature [Ilao *et al.*, 1996]. The activity of most acidic catalysts increases with increasing temperature up to a value of 450°C. Above this temperature, the activity drops rapidly with time on stream due to deactivation of the catalyst by coke deposition [Mochida *et al.*, 1983]. At very high temperatures, the formation of side products other than DME occurs. These include methane, ethane, CO_2 and formaldehyde. At temperatures less than 300°C, even the zeolites are inactive [Ilao *et al.*, 1996]. There is therefore an optimum temperature range in which to operate. This is generally between 300 and 450 °C but varies between catalysts.

Ashina *et al.* [1986] found, over steam treated Mordenite that as the temperature decreased, so did the TMA selectivity. This is in contradiction to the general case and was attributed to the increased diffusion constraints on the TMA at lower temperatures.

1.5.3 Methanol Conversion

The exact product distribution obtained is a strong function of the methanol conversion. Figures 1.10 , 1.11 and 1.12 give an example of the different trends in the selectivity vs. conversion for five different catalysts, *viz.* H-Mordenite, H-Mordenite treated with TEOS, Na-Mordenite, silica-alumina and Rho.

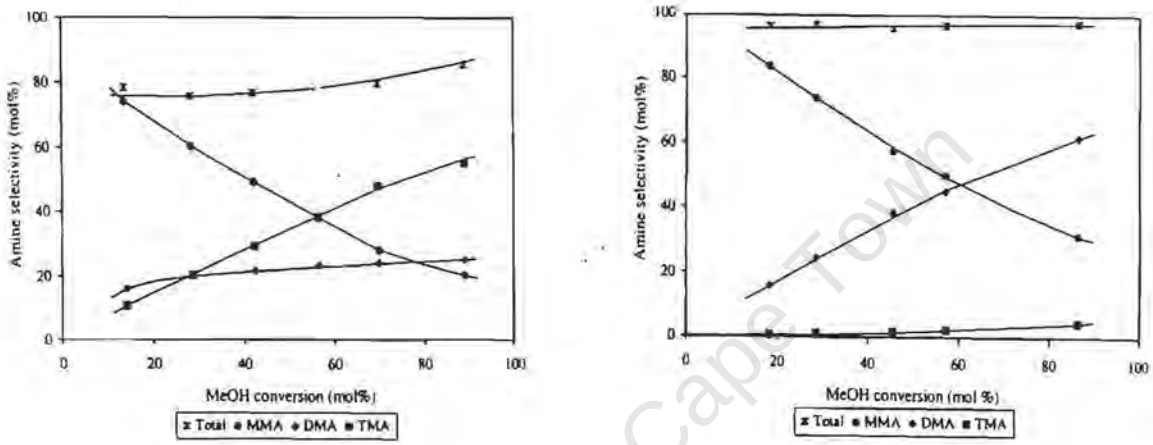

(a) (b)

Figure 1.10: Amine selectivity over H-Mordenite (a) and H-Mordenite treated with TEOS (b) as a function of methanol conversion

($P_{NH3,MeOH}$ = 5 kPa, T = 633 K, C/N = 1) [Gründling et. al., 1996]

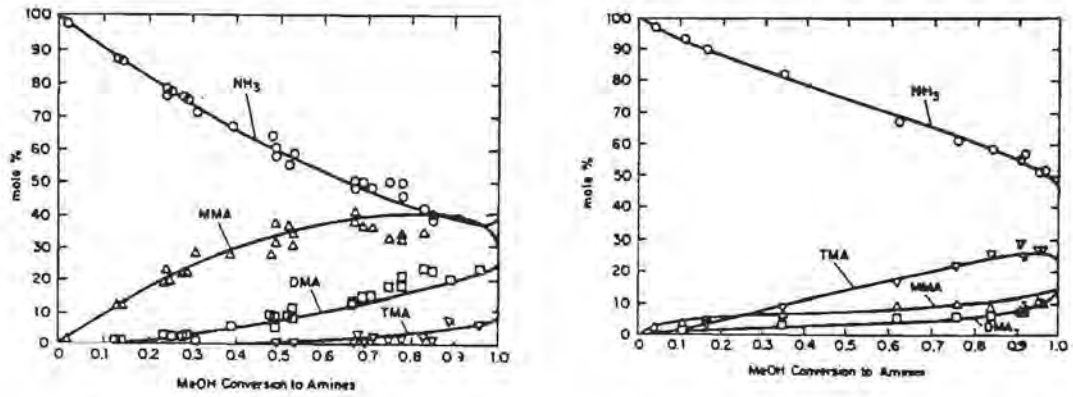

Figure 1.11: Distribution of N containing species over Na-Mordenite (a) and silica - alumina (b) as a function of methanol conversion

(methanol/ammonia=1, T and P_{tot} varied) [Weigert, 1987]

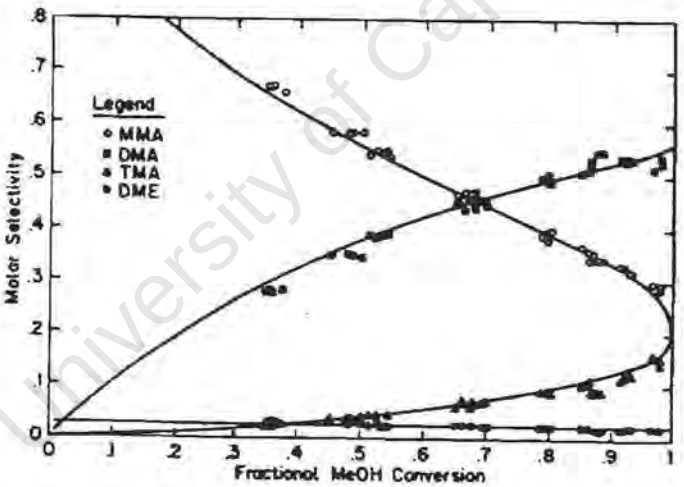

Figure 1.12: Molar selectivity vs. fractional methanol conversion over H-Rho

(methanol/ammonia = 1; temp varied from 250-400°C; P_{tot} = 1atm)

In all cases, as the conversion increases, so does the selectivity to the higher substituted amines as is typical for a series type of reaction. The TEOS treated Mordenite, for example, is highly selective to DMA and produces very little TMA. On the non shape-selective catalysts like silica-alumina, this gives very high TMA selectivities at high conversions.

1.5.4 Addition of Water

It was found that the addition of water to the feed stream over sodium Mordenite decreased the conversion to a greater extent than simple equilibrium could explain. This effect was attributed to competitive adsorption [Weigert, 1987], i.e., the water blocked some of the active sites on the catalyst, hence slowing the reaction. It was also seen that the addition of water changed the selectivity of the MMA disproportionation reaction over alumina. Not all zeolites were seen to be sensitive to the presence of water.

1.6. KINETICS AND THERMODYNAMICS

In order to be able to effectively manipulate any chemical process, it is essential to have a good understanding of the kinetics and thermodynamics of that process. This includes any thermodynamic constraints, the reaction mechanism as well as the overall rate equation. A list of all thermodynamic properties is given in Appendix I.

1.6.1 Thermodynamics of the Methanol Amination Reaction

Thermodynamically, trimethylamine is favoured over mono- and dimethylamine at temperatures less than 400°C. This is caused to a large extent by the fact that MMA and DMA can disproportionate readily to ammonia and TMA [Weigert, 1987; Stull, 1969]. The thermodynamically determined equilibrium distribution is very important as the difference between the compound distribution of the feed and the equilibrium compound distribution is the driving force behind the reaction. Figure 1.13 gives the equilibrium methylamine distribution as a function of temperature.

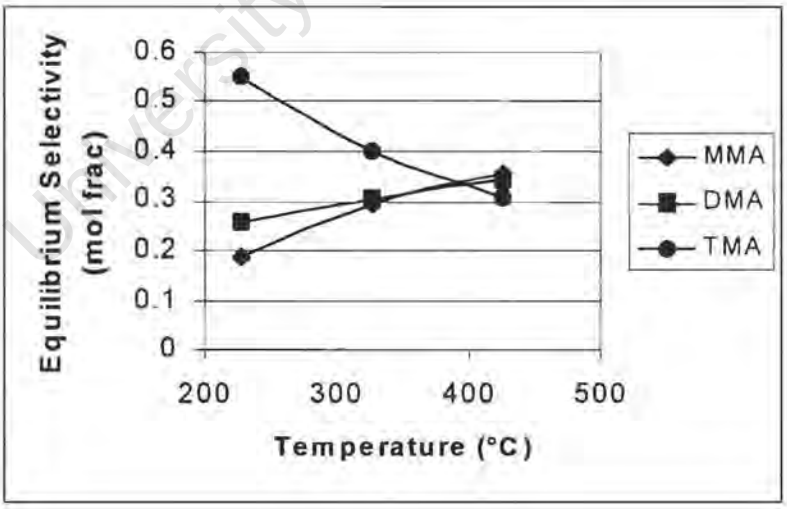

Figure 1.13: Equilibrium Methylamines Distribution

(Calculated using data from Stull *et al.*, [1969], N/C = 1

1.6.2 Reaction Mechanism

Some of the original theories on the mechanism of amination have proposed the adsorption of alcohol on the catalyst followed by the reaction of either ammonia or incompletely substituted amines with the adsorbed methanol. Other theories have proposed dehydrogenation or dehydration of methanol. It has become generally accepted however that the mechanism involves the direct substitution of the hydroxyl group on the methanol with the amino group [Klyuev and Khidekel, 1980]. This can alternatively be viewed as the substitution of one of the hydrogen atoms of the ammonia with the methyl group from the methanol. The exact mechanism however, is highly dependent on the type of catalyst. This is even true of different acidic catalysts.

Many of the earlier proposals assume a six or seven step bimolecular reaction model such as the following:

				$\Delta G°$ [kcal/gmol]
1)	NH_3 + MeOH	$\Leftrightarrow$	MMA + H_2O	-4.13
2)	MMA + MeOH	$\Leftrightarrow$	DMA + H_2O	-7.24
3)	DMA + MeOH	$\Leftrightarrow$	TMA + H_2O	-8.39
4)	2 MMA	$\Leftrightarrow$	DMA + NH_3	-3.11
5)	2 DMA	$\Leftrightarrow$	TMA + MMA	-1.15
6)	MMA + DMA	$\Leftrightarrow$	TMA + NH_3	-
7)	2 MeOH	$\Leftrightarrow$	DME + H_2O	-3.95

[Weigert, 1987, $\Delta G°$ values: Lange, 1979 cited in Keane *et al.*, 1987]

Dingerdissen *et al.* [1991] used a similar mechanism to that shown above. They performed a fairly detailed kinetic analysis. In their analysis however they assumed that the disproportionation reactions were negligible at 60 % methanol conversion, which has subsequently been shown to be incorrect due to the high rate of disproportionation of the amines [Chen *et al.*, 1994]. It was also assumed that diffusion was negligible. What was correct in their analysis however, was that the reaction was between adsorbed ammonia or amines and gas phase methanol.

Recently, there have been a number of proposals made as to the exact mechanism by which the methylamines are formed. These are mostly based on the experimental findings of the authors concerned.

Both Ilao *et al.* [1996] and Kogelbauer *et al.* [1994] have stated that the mechanisms for alkali and protonic catalysts are different. Over Na-Mordenite, the reaction takes place between adsorbed methanol and gas phase ammonia while on H-Mordenite the reaction is between adsorbed ammonia and gas phase methanol. As the protonic form of the catalysts generally show Brønsted acidity and the Na form Lewis acidity, this means that the mechanisms over Brønsted and Lewis acid sites are different. Ilao [1996] has conversely proposed a mechanism in which reaction occurs between adsorbed methanol and adsorbed ammonia.

Chen *et al.* [1994b] stated that ammonia is the preferred adsorbent on Brønsted acidic catalysts. This is seen by the strong decrease in DME production with increasing NH_3 partial pressure. They proposed that the overall reaction mechanism involved the reaction of two species on different strength sites as well as series reactions. They also proposed that the weaker sites were needed to facilitate the desorption of the amines. They stated that if methanol is adsorbed onto the catalyst first it attaches to the less strong sites as evidenced by ammonia adsorption. The methoxy species alone form DME and water in the presence of Methanol.

It has however been shown that the nitrogen containing bases, such as NH_3 and amines, adsorbed more strongly than the methoxy species, formed by the adsorption of methanol and DME. This suggests that methoxy species are not involved in the formation of the amines and would therefore imply that the reaction takes place by adsorbed amines or ammonia reacting with gaseous or weakly adsorbed methanol or DME. It has been seen that disproportionation of the amines also takes place [Weigert, 1988; Chen *et al.*, 1994a].

Gründling *et al* [1996b; 1997a]. have proposed the following reaction mechanism for the formation of methylamines over acid catalysts:

1. Ammonia adsorbs onto the surface
2. Methanol "hydrogen-bonds" to the adsorbed ammonia via an NH group forming the reactive precursor

3. Proton transfer and water release occurs simultaneously, forming the methylamine. This occurs progressively until all four H-atoms have been exchanged for methyl groups, forming the tetramethylammonium ion. A distribution of surface methyl ammonium species is observed.
4. The formation of these surface molecules is not rate controlling. Rather, it is the release of these molecules into the gas phase that controls the rate. This release can occur in one of two ways.
   A: The amine is replaced by NH_3 - adsorption assisted desorption.
   B: Reaction of gas phase ammonia or amine with adsorbed species (methyl group scavenging)

In the above mechanism, gaseous MMA and DMA are formed by either desorption or scavenging but gaseous TMA is only formed by the scavenging route [Gründling *et al.*, 1997a].

1.6.3 Experimentally Determined Kinetics

A number of studies have been performed on the effect of various reaction parameters on the rate of formation of the methylamines. These parameters include the effect of ammonia and methanol partial pressure and the acid site concentration of the catalyst.

Over a number of catalysts, *viz.* Y, Mordenite, ZSM-5 and amorphous silica alumina, Chen *et al.* [1994b] found that the rate of formation of the amines was first order with respect to ammonia over a wide range of temperatures. The rate of formation of amines was greater than 0 order with respect to methanol over H-Mordenite and silica-alumina at very low partial pressures of methanol. The rate with respect to methanol however, rapidly became 0 order at even moderately high partial pressures. Over the other catalysts they found an initial slightly negative order with respect to methanol but this also became 0 order at higher methanol partial pressures. Over the Na-exchanged catalysts, the methanol concentration did not affect the reaction rate but did effect the selectivity [Kogelbauer *et al.*, 1994]. Over Brønsted acid catalysts, the reaction rate was found to be directly proportional to the acid site concentration [Kogelbauer *et al.*, 1994].

Chen *et al.* [1994b] also found that when MMA and DMA are fed to any of the zeolites that they disproportionate very rapidly. The rate of MMA disproportionation, that is the reaction of 2 MMA molecules to form DMA and ammonia, is an order of magnitude higher than the rate of reaction of MMA with methanol to form DMA. Also, the rate of DMA disproportionation is twice that of MMA disproportionation. Mitchell *et al.* [1994] have derived empirical rate equations for the amine disproportionation reactions over amorphous silica-alumina.

If one wants to determine the kinetic rate equation for any catalytic reaction then it is important that all diffusion and adsorption/desorption effects are eliminated. For example, Weigert [1987] has shown that over Na-Mordenite, at greater than atmospheric pressure, the overall reaction order is 0 and that adsorption and desorption control the kinetics. If however only an empirical rate equation is desired, for operational purposes, then this is less important.

Although the formation of DME does not involve ammonia, the DME formation is strongly inhibited by increasing ammonia partial pressure due to the preferential adsorption of ammonia onto the catalyst surface [Kogelbauer *et al.*, 1994,1996]. Even over the alkali exchanged catalysts, the ammonia will adsorb competitively with the methanol although the preference of the surface for ammonia is not as marked over the alkali-exchanged catalysts. The rate of DME production has been observed to be 1st order with respect to methanol over all catalysts tested [Chen *et al.*, 1994b].

1.6.4 Experimentally Determined Reaction Mechanism

As stated above, Chen *et al.* [1994b] found that MMA and DMA disproportionate over the acid catalysts. Similarly, Ilao *et al.* [1996] has found, over both Mordenite and Chabazite, that if the methylamines are adsorbed alone onto the catalyst surface disproportionation reactions take place. As the rate of disproportionation is so great, this must certainly be included in the overall reaction mechanism as they can occur in parallel to the series forward reactions. On co-feeding MeOH with DMA, there was less MMA formed, due to the series reaction of MMA to DMA [Chen *et al.*, 1994b].

The formation of DME is reversible. This is known as it has been found that, when DME is co-fed with ammonia, methanol and amines are observed in the product stream [Chen *et al.*, 1994b]. Also, DME may react with a surface ammonia/amine with the release of methanol.

Gründling *et al.* [1996b] have shown with IR spectroscopy that when the reactants are initially introduced to the catalyst, ammonia adsorption takes place very quickly followed by reaction of the adsorbed ammonia with methanol to form all the adsorbed amines up to the tetramethylammonium ion. All the surface methylammonium species were detected with IR. They also confirmed the absence of adsorbed methanol at the surface. It was seen that, especially for the catalyst treated with TEOS, the concentration of amines in the gas phase was very different to that at the surface [Gründling *et al.*, 1996a; 1997]. Ernst and Pfeifer [1992] had previously shown the presence of the tetramethylammonium ion in the reaction of methanol and ammonia over Na- and H- Mordenite using ^{13}C MAS NMR.

Zhang *et al.* [1994] has proposed that it is only the moderate strength Brønsted acid sites that are responsible for the amination reaction. In general, however, it has been found that increasing acid strength of the catalysts leads to an increase in activity.

In line with the mechanisms proposed in Chapter 1.6.2 there is considerable evidence that the mechanism of this reaction is very different over H- and alkali-exchanged forms of the catalysts. It has been seen that over the alkali-exchanged catalysts the methanol and ammonia are both bound to the cation via the O or N atom. It has also been observed that more methanol than ammonia is bound to the surface when the gas phase concentrations are equivalent. As the Al content of the catalyst increases, so does the lateral interaction between adsorbed molecules. Over Brønsted sites, the amount of ammonia adsorbed is very much higher than that of methanol and this therefore effectively excludes the methanol from the catalyst surface [Kogelbauer *et al.*, 1994; 1996]. Vega and Luz [1988] found that methylamines adsorb preferentially onto the Brønsted acid sites of the catalyst. Weigert [1987] found over Na-Mordenite that the order of the reaction with respect to methanol was zero, indicating a saturated surface. It was also shown that Ba-Mordenite gave more DMA than the acidic form, i.e., it behaved in a similar manner to the Na-Mordenite.

It has been found that in a batch system that the order of introduction of methanol and ammonia is not relevant, because of the local adsorption/desorption equilibrium. [Kogelbauer *et al.*, 1996]

Teunissen *et al.* [1992] found that the H atom of the framework was transferred completely to the ammonia molecule. At low temperatures, the ammonia cation is located near to the Al tetrahedron of the framework. The cation is bonded to the surface via two or three hydrogen bonds.

1.6.5 Reaction Mechanism over Brønsted Acid Catalysts

Taking all of the above theories and proofs into account, it would appear that the mechanism proposed by Gründling *et al.* [1996b] is the closest to the real reaction mechanism over Brønsted acid catalysts. This mechanism accounts for the reaction of adsorbed ammonia or incompletely substituted amines with gas phase methanol. The scavenging mechanism also accounts for the very high rates of disproportionation seen in this system. Figure 1.14 illustrates the reaction mechanism proposed by Gründling *et al.*

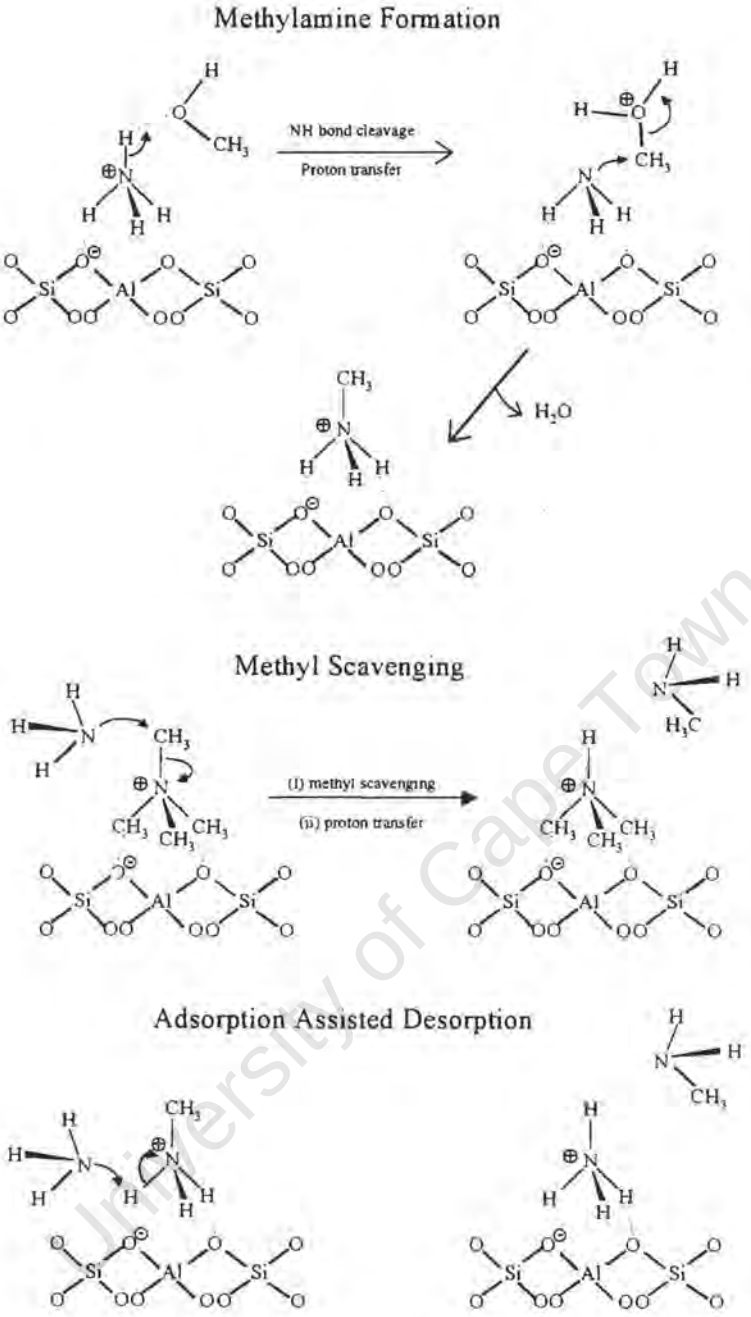

Figure 1.14: Mechanism of Methylamine Formation over Brønsted acid catalysts.

[Copied from Gründling *et al.*, 1997b].

1.7 OBJECTIVES OF RESEARCH

There are a number of questions that arise from the review of the literature as seen in the previous sections of this chapter. One of the first questions posed was of which of the catalysts proposed was the most suitable for the production of methylamines such that the product distribution obtained most closely resembles that of the market demand while maintaining a high activity. From the review of the literature it would seem that the two catalysts most likely to meet these requirements are Rho and Mordenite. It is therefore these catalysts that have been studied in this work. In the initial studies, amorphous silica-alumina was also examined to give a base case against which to compare the two zeolites.

What was also seen in the literature review was that most catalysts require some form of post synthesis modification in order to gain the better performance in terms of selectivity and activity for the methanol amination reaction. While much research has been performed on various types of post synthesis treatment, few systematic time studies of hydrothermal treatment had been performed over Rho, in particular. The second objective of this work was therefore to examine the effect of the duration of hydrothermal treatment on the zeolites, Rho and Mordenite.

The final objective of this work was to attempt to establish a number of links between the different changes caused to the zeolites by the hydrothermal treatment and the changes in the reaction behaviour.

The results shown in this work are then briefly presented as follows. Firstly an initial comparison of the catalysts at different conditions is presented. Included in this is an analysis of the effect of repeated calcination of the catalysts. Secondly, a systematic study of the effect of hydrothermal treatment on the reaction behaviour of the catalysts was performed, along with an investigation of the change in acidity and catalytic structure caused by such treatment. Finally, an in-depth study on the changing adsorption behaviour of catalysts as a function of steaming time was performed.

Experimental Procedure

2. EXPERIMENTAL PROCEDURE

2.1 CATALYSTS

The catalysts used in this project were obtained from either commercial catalyst suppliers or other research groups. The results of the characterisation of the parent catalysts will be shown in chapter 3.1. The details of the characterisation procedures are given in chapter 2.3.

2.1.1 Rho

Two samples of zeolite Rho were obtained from E.I. du Pont de Nemours as powders in the Na/Cs form with a unit cell composition of $Na_7Cs_{3.8}Al_{11}Si_{37}O_{96}$. The parent catalyst therefore had a Si/Al ratio of 3.4.

2.1.2 Mordenite

The Mordenite used in the experiments of this study was a small pore, synthetic Mordenite obtained as a powder from Süd-Chemie in the ammonium form with essentially no residual Na ions. It was determined to have a silica/alumina ratio of approximately 10 using atomic absorption spectroscopy. The Mordenite shown for comparative purposes in the SEM's in section 3.1.2 was synthesised in our Laboratory. This Catalyst was not used for any of the reaction/ adsorption studies.

2.1.3 Silica-Alumina

The amorphous silica-alumina was obtained as 4mm spheres from Kali-Chemie AG, Hanover, Germany. It contained 9 wt% Alumina. The beads were crushed to sub 200 μm particles for reaction purposes.

2.2 POST-SYNTHESIS MODIFICATION TECHNIQUES

2.2.1 Ion Exchange

Zeolite Rho was obtained in the Na/Cs form and therefore needed to be ion-exchanged to the ammonium (NH_4^+) form according to the method given by Bergna *et al.*[1989] and Fischer *et al.* [1989]. This was done by performing four cycles of ion exchange, each in 10 wt% aqueous ammonium nitrate at 90°C under reflux. After each ion exchange the catalyst was filtered under vacuum and fresh ammonium nitrate solution was used for the next ion exchange. After the exchange procedure, the catalyst was washed with de-ionised water by passing the water through the filter cake. The catalyst was then dried on a watch glass in an oven at 100 °C overnight. This ion-exchange procedure was chosen to exchange essentially all of the Na and most of the Cs with ammonium ions.

2.2.2 Calcination

The purpose of calcining the catalysts is twofold. Firstly, it is done to burn off any organics which might have been adsorbed onto the catalyst surface from the atmosphere as these can lead to the formation of coke precursors. Calcination is secondly performed to convert the catalyst from the ammonium form to the protonic form by driving off ammonia.

Two different calcination procedures were used. The first was used if the catalyst was to be used for reaction studies. For this procedure, the catalyst was slowly heated in 60 ml(NTP)/min air to 500 °C over a time period of 2 hrs. It was held at this temperature for 5 hrs before being cooled to reaction temperature. The second calcination procedure was used prior to hydrothermal treatment (see Section 2.2.3 below). Here, the catalyst was slowly heated to 450 °C over 1.5 hrs in 60 ml(NTP)/min air and held there for 2 hrs before being cooled. After calcination, the catalyst was flushed with 60ml (NTP)/min N_2 to remove any O_2 from the system.

2.2.3 Hydrothermal Treatment

Hydrothermal treatment was performed on the catalysts, in the protonic form, using the same apparatus on which the reaction work was carried out (see Chapter 2.4).

For zeolite Rho, steam, with a partial pressure of 30 kPa, was fed to the reactor (cf. Section 2.4.1.) from a water saturator using a nitrogen carrier gas of 60 ml(NTP)/min. The reactor containing 1g of the catalyst was kept at 450 °C and atmospheric pressure. The time of the steaming was varied from 0 to 21 hrs. The catalyst was both heated up and cooled in a flow of inert, N_2 gas. These mild steaming conditions were used as Rho has a moderately unstable framework, which can be damaged at temperatures above 600°C [Shannon *et al.*, 1988], as well as a relatively low Si/Al ratio of 3.4. It could therefore be easily dealuminated.

For Mordenite, which has a more stable framework and a higher Si/Al ratio, two steaming procedures were followed. The first was the same as that for Rho. This was done to obtain a comparison between the catalysts. More severe conditions were also used to gain a more significant change to the catalyst. For these cases, steam, with a partial pressure of 60 kPa at 500 °C, was fed to the reactor with a nitrogen or helium carrier gas of 60 ml (NTP)/min. The duration of the steaming was varied from 0 to 16 hours.

2.3 CATALYST CHARACTERISATION

The types of characterisation performed on the catalysts can be roughly divided into two categories. Firstly, structural analyses (including AA, XRD, FTIR, MAS NMR, BET and SEM) were used to elucidate the physical properties of the catalysts. Secondly, acidity analyses (Thermal Desorption and TGDTA) were performed to examine the strength and quantity of acid sites present on the catalyst.

2.3.1 Structural Analysis

2.3.1.1 Elemental Analysis

Bulk chemical analyses were performed using atomic absorption spectrometry to determine the Si, Al and Na content of the catalysts. Samples were prepared by digestion of the solid in hydrofluoric acid followed by dilution with boric acid and water. The samples were analysed using a Varian SpectrAA-30 spectrometer.

2.3.1.2 XRD (X-Ray Diffraction)

XRD was performed on the catalysts to determine the relative crystallinity and to confirm the structural type of the samples. These spectra were obtained with a Phillips X-ray diffractometer using Cu-Kα radiation (wavelength 1.54Å). The samples were scanned in the range $2\theta = 6°$ to 50°. In all cases the XRD was performed on the hydrated catalyst.

2.3.1.3 FTIR (Fourier Transform Infrared Spectrometry)

Infrared spectra of the catalyst samples were obtained using a Nicolet 5ZDX FTIR Spectrometer in the scanning range 4000 – 400 cm^{-1}. The catalyst samples were initially dried at 100°C and sealed into disks of KBr. These disks comprised 1 part catalyst to 10 parts KBr by weight.

2.3.1.4 ^{27}Al and ^{29}Si MAS NMR

^{27}Al and ^{29}Si MAS NMR were performed on the catalysts to determine the co-ordination state of the Al and the environment of the Si atoms in the catalyst structure. This was done using a Varian Unity 4000 spectrometer.

For the ^{27}Al spectra, a resonance frequency of 104.252 MHz and a spinning rate of approximately 10 kHz were used. The repetition time was 10s and the pulse length was adjusted to 8 μs. The samples were analysed in their hydrated form.

As the degree of hydration of especially Rho affects the crystal structure, this must in turn affect the MAS-NMR studies. 27Al MAS NMR has been used to determine the structural distortion of Rho [Parise *et al.*, 1984]. The NMR used here however is not refined enough to perform fine structural analysis.

2.3.1.5 BET Analysis

BET analysis was used to determine pore volume, pore radius distribution and surface area. These data were obtained using a Micrometrics ASAP 2000 instrument. The catalyst samples are initially dried *in-situ* at 350°C and evacuated. Nitrogen was then adsorbed stepwise until ambient pressure was reached. This needs to be carefully considered however as it does not distinguish between internal and external surface area [Abrams and Corbin, 1995].

2.3.1.6 Scanning Electron Microscopy (SEM)

SEM photographs of the catalyst samples were obtained with a Leica S440 scanning electron microscope.

2.3.1.7 Particle Size Analysis

Particle size distributions of the catalyst samples were obtained using a Malvern Mastersizer S.

2.3.2 Analysis of Acidity

2.3.2.1 Thermal Desorption

Thermal Desorption of ammonia from the catalyst surface was performed to determine the number and strength of acid sites present on the catalyst surface. The system on which the Thermal Desorption was carried out is shown in Figure 2.1. For these experiments, 0.25g of catalyst was loaded into a quartz reactor, which is placed into a furnace. The catalyst is either calcined using the normal calcination procedure (500°C for 5 hrs in 60ml/min synthetic air) or if it has been pre-treated with water then it is dried in 70 ml(NTP)/min flowing air at 200 °C. The catalyst is then flushed with He. 1% ammonia in helium was passed over the catalyst at 150 °C and the uptake of ammonia monitored using a TCD cell. The amount of ammonia adsorbed represents the sum of both physisorbed and chemisorbed ammonia.

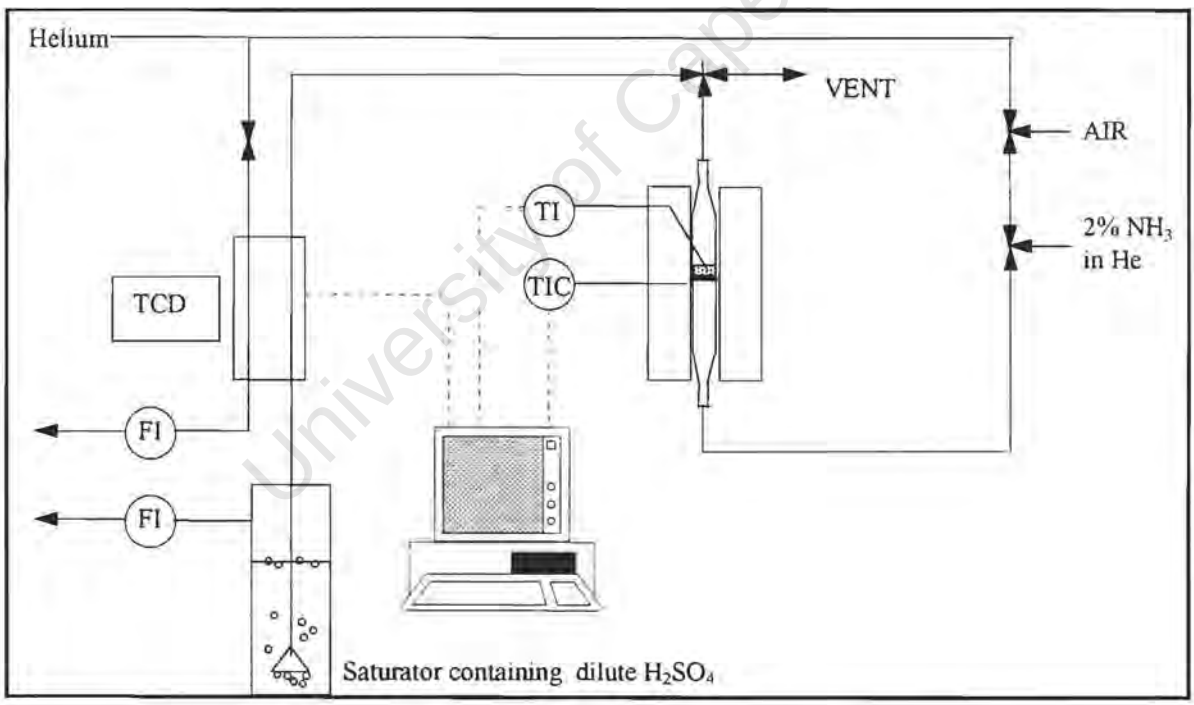

Figure 2.1: Temperature Programmed Desorption Rig

After the adsorption phase, the ammonia is switched off and the catalyst left under flowing helium at 150°C for 16 hours to remove all physisorbed ammonia. The furnace was then heated to 700 °C at 10 °C/min and held there for 1 hr. During this time, the ammonia

desorbing from the catalyst was continuously monitored using a thermal conductivity detector (TCD). The resulting spectra were deconvoluted using a Gaussian model to obtain the individual desorption peaks. While this type of deconvolution is only an estimate of the different peaks, with a fairly large error, it is a very useful tool to separate the individual peaks.

The gas exiting the catalyst was passed through a solution of sulphuric acid, which was made by diluting 20 ml of 1N H_2SO_4 with excess water. The NH_3 dissolved in this solution which was back titrated using 1N NaOH to determine the concentration of ammonia chemisorbed on the catalyst according to:

$$mmol\ NH_3 / gcat = \frac{(vol_{H_2SO_4} * conc_{H_2SO_4})_{initial} - vol_{NaOH} * conc_{NaOH}}{mass\ cat}$$

Theoretically, there should be one ammonia molecule chemisorbed on each acid site of the catalyst. Therefore, the concentration of ammonia found on the catalyst should correspond to the concentration of acid sites on that catalyst. Each aluminium atom in the framework of the catalyst should correspond to one acid site [Kijenski and Baiker, 1989; Martens *et al.*, 1997], although at very high aluminium concentrations the strength of each site becomes less [Kijenski and Baiker, 1989] such that there may be less acid sites detected than the number of aluminium atoms would indicate. The presence of extra-framework, octahedral aluminium within the catalyst may also result in there being fewer acid sites than aluminium atoms. The concentration of acid sites determined using the Thermal Desorption method should therefore be less than or approximately equal to the concentration of aluminium in the framework of the catalyst. Comparing these two results is an indication of the quality of the results obtained from the Thermal Desorption measurements.

2.3.2.2 TG-DTA

Thermogravimetric analyses of the catalyst samples were performed using a Stanton-Redcroft STA780 apparatus to determine a number of phenomena. Firstly, mass loss of the catalyst was determined by ramping the sample from 30 to 700 °C in flowing nitrogen. This analysis was used to monitor the mass loss due to the desorption of water and ammonia from the surface as well mass loss due to dehydroxylation of the catalyst structure at elevated temperatures (close to 700 °C).

Thermogravimetric analysis was also used to monitor mass gain upon adsorption of various molecules and hence to determine the adsorption isotherms.

2.4. REACTION OF METHANOL AND AMMONIA TO FORM METHYLAMINES

2.4.1 Reaction Apparatus

Figure 2.2 shows the flow scheme of the rig used for both reaction and steaming work. Methanol and/or water are fed to the reactor from saturators using nitrogen or helium as a carrier gas. The flows to the saturators are controlled using Brooks 5850 TR Series mass flow controllers. The ammonia is fed as 10 mol% ammonia in nitrogen mixture. Either of the saturators could be bypassed to allow pure nitrogen or synthetic air to flow to the reactor.

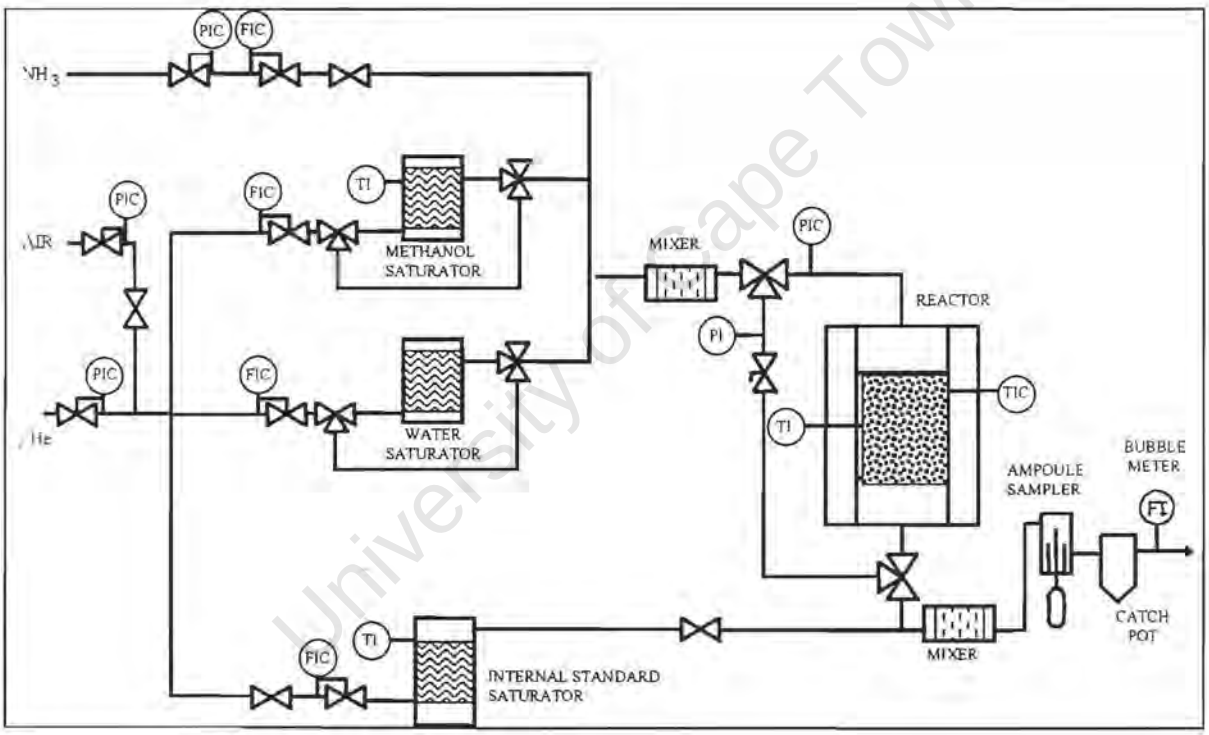

Figure 2.2: Flow sheet of experimental apparatus

The reactor, shown in Figure 2.3, was made from glass. It consists of an outer, preheat zone and an inner tube in which a frit is placed to support the catalyst. The inner tube had an internal diameter of 10mm. This size of inner tube means that very small catalyst samples may be used without getting channelling effects. The inner tube could also be adjusted in height such that the tip of the thermowell always rested at the top of the catalyst bed.

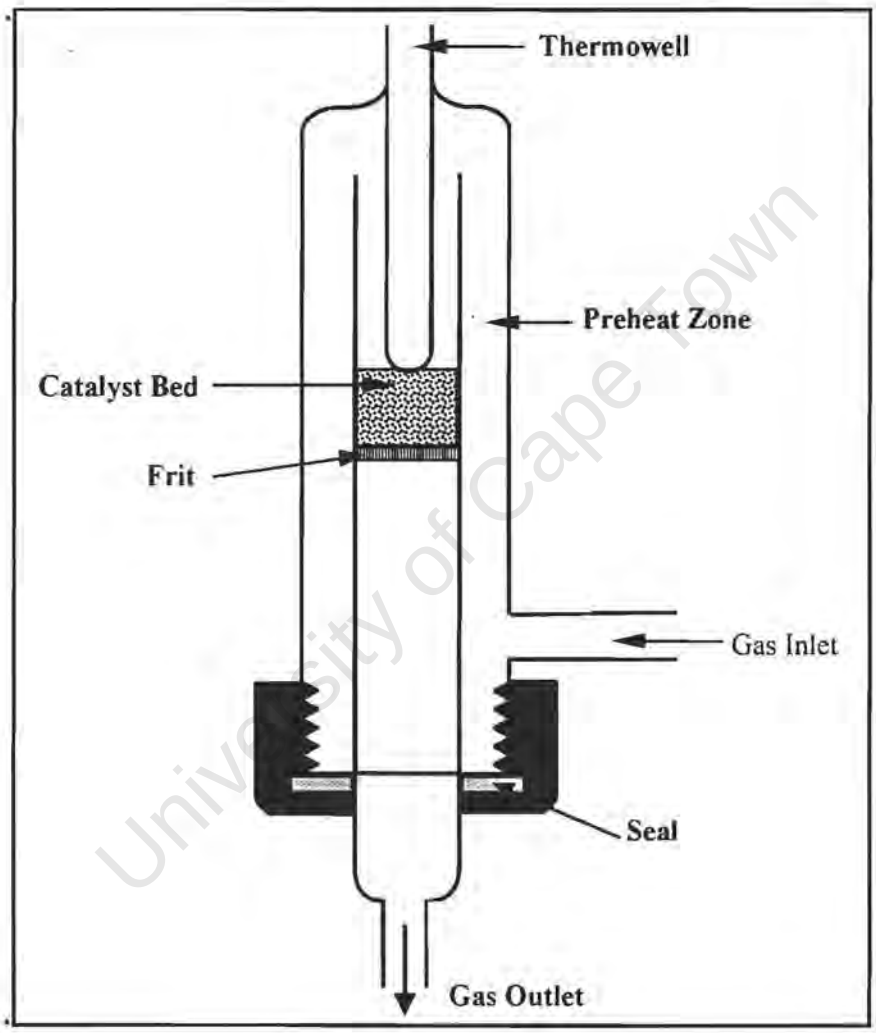

Figure 2.3: Reactor used for methanol amination reactions

n-Hexane, which is used as an internal standard is fed from a saturator and mixed with the reactor product. This mixture is then passed through the ampoule sampling system [Schulz *et al.*, 1984], shown in figure 2.4. The exhaust gas was then passed through a catch pot filled with dilute H_2SO_4 to remove the amines and ammonia from the vent gas.

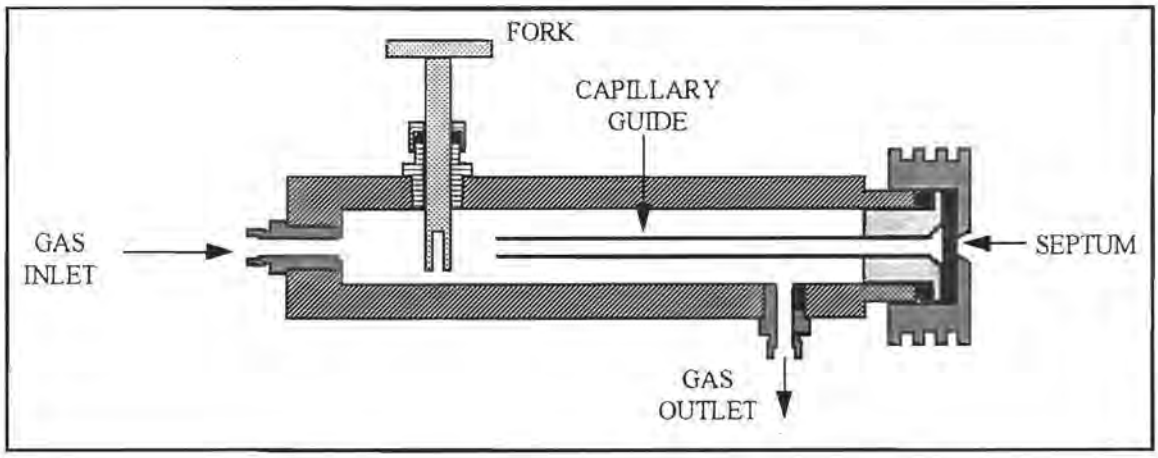

Figure 2.4: Ampoule Sampling System

[Adapted from: Schulz *et al.*, 1984]

2.4.2 Experimental Procedure

For the methanol amination reaction studies, 0.15g of catalyst in powder form were diluted with 1.5g of inert quartz sand ($d_p \approx 0.2$mm). The catalyst samples were first thoroughly dried in 60 ml(NTP)/min inert gas (either nitrogen or helium) at 100 °C for 2 hours prior to reaction. The reactor was then heated to the reaction temperature of 325°C at 5°C/min, still under flowing inert gas. The reaction was carried out by feeding an equimolar mixture of methanol and ammonia, diluted in nitrogen, to the reactor ($p_{MeOH} = p_{NH3} = 8$ kPa; balance N_2; WHSV = 4 g/ g_{cat} /hr).

Mass and carbon balances of the system were performed by adding a constant flow of an n-hexane/ nitrogen mixture to the reactor effluent. Samples were taken using the ampoule technique [Schulz *et al.*, 1984] and analysed using a GC equipped with an FID. The separation of the compounds was achieved using a 4x3 mm I.D. glass column packed with 60/80 mesh Carbopack B/ 4% Carbowax 20M/ 0.8% KOH. Appendix II shows extra information pertaining to the operation of GC including typical GC spectra, response factor determination, sample carbon balance and yield calculations and detector operating conditions.

2.5 ADSORPTION STUDIES

2.5.1 Experimental Procedure

The temperature at which the adsorption experiments were performed was carefully chosen to be as low as possible, so as to, as far as possible, ensure that there would be no reaction between especially the methanol and ammonia during the binary adsorption studies. At the same time it was thought advisable to keep the temperature such that all the compounds were at or above their boiling points. Hence, the temperature was chosen to be 100°C, the boiling point of water.

The adsorption studies were performed in a fixed bed, down-flow reactor (see Figure 2.2). For these studies, a constant helium flow of 130 ml (NTP)/min was passed over a 0.25g sample of the catalyst. The reactor was stabilised at 100 °C prior to the adsorption measurements with pure helium flowing over the catalyst sample. The adsorbates were then switched on instantaneously. Small amounts of the pure compounds (methanol, ammonia and water) or binary mixtures of these were added to the helium flow (130 ml(NTP)/min). The total flow rate thus remained essentially constant. The flow rates of the adsorbate gases used were 0.036 mmol/min (NTP) ammonia (p_{NH3} = 0.6 kPa), 0.124 mmol/min methanol (p_{MeOH} = 2 kPa) and 0.170 mmol/min water (p_{H2O} = 2.5 kPa). The methanol and water flows were obtained by passing a portion of the total He flow through temperature controlled saturators to gain the desired equilibrium partial pressure of these compounds. The ammonia was fed from a pre-mixed gas cylinder. The composition of the effluent gas was analysed continuously using a TCD and an FID in series, taking samples every 3 seconds. The FID only analysed the hydrocarbon (methanol) while the TCD analysed the complete adsorbate flow. The two signals were logged simultaneously and in this manner, the breakthrough curves for the hydrocarbon and total adsorbate mixture were obtained. The non-hydrocarbon breakthrough curve was obtained by subtracting the weighted hydrocarbon breakthrough curve from the total. From the adsorption breakthrough curves, the total amount adsorbed of each compound could be obtained [Berke *et al.*, 1991; Weitkamp *et al.*, 1993].

The method of determining the total, chemisorbed and physisorbed amounts of each adsorbate are illustrated below in Figures 2.5 and 2.6. The total amount adsorbed is determined by integrating the difference between the relative response curves for the empty reactor and the reactor containing the catalyst sample, as shown in Figure 2.5. The amount

total amount adsorbed is then obtained by multiplying this integral which has the units of s^{-1} by the feed rate in $mmol/g_{cat}.s$. The physisorbed amounts of each component were obtained from the difference between the desorption breakthrough curves for the empty reactor and the reactor containing the catalyst sample, as shown in figure 2.6. The chemisorbed amounts were then calculated from the difference between the total amount adsorbed and the amount physisorbed. This method of determination of the chemisorbed amount is not as accurate as the Thermal Desorption method but it does allow for speedy analysis of binary adsorption systems.

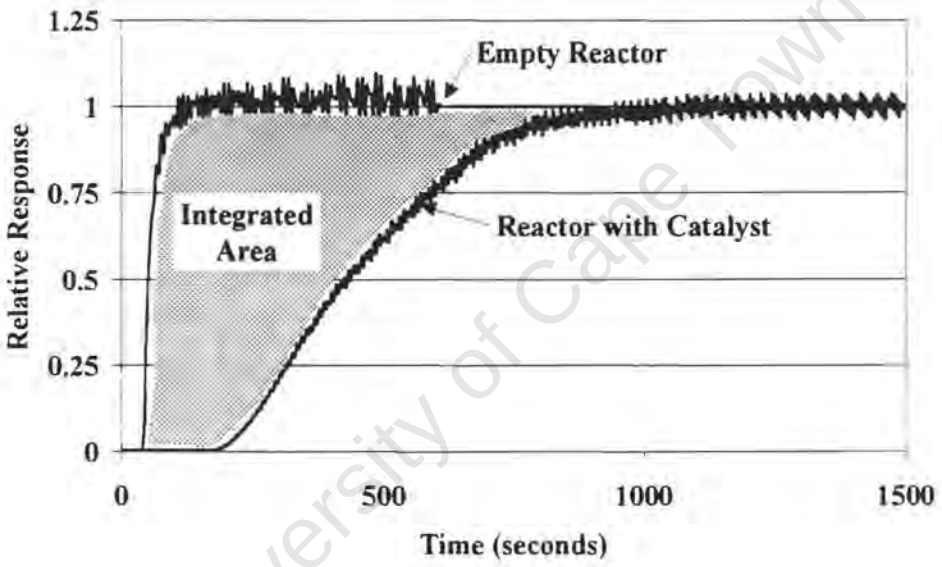

Figure 2.5: Determination of total adsorption capacity

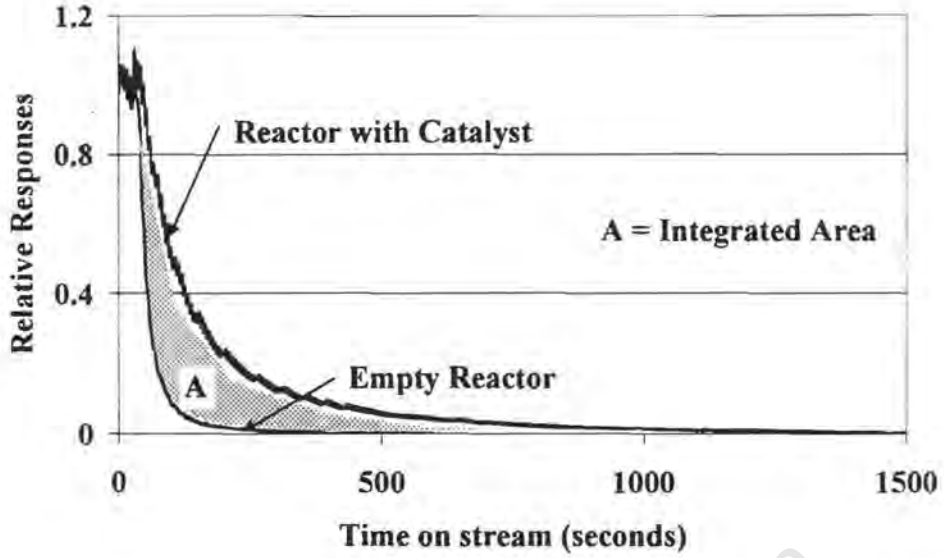

Figure 2.6: Determination of Physisorbed Amount

2.5.2 Thermal Conductivity Analysis

In the adsorption studies, it had first to be determined what degree of dilution was necessary such that the response of the thermal conductivity detector for all the compounds investigated was linear. The signal obtained from a thermal conductivity is a function of the difference in thermal conductivity between a reference gas and the mixture of interest. The following equation gives this relation.

$$S = Ki^2R\left(\frac{\lambda_R - \lambda_M}{\lambda_R}\right)(T_F - T_B) \qquad \text{[McNair and Bonelli, 1968]}$$

Where

S	=	TCD Signal
K	=	Cell constant
i	=	current through the filament
R	=	Resistance of filament
λ_R	=	thermal conductivity of reference
λ_M	=	thermal conductivity of mixture
T_F	=	temperature of filament
T_B	=	temperature of block

As all the physical parameters of the block are kept constant for the experiments, i.e., T_B, T_F, K, i and R, the equation can be simplified as follows:

$$S = C\left(\frac{\lambda_R - \lambda_M}{\lambda_R}\right) \qquad \text{where } C = Ki^2R(T_F - T_B)$$

The thermal conductivity for pure gases can be gained from standard tables or equations and the thermal conductivity of the mixture is determined using the equation

$$\lambda_M = \sum_{i=1}^{n} \frac{y_i \lambda_i}{\sum_j y_j A_{ij}} \qquad \text{[Perry } et\ al.\text{, 1984]}$$

where n is the number of compounds, y_i the mole fraction of each compound and A_{ij} the interaction parameter between the compounds. This can be determined from the equation

$$A_{ij} = \frac{\left[1 + \left(\frac{g_i}{g_j}\right)^{1/2}\left(\frac{M_i}{M_j}\right)^{1/4}\right]^2}{\left[8\left(1 + \frac{M_i}{M_j}\right)\right]^{1/2}}$$ [Perry *et al.*, 1984]

and $$\frac{g_i}{g_j} = \frac{\Gamma_j}{\Gamma_i}\left[\frac{\exp(0.0464\,T_n) - \exp(-0.2412\,T_n)}{\exp(0.0464\,T_q) - \exp(-0.2412\,T_q)}\right]$$

where $$\Gamma = T_c^{1/6} M^{1/2} P_c^{-2/3}$$

The response of the thermal conductivity detector as a function of the percentage dilution can then be calculated as shown in Figure 2.7. As can be seen, it is only at high dilutions ([He] > 95%), that the signal response is linear with respect to concentration. The result of this analysis was that the total concentration of adsorbates in the analysis steam should not exceed 5% of the total stream volume.

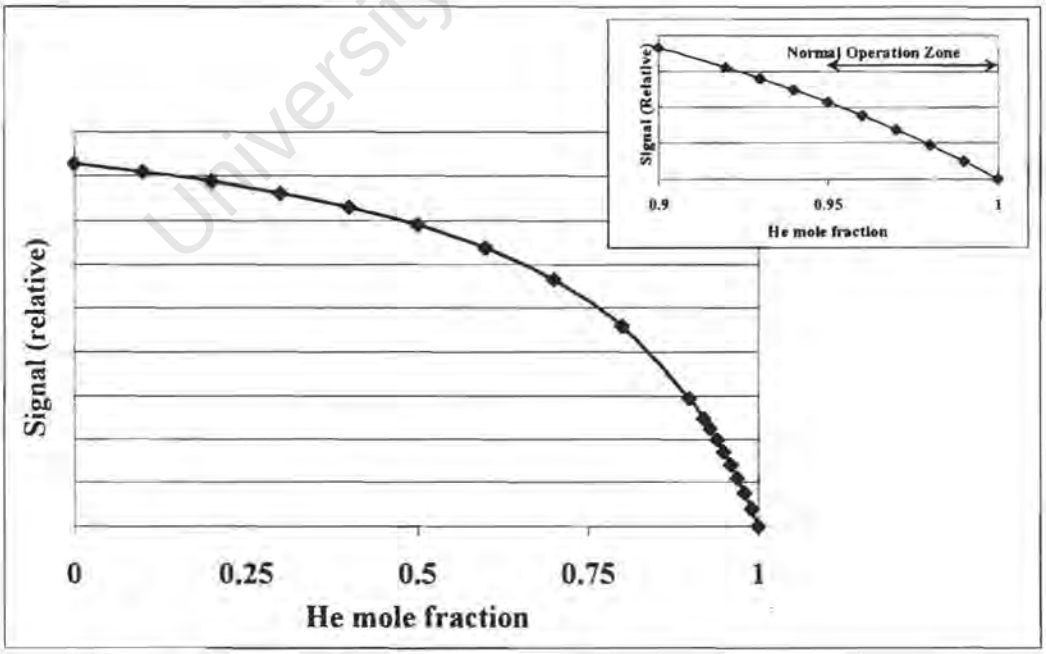

Figure 2.7: Effect of dilution on TCD signal response

(Helium fraction as shown, balance 50/50 mixture of water and methanol)

Initial Studies

3. INITIAL STUDIES

Samples of zeolite Rho, Mordenite and amorphous silica-alumina were characterised and compared for their activity in the methanol amination reaction. This section details the initial characterisation of the parent catalysts used in this study. It also shows the initial reaction studies performed over these catalysts. Furthermore, the effect of catalyst regeneration was investigated to elucidate whether for each experiment fresh zeolite should be taken or whether the catalyst could be regenerated without leading to a change in activity or selectivity.

3.1 CATALYST CHARACTERISATION

3.1.1 Rho

Figures 3.1 and 3.2 show the XRD patterns of the two samples of Rho, which have been used in these studies. In these figures, the major peaks of each species are indicated. The standard XRD spectra for Rho and the impurity phases are given in appendix III. As can be seen, sample B is more crystalline and contains fewer impurities than sample A, although there is still some Chabazite and Analcime within sample B. Even sample A however contains primarily Rho with a smaller percentage of impurities. The XRD spectra show that the major impurities in especially Rho (A) are primarily Analcime (Pollucite) and some Chabazite.

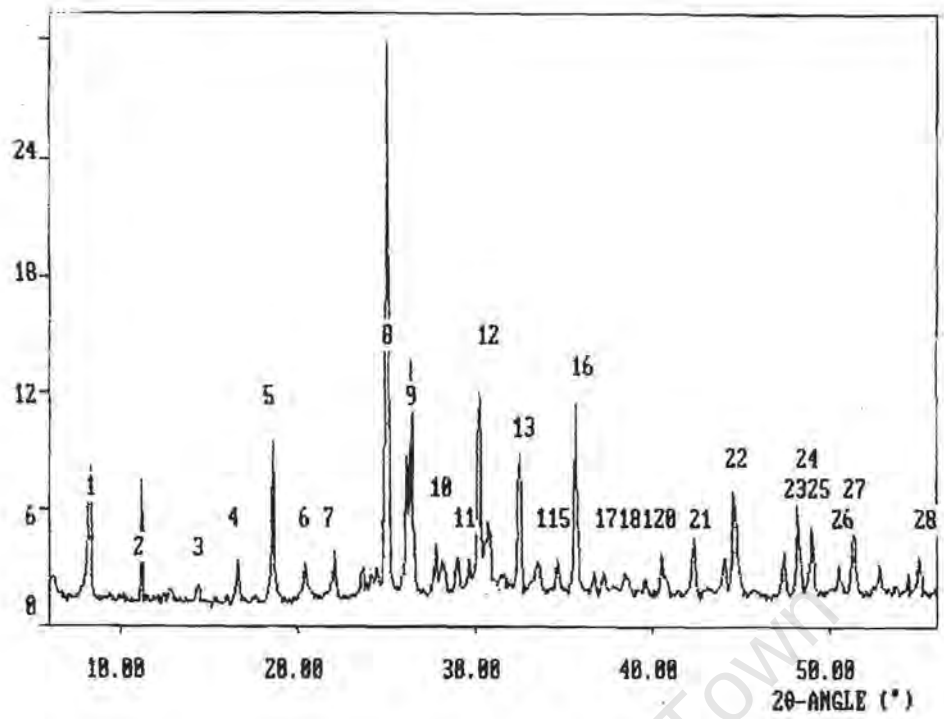

Figure 3.1: XRD patterns of zeolite Na,Cs-Rho (A)

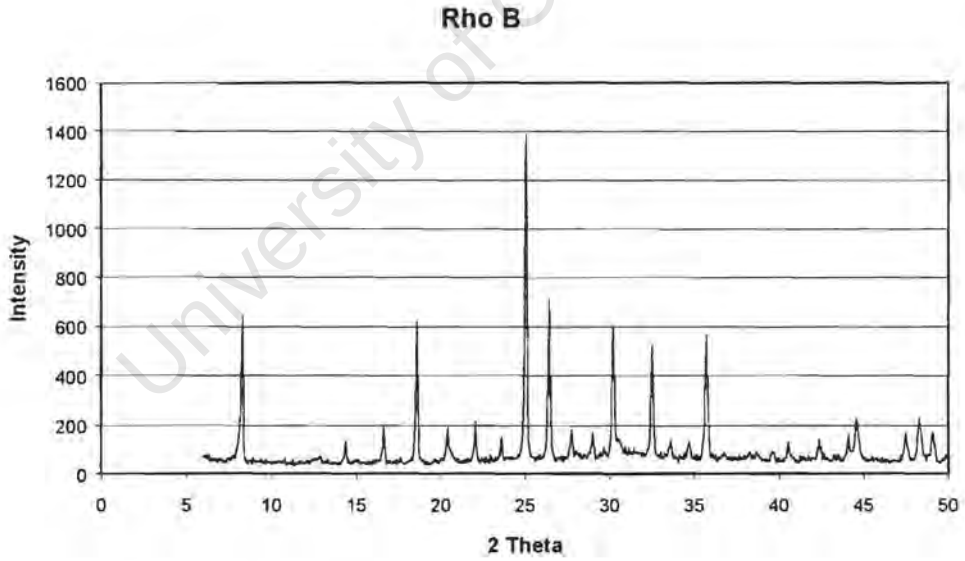

Figure 3.2: XRD Pattern of zeolite Na,Cs-Rho B

Figure 3.3 shows the SEM photographs of both the unsteamed samples of zeolite Rho. It can be seen that both samples appear visually to have a homogeneous phase distribution. In both cases however, the catalyst particles consist of agglomerates made up of much smaller

crystallites. The mean size of the crystallites is approximately 0.5 μm. There is not much variation in the crystallite size and all are rhombohedral in shape. These crystallites in turn form agglomerates of >30 μm. The shape of the agglomerates is more irregular.

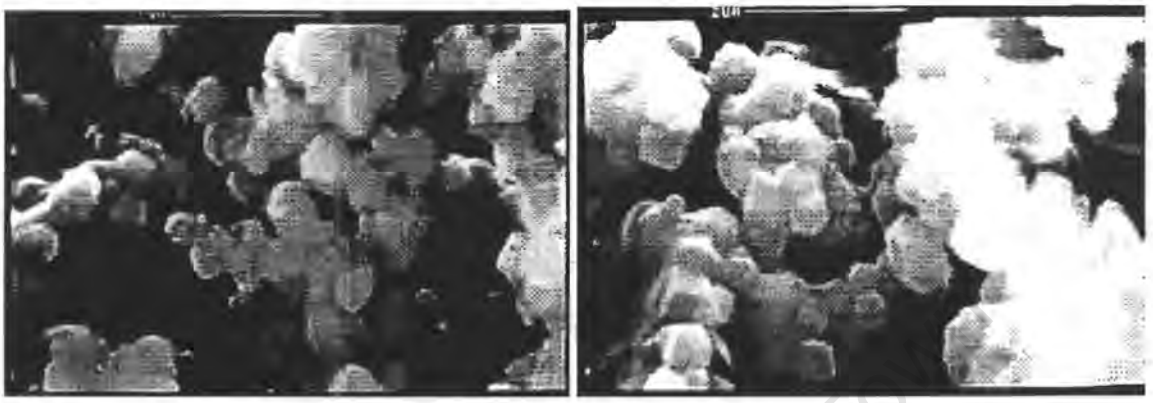

(a) **(b)**

Figure 3.3: SEM photographs of Rho A (a) and Rho B (b)
(white line represents 2μm)

Figure 3.4 gives the ammonia Thermal Desorption spectrum of the ion-exchanged and calcined but unsteamed samples of Rho (A) and (B). These spectra were deconvoluted into three peaks (shown in Appendix IV). It was determined however, using both repeated Thermal Desorption runs and TGDTA that the highest temperature peak, *viz.* 650°C, was caused by dehydroxylation of the catalyst surface and hence not by ammonia desorption. The Thermal Desorption spectra of the two samples were similar but showed some differences. Firstly, Rho (A) had slightly more acid sites than Rho (B). Secondly, the Rho (B) showed less dehydroxylation than Rho (A).

It was determined from the Thermal Desorption spectra that the concentration of the acid sites on the two catalysts were 1.77 mmol/g_{cat} for Rho (A) and 1.59 mmol/ g_{cat} for Rho (B).

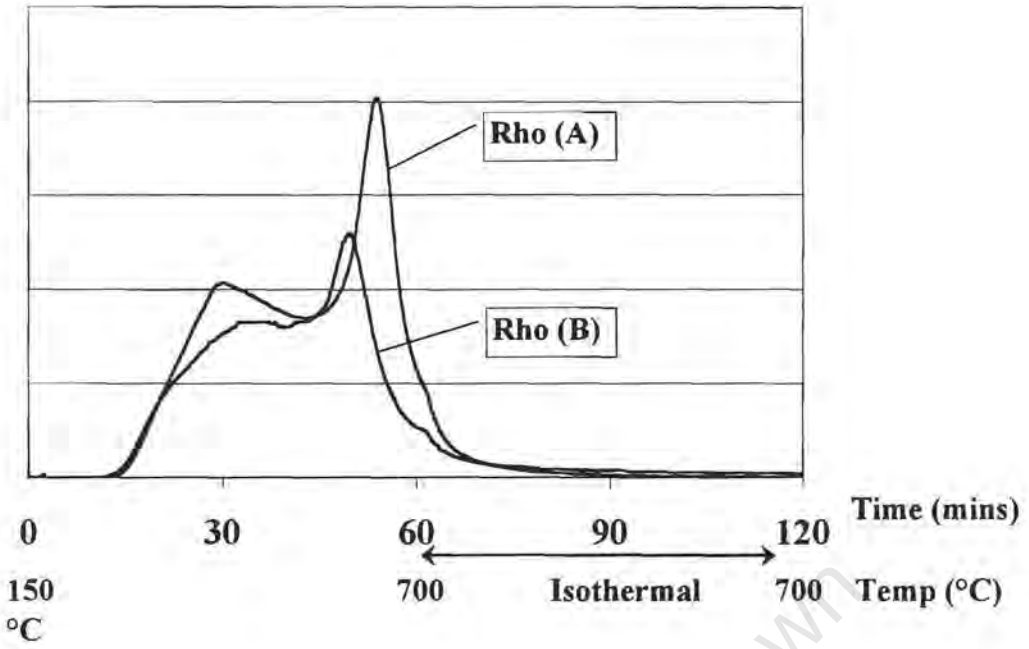

Figure 3.4: Thermal Desorption Spectrum of Rho

(T_{ads}=150°C, heating rate = 9°C/min, t_{ads}=1hr, T_{flush}=150°C, t_{flush}=16hrs, gas flow = 70ml(NTP)/min He)

It was determined using BET measurements that Rho (B), in the ammonium form had a pore volume of 0.24 cm^3/g, of which 0.19 cm^3/g was contained in the micropores of the catalyst.

Infra-red spectra of the calcined and uncalcined samples of Rho were taken (see Appendix III) to determine whether or not the ammonia was removed by the calcination procedure. It was seen that the peak at 1400 cm^{-1}, which is indicative of adsorbed ammonia, was present in the uncalcined sample but not in the calcined sample. This indicated that all the ammonia was removed from the surface of the catalyst during the calcination procedure.

3.1.2 Mordenite

Figure 3.5 shows the XRD spectrum of the Mordenite sample. The complete peak breakdown for this spectrum as well as the standard peak tables for the crystal structure of Mordenite are given in appendix III. It can be seen from the XRD spectrum that this sample is both highly crystalline and has a high phase purity.

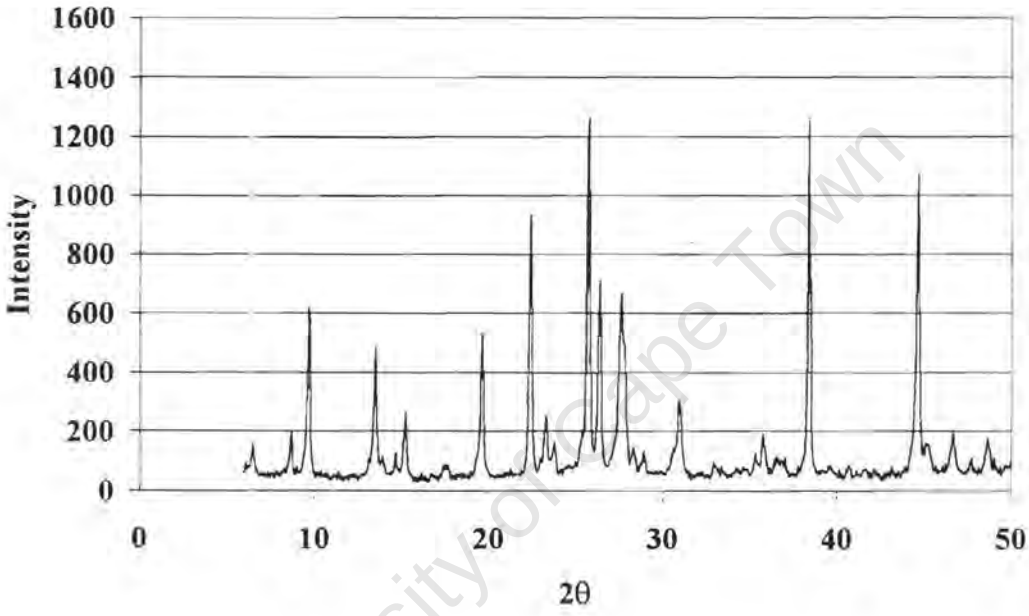

Figure 3.5: XRD Pattern of Mordenite

Figure 3.6 shows the SEM photographs obtained from the Mordenite sample used in this work as well as a highly crystalline Mordenite sample. It can be seen from this figure that there is a large amount variation in the appearance of the catalyst morphology seen between the two catalysts. The sample used in this work has a less well defined surface. In general, the sample is made up of crystallites of approximately 2 to 3 μm. These in turn form agglomerates of ca. 10 μm. The variation in the surface morphology is probably due to the fact that this is a commercial sample of Mordenite, produced in a bulk quantity and hence was subjected to large attrition forces as well as uneven synthesis conditions.

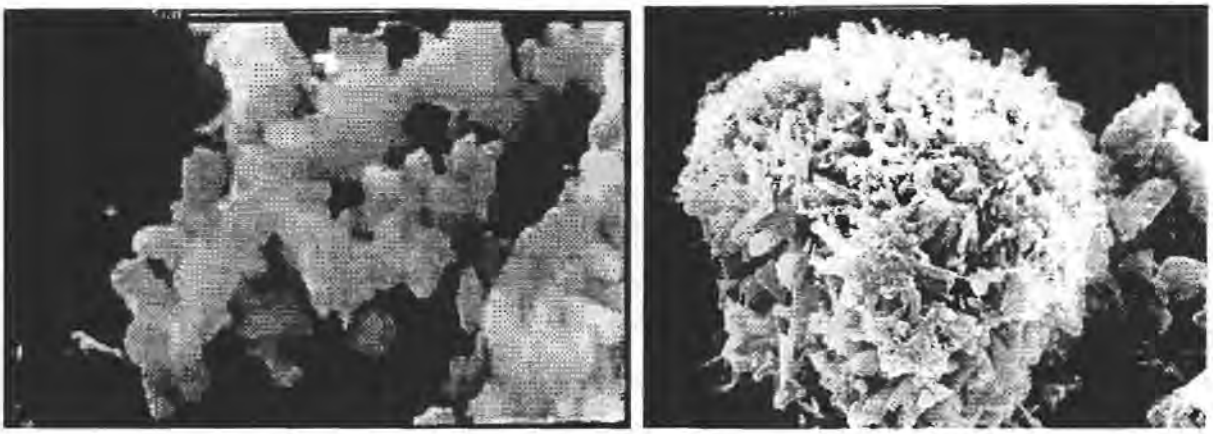

(a) (b)

Figure 3.6: SEM Photograph of the untreated Mordenite used in this work (a) and a highly crystalline Mordenite Sample (b)

(white line = 5μm)

Figure 3.7 shows the Thermal Desorption spectrum of the parent Mordenite. It can be seen that two distinguishable peaks were observed. The first, at ca. 290°C, is very small. The second, at ca. 560°C, is by far the larger of the two peaks. This means that the Mordenite has an almost homogeneous acid site distribution of strong sites. The concentration of acid sites on this catalyst was determined to be 3.38 mmol/ g_{cat}. The single desorption peak of Mordenite is similar to that seen by Miller *et al.* [1992]. The shoulder seen at 700 °C in the Thermal Desorption spectrum is due to the sudden change in temperature program from the ramping to isothermal regimes.

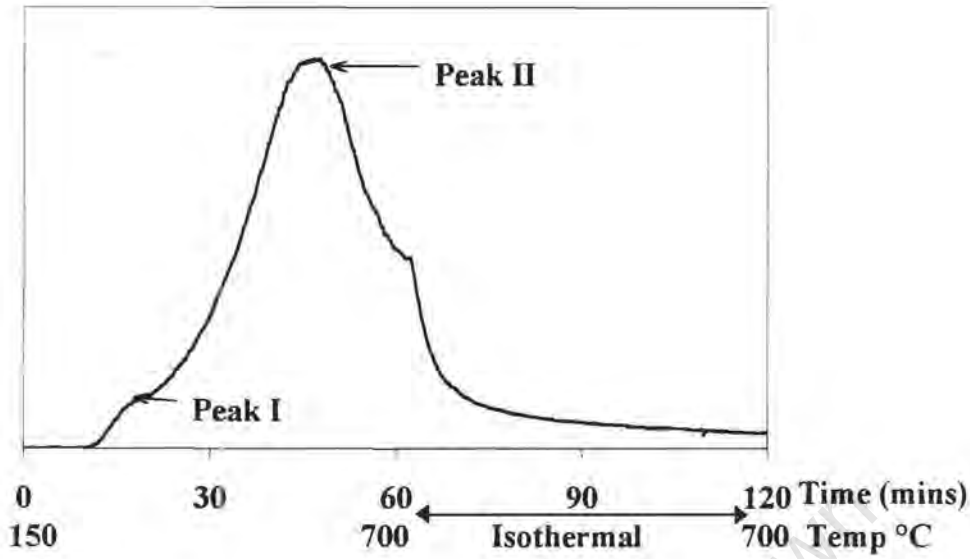

Figure 3.7: Thermal Desorption Spectrum of Untreated Mordenite

(T_{ads}=150°C, heating rate = 9°C/min, t_{ads}=1hr, T_{flush}=150°C, t_{flush}=16hrs, gas flow = 70ml(NTP)/min He)

3.2 REACTION STUDIES

A number of small pore zeolites (Rho, ZK-5 and Chabazite) have been proposed as selective catalysts for the formation of lower substituted methylamines [Keane *et al.*, 1987; Abrams *et al.*, 1990; Ilao *et al.*, 1996]. In addition, Mordenite has been shown to be a good catalyst for the methylamine synthesis [Ashina *et al.*, 1986; Mochida *et al.*, 1983; Weigert, 1987; Segawa and Tachibana, 1992]. Of the catalysts mentioned, zeolites Rho and Mordenite were chosen to be catalysts studied in this work as it seemed that they would give the best results in terms of dimethylamine selectivity. Additionally, Rho has a reasonably stable crystal lattice, an important consideration when choosing a viable catalyst [Shannon *et al.*, 1988a].

The first claim made of these zeolites is that they do not deactivate as rapidly as the amorphous silica-alumina [Shannon *et al.*, 1988a; Ilao, 1992]. The comparison of the deactivation behaviour of the zeolite and silica-alumina was tested, as illustrated in Figure 3.8 by running the methanol amination reaction at 400°C over the three catalysts, Rho (A), Mordenite and amorphous silica-alumina.

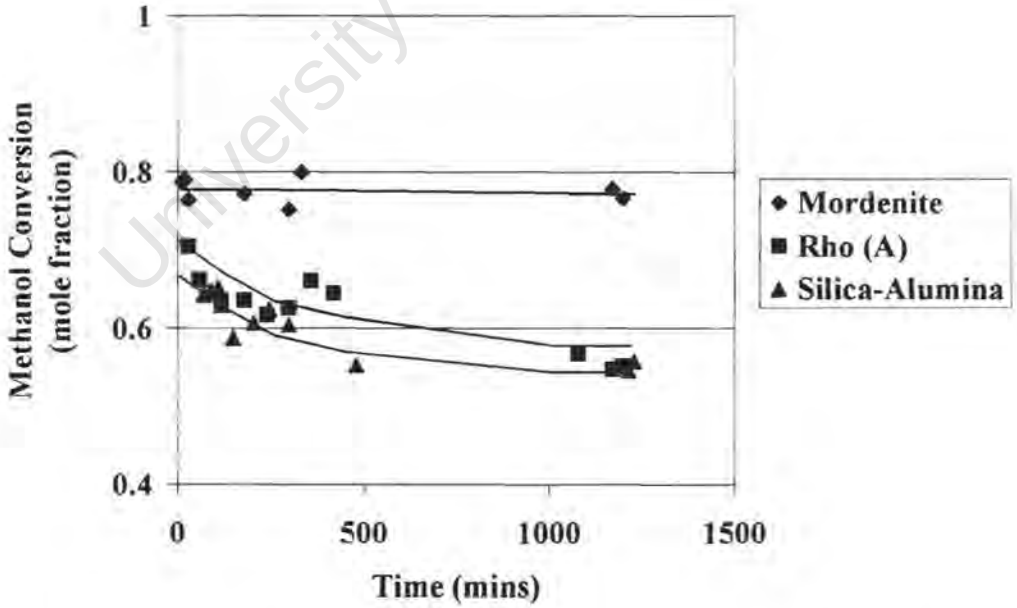

Figure 3.8: Activity in the methanol amination reaction over zeolites Rho (A), Mordenite and silica-alumina at 400°C.

(WHSV=5.8 g MeOH/ g_{cat} /hr; P_{tot} = 1atm; p_{NH3}=p_{MeOH}=8kPa)

As can be seen above, while the performance of the Mordenite is better in that it does not deactivate as rapidly as the other two catalysts. Zeolite Rho seems to have a very similar deactivation rate to the amorphous silica-alumina.

The second claim made in literature is that Rho in particular is highly selective to DMA. In the initial reaction studies performed in this work this was not found to be the case. In the initial scanning of three catalysts (Rho, Mordenite and amorphous silica-alumina), at reaction conditions of 400 °C and 1 atm, it was found that although the activity over the zeolites after 1 hour on stream was somewhat higher than that over the amorphous silica-alumina, there was not as much improvement in selectivity as was expected. Table 3.1 illustrates this comparison between the various catalysts. Both zeolite Rho and Mordenite yielded only 37 mol% TMA in the amine fraction vs. the amorphous silica-alumina which gave 57%. Both zeolites gave an especially higher DMA content in the fraction of amines than the silica-alumina. In the case of Rho, the relative improvement in the DMA yield was more than that in the MMA mole fraction. In contrast, over Mordenite, the relative improvement in yield of MMA and DMA were about constant.

Table 3.1: Initial Reaction Studies at 400°C.

($T_{reaction}$ = 400 °C, p_{tot} = 1 atm, p_{NH3}=p_{MeOH}=8 kPa, $t_{reaction}$=1 hr)

Catalyst		Silica-Alumina	Rho A	Mordenite
WHSV (gMeOH/ g_{cat} /hr)		5.8	5.8	5.8
Methanol Conversion (%)		66	67	79
Amine Content in Amines	**(mol%)**			
	MMA	32	42	46
	DMA	11	22	17
	TMA	57	37	37
Yields (C%)				
	DME	16	2	2
	MMA	8	13	18
	DMA	6	13	13
	TMA	32	35	42
Yield (zeolite)/ Yield (Si/Al[a])		-		
	MMA	-	1.6	2.3
	DMA	-	2.2	2.2
	TMA	-	1.09	1.3

note: a: Si/Al = silica-alumina

The most significant benefit of using the zeolites at 400 °C seems to be in terms of the DME selectivity. Over the silica-alumina, a large fraction of the methanol converted produces DME. Over the zeolites however, this fraction is significantly reduced. This result is consistent with the Thermal Desorption analyses of the parent catalysts, which showed, especially in the case of Mordenite, a strong, homogeneous distribution of high strength Brønsted acid sites (cf. Figure 3.7). Amorphous silica-alumina contains Lewis acidity. Lewis acidity enhances the formation of DME due to the ability of methanol to adsorb competitively with the ammonia on the Lewis acid sites [Kogelbauer *et al.*, 1994,1996].

At lower temperatures it was found that, in contrast to the results at 400 °C, the conversion over the zeolites was significantly higher than that observed over silica-alumina. At 325 °C, the silica-alumina gave almost no conversion. Of the products formed, by far the largest percentage was DME with only small amounts of amines. Table 3.2 gives the results for the two zeolites in initial reaction studies at 325°C. The activity of the two zeolites at 325 °C is very similar. The selectivity however is remarkably different. The performance of the Mordenite at 325 °C in terms of selectivity is very similar to that at 400 °C. Rho A has yielded a far less selective product distribution at the lower temperature. Rho B however has given a product spectrum which gives very high MMA selectivities. It may be said therefore that the level of crystallinity does affect the catalyst performance as Rho (A), which is less crystalline performs worse than Rho B which has the higher crystallinity.

Table 3.2: Initial reaction studies at 325°C.

($T_{reaction}$ = 325 °C, p_{tot} = 1 atm, p_{NH3}=p_{MeOH}=8kPa, $t_{reaction}$=1.5hrs)

Catalyst	WHSV ($gMeOH/ g_{cat}.hr$)	Methanol Conversion (%)	Fraction of total amines (mol%)			DME selectivity (C%)
			MMA	DMA	TMA	
Rho (A)	4.4	28	16	5	79	16
Rho (B)	4.4	40	66	14	20	9
Mordenite	4.4	36	51	13	36	29
Silica-Alumina	4.4	5	[a]	[a]	[a]	98

a: numbers unreliable due to low conversion

It has been seen in this analysis of the untreated catalysts that both Rho and Mordenite perform somewhat better than the amorphous silica-alumina at 400°C both in terms of activity and selectivity. However, neither of them show the desired selectivity to DMA. The most significant benefit of using these untreated zeolites at 400°C is the decreased DME selectivity observed.

The zeolites even in their untreated form do perform better than the amorphous silica-alumina in terms of activity at the lower temperature. Only the highly crystalline Rho however shows a good selectivity at 325°C.

What is interesting to note is the apparently low temperature dependence of the reaction rate over the zeolites as opposed to the silica-alumina.

3.3 REACTION-REGENRATION CYCLES

It was also observed in the initial reaction studies that upon regeneration of the zeolites, in air, after reaction, the performance of each improved both in terms of activity and selectivity. As one of the aims of this work was to find the best possible catalyst for the methanol amination reaction, it was thought to be advisable to study the effect of repeated reaction-regeneration cycles in more detail.

In these studies the catalyst was initially calcined according to the same procedure used for the initial reaction studies and then used for the methanol amination reaction. This formed the first cycle of a series. Subsequent cycles were performed by recalcining the catalyst before performing the reaction step again. Prior to each recalcination, the catalyst was flushed for 1 hr at reaction temperature with inert gas. These cycles of reaction and regeneration were performed many times in order to obtain the trends observed. Figure 3.9 illustrates the procedure used. The results of all reaction experiments are given in appendix V.

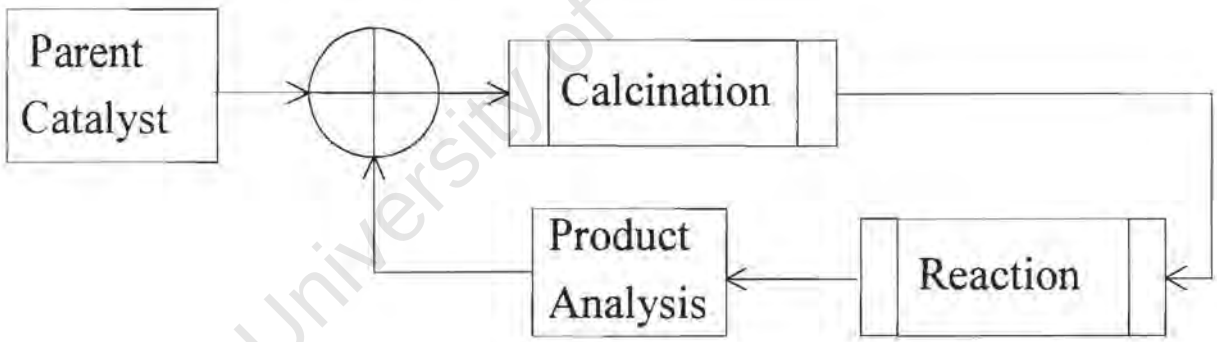

Figure 3.9: Method of Reaction-Regeneration cycles

3.3.1 Zeolite Rho

Further investigation of the change in catalytic performance due to calcination, subsequent to reaction, was performed over zeolite Rho (sample A). Figure 3.10 shows the change in the integral rate of methanol consumption over Rho as a function of cycle number, as well as the rate of formation of amines and dimethyl ether. The catalyst activity, as measured by the integral rate of methanol consumption, increased with increasing cycle number, reaching a plateau after ca. 7 cycles. The rate of amine formation closely followed the rate of methanol consumption, while the rate of formation of DME remained approximately constant with cycle number.

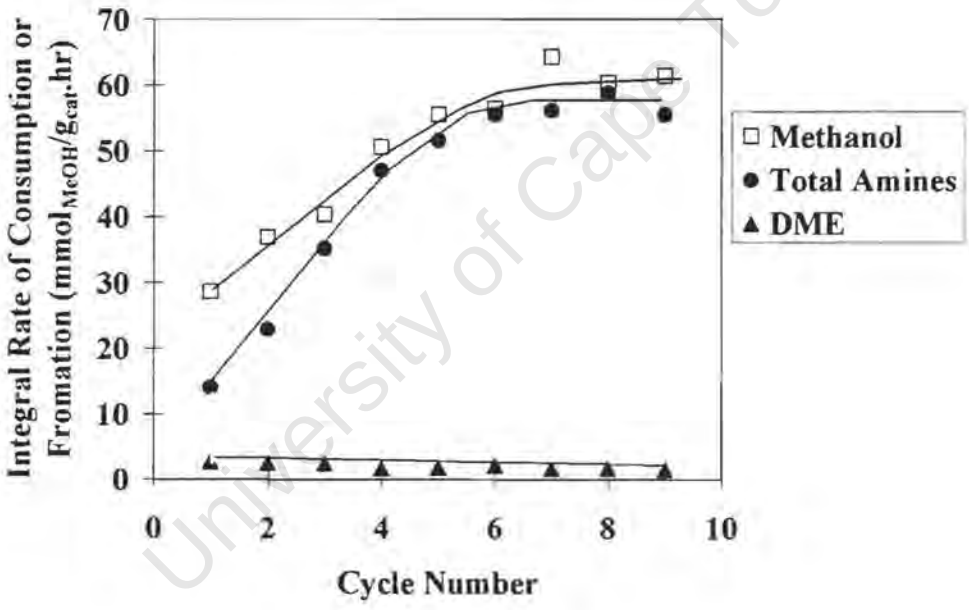

Figure 3.10: Integral Rates of Methanol Consumption and Product formation vs. Number of reaction/regeneration cycles over zeolite Rho A.

($T_{reaction}$ = 325 °C, $t_{reaction}$ = 1.5 hrs/cycle, p_{MeOH} = p_{NH3} = 8 kPa, p_{tot} = 1 atm, $T_{calcination}$ = 500 °C, $t_{calcination}$ = 5 hrs/cycle, calcination gas: synthetic air)

The amine selectivity likewise changed with increasing cycle number. Figure 3.11 shows the amine fractions of the total amines produced over zeolite Rho as a function of cycle number. The trimethylamine selectivity decreased from 79 to 41 mol% while the selectivities of both the mono- and dimethylamine increased from 16 and 5 to 32 and 27 mol% respectively with cycle number. The selectivities reached a plateau after ca. 8 cycles. It can be said therefore, taking the trends in both activity and selectivity into account, that there is an optimum number of cycles that can be performed over the catalyst after which no further improvement can be seen. This occurs for the conditions used here after ca. 7 cycles. That the TMA selectivity starts above thermodynamic equilibrium is an issue that will be discussed extensively in Chapter 4.

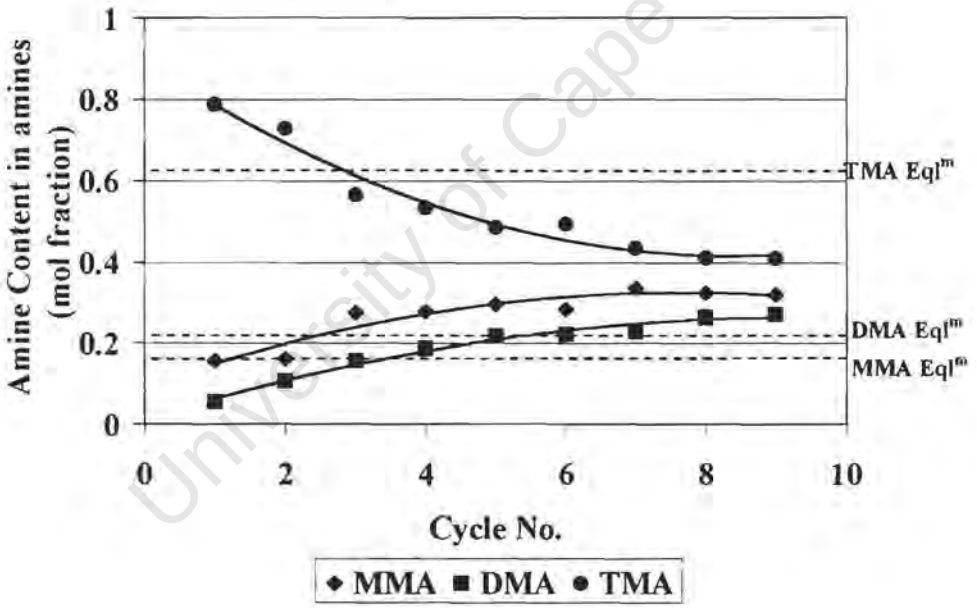

Figure 3.11: Amine content in the fraction of total amines produced as a function of the number of reaction-regeneration cycles over zeolite Rho (A).

($T_{reaction}$ = 325 °C, $t_{reaction}$ = 1.5 hrs/cycle, $p_{MeOH} = p_{NH3}$ = 8 kPa, p_{tot} = 1 atm, $T_{calcination}$ = 500 °C, $t_{calcination}$ = 5 hrs/cycle, calcination gas: synthetic air, dashed lines show thermodynamic equilibrium values)

The question remained as to what exactly happened during the reaction-regeneration cycles to cause the change observed. An initial guess was that the change was occurring either during the reaction phase or during the calcination step in the cycles. Consequently, each of these steps were investigated separately.

Reaction Time

To determine whether or not the trends in activity and selectivity shown above were a function of reaction time, a new series of cycles was performed, in which the time on stream of each cycle was varied. The range of reaction times examined were between 1.5 and 22 hrs /cycle. The results of these cycles are shown in Figures 3.12 and 3.13.

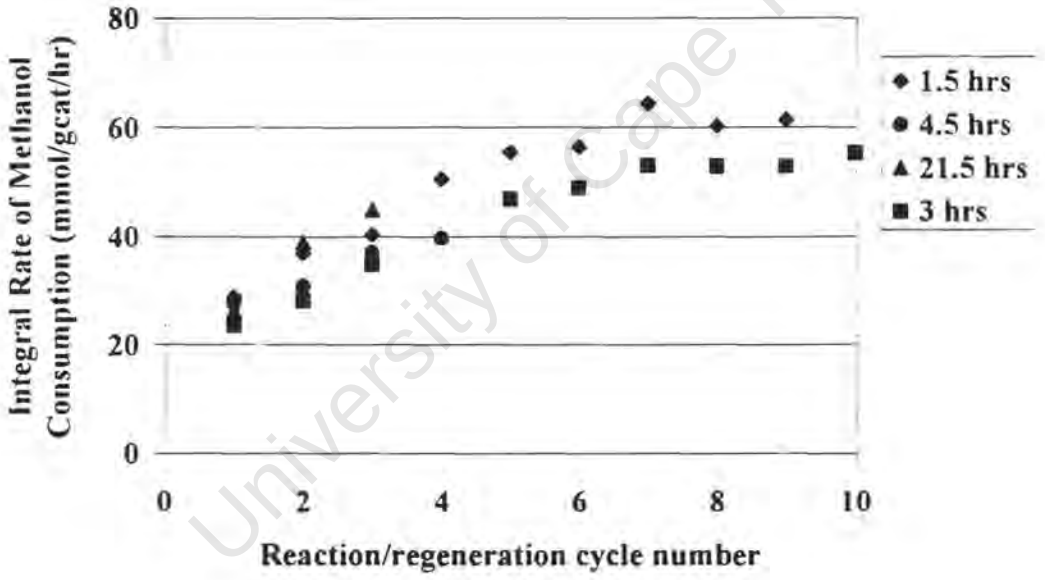

Figure 3.12: Integral rate of methanol consumption as a function of the number of reaction-regeneration cycles under variation of the reaction time per cycle over zeolite Rho (A).

($T_{reaction}$ = 325 °C, p_{MeOH} = p_{NH3} = 8 kPa, p_{tot} = atmospheric, $T_{calcination}$ = 500 °C, $t_{calcination}$ = 5 hrs/cycle)

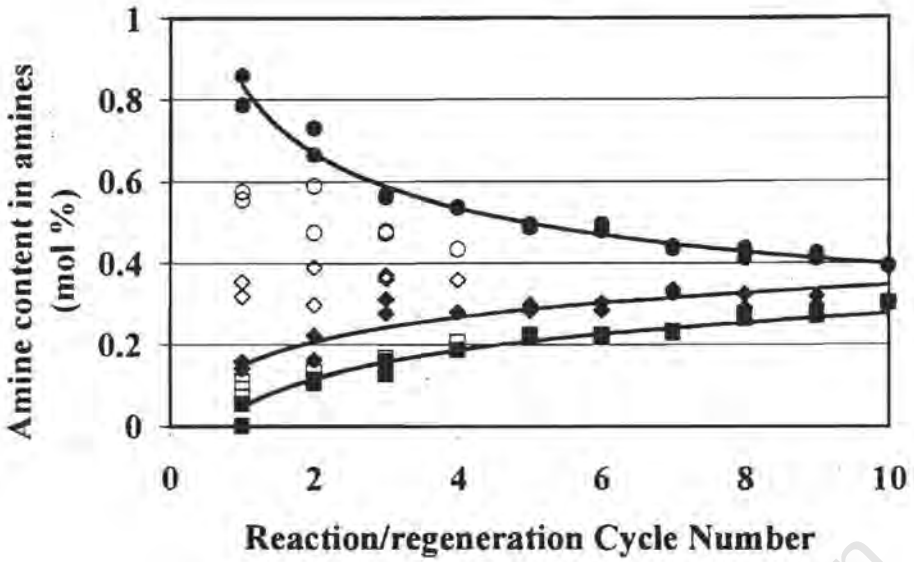

Figure 3.13: Amine content in amine fraction as a function of the number of reaction-regeneration cycles under variation of the reaction time per cycle over zeolite Rho (A).

(♦ MMA(1.5, 3 hrs) ◊ MMA(4.5, 21.5 hrs) ■ DMA(1.5, 3hrs) □ DMA(4.5, 21.5hrs) ● TMA(1.5, 3hrs) ○ TMA(4.5, 21.5hrs)

$T_{reaction}$ = 325 °C, $p_{MeOH} = p_{NH3}$ = 8 kPa, p_{tot} = atmospheric, $T_{calcination}$ = 500 °C, $t_{calcination}$ = 5 hrs/cycle)

It may at first be thought that there is a change in the performance with reaction time. However, on closer examination it was found that the rate decreased with the order in which the experiments were done rather than changing with reaction time. These changes are however related to the difference in particle size of the catalyst.

The decrease in reaction rate observed between the series of 1.5 and 3 hours reaction time was the most distinct, or the furthest apart. It was found that the ratio of the rates of these two curves was the same for all points, including the initial rate. It was therefore concluded that the difference was due to a physical phenomenon, related to the catalyst sample used rather than to the treatment performed on the catalysts.

It was found that the particle size distribution was slightly different between these two samples, which was possibly due to the settling of the catalyst sample in the bottle. It was found that the average particle diameter changed from 7.7 to 9.6 μm. For this size particle, this is a significant change as the particle size influences the degree of axial dispersion and hence the observed reaction rate. The particle size distribution and a discussion of axial dispersion as it relates to particle size is given in Appendix VI.

Calcination time

The next test performed was to determine whether the calcination time had any effect on the observed trends. To do this, a new series was performed in which the calcination time was 15 rather than 5 hours per cycle. The results of this test are shown in Figure 3.14.

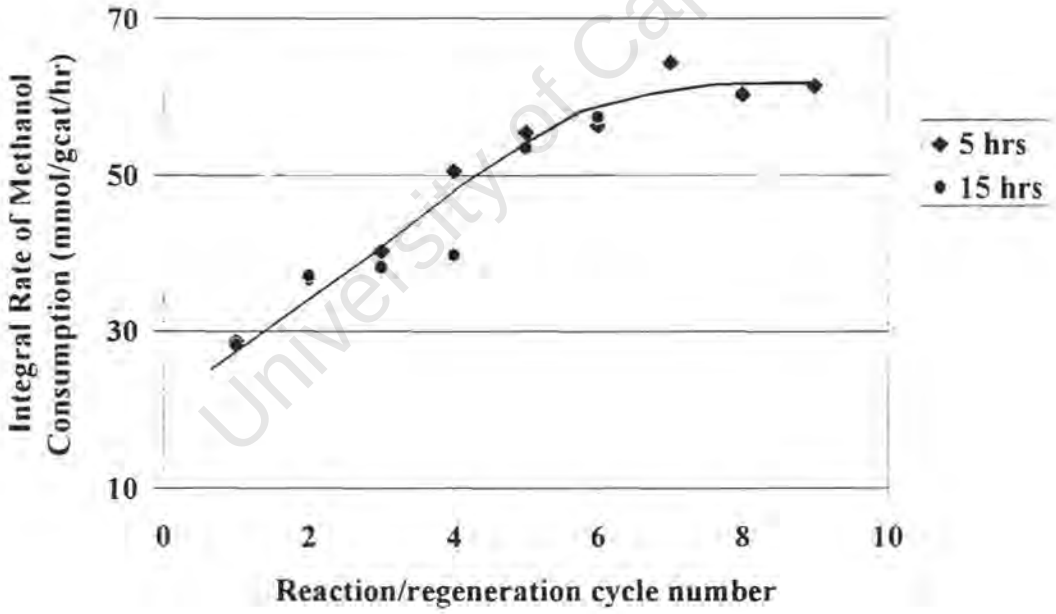

Figure 3.14: Integral rate of methanol consumption as a function of the number of reaction-regeneration cycles under variation of the calcination time per cycle over zeolite Rho (A).

($T_{reaction}$ = 325 °C, p_{MeOH} = p_{NH3} = 8 kPa, p_{tot} = atmospheric, $T_{calcination}$ = 500 °C, $t_{calcination}$ = 5 hrs/cycle)

As can be seen above, between these two widely different calcination times there was no apparent effect of calcination time on the increase in activity observed. It could therefore be concluded that the change observed in the catalyst was not directly related to the calcination step.

At this stage it could be reasoned that if the changes in performance observed were not a function of either reaction or calcination time then they must be caused by either some property of the catalyst itself, though this was thought to be unlikely or to some phenomena occurring over a very short space of time during each of the cycles. This issue will be discussed further in Chapter 3.4.

3.3.2 Mordenite

To determine whether or not the improvements in activity observed over zeolite Rho were specific to that zeolite or a more general occurrence, the same series of reaction- regeneration cycles was performed over Mordenite. The reason for choosing Mordenite as the catalyst of comparison was twofold. Firstly it is a catalyst that has been widely proposed as being effective for the methanol amination reaction [Ashina *et al.*, 1886; Weigert,1987]. Secondly it has a structure completely different to that of Rho, which enables the distinction between structure specific and general catalytic phenomena. Additionally, the particular sample of Mordenite used in this work was an industrial sample, which facilitated the gain of a realistic idea of how this catalyst might behave industrially. The results of the reaction-regeneration cycles over Mordenite are shown in Figures 3.15 and 3.16.

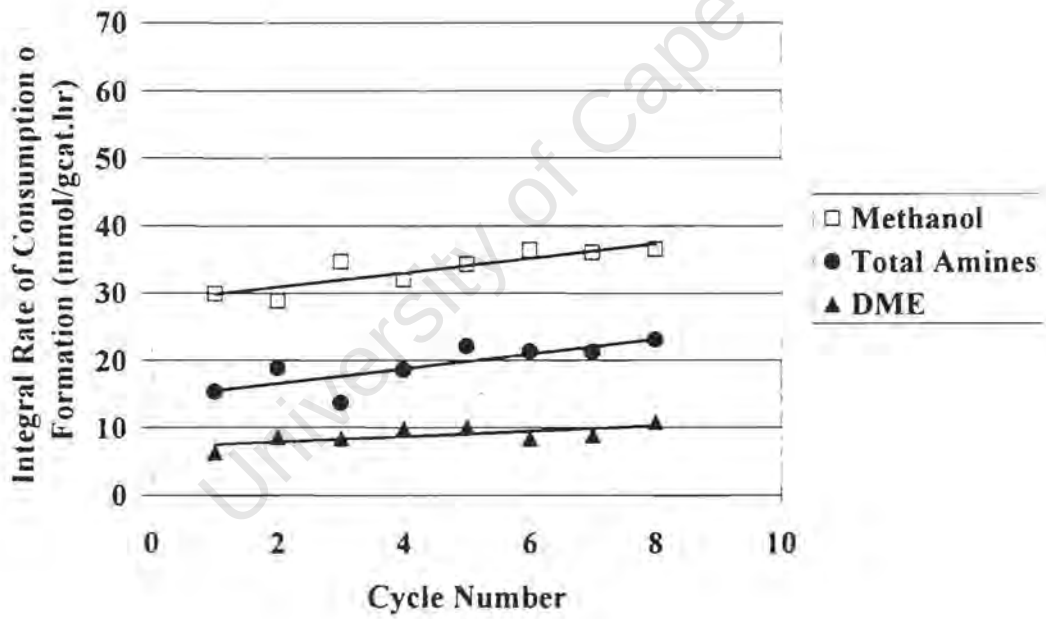

Figure 3.15: Integral Rate of Methanol Consumption and Amine formation as a function of the number of reaction-regeneration cycles over Mordenite.
($T_{reaction}$ = 325 °C, $t_{reaction}$ = 1.5 hrs/cycle, p_{MeOH} = p_{NH3} = 8 kPa, p_{tot} = atmospheric, $T_{calcination}$ = 500 °C, $t_{calcination}$ = 5 hrs/cycle)

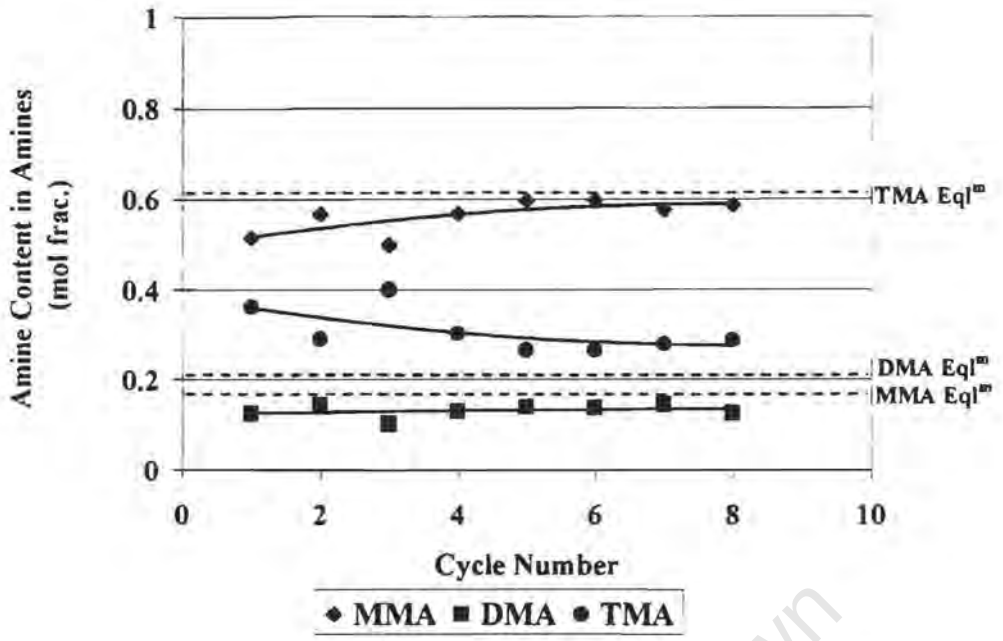

Figure 3.16: Amine content in the fraction of amines as a function of the number of reaction-regeneration cycles over Mordenite.

($T_{reaction}$ = 325 °C, $t_{reaction}$ = 1.5 hrs/cycle, $p_{MeOH} = p_{NH3}$ = 8 kPa, p_{tot} = atmospheric, $T_{calcination}$ = 500 °C, $t_{calcination}$ = 5 hrs/cycle, dashed lines represent equilibrium distribution of amines for these reaction conditions)

It can be seen above that there was a similar, if less distinct, change in performance observed over Mordenite as there was over Rho, the activity and selectivity improving to some degree with cycle number. The difference between the two catalysts is the extent to which the change occurs in each of them. The improvement both in terms of activity and selectivity is far greater over Rho than over Mordenite. In terms of selectivity, however, Mordenite did initially show greater selectivity to monomethylamine and this selectivity improved still further with cycle number at the expense of trimethylamine. The selectivity to dimethylamine however did not change with the varying reaction-regeneration cycle number.

The conclusion therefore is that although Mordenite initially performs better, zeolite Rho, with increasing reaction-regeneration cycles, soon supersedes Mordenite in terms of overall performance. Not only is the activity obtained over Rho higher than that of Mordenite, but also the selectivity to the lower substituted methylamines becomes better over Rho than Mordenite.

3.4 PRESENCE OF WATER

To examine more thoroughly the above phenomena, the exhaust gas from a reactor containing a sample of zeolite Rho over which reaction had occurred was monitored using a GC Mass Spectrometer. After the reaction, the catalyst was flushed with flowing helium (60 ml(NTP)/min) and ramped from 30 to 450 °C at 5 °C/min.

It was observed that at 450 °C all of the reaction products, including water and TMA had desorbed from the surface. This temperature programmed desorption spectrum is shown in Figures 3.17 and 3.18. The eight-peak index of mass spectra [1991] was used for peak identification. A summary of the relative peak intensities of the various compounds is given in appendix VII. Of the peaks shown below, m/e 58 is characteristic of TMA, m/e 44 originates from either DMA or TMA and m/e 30 from either MMA or TMA. Looking at the relative ratios of these ions however at the 400°C peak, it would seem that this peak is caused solely by TMA desorption. With m/e = 45 and 46, seen in the peak at 75 °C could be formed by either DME or the lower substituted amines. The maximum in the water desorption peak, as evidenced by m/e = 18, occurred at the relatively low temperature of 110 °C (see Figure 3.18).

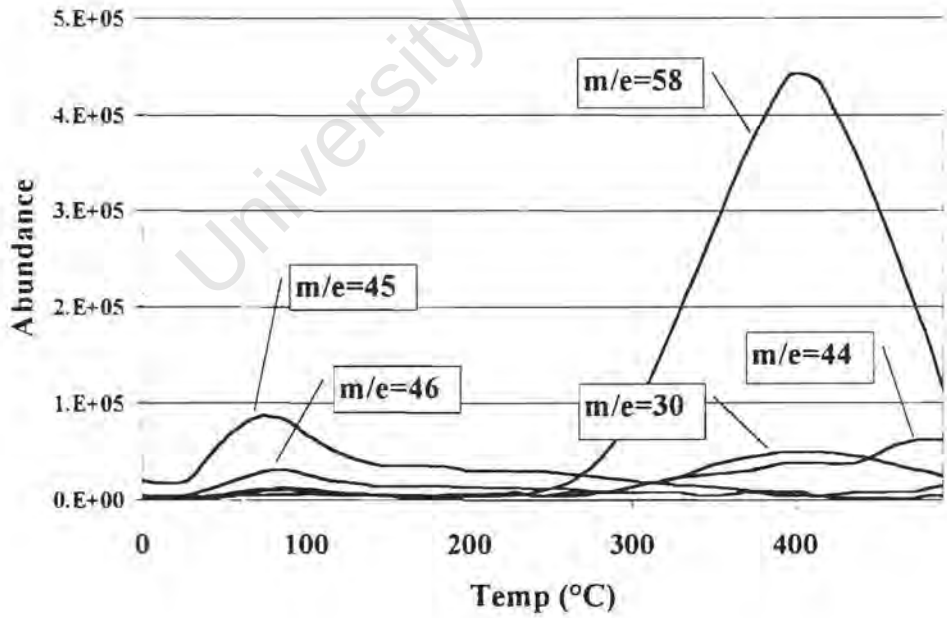

Figure 3.17: Temperature Programmed Desorption of Reaction Products (excluding water) from zeolite Rho after reaction.

(Temperature ramp =5°/min; T_{max}=450°C; Flush Gas:He; $T_{reaction}$=325°C, N/C=1)

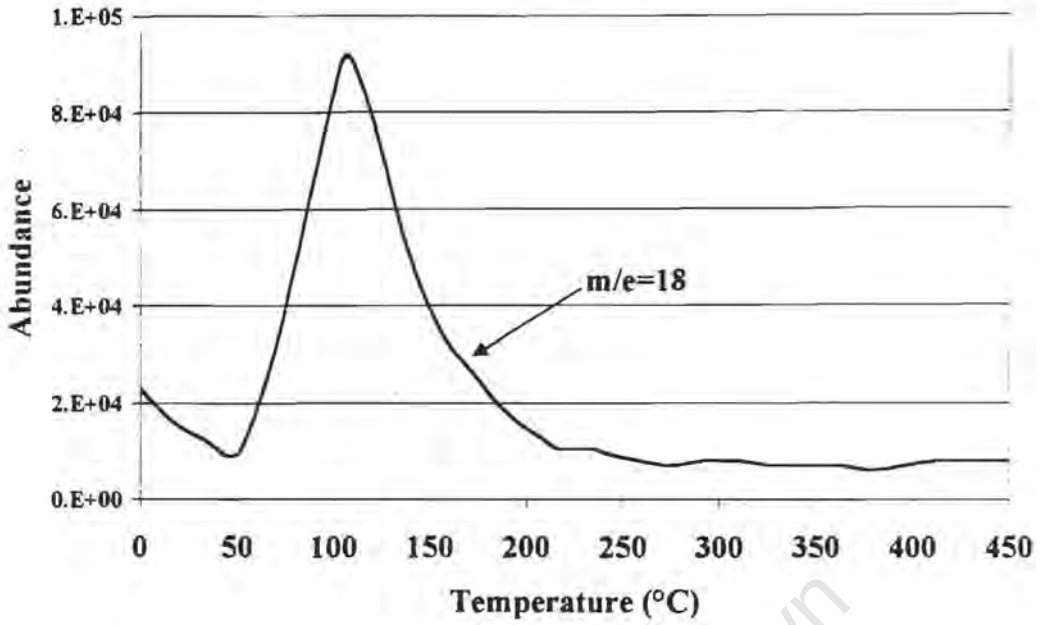

Figure 3.18: Temperature Programmed Desorption of water after reaction from zeolite Rho after reaction.

(Tramp=5°/min; Tmax=450°C; Flush Gas:He)

What these desorption peaks mean firstly, is that in the reaction-regeneration cycles, all of the product desorption should have occurred during the flushing phase between reaction and calcination, before the catalyst was contacted with air. The catalyst change could therefore not have been caused by the reaction of the desorbing amines or dimethyl ether with the oxygen from the air used during calcination.

To test whether there were any residual species left on the catalyst, the same catalyst sample was kept at 450 °C and was contacted with short pulses of dry air. After each of these air pulses, CO, CO_2 and water were observed in the exhaust gas. The water release for the complete experiment is shown in figure 3.19.

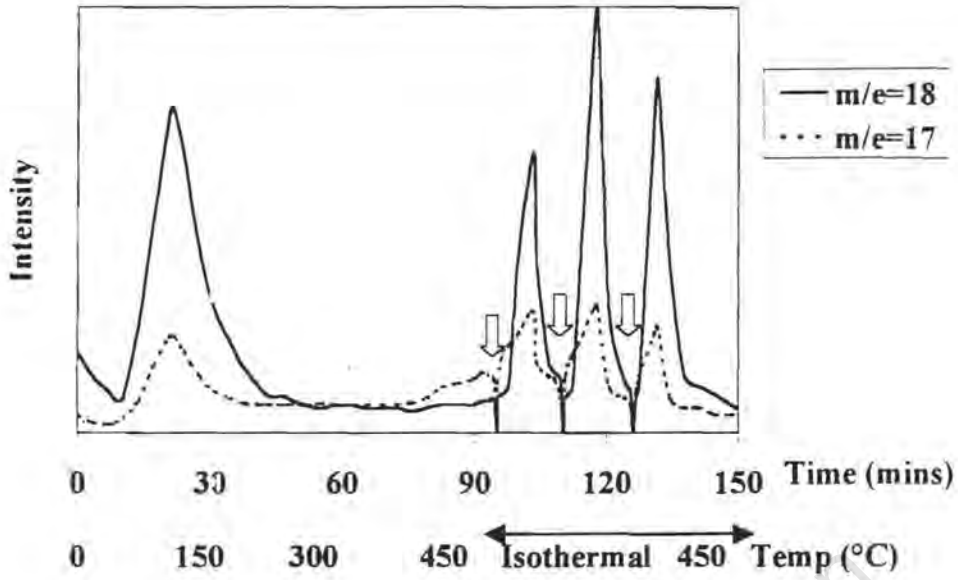

Figure 3.19: Water release during Temperature Programmed desorption of reaction products and following contact with oxygen.

(⇩ = Points at which oxygen was introduced)

The presence of water after the feeding of air meant that there was still some carbonaceous species remaining on the surface of the catalyst after the desorption of the primary reaction products. This is easily explained, since tetramethylammonium (TET) ions were evidenced at the surface of a Mordenite catalyst during the methanol amination reaction [Gründling *et al*., 1996a; 1997a]. These species, being ionic and therefore strongly bound to the surface, are not able to desorb intact and must therefore either remain at the surface or dissociate resulting in gas phase TMA and a residual surface CH_3 group. This process is illustrated in figure 3.20.

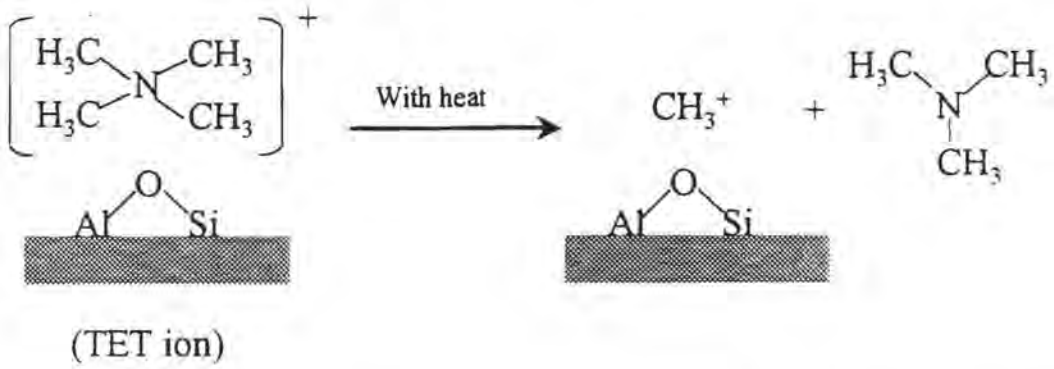

(TET ion)

Figure 3.20: Schematic representation of the dissociation of Tetramethyl ammonium ions on the surface of an acidic catalyst

If the dissociation of the TET ions occurred then the CH_3 groups could be burnt off the surface during the calcination phase. Alternatively, the entire TET ion could be burnt off the surface. In either case, one of the reaction products is water as was evidenced. This then might be the explanation of the change observed in the catalyst, *viz.* water formed at high temperatures might cause dealumination of the catalyst framework.

3.5 DISCUSSION

It has been seen in this section that as put forward in literature [Shannon *et al.*, 1988a; Keane *et al.*, 1987], the deactivation rate of Rho is fairly high at 400°C and much less at 325 °C, making the lower temperature a more appropriate operating point in terms of catalyst lifetime. Although the Mordenite showed no deactivation in the range of operation studied here, it is also known to have a longer lifetime at lower reaction temperatures [Ashina *et al.*, 1986]. As was seen the amorphous silica-alumina can not be operated at the lower temperature due to its low activity. The two untreated samples of Rho show very different selectivities for the methanol amination reaction. Rho (A) gives an almost unselective product distribution whereas Rho (B) shows increased selectivity to MMA but shows no increase in the DMA selectivity. The Mordenite likewise show improvement only in the MMA selectivity, but this is consistent with what is reported in literature [Mochida *et al.*, 1983].

It was also seen how repeated regeneration of the catalysts, Rho(A) and Mordenite, caused an improvement in the performance, both in terms of activity and of amine selectivity. It was determined that this effect was caused *in situ* steaming of the catalysts. The water was generated when residual carbonaceous, surface species were burnt off the catalysts during the calcination.

The final observation from these initial studies is that the Rho(A) and Mordenite were affected differently by the presence of the water generated during the calcination after reaction. The change over Rho was far more significant than that over Mordenite with a larger increase in activity as well as a more significant change in the relative amount of amines.

To further investigate this phenomenon it was decided to carry out more extensive tests into the hydrothermal treatment of the catalysts, Rho and Mordenite.

Hydrothermal Treatment

4. HYDROTHERMAL TREATMENT

Water, formed during the initial stages of the calcination during the reaction - regeneration cycles, is most probably responsible for the change in the catalyst performance. The influence of hydrothermal treatment of the catalysts was therefore investigated systematically. This was to determine whether the same effect, as was seen with the *in situ* steaming caused by the burning of the surface groups, could be obtained with artificial steaming. This was thought to be a valid assumption to make as it is known from literature that hydrothermal treatment can affect the performance of some catalysts [Shannon *et al.*, 1988a,b; Abrams *et al.*, 1989b; Ashina *et al.*, 1986; Dingerdissen *et al.*, 1991, Haag *et al.*, 1984,1994].

The second reason for this study of hydrothermal treatment was to examine effectively the differences in the responses of the two catalysts (zeolites Rho and Mordenite) to steam treatment. Although some studies had been done previously on the steaming of Rho [Shannon *et al.*, 1988a; Abrams *et al.*,1989b] , there were no systematic studies on the effect of steaming time performed. Over Mordenite, many studies on the effect of dealumination have been performed [Ashina *et al.*, 1986; Dingerdissen *et al.*, 1991, Zhang *et al.*, 1994]. A few studies have examined hydrothermal treatment of Mordenite [e.g., Lago *et al.*, 1986] but these were not done in connection with the methanol amination reaction. It was therefore decided that a thorough, systematic study of the effect of steaming time on the methanol amination reaction was required.

In these experiments, the two catalysts were initially steamed at relatively mild conditions. The catalysts were treated for times of 0 to 22 hours with steam (30 kPa partial pressure; 450 °C. water loading = 69 $mmol_{H2O}/g_{cat}.hr$).

4.1 CHARACTERISATION OF ACIDITY

Once it was known that it was the steaming of the zeolites that had caused the change in their behaviour for the methanol amination reaction, is was decided to investigate the structural changes and the changes in acidity that were occurring on the catalysts in more depth.

4.1.1 Temperature Programmed Desorption

Thermal Desorption of ammonia from the catalyst surface was performed to determine the number, strength and concentration of acid sites on the catalyst surface as a function of steaming time. The results of these experiments are shown in Figure 4.1. It is shown here how the desorption of ammonia adsorbed on Rho changes with increasing steaming time.

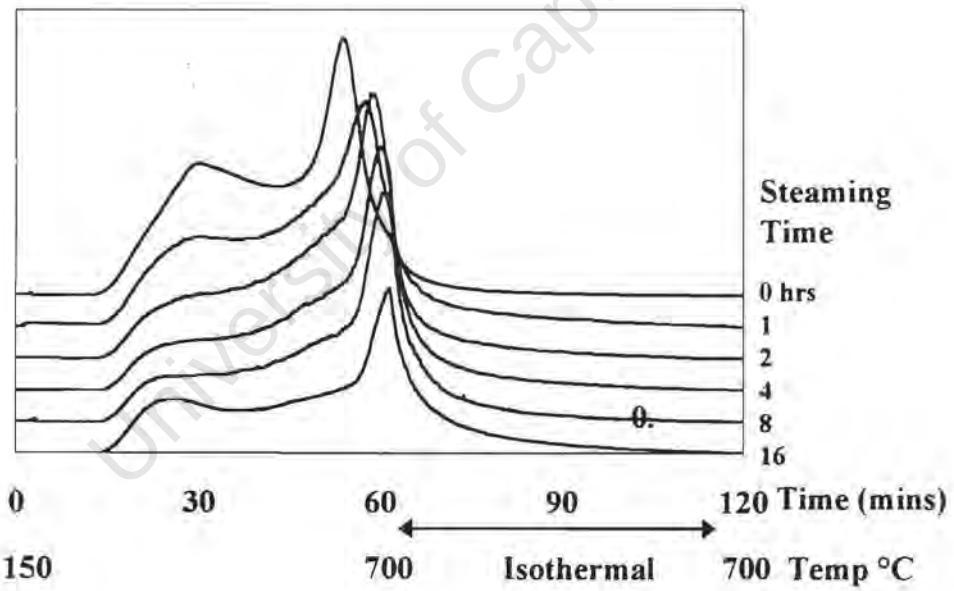

Figure 4.1: Comparison of Thermal Desorption spectra for increased steaming time of zeolite Rho (A)

(T_{ads}=150°C, heating rate = 9°C/min, t_{ads}=1hr, T_{flush}=150°C, t_{flush}=16hrs, gas flow = 70ml(NTP)/min He)

It can be seen in the above spectra that there was more than one peak present in the Thermal Desorption spectra. These spectra were deconvoluted using a simple Gaussian fit of the data. Although this method of deconvolution is not entirely accurate is does serve to give an idea of how the peaks change relative to each other. Figure 4.2 shows a typical fit of three peaks to one of the desorption spectra. The deconvolution of all the Thermal Desorption spectra are given in Appendix IV. A summary of all of these deconvolutions are shown in Table 4.1 below.

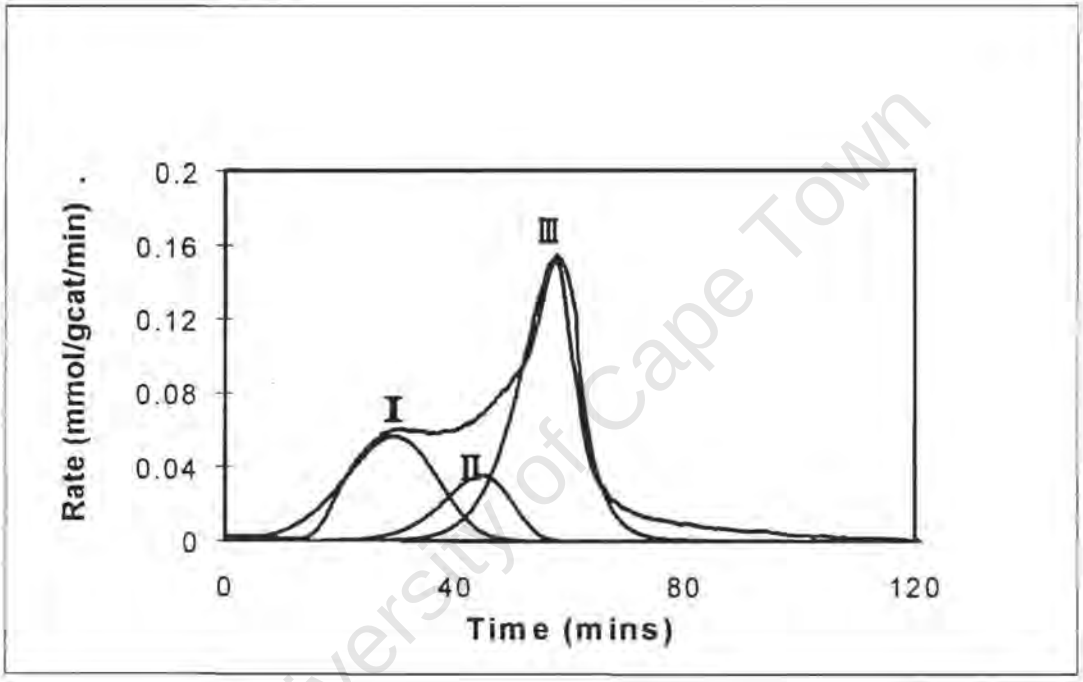

Figure 4.2: Deconvolution of Thermal Desorption Spectrum using Gaussian approximation to the peak shapes.

(0.5 hrs steaming, T_{ads}=150°C, heating rate = 9°C/min, t_{ads}=1hr, T_{flush}=150°C, t_{flush}=16hrs, gas flow = 70ml(NTP)/min He)

Table 4.1: Comparison of Thermal Desorption peaks for zeolite Rho (A) at different steaming times

(T_{ads}=150°C, heating rate = 9°C/min, t_{ads}=1hr, T_{flush}=150°C, t_{flush}=16hrs, gas flow = 70ml(NTP)/min He)

Steaming Time (hours)	Peak I (mmol/ g_{cat})	Peak II (mmol/gcat)	Total desorption (mmol/gcat)	P II / P I	Peak III Normalised
0	1.39	0.38	1.77	0.26	1.00
0.5	1.14	0.53	1.67	0.47	1.00
1	0.81	0.50	1.31	0.61	1.05
2	0.68	0.44	1.12	0.64	0.93
4	0.61	0.39	1.00	0.64	0.89
8	0.65	0.45	1.10	0.69	0.66

It was found in the above Thermal Desorption experiments that Peak III (at 680 °C) was not due to desorption of ammonia but rather to dehydroxylation of the catalyst. This was found firstly from repeated Thermal Desorption studies in which the same catalyst sample was used with the same desorption programme. In these experiments it was found that, although Peaks I and II reoccurred, Peak III did not. That peak III may be caused by framework deterioration was also confirmed by thermogravimetric analysis, in which a precalcined catalyst sample was heated to 700 °C in flowing nitrogen. It was observed that mass loss occurred in the higher temperature range (ca. 600-700°C). The results of these two experiments are shown in Appendix VIII.

The other two peaks, I (450 °C) and II (600 °C), represent desorption of ammonia from two distinct acid sites. The number of strong acid sites (Peak II) can be seen to be approximately constant over the range of steaming time studied here. What can be seen is the definite decrease in the number of weaker and therefore the total number of acid sites. The balance of strong to weak sites on the catalyst therefore shifts towards the stronger sites. As the steaming progresses with time, so the dehydroxylation peak shifts to higher temperatures. The shift of this peak is especially noticeable between the unsteamed and the sample steamed for 0.5 hours. It is for this reason that, in the parent catalyst, the desorption from the strong acid sites is to some extent overshadowed by the dehydroxylation peak.

Thermal Desorption experiments over Mordenite were also carried out. Figure 4.3 shows a comparison of two of these spectra at different steaming times. What this figure shows is firstly that Mordenite initially has an essentially homogeneous acid site distribution, with most of the ammonia desorption occurring at ca. 560°C and only a much smaller amount desorbing at ca. 290°C. With steaming, a second type of weaker acid site is formed at the expense of the original site. Table 4.2 shows the total amount of ammonia desorbed from the Mordenite at different steaming times

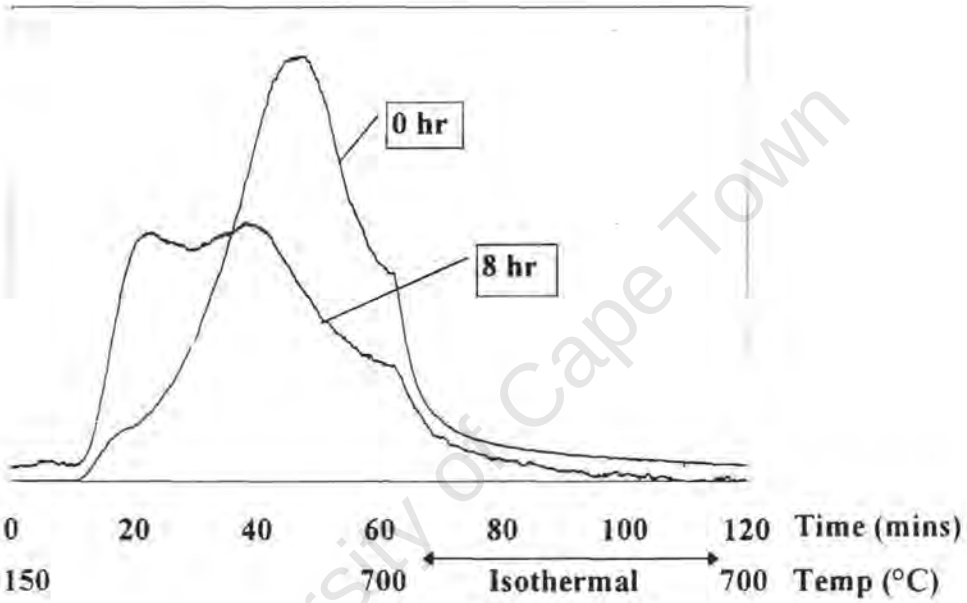

Figure 4.3: Comparison of Thermal Desorption spectra over Mordenite at 0 and 8 hrs steaming

(T_{ads}=150°C. heating rate = 9°C/min. t_{ads}=1hr. T_{flush}=150°C. t_{flush}=16hrs. gas flow = 70ml(NTP)/min He)

Table 4.2: Ammonia desorption from Mordenite steamed for various times

Steaming Time (hours)	Ammonia desorption (mmol/ g_{cat})
0	3.38
8	2.81
16	2.69

It can be seen that the loss of acid sites over Mordenite is relatively not as severe as over Rho. The conclusion that may be drawn from these studies is that the hydrothermal treatment affects the two catalysts is different ways. While over the Rho there is a 35 % net loss of the number of acid sites, there is only a 20% net loss in the number of acid sites over Mordenite with steaming time. This smaller loss over Mordenite is probably due to the higher structural stability of Mordenite but may be related to the generation of the second type of acid site. The response of the Mordenite to steaming seen here is similar to that seen by Miller *et al.* [1992] who also saw a generation of lower temperature ammonia desorption peak in steamed Mordenite.

4.1.2 NMR

It had previously been shown [O'Donovan *et al.*, 1995] that hydrothermal treatment of Mordenite caused some dealumination and the generation of octahedral alumina. Likewise, hydrothermal treatment of Rho has been shown to generate extra-framework aluminium species [Fischer et al., 1987]. The change in distribution of various Al species with steaming time was monitored using ^{27}Al MAS NMR. The NMR spectra for samples which had undergone different steaming times are shown in figure 4.4. The peaks were assigned using the chemical shifts given by Engelhard and Michel [1987]. The peak at 0ppm corresponds to $[AlO_6]^{n-}$ species or octahedral aluminium while that at 65ppm corresponds to $[AlO_4]^{m-}$ species or tetrahedral aluminium. It is the tetrahedral aluminium that is incorporated into the framework of the catalyst. The peak at 90 – 100ppm may be attributed to other forms of extra-framework aluminium or aluminium species which are partly removed from the framework, but has not been conclusively assigned.

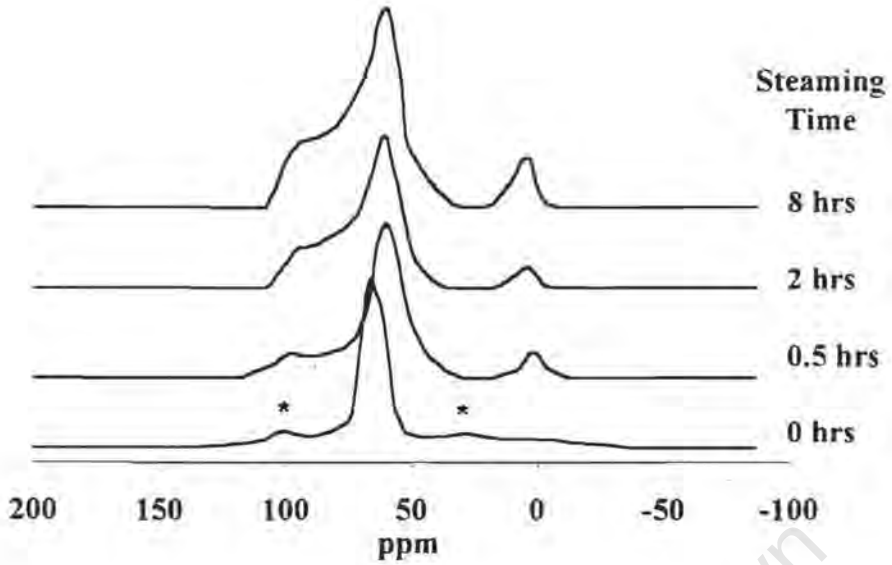

Figure 4.4: ^{27}Al NMR Spectra for increased steaming time of zeolite Rho(A).
(*=spinning side bands. T_{steam}=450°C. p_{water}=30 kPa)

Figure 4.4 indicates that the amount of extra-framework (octahedral) aluminium increases with steaming time while the framework, tetrahedral aluminium decreases. There is also an increase in the peak at 90 ppm with steaming time. It is important to note that this peak is not present in the parent (unsteamed) sample. Although there is a peak at 100 ppm in the parent sample, this is only a spinning side band. It can therefore be said that the steaming of Rho causes progressive dealumination of the catalyst structure.

4.1.3 Atomic Adsorption Spectroscopy

It had also previously been shown [O'Donnovan *et al.*, 1995], using elemental analysis, that hydrothermal treatment of Mordenite did not remove the extra-framework aluminium generated from the catalyst structure. It was also seen in that work that mild acid washing was needed to remove the extra-framework aluminium species from the framework of the catalyst.

Over Rho (B), it was also seen that percentage aluminium in the catalyst remained constant at ca. 18 wt% over the range of steaming times examined. It is therefore evident that much of

the aluminium removed from the catalyst framework is not removed from the catalyst particle. It was not possible, in this work, to tell however whether the extra-framework aluminium is situated within the pores of the catalyst or whether it has migrated to the surface.

It is well known that extra-framework aluminium species generated by hydrothermal treatment can take many forms [Corma, 1989; Martens *et al.*, 1997]. Not all of these species generated need be acidic. It is not contradictory therefore that there should be a loss in the number of acid sites, as seen by Thermal Desorption, on the catalyst without seeing a loss in the total amount of aluminium.

4.2 STRUCTURAL CHARACTERISATION

4.2.1 BET

BET analysis was performed to elucidate the changes in the porosity and surface area of the catalysts with increased hydrothermal treatment. A summary of the information obtained from the BET analysis is given in Appendix IX.

Rho

Figure 4.5 gives the total surface area as a function of steaming time observed over Rho as determined using BET analysis. The surface area is seen to increase substantially with hydrothermal treatment from ca. 460 m^2/g to over 600 m^2/g. The increase in the surface area was also seen to arise mainly from the increase in micropore surface area rather than in mesopore surface area. This large increase in surface area is unexpected. One might expect that with increased dealumination, there was an increase in the mesoporous surface area of the catalyst. As aluminium is removed from the framework, not all of the aluminium atoms that are removed can be replaced with silicon atoms [Barrer, 1982; Martens *et al.*, 1997]. This then leads to the creation of defects within the crystal structure and hence increases the mesoporous volume of the catalyst. In this study of Rho the mesopore surface area increased slightly with increased steaming (see Figure 4.6), which is consistent with the dealumination of the catalyst. It would be expected however that there would be a decrease rather than an increase in the micropore area. One explanation for this could be found in the flexibility of the Rho's crystal structure. It has already been seen how factors such as cation concentration, adsorbent levels and temperature all affect the unit cell dimensions of the catalyst [Parise *et al.*, 1984; Corbin *et al.*, 1990; McCusker, 1984a,b]. It might be expected therefore that the presence of extra-framework aluminium species within the framework could likewise affect the dimensions of the catalyst crystals and that therefore the accessibility of the pore structure would improve.

Figure 4.6 shows the change in the micro- and mesopore volume of Rho as a function of steaming time. As with the surface area, the increase in pore volume arises mainly from the

increase in micropore volume. The increase in mesopore volume seen would be due to the dealumination processes occurring which would lead to some extent to the creation of defect sites within the structure and hence give more mesopores.

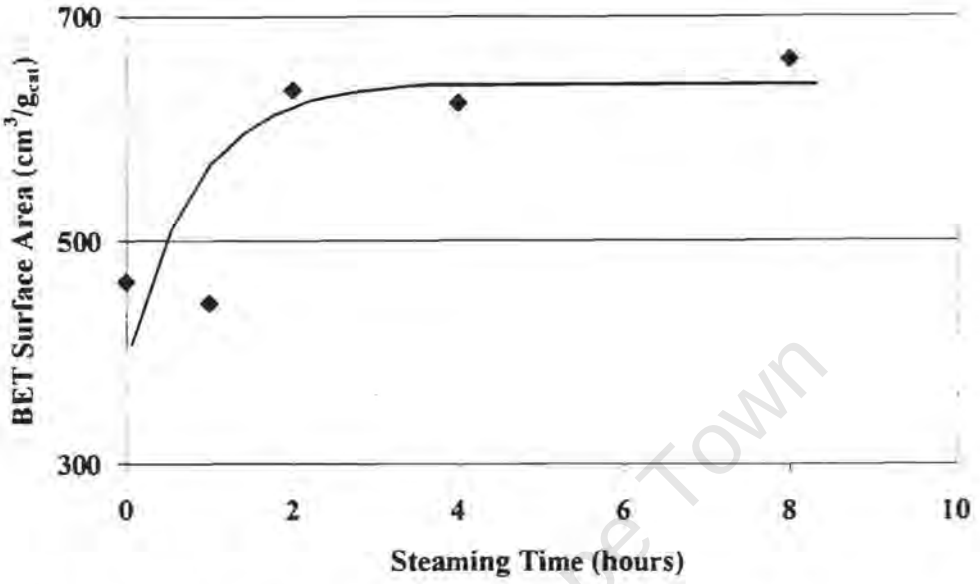

Figure 4.5: Total Surface Area of Rho (B) as a function of Steaming Time as determined by BET analysis

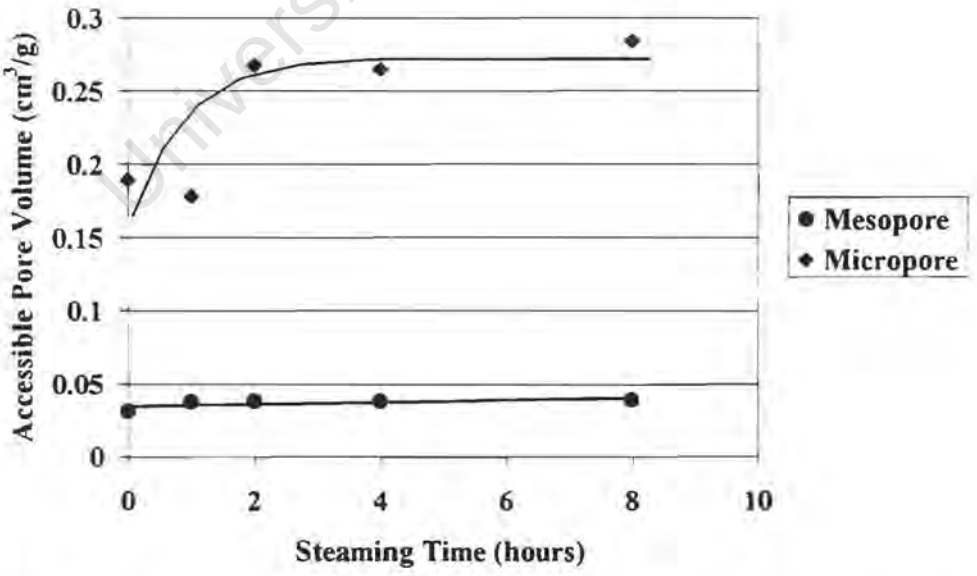

Figure 4.6: Pore volume of Rho (B) as a function of Steaming Time as determined by BET analysis

Mordenite

Figure 4.7 gives an example of the isotherms obtained over Mordenite. It can be seen that a hysteresis is observed, which indicates the mesoporosity is present in the catalyst.

Figure 4.8 shows the change in total surface area, as determined using the BET equation, as a function of steaming time. It can be seen that the total surface area decreases from 520 to 450 m^2/ g_{cat} with the major loss in surface area occurring in the initial hours of steaming. This loss of surface area is consistent with the dealumination evidenced over the catalyst with steaming time. As aluminium is removed from the catalyst structure, there will be a general loss of surface area due to some degree of structural collapse as well as diffusional resistances or pore blockage caused by the presence of extra-framework aluminium species. It had already been shown that steam treatment alone does not remove the aluminium from the catalyst structure [O'Donovan *et al.*, 1995]. Some of the extra-framework aluminium does migrate to the surface of the catalyst [Miller *et al.*, 1992]. There must however be some extra-framework aluminium within the pore structure of the catalyst.

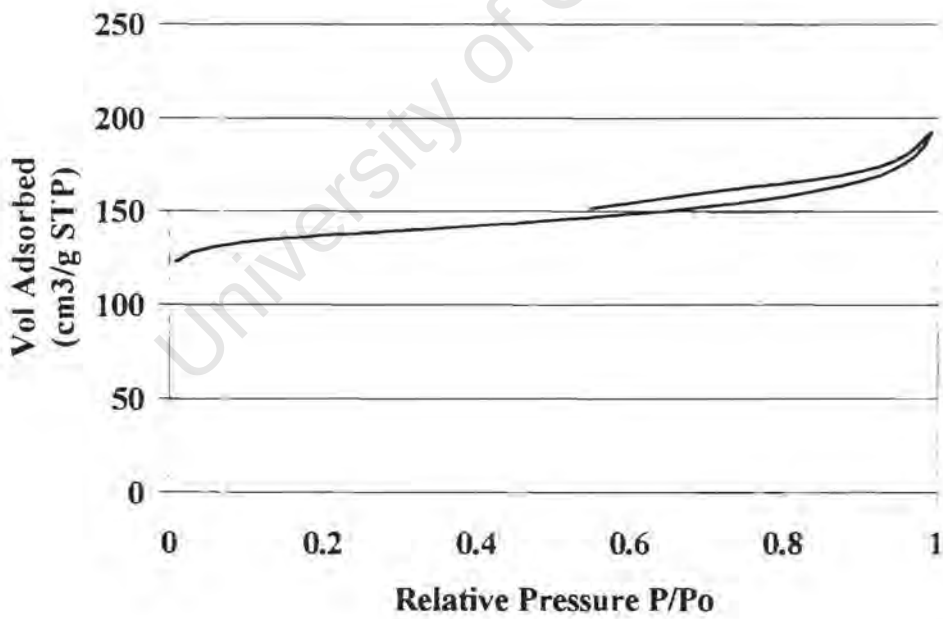

Figure 4.7: BET isotherm for unsteamed H-Mordenite

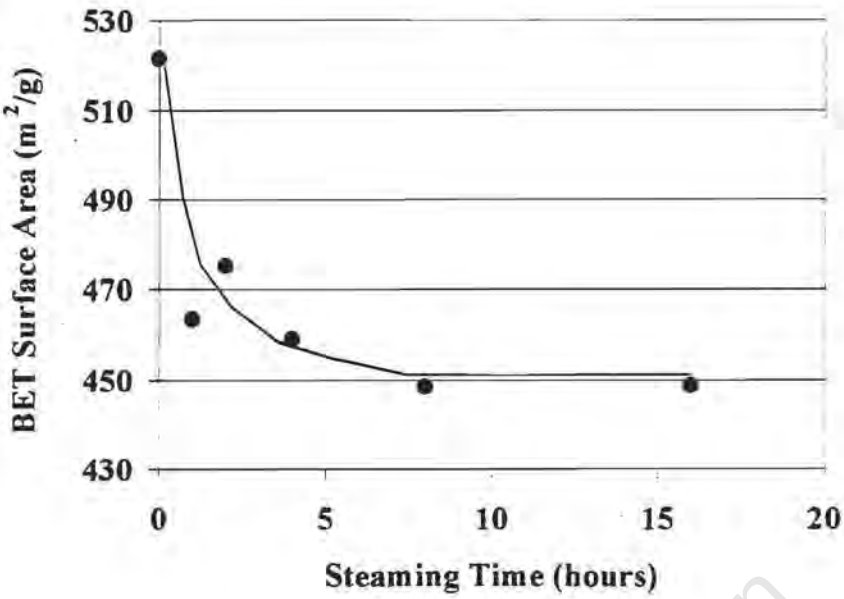

Figure 4.8: Total Surface Area of Mordenite as a function of Steaming Time as determined by BET analysis

Figure 4.9 shows the change in micro- and mesopore volume with steaming time of Mordenite. It can be seen that while there is a significant decrease in the micro-pore surface area from about 440 to 360 m^2/ g_{cat}, the mesopore surface area actually increases slightly with steaming time. This is not surprising considering that the dealumination of the catalyst will cause some defect sites and hence change the nature of the pore structure by creating more mesopores within the catalyst structure. It is a well known phenomenon that dealumination causes an increase in the mesoporosity of catalysts [e.g., Barrer, 1982; Martens *et al.*, 1997]. The response of Mordenite is therefore more typical of catalysts in general than was the response of Rho.

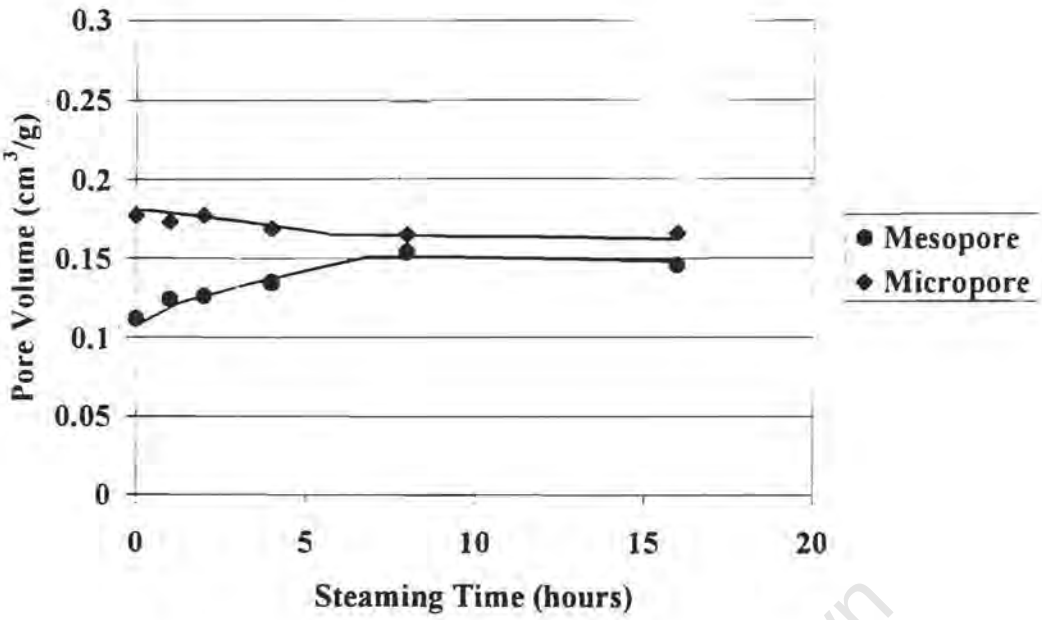

Figure 4.9: Change in Micro- and Mesopore volume of Mordenite with steaming time

4.2.2 SEM

Scanning Electron Micrographs of the catalyst samples were taken to determine if any visible change in morphology had occurred after steaming. Figure 4.10 shows the Scanning electron micrographs of Rho (A) in the untreated form and after 8 hours of steaming. It can be seen that the two samples are essentially identical in appearance.

(a) **(b)**

Figure 4.10: Scanning Electron Micrographs of zeolite Rho (A) in the untreated form (a) and after 8 hours of steaming (b)

(T_{steam}=450°C. p_{water}=30kPa)

Figure 4.11 shows the SEMs of untreated and hydrothermally treated Mordenite. It can be seen that here too there was no discernible change in morphology.

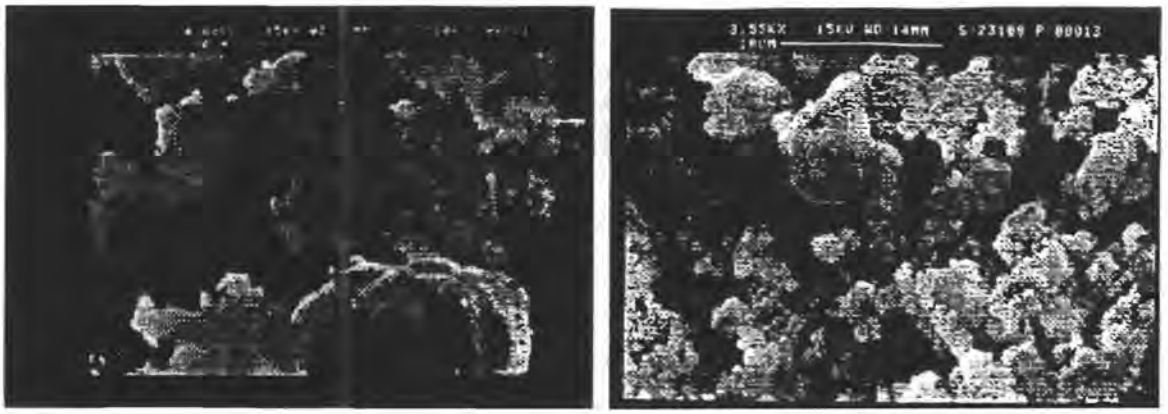

(A) **(B)**

Figure 4.11: Scanning Electron Micrographs of Mordenite in the untreated (A) form and after 1€ hours of steaming (B)

(T_{steam}=450°C, p_{water}=30kPa)

4.2.3 XRD

XRD Spectra of the catalysts were determined and it was seen that there was no change in crystal structure for either Rho or Mordenite after steaming. The XRD Spectra are given in Appendix III. As the machine used in this study has an inherently large standard deviation (Δ_{std} 2θ = 0.1°), it was not possible to determine whether or not there had been framework distortion on zeolite Rho.

4.3 RHO

The results of the hydrothermal treatment of Rho on the integral rate of consumption of methanol and ammonia as a function of steaming time are presented in figures 4.12 and 4.13. It can be seen from these graphs that the activity, as indicated by the integral rate of methanol consumption, increased from about 40 mmol MeOH/ g_{cat}.hr for the untreated catalyst to ca. 120 mmol MeOH/ g_{cat}. hr after 3 hours of steaming. This represents a threefold improvement in catalyst activity. At longer steaming times, the activity dropped off steadily. In contrast, the rate of ammonia consumption increases steadily with steaming time. At first the increase is rapid but this plateaus at longer steaming times. The selectivity to the lower substituted methylamines (see Figure 4.13), *viz.* MMA and DMA, increased from 27 and 2 mol% to 53 and 38 mol% respectively with steaming time, ultimately reaching a plateau after ca. 5 hours of steaming. The decrease in TMA selectivity from 72 to 9 mol% was very marked.

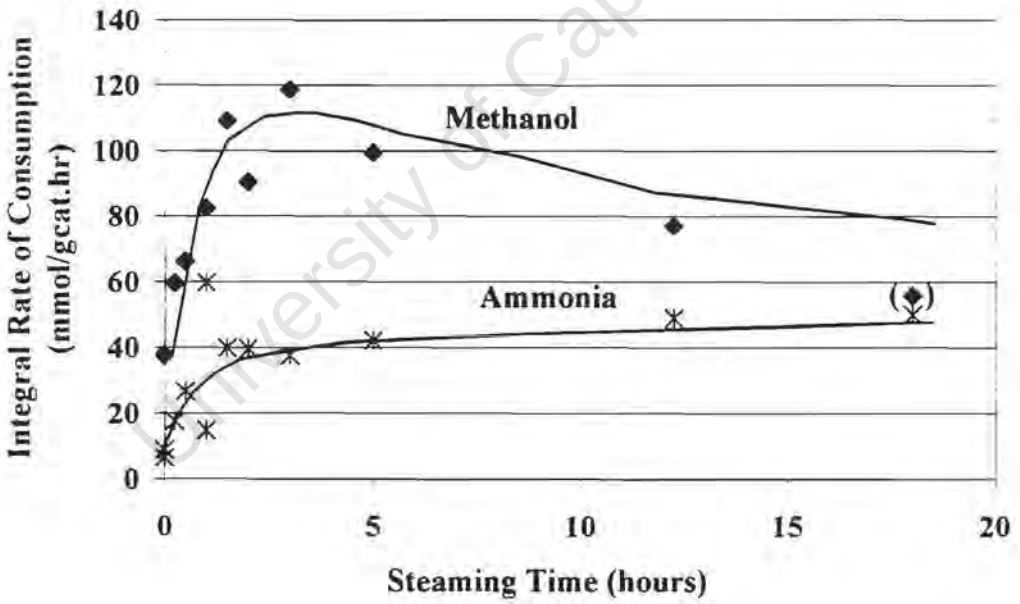

Figure 4.12: Integral rate of methanol and ammonia consumption as a function of steaming time over zeolite Rho (A).

(WHSV= 4.4 gMeOH/g_{cat}.hr. T_{steam} = 450 °C, p_{steam} = 30 kPa, $T_{reaction}$ = 325 °C, p_{MeOH} = p_{NH3} = 8 kPa, p_{tot} = atmospheric. Value in parentheses unreliable due to high carbon balance of that point)

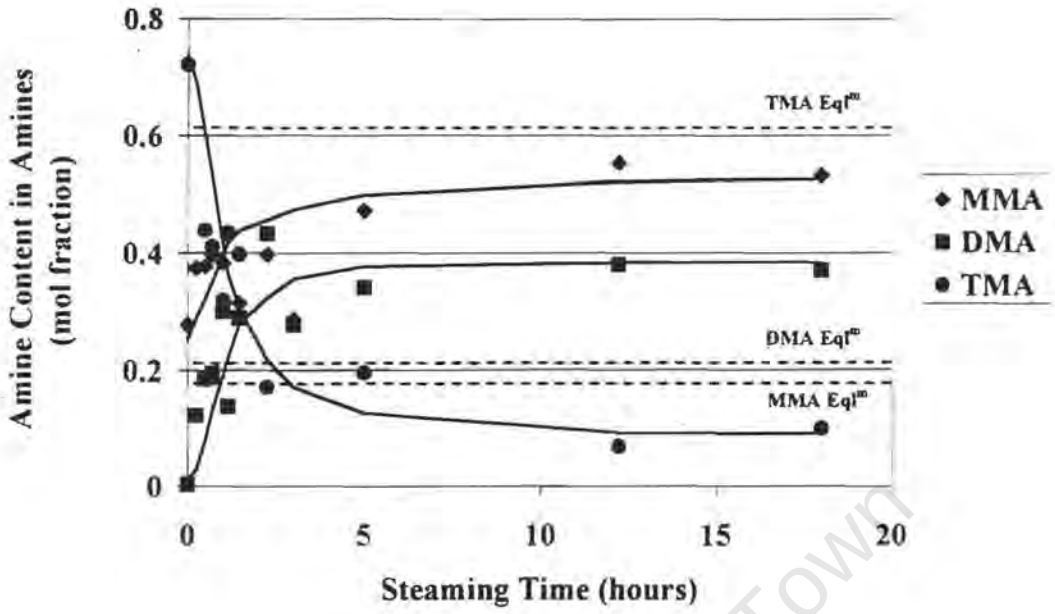

Figure 4.13: Amine content in the fraction of amines as a function of steaming time over zeolite Rho (A).

(WHSV=4.4 gMeOH/g_{cat}.hr. T_{steam} = 450 °C. p_{steam} = 30 kPa. $T_{reaction}$ = 325 °C. $p_{MeOH} = p_{NH3}$ = 8 kPa. p_{tot} = atmospheric. dashed lines represent thermodynamic equilibrium values for these reaction conditions.)

These results are similar to those obtained with the reaction - regeneration cycles, in that in both cases, the activity increased initially with treatment. Also, with both types of treatment the selectivity to MMA and DMA increased while the selectivity to TMA decreased. As both the trends in activity and selectivity were similar for the reaction - regeneration cycles and the hydrothermal treatment, it is possible to infer that the water formed during the initial stages of the calcination phase in the reaction - regeneration cycles might be the cause of the change observed over the catalysts.

There were however three major differences between the results obtained for the reaction regeneration cycles and the hydrothermal treatment. Firstly, the increase in activity is far greater with the hydrothermal treatment than with the reaction - regeneration cycles. During the hydrothermal treatment, the reaction rate increased from 40 to 120 mmol MeOH/ g_{cat}.hr

whereas the activity observed for the reaction - regeneration cycles increased from 28 to 60 mmol MeOH/ g_{cat}.hr. The different starting reaction rates are a function of the different space velocities used. The difference in the percentage increases in the reaction rates could be due to the fact that even though very mild conditions were used during the steaming procedure, they were still more severe than the *in situ* conditions generated during the calcination phase. It is well known that steaming causes dealumination of the framework of many catalysts [Corma *et al.*, 1989; 1996; Englehardt *et al.*, 1987; Burgfels and Schmidt, 1995; Martens *et al.*, 1997; Haag, 1987]. For any set of conditions, the potential to affect the catalyst is different [Scherzer *et al.*, 1984; Haag, 1987]. In general however, the more severe the steaming conditions however, the higher the amount of aluminium it is possible to remove from the framework [O'Donovan *et al.*, 1995; Burgfels *et al.*, 1995]. For any set of conditions, the potential to affect the catalyst is different. At very severe conditions however, the collapse of the crystal structure might occur. This will however be dependent on the initial concentration of aluminium in the framework as well as the structural type, as some catalysts are more inherently stable than others. For example, Mordenite is rather stable under even severe hydrothermal treatment (650°C, 1 atm steam for 24 hrs [Miller *et al.*, 1992]) whereas for example, ZK5 degrades under relatively mild treatment conditions (500°C, 4 hrs [Shannon *et al.*, 1989]).

The second difference between the reaction - regeneration cycles and the hydrothermal treatment is the fact that the activity goes through a maximum with steaming time but not with the number of cycles during reaction-regeneration. This is probably due to the fact that not enough cycles were performed to see a decrease in activity. Referring back to Figure 3.3 it can be seen that a plateau in the activity was reached after ca. 7 cycles and did not drop again by 10 cycles. It is still possible that the decrease in activity seen with the long steaming times is caused by a different phenomenon. For example, pore blockage may not occur with the reaction-regeneration cycles. This is due to the very low concentration and short exposure time to water in this method of treatment which may not be sufficient to generate the quantities of extra-framework aluminium species necessary to can diffusional constraints to the product molecules. Under steaming conditions however, enough extra-framework aluminium may be formed to cause pore blockage. This would introduce diffusional constraints and hence cause a decrease in activity. The loss of activity seen at longer steaming

times may also be due to loss of the total number of acid sites caused by the hydrothermal treatment.

It is also interesting to note that although the activity, as evidenced by the integral rate of methanol consumption, goes through a maximum with steaming time, which the selectivity does not. It rather reaches a constant value. It may therefore be stated that at least two separate changes are occurring on the catalyst with hydrothermal treatment. The rate of reaction or rather the conversion in the system and the selectivity obtained are linked. The changes observed here however do not appear to be entirely related to of each other. This will be discussed in more detail in chapter 4.5.

The final difference between these experiments with steaming and the reaction - regeneration cycles was the greater change in particularly the TMA selectivity. With hydrothermal treatment, the TMA selectivity was lowered to 10 mol%, whereas it was only lowered to 42 mol% in the reaction - regeneration cycles. Once again, this might be ascribed to the difference in severity of the treatment conditions.

4.4 MORDENITE

Initially, the hydrothermal treatment conditions used for the Mordenite were identical to those used for Rho. The reason for doing this was twofold. Firstly, it was done to test whether the similarities and differences between the reaction-regeneration cycles and the hydrothermal treatment would be the same over Mordenite as they were over Rho. If this was found not to be the case then it would mean that the comparison between the reaction - regeneration cycles and the hydrothermal treatment was specific for Rho and not for zeolites in general. The results obtained over Mordenite are shown in Figures 4.14 and 4.15. In Figure 4.14 the reaction rate change over Rho and Mordenite are plotted simultaneously for comparative purposes.

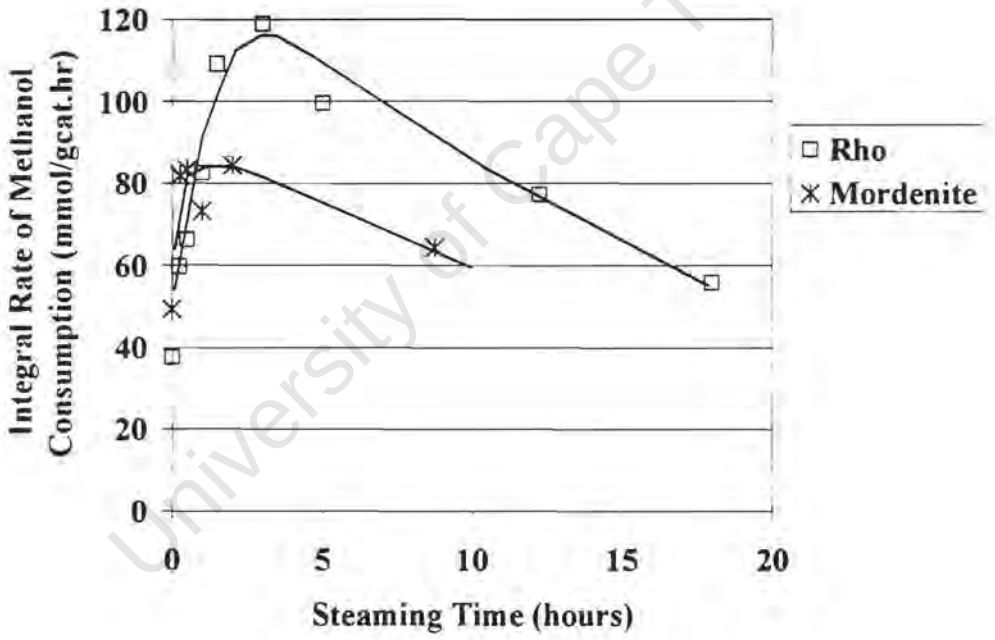

Figure 4.14: Integral Rate of Methanol Consumption over Rho (A) and Mordenite as a function of steaming time.

(WHSV=4.4 gMeOH/g_{cat}.hr, T_{steam} = 450 °C, p_{steam} = 30 kPa, $T_{reaction}$ = 325 °C, p_{MeOH} = p_{NH3} = 8 kPa, p_{tot} = atmospheric.)

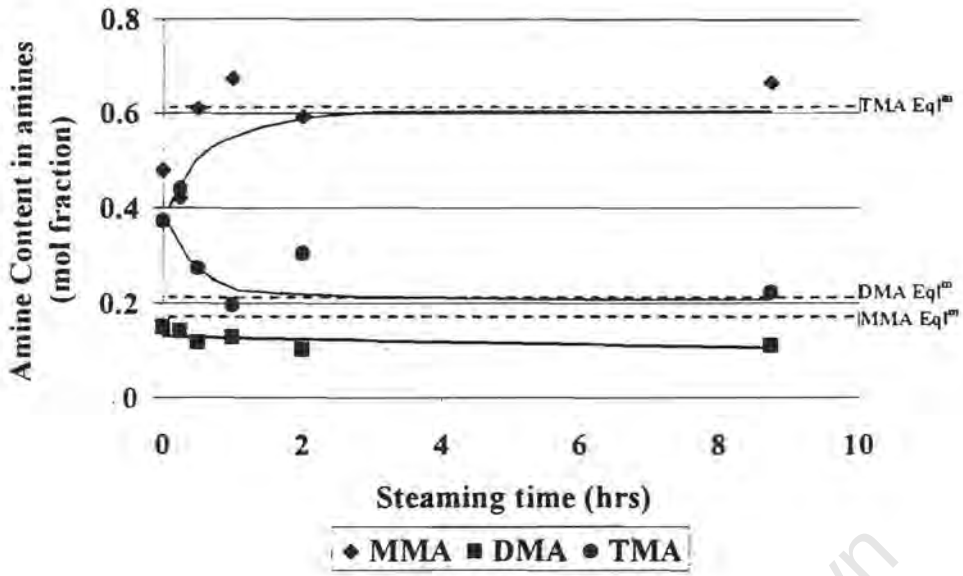

Figure 4.15: Amine content in the fraction of amines as a function of steaming time over Mordenite.

(WHSV=4.4 gMeOH/g_{cat}.hr. T_{steam} = 450 °C. p_{steam} = 30 kPa. $T_{reaction}$ = 325 °C. p_{MeOH} = p_{NH3} = 8 kPa. p_{tot} = atmospheric. dashed lines represent thermodynamic equilibrium values for these reaction conditions)

It can be seen above that with Mordenite as with Rho, the activity went through a maximum with steaming time. The methanol conversion over Mordenite increased from 36 mol% on the untreated sample to a maximum of ca. 60 mol%. At the higher steaming times, the activity dropped off. The selectivity to monomethylamine increased at the expense of the trimethylamine selectivity, which decreased with steaming time. Both the monomethylamine and trimethylamine selectivities reached a plateau after ca. 4 hours of steaming. The dimethylamine selectivity was virtually unchanged over the range of steaming times studied.

As was seen over Rho, the trends of activity and selectivity, over Mordenite in the reaction - regeneration cycles and the hydrothermal treatment, were similar. In both studies, there was an initial increase in the rate with steaming time. Also, the selectivity to monomethylamine increased while that of dimethylamine remained constant and the trimethylamine selectivity decreased. This very high MMA selectivity over Mordenite could be due to the unidimensional structure of this catalyst. The selectivity over Mordenite may therefore be

controlled by diffusion within the channels. An increase in the diffusional constraints caused by steaming would further increase the diffusional constraints within the catalyst.

The difference between the reaction - regeneration cycles and the hydrothermal treatment over Mordenite was once again similar to that of Rho in that the activity went through a maximum with steaming time but not with reaction-regeneration cycles. Over Mordenite however, the degree to which the selectivity changed was fairly similar between the two forms of treatment. The maxima in the activities were almost identical. The maximum monomethylamine selectivity was 68 % with hydrothermal treatment and 60% with the reaction-regeneration cycles. This is as opposed to Rho where the maximum monomethylamine selectivities were vastly different for the two types of treatment, *viz.* 55% with hydrothermal treatment and 30 % with reaction-regeneration cycles.

Another similarity between Rho and Mordenite is that while the activity of both catalysts passed through a maximum with steaming, the selectivity remained steady at longer steaming times. This phenomenon will be discussed in more detail in Chapter 4.5.

4.4.1 Severe Hydrothermal Treatment

The change in activity and selectivity over Mordenite when using the initial, mild steaming conditions (T_{steam}=450°C, p_{steam}=30kPa) was rather modest. It was therefore decided to investigate the use of more severe conditions. To gain these more severe conditions, both the steaming temperature and the water partial pressure were raised, the steaming temperature to 500 °C and the water vapour pressure 57 kPa. The results of these new experiments are shown in Figures 4.16 and 4.17.

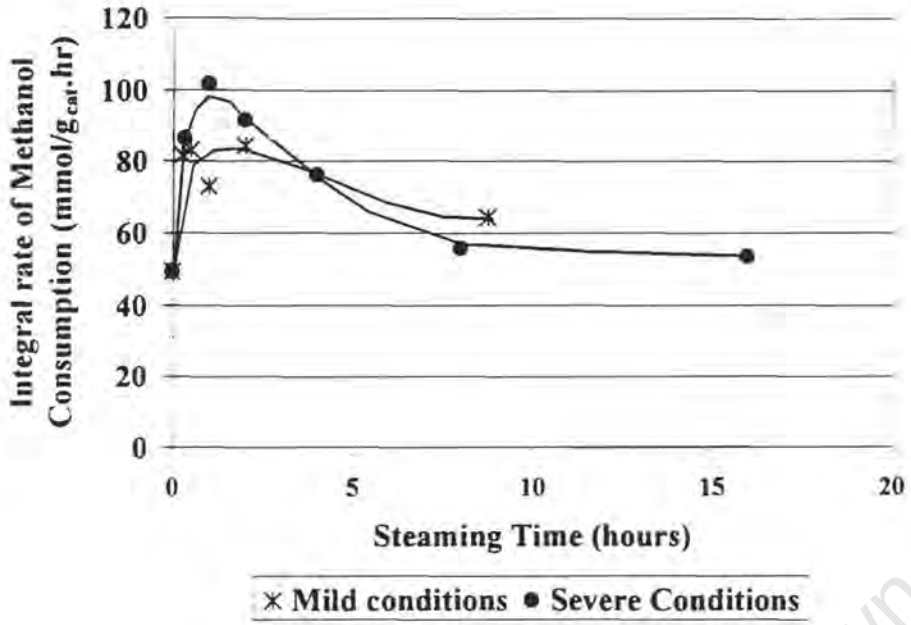

Figure 4.16: Integral rate of Methanol consumption a function of over Mordenite.

(Mild steaming: T_{steam} = 450 °C, p_{steam} = 30 kPa; Severe steaming: T_{steam} = 500 °C, p_{steam} = 57 kPa; WHSV=4.4 gMeOH/g_{cat}.hr, $T_{reaction}$ = 325 °C, p_{MeOH} = p_{NH3} = 8 kPa, p_{tot} = atmospheric.)

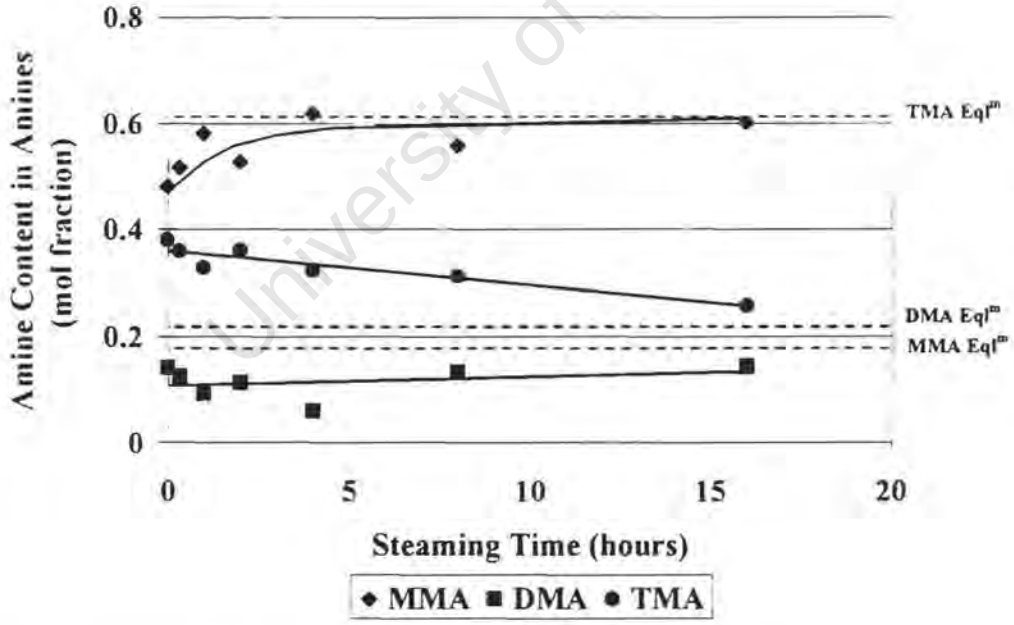

Figure 4.17: Amine content in the fraction of amines as a function of steaming time over Mordenite for severe steaming conditions.

(WHSV=4.4 gMeOH/g_{cat}.hr, T_{steam} = 500 °C, p_{steam} = 57 kPa, $T_{reaction}$ = 325 °C, p_{MeOH} = p_{NH3} = 8 kPa, p_{tot} = atmospheric, dashed lines represent thermodynamic equilibrium values for these reaction conditions.)

It can be seen that the increase in activity for the more severely treated Mordenite is somewhat more than that of the more mildly treated one. Here, the increase in conversion is doubled whereas for the mild steaming conditions, the increase was by 70%. The position of the maximum in activity is also earlier, at 1 hour, compared to the previous case where the maximum occurred after only 2.5 hours. In this study, as in the case of the milder hydrothermal treatment, the change in amine selectivity is not very significant. A very slight decrease in TMA selectivity is seen.

It may therefore be concluded that not much benefit is gained from using more severe steaming conditions on the Mordenite.

4.5 DISCUSSION

4.5.1 Contradiction Between Activity and Selectivity

As has been shown in this chapter, in both the case of the hydrothermal treatment and reaction - regeneration cycles over Rho and Mordenite, there was an increase in activity accompanied by an increase in selectivity to lower substituted methylamines. These trends are seemingly contradictory for a series type reaction, as it would be expected that with increasing methanol conversion there would be a decrease rather than an increase in the selectivities of monomethylamine and dimethylamine. In a set of series type reactions, the selectivity to products vs. reactant conversion would be expected to follow the trend shown in Figure 4.18. In this type of system, as the conversion of the primary reactant increases, the yield of the products changes, with the final product in the series increasing.

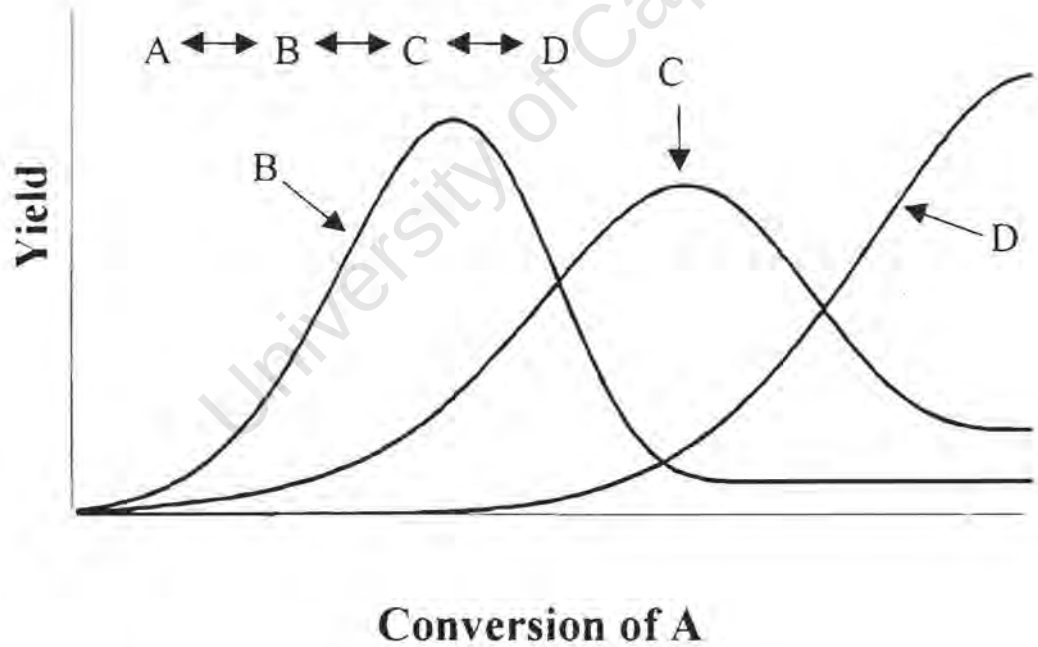

Figure 4.18: Theoretical Progression of Yield vs. Conversion for a series of three reversible reactions

The results seen with hydrothermal treatment of Rho however show a decreased selectivity to trimethylamine, the final product, when the ammonia conversion increases. This means that the selectivity change seen upon hydrothermal treatment in not merely a thermodynamic effect. The changes in activity and selectivity with treatment must therefore be separate phenomena and when an explanation for these changes is sought at least two changes to the catalytic properties of the Rho and Mordenite should be found.

Alternatively, the above results may be due to the fact that the mechanism is not a simple series type. This would fit in with the mechanisms proposed for this reaction [Gründling *et al.*, 1996b,1997; Ernst and Pfeifer, 1992]. However, this still does not explain the increasingly non-thermodynamic distribution of amines seen with increased conversion. Initially, without treatment, there is more TMA produced than MMA or DMA, which would be expected from thermodynamic equilibrium, but as the treatment, and hence the change in the catalyst progresses, a far smaller percentage of TMA is seen.

4.5.2 Rho

Hydrothermal treatment of Rho leads to significant changes in the catalyst, both in terms of the number of acid sites and the pore volume. It was observed that there is an overall loss in acidity from the catalyst with increased steaming time (cf. Thermal Desorption experiments). What is significant to note however is that this loss has occurred mainly from the weaker of the two acid sites present on the catalyst. At the same time, the ^{27}Al MAS NMR studies of the steamed samples showed a change in the distribution of aluminium species within the catalyst with increased steaming. It is seen that while the unsteamed sample contains primarily tetrahedral aluminium, there is a progressive increase in the amount of octahedral aluminium with steaming time as well as the formation of a third aluminium species that was not present in the parent catalyst. It is possible for some of the extra-framework aluminium species to be neutral [Corma, 1989]. This would then account for the loss in total number of acid sites seen over the catalysts. Also, the formation of aluminium agglomerate species, i.e., Al_xO_y would result in a loss of the total number of acid sites.

From a structural point of view it has been seen that there is an increase in the surface area and pore volume of Rho with increased steaming. More importantly, there is no significant change seen in the mesopore volume and as such the increase in pore volume seen is almost solely caused by an increase in the micropore volume. A possible explanation for this is the structural flexibility of Rho. It is well known that the pore dimensions of Rho are a strong function of cation concentration, adsorbent levels and temperature [Parise *et al.*, 1984a,b; Corbin *et al.*, 1990; McCusker, 1984a,b]. The is also evidence that hydrothermally treatment Rho shows a larger cell constant, a = 15.0602 Å [Fischer et al., 1987], than the untreated, dehydrated catalyst, a = 14.87 Å [Parise et al., 1984b]. This would then be consistent with the increase in especially the micropore volume of the catalyst, as a change in the unit cell dimensions would not affect the mesopore volume. The XRD and SEMs have also shown that at the levels of hydrothermal treatment used here, there is no measurable loss of crystallinity or change in crystallite morphology.

From the reaction studies over the Rho steamed for various times it has been seen that there is a significant change in the catalyst's performance both in terms of activity, as evidenced by the rate of consumption of both methanol and ammonia, and in terms of the selectivity where an increase in the selectivity to the lower substituted amines, MMA and DMA was seen with

steaming time. The two major points of interest in these reaction studies are the decrease in methanol conversion seen at prolonged steaming times as well as the shift in the selectivity, apparently away from thermodynamic equilibrium with steaming time.

The increase in conversion can not be related to the acid site concentration, as the acid site concentration decreased while there is an increase in inactivity. The increased conversion must therefore be related to one of the other changes occurring on the catalyst. The one possibility is the increased pore volume seen in the catalyst since increased accessibility of the pore structure obtained could give rise to an increase in activity. This does not however explain the change in selectivity seen with increased hydrothermal treatment.

It is possible that the hydrothermal treatment causes a change in the adsorption behaviour of the catalyst by affecting the acid site strength and hence the affinity for different adsorbates. This would cause a change in the distribution of surface species on the catalyst. The local concentration of species at the catalyst surface would naturally affect the local equilibrium of the system and in turn the product distribution observed. In addition, a change in the local concentrations can affect the activity of the system. A similar situation was observed by Grundling *et al.* [1996] over modified Mordenite where an increase in the concentration of the higher substituted methylamines at the surface was found to lead to greater activity due to the increased nucleophilic behaviour of these species.

The decrease in methanol consumption at longer steaming times may be ascribed to the formation of extra-framework alumina within the catalyst. As large amounts of EFAl are formed, as seen from the NMR experiments, this may cause blockage of the pore structure of the catalyst and hence a lower accessibility to the reactant or product molecules. This would be in agreement with the findings of Segawa and Tachibana [1993] who showed in the reaction of methanol and ammonia over Mordenite that dealumination of the catalyst lead to a loss of activity. Similar effects have been seen with other catalysts [Bamwenda *et al.*, 1994,1995; Miller *et al.*, 1992]. The eventual decrease in activity observed may also be due to the acid site loss. It has been proposed that cationic extra-framework aluminium species lower the activity of catalysts by partial charge balancing of catalyst and hence the excluding protons from the catalyst surface [Kubelkova *et al.*, 1992].

It may be postulated that there are several different changes occurring on the catalyst with hydrothermal treatment. Particularly, there are two factors affecting the activity. One, the

increased accessibility of the pore structure and/or a change in the adsorption behaviour are causing the increase in activity seen especially at shorter steaming times. In contrast, there is also some catalyst degradation, in the form of acid site loss or general structural deterioration that causes a decrease in activity. The change in selectivity may or may not be related to the change in activity. In Chapter 5, the change in the adsorption behaviour of the catalysts will be examined in more detail.

The initially high trimethylamine selectivity observed, which is above that expected from equilibrium thermodynamic considerations, is not unique to this work. There have been other reports of trimethylamine selectivities higher than thermodynamic equilibrium. For example, Keane *et al.* [1987], report trimethylamine selectivities of 73 and 69 mol% over HY and Mordenite respectively for an equimolar feed of methanol and ammonia at 325°C. At these conditions, the expected trimethylamine selectivity is 62 mol%. Also, Shannon *et al.* [1988], over Pollucite at 93% methanol conversion, and Ilao *et al.* [1996], over H-ZSM-5 at 80% methanol conversion, reported trimethylamine selectivities greater than 62 mol% at reaction temperatures of 325°C.

4.6.2 Mordenite

In the case of Mordenite it has been seen in this work that the hydrothermal treatment causes some overall loss in acidity but more importantly that there is a definite generation of a second, weaker acid site with steaming time. There was also dealumination of Mordenite seen with hydrothermal treatment. The change in the acidity of the Mordenite as opposed to the Rho with steaming time is markedly different. Whereas Rho underwent acid site loss without the formation of new acid sites, Mordenite showed a shift in the type of acid site, as seen with the Thermal Desorption experiments, with a loss in the number of acid sites which is less than for Rho.

The structural changes over Mordenite were likewise different to those over Rho. Here, a decrease in the surface area was seen with increased hydrothermal treatment, most of which is due to a loss of micropore surface area. As with the Rho, this catalyst does not show discernible changes in crystallinity or morphology.

In the reaction studies, Mordenite shows some improvement in activity after hydrothermal treatment. This is not however as much as that seen over Rho. The change in selectivity observed over Mordenite is likewise less noticeable. Particularly, there is no increase in the selectivity to DMA observed. Even using more severe steaming conditions did not further improve the performance of the Mordenite.

In general, the effect of the hydrothermal treatment on Mordenite is somewhat less than on Rho. The integral rate of methanol consumption increases by ca. 70% to 100% with the Mordenite, depending on the severity of steaming, while the increase over Rho is almost 200%.

It may therefore be concluded that Rho was far more greatly affected by the hydrothermal treatment than was the sample of Mordenite. This was not all that unexpected or unreasonable for two reasons. Firstly, it is known that the crystal structure of Mordenite is inherently very stable and is stable at quite severe treatment conditions [Miller *et al.*, 1992]. Rho, on the other hand suffers structural collapse at moderately severe treatment conditions [Shannon *et al.*, 1988a]. It may therefore be said that the framework of Mordenite is more stable than that of Rho. The large degree to which the framework of Rho distorts upon the insertion of different adsorbates [McCusker, 1984; Parise *et al.* 1984; Corbin *et al.*, 1990] is another strong indication of the ease by which the structure of this catalyst may be altered. Secondly, the percentage aluminium in the framework of Rho is higher than that in the Mordenite. The silicon/aluminium ratio of the Rho was 6 whereas that for the Mordenite was 10. When there is more aluminium in the framework, as with the Rho, it is easier to remove larger quantities of that aluminium from the framework.

Adsorption Studies

5. ADSORPTION STUDIES

In the previous two chapters it was shown that hydrothermal treatment caused dealumination of the zeolites Rho and Mordenite. It was also shown how this form of treatment influenced the performance of the catalysts for the methanol amination reaction in terms of their activity, which increased, and selectivity, which shifted towards the lower substituted methylamines. This and the characterisation results indicated that more than one change was occurring over the catalysts, specifically it appeared that contradictory changes were occurring in the catalysts with steaming and hence that there was an optimum degree of hydrothermal treatment at which the best combination of activity and selectivity could be achieved

In other work, Shannon *et al.* [1984] noticed that there was improvement in the structural stability of zeolite Rho after steaming. In a study of ZSM-5 and T-zeolite catalysts, Hermann *et al.* [1988] assume that the extra-framework aluminium (EFAl) remains within the interior of the catalyst and thus improves selectivity by increasing diffusional constraints. Increasing the diffusional constraints within the catalyst most severely affects the largest amine, TMA, and therefore allows this to be reconverted within the catalyst pore structure to lower substituted amines. There are however researchers who disagree that extra-framework aluminium is beneficial to the methanol amination reaction [Shannon *et al.*, 1988; Segawa and Tachibana, 1993; Ilao *et al.*, 1996]. They found that dealumination hindered the catalyst performance by decreasing the catalyst activity. They also found that γ-alumina (amorphous alumina), which can be formed during the dealumination process [Corma, 1989], produced exclusively dimethyl ether.

Although it has been shown that hydrothermal treatment causes dealumination, which could in turn increase the diffusional constraints, there are a number of conflicting observations that have arisen from this work. Firstly, the improvement in both methanol and ammonia conversion with increasing extent of dealumination by steaming would seem to indicate that there is not an increase in the diffusional constraint. If diffusional constraints played a role here, the increase in conversion should then indicate a decrease in the diffusional constraints. The change in selectivity to the smaller molecules, *viz.* monomethylamine and dimethylamine, on the other hand is consistent with an increase in the diffusional constraints. Another reason for the change in selectivity could be a change in the concentration within the

pores that would shift the local equilibrium distribution and hence change the observed selectivity.

In this study, single component adsorption studies of methanol, ammonia and water as well as binary adsorption studies of the methanol/ammonia and methanol/water pairs are reported with a view to elucidating the change in reaction behaviour of zeolites Rho and Mordenite upon steaming from a different point of view. The results of the adsorption studies of each catalyst will first be considered individually and then compared. The results of all adsorption experiments are tabulated in appendix X. The method of determining the amounts of chemisorption versus physisorption has been described in chapter 2.

5.1 RHO

5.1.1 Pure Component Adsorption

The adsorption studies were performed on Rho(B). The adsorption capacities for the three pure compounds were determined as a function of steaming time. The total amount adsorbed of all pure components is shown in Figure 5.1. It can be seen that each curve passes through a maximum after a steaming time of ca. 2 hours. Table 5.1 shows the adsorption capacity of the parent catalyst and the maximum adsorption capacity obtained over zeolite Rho(B) after 2 hours of steaming at 450 °C. The relative increases in the amount of methanol and ammonia adsorbed were identical (at ca. 34%). The increase in the amount of water adsorbed is however relatively more at 50%.

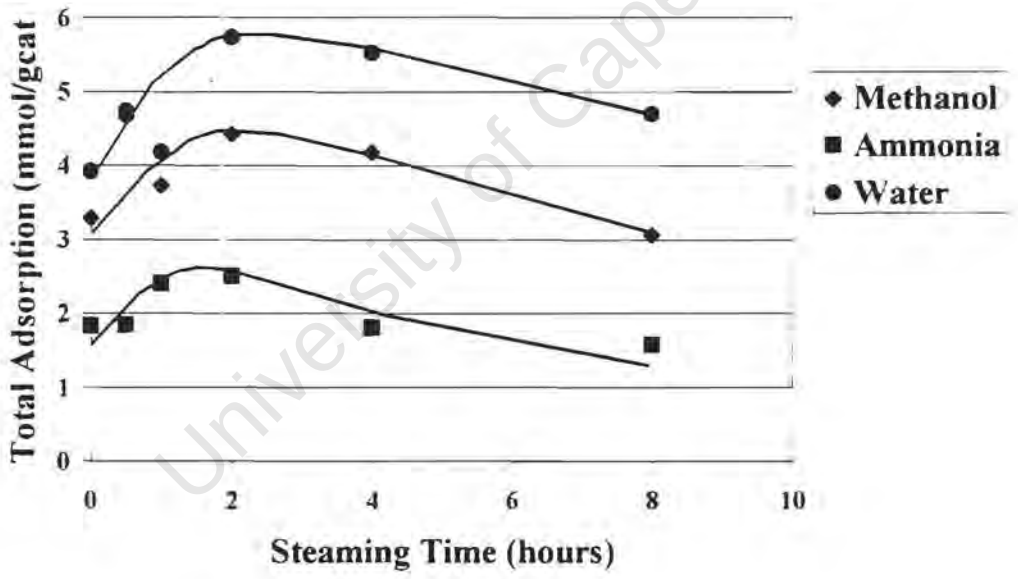

Figure 5.1: Total adsorption capacity of pure compounds as a function of steaming time for zeolite Rho(B).

(T_{ads} = 100°C. p_{H2O} = 2.5 kPa. p_{MeOH} = 2 kPa. p_{NH3} = 0.6 kPa. balance He. P_{tot} = atmospheric)

Table 5.1: Increase in adsorption capacities of pure compounds over zeolite Rho(B) with steaming time.

(T_{ads}=100°C, p_{MeOH}=2 kPa, p_{NH3}=0.6 kPa, p_{H2O}=2.5 kPa)

Adsorbate	Initial Adsorption Capacity (mmol/ g_{cat})	Maximum Adsorption Capacity (mmol/g_{cat})	Percentage Increase
Ammonia	1.8	2.4	33
Methanol	3.2	4.3	34
Water	3.8	5.7	50
Methanol & Water	5.4	8.0	47
Methanol & Ammonia	3.2	4.3	24

The maximum observed in the total adsorption capacity over Rho might be explained in terms of the pore structure of the catalyst with steaming time. As the catalyst is dealuminated, there is an increase in the pore volume, as seen by the BET measurements (cf. Chapter 4.2). This increased pore volume in the initial stages of hydrothermal treatment leads to the initial increase seen in the adsorption capacity. The increase in pore volume, as was discussed in Chapter 4, may be due to the flexibility of the framework of Rho, which is known to be highly flexible and dependent on the presence of cations, temperature and adsorbates [Parise *et al.*, 1984; Corbin *et al.*, 1984,1990; McCusker, 1984a,b]. It is not unreasonable to expect therefore that the presence of extra-framework aluminium would likewise affect the pore structure of Rho.

It has already been discussed how any cationic extra-framework aluminium species could cause partial acid site loss due to it taking over the function of charge balancing the catalyst framework [Kubelkova *et al.*, 1989]. This leads to the decrease in adsorption capacity with longer times on stream. Larger amounts of extra-framework aluminium can also lead to decreased adsorption capacity due to pore blockage as has been seen with other catalysts [Bamwenda *et al.*, 1994,1995; Miller *et al.*, 1992].

Figure 5.2 shows the chemisorbed component of the total adsorption. The amount chemisorbed, in a similar manner to the total adsorption, reached a maximum after about 2 hours and then decreased at longer steaming times. This is consistent with the Thermal Desorption experiments, which also showed a decrease in the ammonia in adsorption

capacity at longer steaming times, although these two experiments were performed at different conditions. The Thermal Desorption experiments did not however show an initial increase in ammonia adsorption capacity but rather seemed to remain essentially constant in the initial steaming times. This might be due to the fact that in the Thermal Desorption experiments measure the amount chemisorbed from desorption whereas the adsorption experiments measure the chemisorption amount from the difference between total adsorption and physisorption. The amount of physisorbed ammonia in the adsorption experiments was difficult to determine and contains a large error.

The decrease in chemisorption capacity can be ascribed to the decrease in the number of acid sites with increasing steaming time. In theory, each framework aluminium atom corresponds to one acid site. It is also expected that each chemisorbed molecule is attached to one acid site and that there is no more than one molecule per site. Therefore as the dealumination causes a loss in the number of acid sites, the chemisorption capacity will decrease. What is interesting to note is that the amounts of pure methanol and water chemisorbed are substantially higher than the amount of pure ammonia chemisorbed. The ammonia chemisorption corresponds to the number of acid sites as seen by Thermal Desorption (1.77 mmol/g_{cat}). This indicates that the amounts of methanol and water chemisorbed are more than the number of acid sites, indicating multi-layer adsorption.

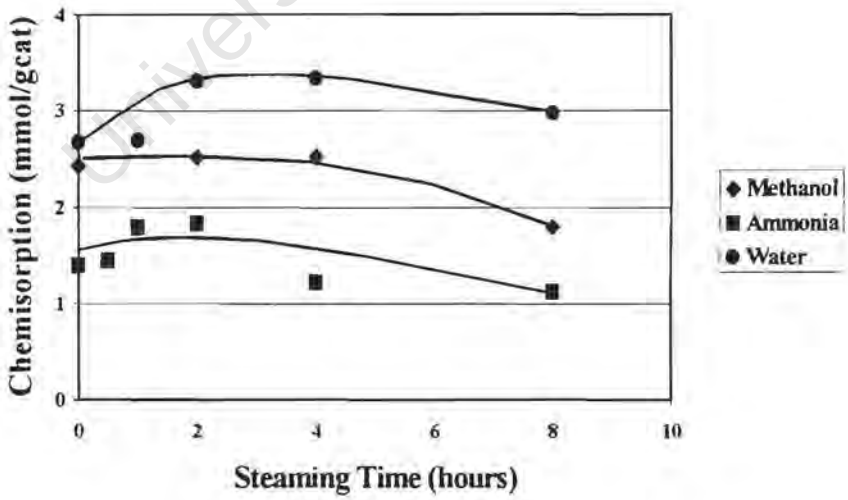

Figure 5.2: Chemisorption capacity of pure compounds as a function of steaming time for zeolite Rho(B).

(T_{ads} = 100°C, p_{H2O} = 2.5 kPa, p_{MeOH} = 2 kPa, p_{NH3} = 0.6 kPa, balance He, P_{tot} = atmospheric)

Figure 5.3 shows the physisorbed component of the total adsorption. It is seen that the physisorbed amount of ammonia is low in comparison to that of the other two compounds and seems to be less dependent on steaming time. Initially, the physisorbed amounts of methanol and water increase rapidly with steaming time and pass through clear maxima at 2 hours of steaming before declining. The large differences in the amounts of the pure compounds physisorbed is probably due to the differences in the partial pressures used. As far as the physisorbed amount is concerned, there is a direct relationship between the partial pressure of the gas and the amount adsorbed. This is confirmed by the ratios of the initial amounts adsorbed. The ratio of ammonia: methanol: water in the gas phase was 1:2.9:3.6 and the ratio of the physisorbed amounts was 1: 2.3:3.1. These ratios are similar, though not exactly the same.

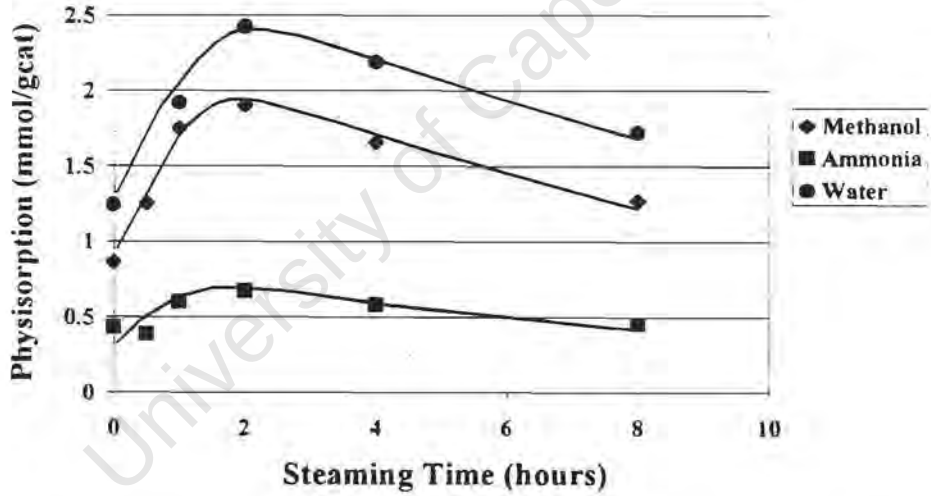

Figure 5.3: Physisorption capacity of pure compounds as a function of steaming time for zeolite Rho(B).

(T_{ads} = 100°C, p_{H2O} = 2.5 kPa, p_{MeOH} = 2 kPa, p_{NH3} = 0.6 kPa, balance He, P_{tot} = atmospheric)

5.1.2 Binary Adsorption Studies

Although the adsorption of pure compounds yields valuable information on the adsorption capacity of zeolites, the preference of the zeolite for one compound or the other, *viz.* the relative strength of adsorption, must be considered if adsorption measurements are used to explain the behaviour of the zeolite in a reaction mixture. Two mixtures were chosen for the studies of binary adsorption behaviour, *viz.* methanol/water and methanol/ammonia.

Methanol - Water

Firstly, a mixture of methanol and water in order to obtain information as to the changing hydrophobicity of the catalyst [Kiss *et al.*, 1991; Weitkamp *et al.*, 1993]. Figure 5.4 shows the ratio of total methanol to water adsorption over zeolite Rho as a function of steaming time. It can be seen that the hydrophobicity of the catalyst goes through a sharp maximum at ca. 2 hours steaming time. The strong decrease in the ratio after two hours steaming might be ascribed to the greater affinity of water for the extra-framework aluminium species.

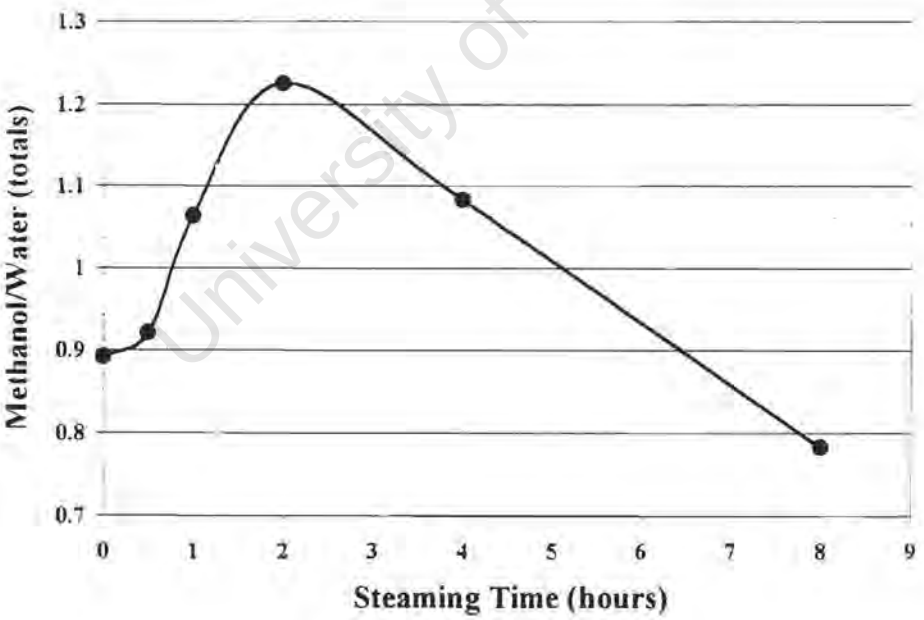

Figure 5.4: Ratio of total Methanol to Water adsorption over zeolite Rho(B) vs. steaming time.

(T_{ads} = 100°C, p_{H2O} = 2.5 kPa, p_{MeOH} = 2 kPa, balance He, P_{tot} = atmospheric)

Figure 5.5 shows the ratio of methanol to water chemisorption over Rho as a function of steaming time. It can be seen that the ratio of chemisorbed methanol to water initially remains constant but decreases with longer steaming times. This means that with prolonged hydrothermal treatment there is an increase in the relative amount of water chemisorbed at the surface. On this catalyst, this trend is not however very pronounced. It has already been established that the hydrothermal treatment causes dealumination of the catalyst. As the aluminium is removed from the framework, it forms a variety of species [Corma *et al.*, 1989; Martens *et al.*, 1997]. When completely dehydrated, these would have the general formula $[Al_xO_y]^{n-}$. These species can react with water to form species of the form $[Al_xO_yH_z]^{m-}$. This reaction can explain the increased water adsorption seen with increasing dealumination.

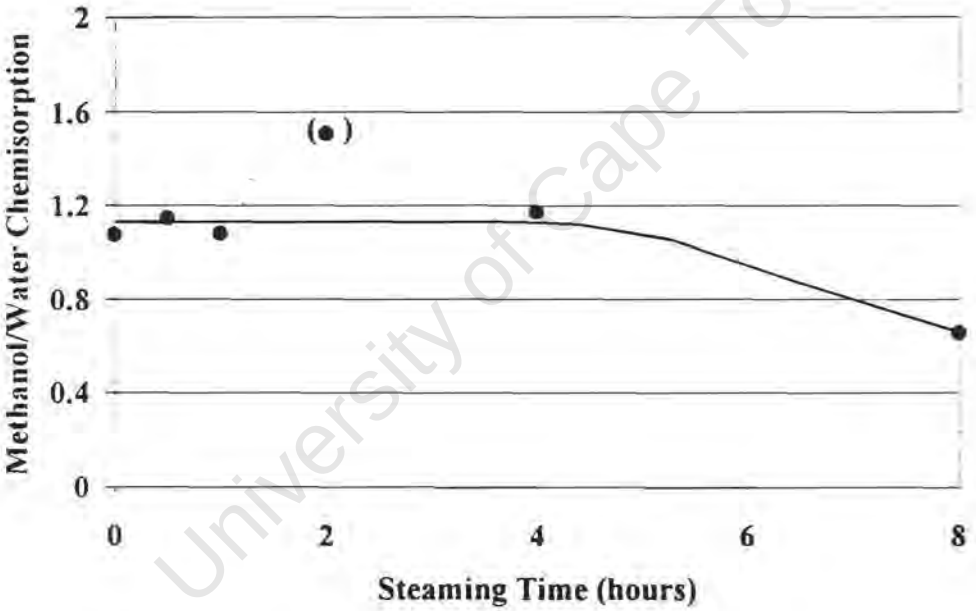

Figure 5.5: Ratio of total Methanol to Water adsorption over zeolite Rho(B) vs. steaming time.

(T_{ads} = 100°C, p_{H2O} = 2.5 kPa, p_{MeOH} = 2 kPa, balance He, P_{tot} = atmospheric)

Ammonia - Methanol

The second binary mixture tested was that of methanol and ammonia. Figure 5.6 shows the ratio of chemisorbed ammonia to methanol over zeolite Rho as a function of steaming time for the binary mixture. The amount of ammonia relative to methanol chemisorbed is high and increases with increasing steaming time. Ammonia is a stronger base than methanol and the generation of stronger acid sites (cf. Thermal Desorption results in Chapter 4.1) should favour the chemisorption of the stronger base. This increase in the ratios of chemisorption was also found to be purely a function of the changing nature of the acid sites and not a function of the adsorption capacities of the two molecules.

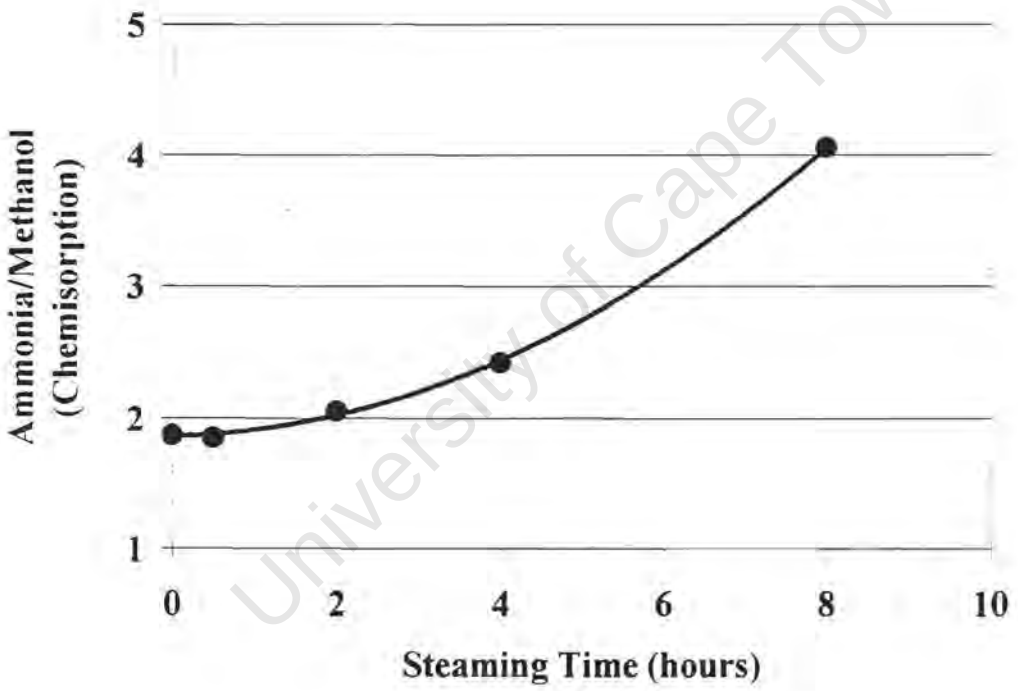

Figure 5.6: Ratio of ammonia to methanol chemisorption over zeolite Rho(B) vs. steaming time.

(T_{ads} = 100°C, p_{MeOH} = 2 kPa, p_{NH3} = 0.6 kPa, balance He, P_{tot} = atmospheric)

Figure 5.7 shows the ratio of physisorbed ammonia to methanol, i.e., ammonia and methanol which is not bonded to the catalyst surface, as a function of steaming time. It can be seen that the trend observed in the physisorbed ratios is opposite to that which was observed in the chemisorption in that the ratio of physisorbed ammonia to methanol decreases with increasing steaming time. This means that the amount of methanol physisorbed is much higher than that of ammonia and increases relative to ammonia with steaming time.

For the untreated sample (0hrs steaming) the relative concentrations physisorbed in the pores is approximately that in the gas phase. Upon steaming, the amount of ammonia physisorbed in the pores relative to that of methanol is less than in the gas phase. The composition of physisorbed species within the pores is thus richer in methanol.

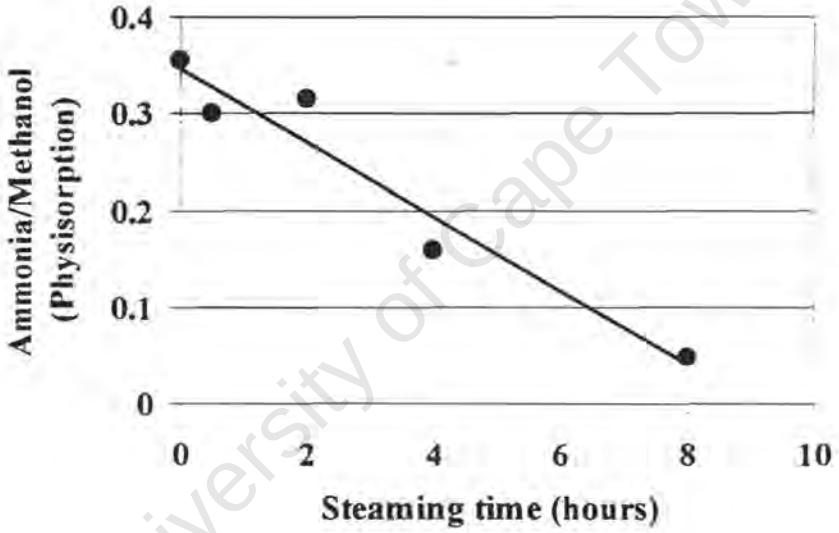

Figure 5.7: Ratio of ammonia to methanol physisorption over zeolite Rho(B) vs. steaming time.

(T_{ads} = 100°C, p_{MeOH} = 2 kPa, p_{NH3} = 0.6 kPa, balance He, P_{tot} = atmospheric)

5.2 MORDENITE

Similar adsorption studies to those carried out over Rho were carried out over Mordenite. The Mordenite samples studied here are those that were subjected to the more severe hydrothermal treatment regime, *viz*. $T_{adsorption}$ = 500°C, p_{H2O} = 57 kPa. The reaction studies corresponding to these samples are shown in Chapter 4.4.1.

5.2.1 Pure Component Adsorption

The adsorption capacities of the three pure compounds on Mordenite as a function of steaming time are shown in Figure 5.8. What is seen in this figure is that there is a systematic decrease in the amount of all compounds adsorbed with increased steaming time. In particular, the responses of water and methanol adsorption to hydrothermal treatment, which are very similar, show an initially rapid drop in the total amount adsorbed. The response of the total ammonia adsorption capacity to hydrothermal was however more linear. These results are in contrast to the results obtained over Rho where a maximum in the adsorption capacity with steaming time was seen. Table 5.2 shows the initial total adsorption capacity and the total adsorption capacity after 16 hours of steaming. It can be seen that the most significant decrease is seen in the amount of water adsorbed.

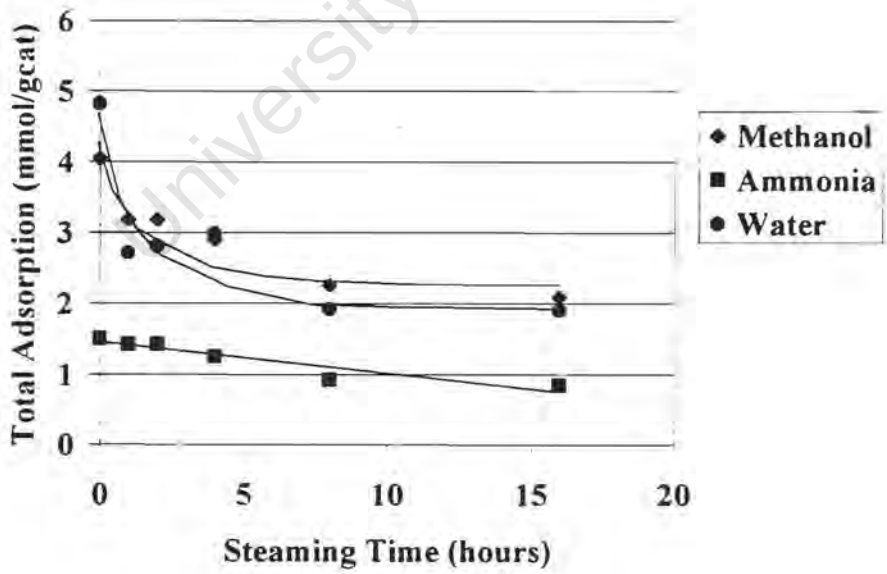

Figure 5.8: Total adsorption capacity of pure compounds as a function of steaming time for Mordenite.

(T_{ads} = 100°C, p_{H2O} = 2.5 kPa, p_{MeOH} = 2 kPa, p_{NH3} = 0.6 kPa, balance He, P_{tot} = atmospheric)

Table 5.2: Decrease in adsorption capacities of pure compounds over Mordenite with steaming time.

(T_{ads}=100°C, p_{MeOH}=2 kPa, p_{NH3}=0.6 kPa, p_{H2O}=2.5 kPa, values in parentheses estimated)

Adsorbate	Initial Adsorption Capacity (mmol/ g_{cat})	Final Adsorption Capacity (mmol/ g_{cat})	Percentage Decrease
Methanol	4.04	2.09	48
Ammonia	(1.5)	0.84	44
Water	4.84	(1.92)	60
Methanol & Water	4.44	3.23	27
Methanol & Ammonia	4.17	2.26	46

The behaviour of especially the methanol and water total adsorption as a function of steaming time closely follows the results of the BET measurements which showed a decrease in the surface area (cf. Figure 4.8). It is hardly surprising that as the surface area and pore volume decrease that so does the total adsorption capacity of the catalyst.

Figure 5.9 shows the chemisorption capacity of Mordenite as a function of steaming time. It can be seen that the response of the chemisorption of all three compounds is similar. All the adsorbates show an initially fast decrease in chemisorption capacity, which slows down but still decreases with further steam treatment. These results are similar to the Thermal Desorption results, which showed a similar decrease in the adsorption of ammonia, though the adsorption conditions of the Thermal Desorption were different ($T_{ads\ Thermal\ Desorption}$ =150°C). Again, the chemisorbed amount in the adsorption studies is a difference measurement and thus is associated with a larger error of measurement. The adsorption studies show a 40 % decrease in the amount of ammonia chemisorbed while the Thermal Desorption experiments show a 20 % loss in the concentration of acid sites. The decrease in chemisorption can therefore be compared to the loss of acid sites with hydrothermal treatment although it is not a direct correlation.

Figure 5.10 shows the physisorption capacity of the Mordenite as a function of steaming time. It is seen that there was a decrease in the physisorbed amounts of all compounds but that that of water shows the most significant decrease in the initial steaming times. As with Rho, the physisorbed amount of ammonia is significantly less than that of either of the other two compounds.

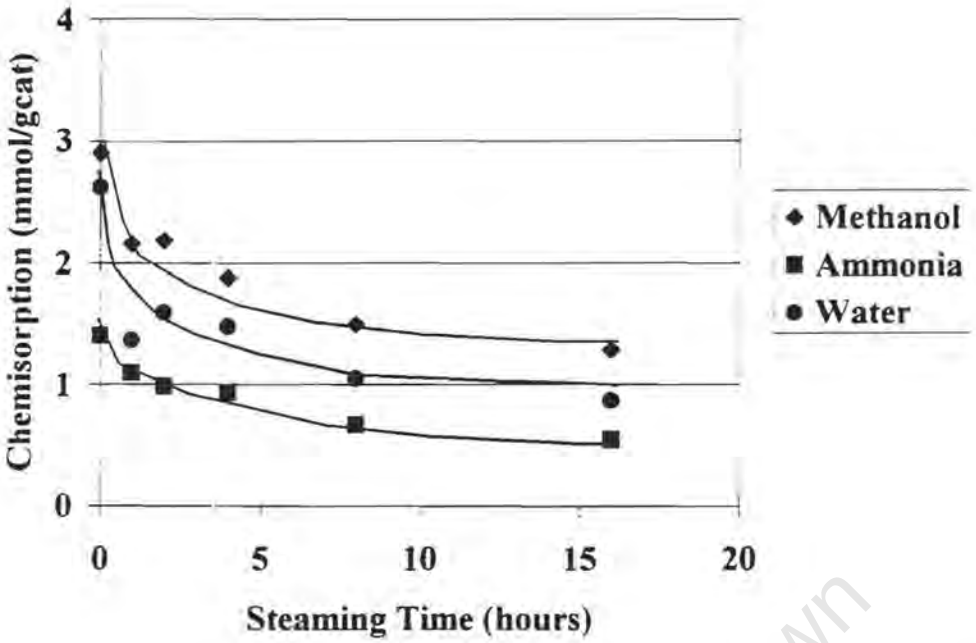

Figure 5.9: Chemisorption capacity of pure compounds as a function of steaming time for Mordenite.

(T_{ads} = 100°C, p_{H2O} = 2.5 kPa, p_{MeOH} = 2 kPa, p_{NH3} = 0.6 kPa, balance He, P_{tot} = atmospheric)

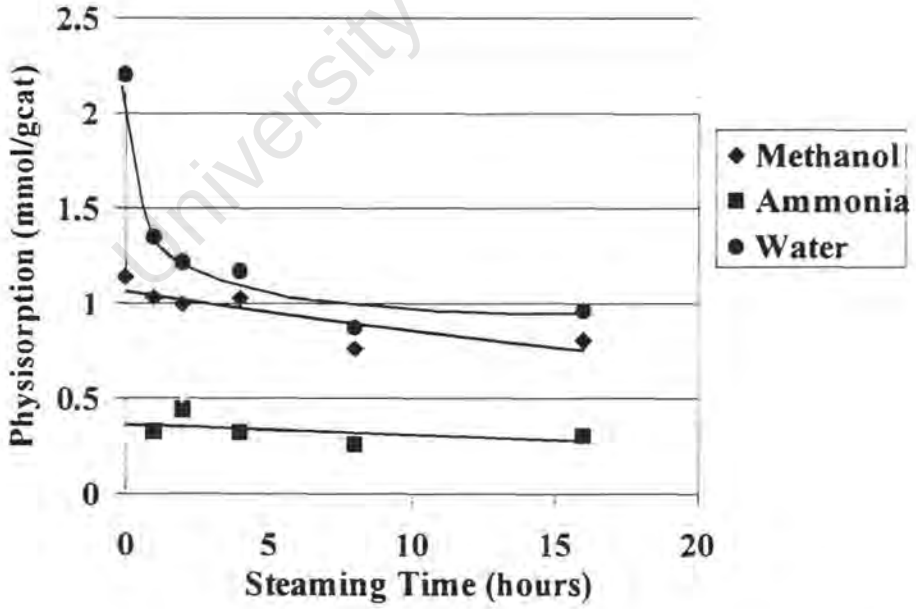

Figure 5.10: Physisorption capacity of pure compounds as a function of steaming time for Mordenite.

(T_{ads} = 100°C, p_{H2O} = 2.5 kPa, p_{MeOH} = 2 kPa, p_{NH3} = 0.6 kPa, balance He, P_{tot} = atmospheric)

5.2.2 Binary Adsorption Studies

As with Rho, the binary adsorption studies over Mordenite show more interesting results than the simple single component adsorption studies.

Methanol – Water

Figure 5.11 shows the ratio of the total methanol to water adsorption from a binary mixture as a function of steaming time. It appears that this passes through a maximum with steaming time. This may however be an anomaly of the experimental error, in which case the ratio of the total adsorptions could be said to have remained essentially constant with steaming time.

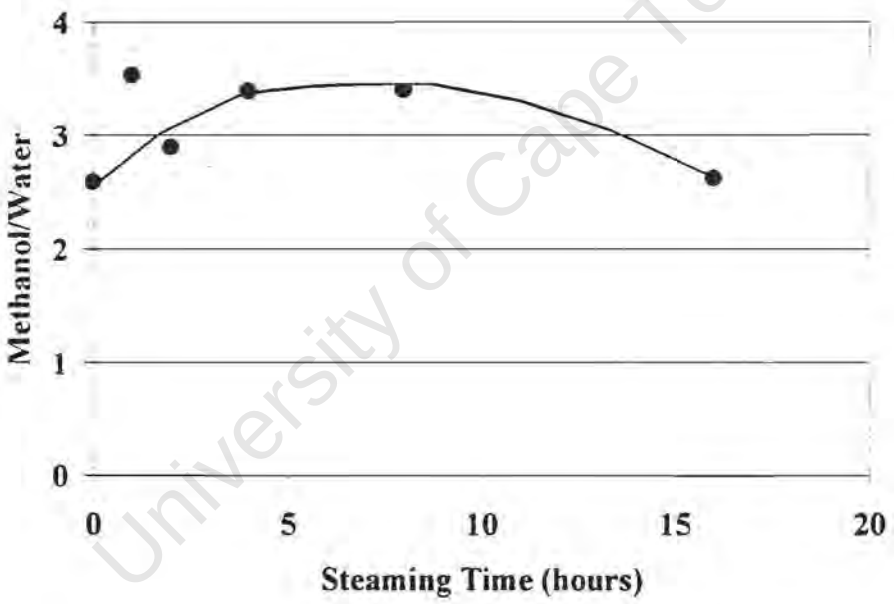

Figure 5.11: Ratio of total Methanol to Water adsorption over Mordenite vs. steaming time.

(T_{ads} = 100°C, p_{H2O} = 2.5 kPa, p_{MeOH} = 2 kPa, balance He, P_{tot} = atmospheric)

Figure 5.12 shows the ratio of methanol to water chemisorption over Mordenite as a function of steaming time. It can be seen that there was a significant decrease in this ratio. This indicates that with prolonged steaming of the Mordenite that there was significantly more water chemisorbed onto the catalyst. A possible explanation for this could be related to the

dealumination of the catalyst. As the aluminium is removed from the framework, it can form a number of extra-framework species. In the completely dehydrated form of the catalyst, most of these would have the general formula $[Al_xO_y]^{n+}$. These species could then react with water to form $[Al_xO_yH_z]^{m+}$. This would then explain the relative increase in the amount of water vs. methanol chemisorption with increased dealumination of the catalyst. It is well known that alumina (Al_2O_3) in particular can undergo this reaction with water.

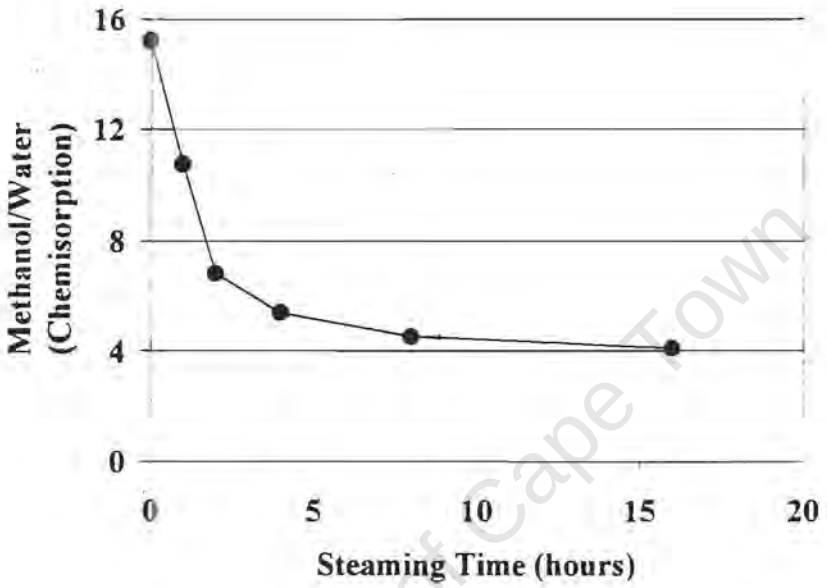

Figure 5.12: Ratio of Methanol to Water Chemisorption over Mordenite vs. steaming time.

(T_{ads} = 100°C, p_{H2O} = 2.5 kPa, p_{MeOH} = 2 kPa, balance He, P_{tot} = atmospheric)

Figure 5.13 shows the ratio of physisorbed methanol to water as a function of steaming time. It can be seen that this ratio increases with steaming time as opposed to the chemisorption, which decreased.

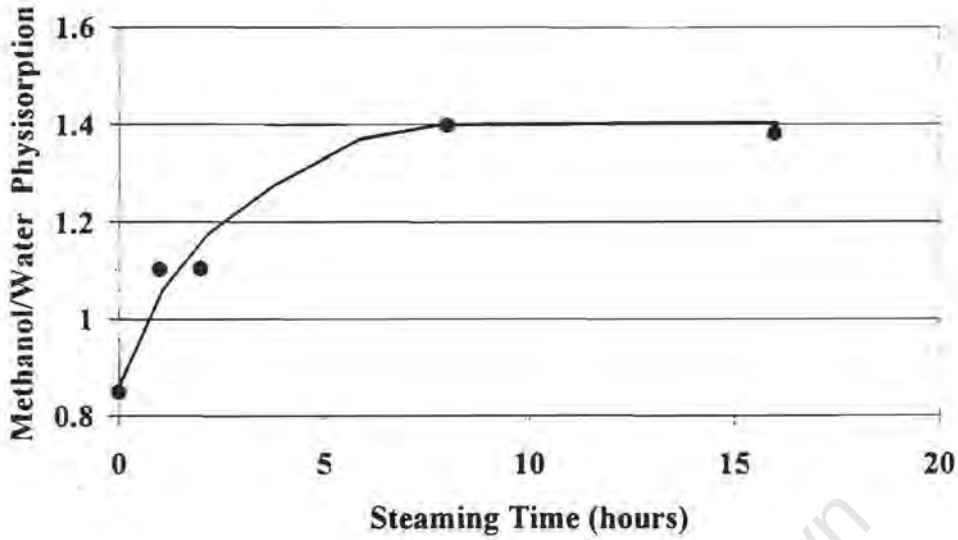

Figure 5.13: Ratio of Methanol to Water Chemisorption over Mordenite vs. steaming time.

(T_{ads} = 100°C, p_{H2O} = 2.5 kPa, p_{MeOH} = 2 kPa, balance He. P_{tot} = atmospheric)

Ammonia – Methanol

Figure 5.14 shows the ratio of chemisorbed ammonia to methanol from a binary mixture as a function of steaming time. Initially there was more ammonia than methanol adsorbed on the surface but this decreased with prolonged hydrothermal treatment. This indicates a change in the affinity of adsorption of the methanol and ammonia on the catalyst surface and hence indicates a change in the nature of the catalyst's acidity. This finding is in agreement with the results of the Thermal Desorption which showed the formation of a second, weaker type of acid site with increased steaming of the catalyst. As mentioned in the discussion of the adsorption on Rho, ammonia is a stronger base than methanol and would therefore react preferentially with a strong acid site. On a weaker acid site, the weaker base (methanol) would have a stronger chance of reacting with the surface. This is what was observed in this study, that the chemisorption of methanol increases as the acid site strength decreases.

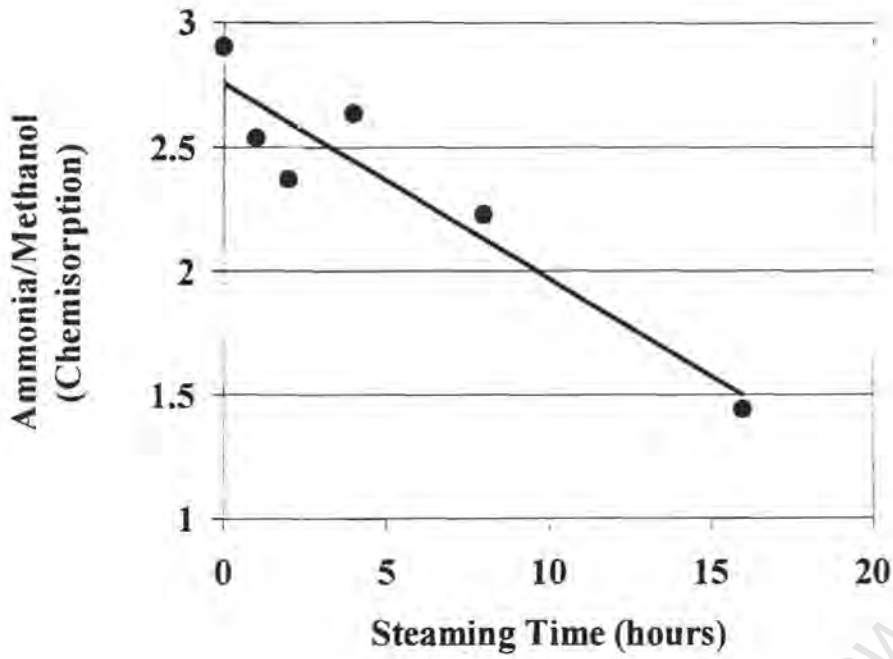

Figure 5.14: Ratio of ammonia to methanol chemisorption over Mordenite vs. steaming time.

(T_{ads} = 100°C. p_{MeOH} = 2 kPa. p_{NH3} = 0.6 kPa. balance He. P_{tot} = atmospheric)

Figure 5.15 shows the absolute amounts of ammonia and methanol physisorbed from a binary mixture over Mordenite as a function of steaming time. It was observed that for all catalyst samples, the amounts of ammonia physisorbed were extremely small, such as to make a comparison of the ratio of physisorbed ammonia to methanol unreliable. The amount of methanol physisorbed decreased with increasing hydrothermal treatment but this fits in with the general decrease in adsorption capacity observed for Mordenite with steaming.

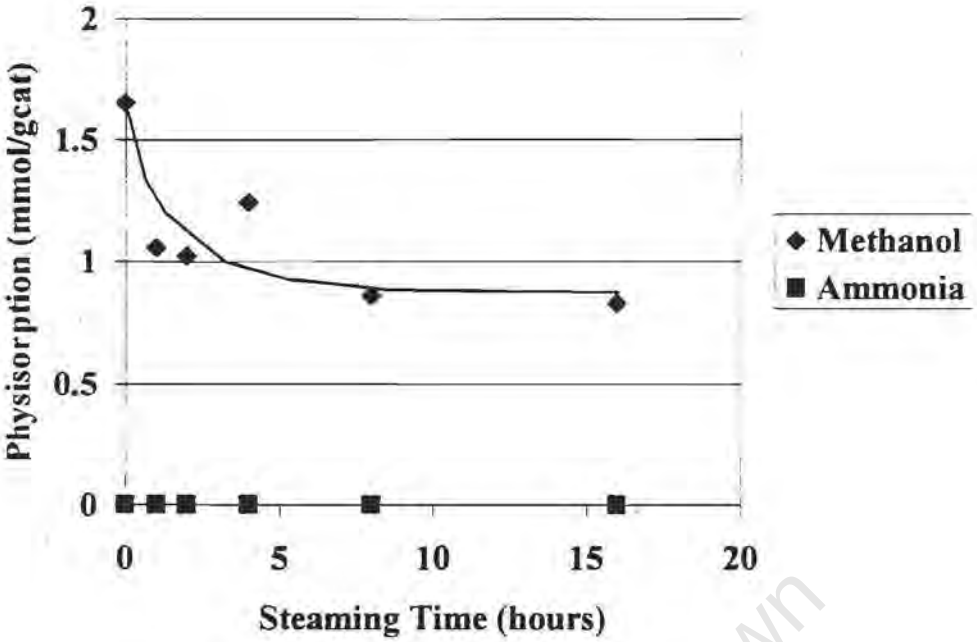

Figure 5.15: Ammonia and Methanol physisorption from a binary mixture over Mordenite as a function of steaming time.

(T_{ads} = 100°C, p_{MeOH} = 2 kPa, p_{NH3} = 0.6 kPa, balance He, P_{tot} = atmospheric)

5.3 DISCUSSION

An interesting observation is made when considering the total amount of all the compounds adsorbed relative to the pore volume of the catalysts. Take for example the adsorption of methanol where in the range of results obtained in this study, the concentration within the catalyst (either Rho or Mordenite) varies between 2 and 7 mol/litre. This is far more than the gas phase where the concentration fed was 0.09 mol/lit. Thus the concentration of methanol within the pores is a factor of ca. 40% higher. This is still lower than the concentration of a liquid however, which is ca. 30 mol/litre.

5.3.1 Rho

The Thermal Desorption experiments showed that, while the ratio of strong to weak acid sites increased with steaming time, the total number of acid sites decreased. It may therefore be questioned whether the observed increase in adsorption capacity is due to increased adsorption on the active sites or only to an increase in the physisorbed species within the catalyst structure. It has already been shown, with the BET measurements, how the steaming causes an increase in the pore volume of the catalyst. This increased pore volume would naturally lead to an increase in the physisorption capacity of the catalyst. However, as both the physisorption and chemisorption went through maxima with steaming time (cf. Figures 5.2 and 5.3) it is not one or other type of species that is increasing but rather a combination of both. These two types of adsorption are however linked in that a higher adsorbate concentration within the catalyst pores would shift the adsorption equilibrium in such a way that the concentration of chemisorbed species would also increase. To test this hypothesis, the ratio of chemisorbed to physisorbed species can be examined as a function of steaming time (see Figure 5.16). It can be seen that the ratio of chemisorbed to physisorbed species does not remain constant with steaming time. This means that the increase in chemisorbed species was not simply due to a change in the overall concentration within the pores and hence a shift in the equilibrium. These data rather confirm the changing nature of the catalyst surface, in particular the acid sites.

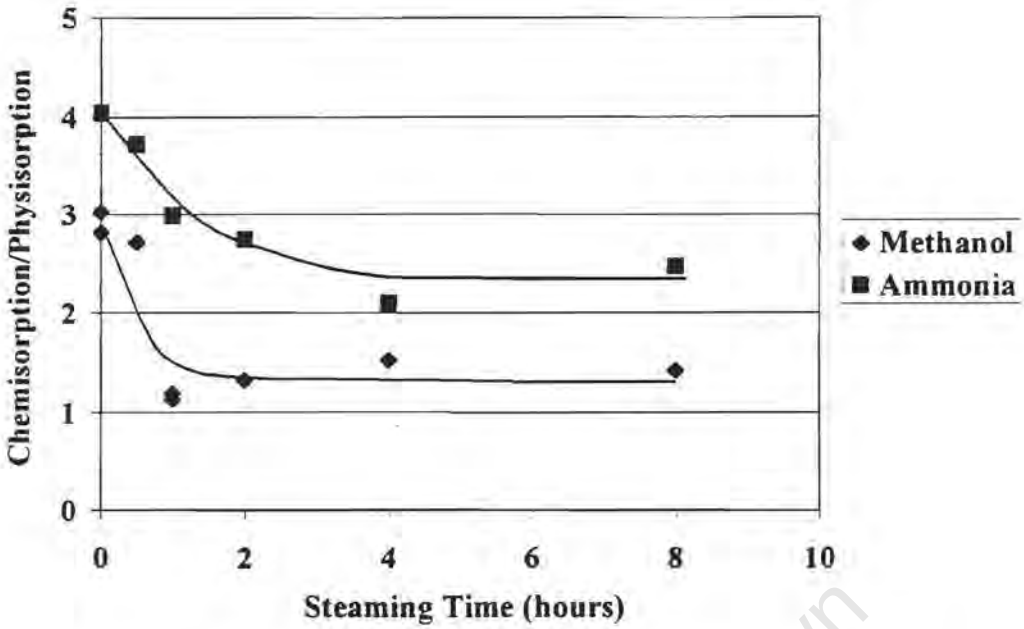

Figure 5.16: Ratio of Chemisorption to Physisorption vs. steaming time over zeolite Rho for pure Methanol and Ammonia.

(T_{ads} = 100°C, p_{MeOH} = 2 kPa, p_{NH3} = 0.6 kPa, balance He, P_{tot} = atmospheric)

The change in the ratio of ammonia to methanol physisorption seen in the binary adsorption studies of this work is consistent with the increase in activity seen in the methanol amination reaction with steaming time. To explain this, it is first necessary to remember that it has been shown that the mechanism of formation of the methylamines from methanol and ammonia occurs via a three-step process. Gründling *et al.* [1997] showed that firstly ammonia adsorbs onto the surface of the catalyst. This is followed by reaction of gas phase methanol with the adsorbed ammonia or incompletely substituted methylamines at the surface to form more highly substituted sorbed methylamines accompanied by the release of water. In the final step, the gas phase amines are formed either by adsorption-assisted desorption of the sorbed amines or through methyl group scavenging. When the concentration of methanol within the pores of the catalyst increases, as has been seen to occur in the adsorption studies of the physisorbed binary methanol/ammonia mixture, the equilibrium of the surface species shifts in favour of the more highly substituted species. This means that the concentration of methyl groups, as part of sorbed methylammonium ions, increases as the concentration of methanol within the pores increases. Veefkind *et al.* [1998] have shown that the rate of amine

formation is dependent on the concentration of methyl groups, in methylammonium species, at the surface rather than the concentration of acid sites. Hence, as the concentration of methyl groups at the surface increases, the rate of methylamine formation should increase leading to a higher rate of ammonia conversion, which was found to be the case in this present study, up to 5 hours steaming.

What remains however is to explain the apparently contradictory change in selectivity that was observed in the initial steaming times. The fact that the ratio of chemisorbed ammonia to methanol from the binary mixture increased with steaming time while the ratio in the adsorption experiments of the pure compounds remained constant indicates that the change in the adsorption ratios of the binary mixture must be due to a change in the affinity for adsorption of the catalyst caused by the hydrothermal treatment. As the ammonia is the more basic compound, this would seem to indicate that there is an increase in the acid strength of the catalyst. This is consistent with the Thermal Desorption experiments, which showed an increase in the percentage of strong acid sites as a function of steaming time. The increase in acid site strength means that there should be no difference in the amount of dimethyl ether formed during the reaction. There was indeed no measurable change in the amount of DME formed with steaming time. The DME yield remained constant within error of measurement at ca. 4 C% for the entire scope of the reaction studies.

While the distribution of the chemisorbed species gives information about the nature of the catalytic acid sites, with respect to their affinity for adsorption of different molecules, the reaction is also affected by the distribution of the free molecules in contact with the adsorbed species, i.e., the distribution of the physisorbed species. This is because the reaction takes place between the adsorbed methylammonium species and the gas phase molecules. As mentioned above, the decreasing ratio of physisorbed ammonia to methanol indicates that the concentration of free methanol relative to ammonia within the pores of the catalyst must increase with increasing steaming time. The logical hypothesis to arise from this observation is that, during reaction studies, the thermodynamic equilibrium is shifted towards the higher substituted amines and that therefore the proportion of trimethylamine in the amine mixture should be higher. The product spectrum would therefore be based on the equilibrium given by the concentration within the pores of the catalyst rather than the concentration within the gas phase. If the plot of amine yield as a function of ammonia conversion (cf. Figure 4.20) is more closely examined, it can be seen that at low conversions the yields of

monomethylamine and dimethylamine are very low in comparison to that of trimethylamine. It is only once the consumption of methanol nears completion, i.e., $X_{NH3} > 0.33$, that the yields of monomethylamine and dimethylamine start to increase. It is also at this point that the yield of trimethylamine starts to decrease rapidly.

This means that the product distribution is affected by the conversion within the system, or more precisely the effective conversion within the individual catalyst particles. Initially, the methanol is consumed faster than the ammonia and the highly substituted trimethylamine is formed preferentially. At higher conversions, as the methanol consumption nears completion, the concentration of methanol within the pores decreases and the methanol consumption slows down while the disproportionation reactions of trimethylamine and ammonia to dimethylamine and monomethylamine become relatively more important. The result of this is that apparently similar methanol conversions could give quite different product selectivities.

5.3.2 Mordenite

The change in adsorption behaviour over Mordenite was seen to be completely different to that of Rho. It was seen in the case of Mordenite, that the hydrothermal treatment lead to an increase in the affinity of the catalyst surface for methanol which in turn lead to the increased rate of DME formation at the expense of the formation of amines. In addition, the hydrothermal treatment of Mordenite leads to a loss in the total adsorption capacity and hence the overall reaction rate is seen to decrease.

Over Rho it was observed that the change in the ratio of the physisorbed methanol to ammonia could be correlated with the increase in activity seen for the methanol amination reaction. Although Mordenite likewise showed an increase in activity over short steaming times, the fact that the amount of ammonia physisorbed for all samples was below the accuracy of measurement for the procedure used in this work makes a similar comparison difficult. It may be expected however that there is a relationship between the decrease in total adsorption capacity and the decrease in activity seen at steaming times greater than about 2 hours.

The increase in the relative amount of methanol chemisorbed on the Mordenite should correspond to an increase in the amount of DME formed. This is indeed the case. Figure 5.17 shows the yield of DME and total amines formed over Mordenite as a function of steaming time. It can be seen that the yield of DME increased significantly with increased hydrothermal treatment. It is important to note that the rate of formation of DME was increasing, even while the rate of methanol conversion was decreasing, making the increase in DME selectivity even more pronounced.

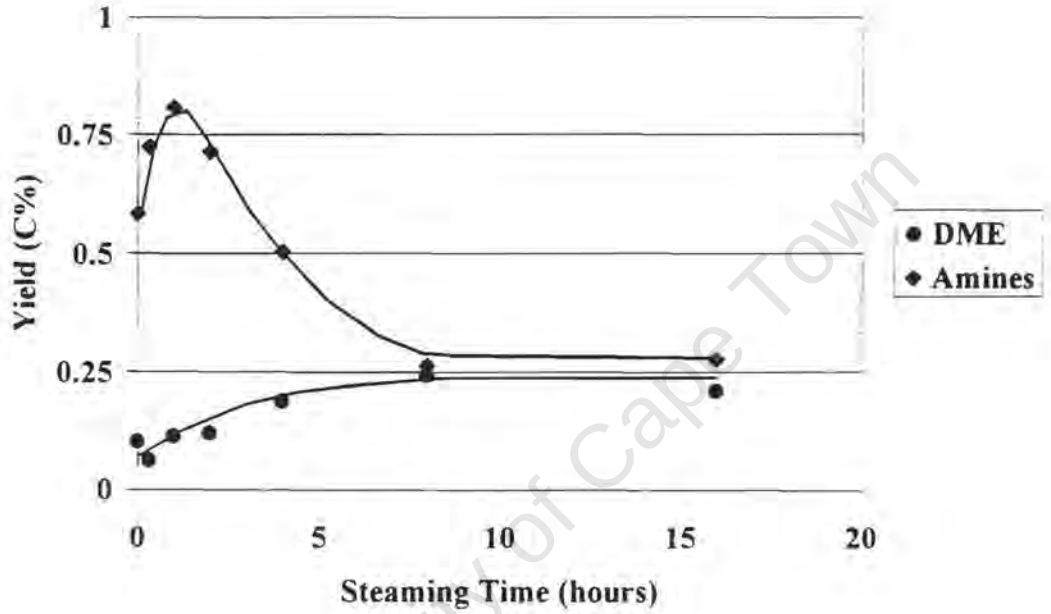

Figure 5.17: Yield of Dimethyl ether and total Amines over Mordenite as a function of steaming time.

Although there was a small change in the amine content in amines seen over Mordenite with steaming time, it is questionable whether this is a true improvement in the catalyst performance or simply a function of the decreased total rate of formation of amines. Not only does the overall conversion of methanol decrease, but the relative rate of formation of DME increases to approximately half of the product spectrum on a carbon basis, making the decrease in the rate of formation of amines more marked than the decrease in the rate of amine conversion. This could then be responsible for the slight change in amine selectivity seen with steaming time.

Discussion

6. DISCUSSION

One of the most significant results to come from this work must be the difference in the responses of the zeolites, Rho and Mordenite to the hydrothermal treatment. While this method of post-synthesis modification was seen to be beneficial, with respect to activity and selectivity, to the results obtained for the methanol amination reaction in the case of Rho, little or no benefit was seen to be gained from steaming Mordenite. It was also seen that hydrothermal treatment of both Rho and Mordenite results in changes to the catalyst structures and acidic natures.

6.1 COMPARISON OF CATALYST CHANGES CAUSED BY HYDROTHERMAL TREATMENT

6.1.1 Changes in Reaction Behaviour

In terms of the reaction studies performed over the two zeolites as a function of steaming time, what is most obvious is that Rho could be manipulated to a much larger extent than could Mordenite to yield a more favourable performance both in terms of activity and selectivity for the methanol amination reaction. Over Rho, a significant increase in the rate of reaction was seen as well as a marked increase in the selectivity to the lower substituted amines. Mordenite, on the other hand, showed only some moderate improvement in methanol consumption and amine selectivity with steaming. It moreover showed a marked increase in the yield of DME with steaming time.

Both catalysts showed a decrease in the rate of formation of amines with long steaming times. This means that for both there is an optimum degree of hydrothermal treatment, such that the best combination of activity and selectivity, i.e., yield, can be obtained.

6.1.2 Structural and Acidic Changes

To gain a better understanding of why the responses of the two zeolites to hydrothermal treatment is so different, it is necessary to look to the changes in both the structural and acidic properties of the catalysts that have been caused by the steam treatment. Let us first examine the change in acidity of the two catalysts as a function of steaming time.

It was seen from the Thermal Desorption experiments (cf. Chapter 4.1) that the change in the acidic character of the two catalysts as a function of steaming time was quite different. On the Rho, which initially had two distinct types of acid sites, as observed from the Thermal Desorption spectra, it was seen that there was a general loss in the number of acid sites caused by the steaming and that this loss occurred primarily from the weaker of the two acid sites. On the Mordenite, in contrast, the initial acid site distribution was essentially homogeneous. With steaming of Mordenite however, although there was some overall loss in the number of acid sites, it is interesting to note that there was a generation of a second type of acid site, which had a weaker affinity for ammonia than did the original site type. These results mean that the actual acidic natures of the two catalysts are being altered in different ways by the hydrothermal treatment. While the average acid site strength of the Rho is increasing, that of the Mordenite decreases.

The Thermal Desorption experiments also illustrated the fact that the framework of the Rho is less stable than that of the Mordenite in regard to dehydroxylation. This can be seen because while dehydroxylation in the case of Rho is seen at temperatures of ca. 650°C, the Mordenite shows no dehydroxylation even up to 700°C.

The NMR studies of the two catalysts showed that there was generation of octahedrally co-ordinated aluminium in both catalysts caused by the hydrothermal treatment. The increase in octahedral aluminium in the structure is indicative of dealumination of the catalysts leading to the formation of extra-framework aluminium species. EFAl species have been shown to exhibit Lewis acidity [Kubelkova *et al.*, 1989; Mirodatos and Barthomeuf, 1981; Shertrukde *et al.*,1993]. Now, as has been discussed in Chapter 4, extra-framework aluminium species can take different forms [Corma, 1989; Martens *et al.*,1997] leading to Lewis acid sites of differing strengths. It has also been shown that this type of Lewis acidity favours the formation of dimethyl ether [Ilao *et al.*, 1996]. It may be postulated therefore that the extra-framework aluminium species, which form on Rho and Mordenite, are different. It would

seem the acid sites generated on Mordenite are of a reasonably weak Lewis nature as they correspond well to the increased formation of dimethyl ether seen over Mordenite with increased steaming. Steaming of zeolite Rho did not generate these weak Lewis acid sites which desorb ammonia in the Thermal Desorption experiments at ca. 325°C. Furthermore, steaming of Rho did not enhance the formation of DME with increased hydrothermal treatment.

The next changes caused to the catalyst are those of the catalyst structure. One of the most striking differences seen over the two catalysts must be in the pore volumes as seen by the BET measurements. The changes to the pore volumes of the two catalysts were almost exactly opposite. While the surface area and pore volume of the Rho increased with steaming time, those of Mordenite decreased. It is also interesting to note that these contradictory changes seen for the two catalysts are due to the change in the micropore volume of each which increases significantly over Rho and decreases over Mordenite. As was already noted in Chapter 4.6, the phenomenal increase in the micropore volume of Rho is in all likelihood due to its unique structural flexibility. It is probable that the generation of extra-framework aluminium species within this catalyst cause it to take on the more open, symmetrical orientation of its framework and hence make the internal pore structure more accessible to adsorbant molecules. The structural flexibility of Rho is unique [Corbin *et al.*, 1990]. Mordenite shows no such framework flexibility and therefore, complete dehydration of its structure would not cause any problems in terms of framework accessibility, as is the case with Rho.

The mesopore volume of both catalysts was seen to increase slightly. This is hardly surprising as dealumination of either structure must necessarily lead to the formation of some defect sites within the pore structure of the catalyst and hence cause an increase in the volume of mesopores seen.

6.1.3 Change in Adsorption Behaviour

The change in the adsorption behaviour of the two catalysts also illustrates the contradictory changes over these two zeolites. While the single component adsorption studies gave information about the changing capacities of the catalysts, the binary adsorption studies gave information about the changing nature of the catalyst surfaces and about the affinity of those surfaces for the different adsorbates.

The first difference between the zeolites is that of the changing total adsorption capacities. While Rho showed a distinct maximum in the total adsorption capacity of all three compounds (methanol, water and ammonia), Mordenite showed a systematic decrease. Over both catalysts, the change in the total adsorption capacity was seen to be due to contributions from both chemisorption and physisorption, i.e., the changes in chemisorption and physisorption were similar rather than acting in opposition to each other. The total adsorption capacities may be related to pore volumes of the catalysts. In Rho, as the accessible pore volume increases, so does the adsorption capacity. In Mordenite, the adsorption capacity decreases with decreasing pore volume.

Where this correlation between pore volume and adsorption capacities falls short however, is in the longer (>4 hours) steaming time of Rho. Although the pore volume of Rho, as determined by the BET measurements was seen to remain constant at longer steaming times, there was a decrease in the total adsorption capacity of Rho with prolonged hydrothermal treatment. An alternative explanation must therefore be sought for the decrease in the total adsorption capacity over Rho at longer steaming times. A possible explanation for the decrease in the total adsorption capacity has already been discussed in terms of the presence of extra-framework aluminium. It was noted that the decrease in adsorption capacity could be caused by cationic extra-framework aluminium species taking over the function of charge balancing the catalyst framework [Kubelkova, 1989]. Extra-framework aluminium could also lead to pore blockage [Bamwenda, 1994,1995; Miller, 1992], which would also cause a decrease in the adsorption capacity.

The results obtained over the two catalysts in the binary adsorption studies are also quite different. The ratio of total methanol to water adsorbed from a binary mixture is an indication of the relative hydrophobicity of the catalysts. Initially, it was seen that this ratio was far less over Rho than over Mordenite, indicating that the Mordenite is more hydrophobic than Rho.

Even though this ratio changes over both catalysts as a function of steaming time, the total methanol to water adsorption ratio over Mordenite was always higher than that over Rho.

The ratio of total methanol to water adsorbed changed more significantly on Rho than it did on Mordenite. While both catalysts showed a maximum in the ratio of total methanol to water adsorption with steaming time, the relative increase over Rho is ca. 36% as opposed to Mordenite which showed an increase of ca. 28%. Also, the maximum in this ratio over Rho is sharp and occurs after two hours steaming time while that over Mordenite was less distinct and occurred later at ca. 8 hours steaming. Together these results indicate that the hydrophobicity of Mordenite, while always being higher than that of Rho, is not as strongly affected by the hydrothermal treatment.

A more dramatic difference between the two catalysts was found in the ratio of chemisorbed methanol to water as a function of steaming time. While there was a slight decrease in this value over Rho, the ratio over Mordenite dropped dramatically in the initial hours of steaming to ca. 30% of its initial value. This is indicative of the fact that there is some change to the surface of the Mordenite which does not occur on or is not the same on Rho. A possible explanation for this could be related to the dealumination of the catalyst. As the aluminium is removed from the framework, it can form a number of extra-framework species. In the completely dehydrated form of the catalyst, most of these would have the general formula $[Al_xO_y]^{n-}$. These species could then react with water to form $[Al_xO_yH_z]^{m+}$. This would then explain the increased amount of water chemisorption with increased dealumination of the catalyst.

When the results of the binary adsorption of ammonia and methanol were examined, it was seen that the change in the relative affinity of the surface of the catalysts for these two compounds was opposite. While the ratio of ammonia to methanol chemisorption over Rho increased, that over Mordenite decreased. These results are however consistent with the changes in the acid sites of the catalysts, as seen with the Thermal Desorption experiments. It was seen that Lewis acid sites were generated on Mordenite while there was no such generation of Lewis acidity on Rho. It has been shown that methanol can adsorb competitively on Lewis acid sites [Kogelbauer *et al.*, 1994,1996]. This then explains the increased chemisorption of methanol on steamed Mordenite. The increased ammonia chemisorption on steamed Rho can be explained by considering the fact that ammonia is a far

more basic molecule than is methanol. It is also known that a stronger acid site will shown more preference for a strong base than will a weak acid site. The changes in the affinity of the catalyst surfaces of Rho and Mordenite with steaming time for ammonia and methanol are therefore perfectly reasonable.

It was more difficult to compare the ratios of ammonia to methanol physisorption over the two catalysts. This was due to the fact that there was very little ammonia physisorption at any stage seen in these adsorption experiments using Mordenite.

6.2 RELATIONSHIP BETWEEN CATALYST CHANGES AND REACTION PERFORMANCE

6.2.1 Rho

With the difference in the changes evidenced over the catalysts having been discussed in the previous section, it remains to correlate the changes on each catalyst with its reaction performance and to see how these correlations give further understanding to the reaction behaviour of catalysts in general.

Over the Rho, the conversion or rate of reaction of ammonia initially increases as a function of steaming time and reaches a plateau within the range of steaming times considered in this study. This increase closely matches the increase in pore volume seen with the BET measurements. To test this theory, the ammonia conversion was plotted against the pore volume of the catalyst as shown in Figure 6.1. It can be seen from this graph that there is a reasonable correlation between the pore volume and the rate of ammonia consumption although there is a large gap in the data.

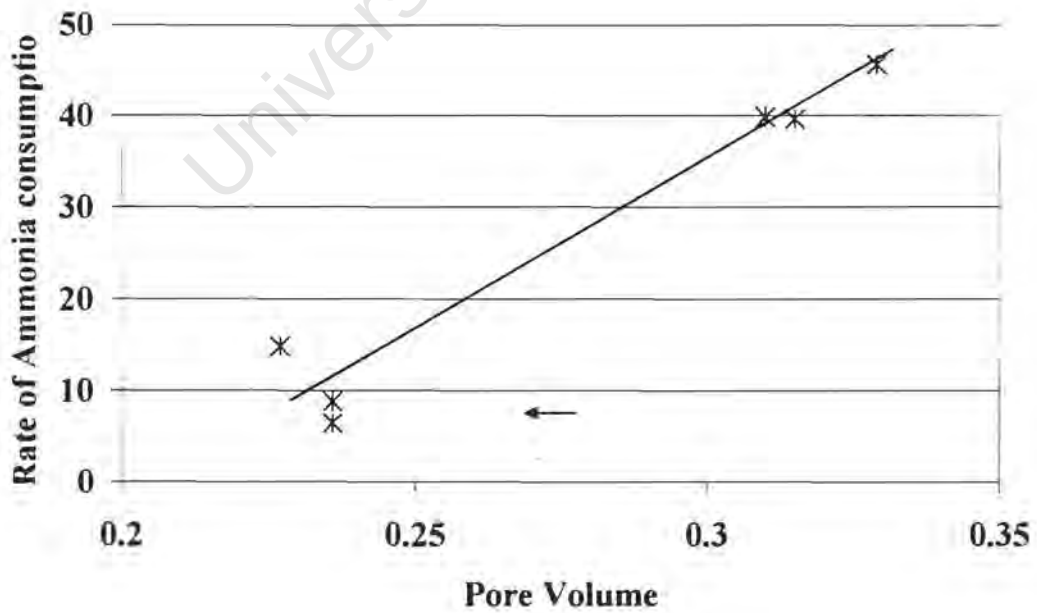

Figure 6.1: Comparison of Pore Volume and Rate of Ammonia consumption over Rho

The change in the rate of methanol consumption over Rho as a function of steaming time is more complex. It was seen that the methanol consumption (cf. Figure 4.12) went through a maximum with steaming time, in contrast to the ammonia consumption, which reached a plateau. There are some trends in the changes to Rho, which might account for this change observed in the rate of methanol consumption. Firstly, it could be related to the total adsorption capacity (cf. Figure 5.1), which showed a similar maximum with steaming time. Secondly, it could also be related to the hydrophobicity of the catalyst (cf. Figure 5.4), which likewise showed a maximum as a function of steaming time, although given the reaction mechanism, this does not seem likely. The third option is to consider the increase and decrease in the rate of methanol consumption as different phenomena. The total adsorption capacity seems a likely option for comparison as increasing the adsorption capacity will increase the concentration of methanol in the pores and hence affect the distribution of surface species. As the concentration of methanol in the pores increases, there would be a shift towards the more highly substituted surface species. It is known that the rate of formation of amines is proportional to the concentration of methyl groups, in methyl ammonium species, at the surface [Veefkind, 1998].

The decrease in the methanol consumption may also be due to the shifting product distribution observed. This means that while the rate of ammonia conversion reaches a plateau, the substitution of each of these reacted molecules is lowered, leading to an observed decrease in the methanol consumption. It remains to propose an explanation for the change in amine selectivity observed. While all the adsorption studies indicate that there should be an increase in the amount of TMA formed, this is obviously not the case. The relatively low concentration of physisorbed ammonia within the pores should lead to an increase rather than a decrease in the substitution of product amines. The decrease in the selectivity of TMA produced can in some part be explained by the fact that as the methanol conversion increases the amount of ammonia physisorbed within the pores can increase and hence yield more of the lower substituted amines. This does not however account for the observed decrease in the amount of TMA being lower than the value being expected from thermodynamic equilibrium. To explain this, it is necessary to reconsider the framework structure of Rho. Rho consists of large sodelite cages, which are connected by narrow double membered rings. It has also been shown that the charge balancing cations tend to be situated within these double rings rather

than in the large cages [Szostak, 1992]. It is reasonable therefore to suspect that as the framework is dealuminated and large amounts of extra-framework aluminium species are formed, that especially any charged aluminium species may locate themselves within the pore openings of the catalyst and hence increase the diffusional constraints of the larger molecules. This would mean that the increased selectivity of the lower substituted amines observed was due to an induced product shape selectivity of the catalyst, caused by the hydrothermal treatment.

6.2.2 Mordenite

The changes observed over Mordenite, as discussed in Chapter 6.1, were both different to and less significant than those observed over Rho. The most significant change seen here was the large increase in the rate of formation of DME and this has been attributed to the formation of Lewis acid sites within the catalyst. Although the DME can itself react with adsorbed ammonia to form methylamines, the large loss of acid sites favourable to ammonia adsorption mean that the total rate of amine formation is slowed considerably.

As mentioned in Chapter 5, the small change in the relative amine selectivity seen over Mordenite with steaming time, should not be ascribed to a true improvement in the catalyst performance. It was rather seen to be simply a function of the decreased total rate of formation of amines. The decrease in the rate of total amine formation seen was more than adequate to explain the small change in amine selectivity observed.

Conclusions

7. CONCLUSIONS

To reiterate, the objectives of this study, as discussed in Chapter 1.7, were briefly as follows. Firstly, the original question asked was as to which of the catalysts studied was the most suitable for the methanol amination reaction. The second objective was to find the optimal performance achievable from any catalyst using hydrothermal treatment. The third, and possibly most important, objective was to elucidate changes caused to any given catalyst by hydrothermal treatment. With this in mind the findings of this work will be reviewed.

The first conclusion from this work is that the zeolites can be used for the methanol amination reaction at lower temperatures as suggested in literature [Shannon *et al.*, 1988a; Keane *et al.*, 1987]. Zeolites did show some improvement in selectivity to the lower substituted amines but it was only the hydrothermally treated forms of Rho that showed significantly improved product spectra.

Secondly, it was seen how hydrogen containing species on the surface of Rho and Mordenite, which are not desorbed during normal flushing procedures, are burnt off the surface, yielding water as a product. This water then act acts an *in situ* steaming agent and as such causes changes to the reaction behaviour of the catalyst. This is an important observation as it indicates that care should be taken when regenerating catalysts after reaction as inadvertent steaming of the catalyst can occur. The ease with which these catalysts are affected by steam is also significant because it means that any conditions under which some water is present at high temperatures over the catalyst could cause steaming and hence dealumination to occur. For example, the deep bed calcination conditions used by some researchers, where the desorbing gasses are not removed effectively could lead to steaming of the catalyst. This might not however be undesired.

One of the most significant findings of this work must be the difference in the manner in which the two zeolites, Rho and Mordenite, are affected by the hydrothermal treatment. The two most important physical differences in the response of the two catalysts to hydrothermal treatment are the change in the nature of the acid sites and the change in the surface area and pore volume seen. Hydrothermal treatment of Rho causes a loss in the total number of acid sites in the catalyst and this loss is primarily from the weaker of the two acid sites. Treatment of Mordenite on the other hand causes less loss in the total number of acid sites in the catalyst

but the treatment also causes a second type of acid site to be formed. Steaming of Rho leads to an increase in especially the micropore surface area and pore volume of the catalyst whereas steaming of Mordenite causes a decrease in the microporous structure of the catalyst. Where the response of the catalysts are the same, is in the fact that steaming causes the generation of extra-framework aluminium species in both catalysts. The mesoporous structure of both catalysts is also increased by the hydrothermal treatment due to the formation of defect sites within the catalyst structure.

The hydrothermal treatment also causes contradictory effects in the adsorption behaviour of the two catalysts. The steaming caused the total adsorption capacity of Rho to go through a maximum while that of Mordenite to decrease. The initial changes in the adsorption capacity were due directly related to the changing pore volumes of the catalysts. The decrease in adsorption capacity over Rho at longer steaming times was ascribed to the presence of extra-framework aluminium within the pore structure of the catalyst. The hydrothermal treatment also causes different changes in the affinity of chemisorption of the various compounds studied in this work. Over Rho the affinity for ammonia, as opposed to Methanol, is increased by the steaming while that over Mordenite is decreased.

The changes in the performance of the catalysts for the methanol amination reaction can be correlated to the changes in acidity, structure and adsorption capacity of the two catalysts. Over Rho it was seen that a number of effects with contradictory consequences were occurring. The increase in the rate of reaction of ammonia can be correlated with the pore volume of the catalyst, or to the increasing concentration of methyl groups, in methylammonium species, at the surface. The rate of reaction of methanol initially increases due to the overall increase in activity. The later decrease in the rate of methanol consumption is caused by the changing selectivity of the system and to the decreasing total adsorption capacity of the catalyst.

As the selectivity changes towards the lower substituted amines, so the consumption of methanol decreases. The change in amine selectivity seen over Rho with steaming time is caused by the generation of extra-framework aluminium within the pore structure of the catalyst. The presence of the extra-framework aluminium may cause increased diffusional constraints within the pores of the catalyst. This would be enough to constrain the larger, TMA, molecule but not enough to constrain the smaller, MMA and DMA, molecules. The

rate of ammonia reaction is not slowed by this constraint because the rate of TMA disproportion is very high compared to the series formation of amines.

The presence of extra-framework aluminium may also be responsible for the decrease in the total adsorption capacity seen over Rho at longer steaming times. As less pore volume is available, so the rate of reaction decreases.

The generation of larger amounts of dimethyl ether over Mordenite was seen to be due to the formation of the second type of acid site. This site, which is probably of a Lewis acidic nature, has a far higher affinity for methanol and hence leads to an increase in the chemisorption of methanol at the catalyst surface and hence to the higher rate of formation of dimethyl ether.

The large loss of the original acid site type in the Mordenite, which was selective to amines, caused the decrease in the overall formation of amines.

References

REFERENCES

Abrams, L., Keane, M. and Sonnichsen, G. C.: "Selective Synthesis of DMA over Small-Pore Zeolites: Catalytic Selectivity and Sorption Behaviour", *J. Catal.*, **115** (1989) 410-419.

Abrams, L., Corbin, D. R. and Shannon, R. D.: "Zeolite Rho and ZK-5 Catalysts for conversion of Methanol and Ammonia to Dimethylamine", *U.S. Patent* 4,814,503, (1989).

Abrams, L., Corbin, D. R. and Keane, M.: "Synthesis of DMA by Zeolite Rho: A Rational Basis for Selectivity", *J. Catal.*, **126** (1990) 610-618.

Abrams, L. and Corbin, D. R.: "Sorption Properties of Zeolite Rho", *J. Catal.*, **127** (1991) 9-21.

Abrams, L. and Corbin, D.R.: "Probing Intrazeolite Space", *J. Inclusion Phenomena*, **21** (1995) 1-46.

Ashina, Y., Fujita, T., Fukatsu, M., Niwa, K. and Yagi, J.: "Manufacture of Dimethylamine Using Zeolite Catalyst", *Stud. Surf. Sci. Catal.*, **28** (1986) 779-786.

Baiker, A. and Richarz, W.: "Catalytic Amination of Long Chain Aliphtic Alcohols", *Ind. Eng. Chem., Prod. Res. Dev.*, **16** (1977) 261-266.

Baiker, A. and Richarz, W.: "Synthesis of Long Chain Aliphatic Amines from the Corresponding Alcohols", *Tetrahedron Letters*, **22** (1977) 1937-1938.

Baiker, A. and Kijinski, J.: "Catalytic Synthesis of Higher Aliphatic Amines from the Corresponding Alcohols", *Catal. Rev.-Sci. Eng.*, **27** (1985) 653-697.

Bamwenda, G. R., Zhao, Y. X. and Wojciechowski, B. W.: "The Inactivity of Extra Framework Aluminium in the Cracking of 2,3 Dimethylbutane on USHY", *J. Catal.* **150** (1994) 243-253.

Bamwenda, G. R., Zhao, Y. X., Groten, W. A. and Wojciechowski, B. W.: "The Effects of EFAl Extraction on 2-Methylpentane Cracking over Steamed HY", *J. Catal.* **157** (1995) 209-221.

Barrer, R. M. and Rosemblat, M. A.: "Zeolite Rho. Part III. Sorption of inorganic Gases and Hydrocarbons," *Proc. 6th Int. Zeo. Conf.*, (Olson & Bisio eds), (1983) 115 276–287.

Barrer, R.M., "Hydrothermal Chemistry of Zeolites," *Academic Press* (1982).

Bergna, H.E., Keane, M., Ralston, D., Sonnichsen, G., Abrams, L. and Shannon,R.: "Selective Synthesis of DMA over Small-Pore Zeolites : IV Effects of SiO_2 and Al_2O_3 Coatings", *J. Catal.*, **115** (1989) 148-158.

Berke, C.H., Kiss, A., Kleinschmidt, J. and Weitkamp, J.: "Der Hydrophobizitäts-Index: Eine neue Methode Zur Charakterisierung der Oberflächeinegenachafter zeolithischer Adsorbentiene", *Chem. Ing. Tech.*, **63** (1991) 623-628.

Burgfels, G. and Schmidt, F. "Tayloring the dealumination Behaviour of Synthetic Zeolite Mordenite by Controlled Synthesis Conditions," *Science and Technology in Catalysis*, (1995) 465-467.

Cairon, O., Sellem, S., Potvin, C., Manoli, J.M. and Chevreau, T.: "Dealumination and acidity measurement of HEMT zeolites modified by steaming and leaching", *Zeolites*, (1995) 513–518.

Carvajal, R., Chu, P.-J. and Lunsford, J.H.: "The role of Polyvalent Cations in Developing Strong Acidity: A study of Lanthanum-Exchanged Zeolites", *J. Catal.*, **125** (1990) 123-131.

Chatelain, T., Patarin, J., Fousson, E., Soulard, M., Guth, J.L. and Schulz, P.: "Synthesis and Characterisation of high-silica zeolite RHO prepared in the presence of 18-crown-6 ether as organic template", *Microporous Materials*, **4** (1995) 231-238

Chen, D.T., Sharma, S.B., Filimonov, I. and Dumesic, J.A.: "Microcalorimetric studies of zeolite acidity", *Cat. lett.*, **12** (1992) 201-212.

Chen, D.T., Zhang, L., Chen, Y. and Dumesic, J.A.: "Methylamine Synthesis over Solid Acid Catalysts: Microcalorimetric and Infrared Spectroscopic Studies of Adsorbed Species", *J. Catal.*, **146** (1994) 257-267.

Chen, D.T., Zhang, L., Kobe, J.M., Chen, Y. and Dumesic, J.A.: "Methylamine synthesis over solid acid catalysts: reaction kinetic measurements", *J. Mol. Cat.*, **93** (1994) 337-355.

Constantinescu, F. and Blum, J.: "Adsorption Characterisation of the Dealumination Effect on H-Mordenites", *Journal of Pourous Materials*, **2** (1995), 35-41.

Corbin, D.R., Abrams, L., Jones, G.A., Eddy, M.M., Harrison, W.T.A., Stucky, G.D. and Cox, D.E.: " Flexibility of the Zeolite Rho Framework. In Situ X-ray and Neutron Powder Structural Characterisation of Divalent Cation-Exchanged Zeolite Rho.", *J. Am. Chem. Soc.*, **112** (1990) 4821-4830.

Corbin, D.R., Keane, M., Abrams, L., Farlee, R.D., Bierstedt, P.E. and Bein, T.: "Designing Zeolite Catalysts for Shape Selective Reactions: Chemical Modification of Surfaces for Improved Selectivity to DMA in Synthesis from Methanol and NH_3", *J. Catal.*, **124** (1990) 268-280.

Corbin, D.R., Schwarz, S., and Sonnichsen, G.C.: "Methylamine Synthesis: A Review," *Cat. Today*, **37** (1997) 71-102.

Corma, A.: "Application of Zeolites in Fluid Catalytic Cracking and Related Processes", *Stud. Surf. Sci. Catal.*, **49** (1989) 49-67.

Corma, A.: "Inorganic Solid Acids and Their Use in Acid Catalysed Hydrocarbon Reactions", *Chem. Rev.*, **95** (1995) 559 - 614

Corma, A., Martinez, A. and Martinez, A., "The Role of Extraframework Aluminium Species in USY Catalysts During Isobutane/ 2-Butene Alkylation", *Appl. Cat.* **134** (1996) 169-182.

Cotterman, R.L., Hickson, D.A. and Shatlock, M.P., in "Characterisation and Catalytic Development: An Interactive approach." (S.A.Bradley, M.J.Galtuso, R.J.Bertolacini, eds.), *Am. Chem. Soc.* (1989).

Csicsery, S.M.: "Catalyst testing: How and How Not To Test Catalysts", *Catalyst Consultants Publishing*, (1992).

Deeba, M.: "Amines Via the Amination of Alkanols Using Dealuminated Zeolites", *European Patent* - 180983 A1, (1985).

Deeba, M., Ford, E. and Johnson, T. : "Direct Amination of Ethylene by Zeolite Catalysis", *J. Chem. Soc., Chem. Commun.*, (1987) 562-563

Deeba, M.: "Shape Selective Catalysis for C2 to C4 Alkanol Amination", *European Patent* - 311900 A2 (1988).

Deeba, M. and Ford, M.E.: "Direct Amination of Olefins: A Comparative Study over Erionite and Y Zeolites", *Zeolites*, **10** (1990) 794-797.

Dingerdissen, U.: "Herstellung von Niederen Aminen an Zeolithkatalysatoren", PhD Thesis, *Technischen Hochschule Darmstadt*, Darmstadt, 1990.

Dingerdissen, U., Nagy, E. and Fetting, F.: "Zur Kinetik der Aminierung von Methanol an dem Zeolith-Katalysator ZK-5", *Chem. Ing. Tech.*, **63** (1991) 625-628.

Engelhardt, G., Jerschkewitz, H.-G. and Lohse, U., "500 MHz ^{1}H-MAS NMR Studies of Dealuminated HZSM-5 Zeolites," *Zeolites*, 7 (1987) 289-292.

Ernst, H. and Pfeifer, H.: "Synthesis of Methylamines Studied by In Situ Carbon-13 MAS NMR Spectroscopy", *J. Catal.*, **136** (1992) 202-208.

Fetting, F., Petry, T. and Dingerdissen, U.: "Einfluß der Art des Katalytisch Aktiven Zentrums auf das Katalytische Verhalten bei der Aminierung von C1 bis C3-Alkoholen an Zeolith-Katalysatoren", *Chem. Ing. Tech.*, **63** (1991) 492-495.

Fetting, F. and Dingerdissen, U.: "Production of methylamines over ZK-5 Zeolite Treated with Tetramethoxysilane", *Chem. Eng. Tech.*, **15** (1992) 202-212.

Fischer, R.X., Baur, WH., Shannon, R.D. and Staley, R.H.: "Weakly Acidic Bridging Hydroxyl Groups and NONframework Aluminium Species in Zeolite D-Rho Shallow-Bed Calcined in Steam", J. Phys. Chem., 91 (1989) 2227-2230.

Fischer, R.X., Baur, W.H., Shannon, R.D., Parise, J.B., Farber, J. and Prince, e.: "New Different Forms of Ammonium Loaded and Partly Deammoniated Zeolite Rho Studied by Neutron Powder Diffraction", *Acta Cryst.*, **C45** (1989) 983-989.

Fritz, P.O. and Lunsford, J.H.: "The Effect of Sodium Poisonong on Dealuminated Y-Type Zeolites", *J.Catal.*, **118** (1989) 85-98.

Gier, T.E., Shannon, R.E., Sonnichsen, G.C., Corbin, D.R. and Keane, M.Jr.: "Zeolite Rho as Catalyst for Conversion of Methanol and Ammonia to Dimethylamine", *United States Patent* - 4 8006 689, (1985).

Gründling, C.: "Elementary Steps in the Synthesis of Methylamines over Molecular Sieve Catalysts", PhD Thesis, Universiteit Twente, The Netherlands, 1995.

Gründling, C., Eder-Mirth, G. and Lercher, J.A.: "Selectivity Enhancement in Methylamine Synthesis via Postsynthesis Modification of Brønstead Acidic Mordenite", *J. Catal.*, **160** (1996) 299-308.

Gründling, C., Veefkind, V.A., Eder-Mirth, G. and Lercher, J.A.: "On the Mechanism of Zeolite Catalysed Amine Synthesis", *Proc. 11th Int. Zeo. Conf.*, (1996) Po-005.

Gründling, C., Veefkind, V.A., Eder-Mirth, G., and Lercher, J.A.: "New Insight Into The Mechanism of Zeolite Catalyzed Nucleophilic Amination *Via In Situ* Infrared Spectroscopy", *Stud. Surf. Sci. Cat.*, **105** (1997) 591-598.

Gründling, C., Eder-Mirth, G. and Lercher, J.A.: "Surface Species in the Direct Amination of Methanol over Brønsted Acidic Mordenite Catalysts", *Res. Chem. Intermed.*, **23** (1997) 25-40.

Haag, W.O. and Dessau, R.M.: "Duality of Mechanism for Acid-Catalysed Paraffin Cracking", *Proc. 8th Int. Cong. Catal.*, **2** (1984) 305.

Haag, W.O. and Chen, N.Y.: "Catalyst Design with Zeolites" in "Catalyst Design: Progress and Perspectives." *John Wiley and Sons* (1987).

Haag, W.O.: "Catalysis by Zeolites – Science and Technology", *Stud. Surf. Sci. Catal.*, **84** (1994) 1375-1394.

Haase, F., and Sauer, J.: "Interaction of methanol with Brønstead Acid Sites of Zeolite Catalysts: An ab Initio Study," *J. Am. Chem. Soc*, **117** (1995) 3780-3789.

Herrmann, C., Fetting, F. and Plog, C.: "Amine Production from Methanol and Ammonia over ZSM-5 and T-Zeolite Catalysts", *Appl. Cat.*, **39** (1988) 213-326.

Hao, M.C., Yamamoto, H. and Segawa, K.: "Shape-Selective Methylamine Synthesis over Small-Pore Zeolite Catalysts", *J. Catalysis*, **161** (1996), 20-30.

Kaeding, W.W.: "Production of Aliphatic Amines Utalizing a Crystalline Aluminosilicate Catalyst of ZSM-5, ZSM-11 or ZSM-21", *United States Patent* - 4.082,805 (1978).

Karge, H.G., Kosters, H. and Wanda, Y.: "Dehydration of Cyclohexanol as a Test Reaction for Zeolite Acidity", in *Proc. 6th Int. Zeo Conf.* (D. Olson and A Bisio, eds.), Butterworths, U.K., (1983) 308.

Karge, H.G. and Weitkamp, J.: "Untersuchunungen an Dealuminierten Mordenit – Katalysatoren", *Chem -Ing. Tech.*, **58** (1986) 946-959.

Karge, H.G. and Boldingh, E.: "Spectroscopic investigations on Deactivation of Zeolite Catalysts during Reactions of Olefins", *Catal. Today*, **3** (1988) 379.

Keane, M., Sonnichsen, G.C., Abrams, L., Corbin, D.R., Gier, T.E. and Shannon, R.D.: "Selective Synthesis of Dimethylamine over Small Pore Zeolites", *Appl. Cat.*, **32** (1987) 361-366.

Kemball, C.: "Thermodynamic Factors in Adsorption and Catalysis - Equilibria in the Adsorbed phase" (1966) 190-199.

Kijenski, J. and Baiker, A.: "Acidic Sites on Catalyst Surfaces and Their Determination", *Cat. Today*, **5** (1989), 65-70 and 93-98.

Klyuev, M.V. and Khidekel, M.L.: "Catalytic Amination of Alcohols, Aldehydes and Ketones", *Russian Chem. Rev.*, **49** (1980) 14-27.

Kogelbauer, A., Gründling, C. and Lercher, J.A.: "Correlation of Adsorption Structure and Reactivity in Zeolite Catalysed Amination", *Stud. Surf. Sci. Catal.*, **84B** (1994) 1475-1482.

Kogelbauer, A., Gründling, C. and Lercher, J.: "Influence of the Chemical Composition upon Adsorption, Coadsorption, and Reactivity of Ammonia and Methanol on Alkali-Exchanged Zeolites", *J. Phys. Chem.*, **100** (1996) 1852-1857.

Kubelkova, L., Beran, S., Maleka, A and Mastikhin, V.M.: "Acidity of Modified Y Zeolites: Effect of Nonskeletal Al, Formed by Hydrothermal Treatment, Dealumination with $SiCl_4$ and Cationic Exchanged with Al", *Zeolites*, **9** (1989) 12.

Kustanovich, I., Luz, Z., Vega, S., & Vega, A.J.: "Sorption of Mono-, Di-, and Trimethylamine on ZK-5 Zeolites Studied by Deuterium NMR," *J. Phys. Chem.*, **94** (1990) 3138-3144.

Lago, R.M., Haag, W.O., Mikovsky, R.J., Olson, D.H., Hellring, S.D., Schmitt, K.D. and Kerr, G.T., "The nature of the Catalytic Sites in HZSM-5 Activity Enhancement", *Stud. Surf. Sci. Catal.*, **28** (1986) 677.

Larsson,R.: "On transient Species and Activation Energies in Heterogeneous Catalysis", *Cat. Let.*, **36** (1996) 171-173.

Lercher, J.A., Gründling, C. and Eder-Mirth, G.: "Infrared Studies of the Surface Acidity of Oxides and Zeolites Using Adsorbed Probe Molecules," *Catal. Today*, **27** (1996) 353-376.

Li, K. & Peng, Y.: "Methylation of n-butylamine over solid-acid catalysts", *Appl Cat. A:Gen.*, **109** (1994) 225-233.

Lobo, R.L., Schwarz, S., Corbin, D.R.: "Method of Making Methylamines Using Chabazite Catalysts", *PCT Int. Appl.*, WO9902483, (1999).

Marney, L., Khabtou, S., Marzin, M., Lavalley, J.C., Chambellan, A. and Chevreau, T.: "Acidity and Reactivity of Steamed HY Zeolites Obtained by Progressive Extraction of Extraframework Al Species", *Zeolites*, (1995) 501-506.

Martin, A., Lücke, B., Wieker, W. and Becker, K.: "Amination of Dimethyl Ether on Zeolite Catalysts. I.Influence of Alkali-Cation Content of T-zeolite on the Dimethyl Ether Conversion and Methylamine Distribution", *Catalysis Letters*, **9** (1991) 451-460.

Martin. A., Berndt. H., Wolf. U. and Lücke. B.: "Amination of Dimethyl Ether on Zeolite Catalysts. 2.Acidic Properties of the Used T-Zeolites and Their Influence on the Catalytic Reaction", *Catalysis Letters*, **14** (1992) 359-371.

Martens. J.A., Souverijns. W., Van Rhijn. W and Jacobs. P.A.: "Acidity and Basicity in Zeolites", in Handbook of Heterogeneous Catalysis (G.Ertl. H. Knötzinger. J. Weitkamp. Eds.) **vol 1** (1997) 324-365.

McCusker. L.B., & Baerlocher. C.: "The Effect of Dehydration upon the Crystal Structure of Zeolite Rho", *Proc 6th Int. Zeolite Conf. Olson & Bisio eds.*, (1983). 812-821.

McCusker. L.B.: "Crystal structures of the Ammonium and Hydrogen Forms of Zeolite Rho," *Zeolites*, **4** (1984) 51-55.

Meier. W.M. and Olson. D.H.: "Rho", *Zeolites*. **12** (1992) 166-167.

Merz. C. and Fetting. F.: "Synthese des Zeoliths Rho", *Chem. Ing. Tech.*, **66** (1994) 730-732.

Merz. C. and Fetting. F.: "Characterisation of Small- and Intermediate-Pore Zeolites by means of Temperature-Progammed Desorption of Amines", *Chem. Eng. Tech.*, **19** (1996) 526-537.

Mikovsky. R.J. and Marshall. J.F., *J. Catal.*, **44** (1976) 170.

Miller. J., Hopkins. P.D., Meyers. B.L., Ray. G.J., Roginski. R.T., Zajac. G.W. and Rosenbaum. N.H.: "The Effect of Nonframework Aluminum on Acidity in Dealuminated Mordenite", *J. Catal.*, **138** (1992) 115-128.

Mirodatos. C., Barthomeuf. D.: "Superacid Sites in Zeolites", *J. Chem. Soc., Chem. Commun.*, (1981) 39.

Mitchell. J.W., Hayes. K.S. and Lutz. E.G.: "Kinetic Study of Methylamine Reforming over a Silica-Alumina Catalyst", *Ind. Eng. Chem. Res.* **33** (1994) 181-184.

Mizuno. N., Tabata. M., Uematsu. T. & Iwamoto. M.: "Amination of 2-Methylpropene over Proton Exchanged ZSM-5 Zeolite Catalysts", *J. Catal.*, **146** (1994) 249-256.

Mochida I., Yasutake A., Fujitsu H. and Takeshita K.: "Selective Synthesis of Dimethylamine from Methanol and Ammonia over Zeolites", *J. Catal.*, **82** (1983) 313-321.

Musa. M., Tarină. V., Stoica. A.D., Ivanov. E., Pop. E., Pop. G., Plotinaru. D., Ganea. R., Birjega . R., Muscă. G. and Paukshtis. E.: "Some Structural Characteristics of Dealuminated Mordenites", *Zeolites*, 7 (1987) 427-432.

Nekrasova. V.A. and Shuikin. N.I.: "Catalytic Methods of Preparing Aliphatic and Alicyclic Amines", *Russian Chem. Revs.*, **34** (1965) 843-853.

O'Donovan. A.W., O'Connor. C.T. and Koch. K.R.: "The effect of Acid and Steam Treatment of Na- and H-Mordenite and their Structural. Acidic and Catalytic Properties.", *Microporous Materials*. **5** (1995) 185-202.

Olson. K.D.: "Process for the Production of Alkylamines", *European Patent* - 324 367 A1. (1988).

Parrillo. D.J., Gorte. R.J. and Farneth. W.E.: "A Calorimetric Study of Simple Bases in H-ZSM-5: A Comparison with Gas-Phase and Solution-Phase Acidities", *J. Am. Chem. Soc.*, **115** (1993) 12441-12445.

Parise. J.B., Gier. T.E., Corbin. D.R. and Cox. D.E.: "Structural Changes Occurring upon Dehydration of Zeolite Rho. A Study Using Neutron Powder Diffraction and Distance least-Squares Structural Modelling", *J. Phys. Chem.*, **88** (1984) 1635-1640.

Parise. J.B., Abrams. L., Gier. T.E., Corbin. D.R., Jorgensen. J.D. and Prince. E.: "Flexibility of the Framework of Zeolite Rho. Structural Variation from 11 to 573 K. A Study Using Neutron Powder Diffraction Data", *J. Phys. Chem.*, **88** (1984) 2303-2307.

Pearlstine, K.A., and Friend, C.M.: "Surface Chemistry of Alkyl Amines. 2. Methylamine and Trimetylamine on W(100), W(100)-(5X1)-C, and W(100)-(2X1)-O," *J. Am. Chem. Soc.*, **108** (1986) 5842-5847.

Pelmenschikov, A.G., Paukshtis, E.A., Edisherashvili, M.O., and Zhidomirov, G.M.: "On the Loewenstein Rule and Mechanism of Zeolite Dealumination." *J.Phys.Chem.*, **96** (1992) 7051-7055.

Perry, R.H. and Green, D., "Perry's Chemical Engineers' Handbook." *McGraw Hill*, Singapore, 1984.

Roundhill, D.M.: "Transition Metal and Enzyme Catalysed Reactions involving Reactions with Ammonia and Amines", *Chem. Rev.*, **92** (1992) 1.

Ruthven, D.M.: "Principles of Adsorption and Adsorption Processes", *John Wiley and Sons*, U.S.A., (1984)

Scherzer, J., *Catal. Rev. Sci. Eng.*, **31** (1989) 215.

Schultz, H., Böhringer, W., Kohl, C., Rahmano, N. and Will, A., *D6MK-Forschungsbericht 320*, D6MK, Hamburg, 1984.

Schwarz, S., Corbin, D.R. and Sonnichsen, G.C.: "Comparison of ZK-5's Derived from K,Cs and K,Sr Synthesis Gels and Rho for Methylamine Synthesis." *Proc. of the 11th Int. zeolite conf.*, (1996) Po-006.

Schwarz, S., Corbin, D.R. and Sonnichsen, G.C.: "The effect of Crystal Size on the Methylamine Synthesis Performance of ZK-5 Zeolites", *Microporous and Mesoporous Materials*, **22** (1998) 409-418.

Segawa, K. and Tachibana, H.: "Highly Selective Methylamine Synthesis over Modified Mordenite Catalysts", *J. Catal.*, **131** (1991) 482-490.

Segawa, K. and Tachibana, H.: "Shape Selective Reactions for Methylamine Synthesis from Methanol and Ammonia", *Proc. 10th Int. Congress Catal.* (Guczi *et al.*, eds.), (1992) 1273-1283.

Segawa, K., and Ilao, M.C.: "Methanol Amination over Small-Pore Zeolite Catalysts." *Stud. Surf. Sci. Cat.*, **105** (1997) 1219-1226.

Sewell, G., O'Connor, C. and van Steen, E.: "Reductive Amination of Ethanol with Silica-Supported Cobalt and Nickel Catalysts", *App. Cat. A: General*, **125** (1995) 99-112

Shah, R., Payne, M.C., Lee, M.-H. and Gale, J.D.: "Understanding the catalytic Behaviour of Zeolites: A First Principles Study of the Adsorption of Methanol." *Science*, **271** (1996) 1395 - 1397.

Shannon, R.D., Keane, M., Abrams, L., Staley, R.H., Gier, T.E., Corbin, D.R. and Sonnichsen, G.C.: "Selective Synthesis of DMA over Small-Pore Zeolites. I. H-Rho.", *J. Catal.*, **113** (1988), 367-382.

Shannon, R.D., Keane, M., Abrams, L., Staley, R.H., Gier, T.E., Corbin, D.R. & Sonnichsen, G.C.: "Selective Synthesis of DMA over Small-Pore Zeolites. II Effects of Impurities on Catalytic Properties of H-Rho", *J. Catal.*, **114** (1988) 8-16.

Shannon, R.D., Keane, M., Abrams, L., Staley, R.H., Gier, T.E. and Sonnichsen, G.C.: "Selective Synthesis of DMA over Small-Pore Zeolites. III. H-ZK-5", *J. Catal.*, **115** (1989) 79-85.

Sharma, S.B., Meyers, B.L., Chen, D.T., Miller, J. and Dumesic, J.A.: "Characterisation of Catalyst Acidity by Microcalorimetry and Temperature-Programmed Desorption", *Appl. Cat.*, **102** (1993) 253 - 265.

Shen, J.-P., Ma, J., Jiang, D.-Z. and Min, E.-Z.: "Selective Synthesis of Ethylamine over β Zeolite", *Catalysis Letters*, **26** (1994) 291-295.

Shen, V. and Bell, A.T.: "Computer Simulation of the Interactions of Tetraalkylammonium Cations with ZSM-5 and ZSM-11." *Microporous Materials*, **7** (1996) 187-199.

Shertukde, P.V., Hall, W.K., Dereppe, J.-M. and Marcelin, G.: "Acidity of H-Y zeolites: Role of Extralatice Aluminium", *J.Catal.*, **139** (1993) 468-481.

Shiokawa, K., Ito, M. and Itabashi, K.: "Crystal Structure of Synthetic Mordenites." Zeolites, 9 (1989) 170-176.

Silva, J.M., Ribeiro, M.F., Ramôa Ribeiro, F., Benazzi, E., Gnep, N.S. and Guisnet, M., "Influence of the Treatment of Mordenite by Ammonium Hexafluorosilicate on Physicochemical and Catalytic Properties", *Zeolites*, **16** (1996) 275-280

Stach, H. and Jänchen, J., "Relationship between Acid-Strength and Framework Aluminium Content in Dealuminated Mordenites," *Zeolites*, **12** (1992) 152-154.

Stach, H., Jänchen, J. and Lohse, U., "Relationship between Acid Strength and Framework Aluminium Content in Dealuminated Faujasites," *Zeolites*, **12** (1992) 152-154.

Stockenhuber, M. and Lercher, J.A.: "Characterisation and Removal of Extra Lattice Species in Faujasites", *Microporous Materials*, **3** (1995) 457-465.

Stull, D.R., Westrum, E.F. and Sinke, G.C.: "The Chemical Thermodynamics of Organic Compounds", *John Wiley & Sons*, New York, 1969.

Schweizer, A.E., Fowlkes, R.L., McMakin, J.H. and Whyte, T.E.Jr.: "Lower Aliphatic Amines" in *Kirk-Othmer*, 2 (1992) 272-295.

Sykes, P.: "A Guidebook to Mechanism in Organic Chemistry", *Longman Scientific & Technical*, Singapore, 1988.

Szostak, R.: "Handbook of Molecular Sieves", *Van Nostrand Reinhold*, New York, 1992.

Teunissen, E.H., Jacobs, W.P.J.H., Jansen, A.P.J. and van Santen, R.A.: "Spectroscopy, Energetics and Siting of NH_4^+ in Zeolites: Theory and Experiment" *Proc. 9th Int. Zeolite Conf.*, (1993), 469-478.

Treacy, M.M.J., Higgins, J.B. and von Ballmoos, R.: "Collection of simulated XRD Powder Patterns for Zeolites", *Zeolites*, **16** (1996) 327-802.

Veefkind, V.A., Gründling, C. and Lercher, J.A.: "Steric Aspects in Methylamine and Dimethylether Synthesis over Acidic Mordenites", *J. Mol. Cat.: A Chem.*, **134** (1988) 111

Vega, A.J. & Luz, Z.: "Characterisation of the Sorption of Mono, Di-, and Trimethylamine in Zeolite H-Rho by Deuterium NMR.", *Zeolites*, **8** (1988) 19-26.

Weigert, F.: "Selective Synthesis and Equilibration of Methylamines on Sodium Mordenite", *J. Catal.*, **103** (1987) 20-29.

Weitkamp, J., Kleinschmidt, P., Kiss, A. and Birke, C.H. in von Ballmoos,R., Higgins, J.B. and Treacy, M.M.J.: "The Hydrophobicity Index – A valuable Test for Probing the Surface Properties of Zeolitic Adsorbents in Catalysts", *Proc. 9th Int. Zeolite Conf.*, Butterworth-Heinemann, Stoneham Massachusettes, vol 2, (1993) 79-87.

Witzel, F., Karge, H.G. and Gutze, A.: "ESR Measurements for the Characterisation of Acidic Lewis Sites in Zeolites", in *Proc. 9th int zeolite conf.* (R.van Ballmoos, J.B.Higgins and M.M.J.Treacy, eds.) **vol II** (1993) 563.

Wu, P., Komatsu, T., Yashima, T.: "Acidic and Catalytic Properties of Aluminated Zeolite: Effect of Extraframework Aluminium." *J. Chem. Soc., Faraday Trans.*, (1996), 92, 861-870.

Zhang, Y.-Z., Xu, Z.-L., Wang, J. and Ke, Y.-Y.: "Studies on the Nature of Catalysis for the Selective Synthesis of Methylamine", *Stud. Surf. Sci. Catal.*, **84C** (1994) 1927-1933.

Zhao, S.: "Zeitliche Selektivitäts und Aktivitätsänderungen bei der Umsetzung von Methanol und n-Dodecan am Zeolith HZSM-5 und anderen sauren Katalysatoren", PhD Thesis, Universität Karlsruhe, Germany, 1991.

Appendices

APPENDIX I: THERMODYNAMIC DATA

VAPOUR PRESSURE DATA

Compound	Vapour Pressure (mmHg)									
	1	5	10	20	40	60	100	200	400	760
	Temperature (°C)									
Helium	-271.7	-271.5	-271.3	-271.1	-270.7	-270.6	-270.3	-269.8	-269.3	-268.6
Water	-17.3	1.2	11.2	22.1	34	41.5	51.6	66.5	83.0	100
Methanol	-44	-25.3	-16.2	-6	5	12.1	21.2	34.8	49.9	64.7
Ammonia	-109.1	-97.5	-91.9	-85.8	-79.2	-74.3	-68.4	-57.0	-45.0	-33.6
MMA	-95.8	-81.3	-73.8	-65.9	-56.9	-53.3	-43.7	-32.4	-19.7	-6.3
DMA	-87.7	-72.2	-64.6	-56	-46.7	-40.7	-32.6	-20.4	-7.1	7.4
TMA	-97.1	-81.7	-73.8	-65	-55.2	-48.8	-40.3	-27	-12.5	2.9

[Taken from Perry *et al.*, 1984]

THERMODYNAMIC PROPERTIES

Property	Methanol	Ammonia	MMA	DMA	TMA	Water	DME
Formula	CH_3OH	NH_3	CH_3NH_2	$(CH_3)_2NH$	$(CH_3)_3N$	H_2O	$(CH_3)_2O$
Mol. Wt. (g/mol)	32	17	31	45	59	18	46
Mp (°C)	-97	-77.7	-92.5	-96	-124	0	-138.5
Bp (°C)	64.7	-33.4	-6.7	7.4	3.5	100	-23.7
$\Delta H_{f\,(600K)}$ kcal/mol	-50.34	-10.96 [1]	-8.09	-7.96	-9.83	-58.5	-43.06 [1]
$\Delta G_{f\,(600K)}$ kcal/mol	-28.52	-3.903 [1]	22.20	38.79	55.19	-51.16	-26.06 [1]
$Cp_{(600K)}$ cal/mol.K	16.02	6.7+0.0063T [2]	18.86	28.41	38.34	8.68	
Sg_{liq}	0.792		0.699	0.68	0.662	1	
Tc (K)	513	132.4	430.1	437.7			126.9
Pc (atm)	78.5	111.5	73.6	52.4			52
Log Kp_{600}	10.389		-8.085	-14.13	-20.103	18.634	
pKa		9.25	10.64	10.77	9.8	14	

1. 298K
2. Temperature Range 200-800K

Data taken from: Stull, 1969; Perry *et al.*, 1984; Sykes, 1988

INTERACTION PARAMETERS: (A_{IJ})

i↓ j→	Methanol	Water	Helium
Methanol	1	1.713	0.203
Water	0.6733	1	0.3038
Helium	5.918	3.659	1

[Taken from Perry. 1984]

APPENDIX II: GAS CHROMATOGRAPHY

Gas Chromatograph Operating Conditions

1. Reaction Sample Analysis

Column: 4x3 mm I.D. glass column packed with 60/80 mesh Carbopack B/ 4% Carbowax 20M/ 0.8% KOH

Carrier Gas	Hydrogen
Carrier Flow rate	30 ml(NTP)/min
Initial Column Temperature	40 °C
Initial Hold Time	10 mins
Temperature Ramp	20 °C/min
Final Temperature	180 °C
Final Hold Time	14 mins
Detector	FID
Detector Temperature	200 °C

2. Adsorption Studies

Continuos Analysis. TCD and FID in series, no column used.

Oven Temperature	100 °C
Injector Temperature	130 °C
FID temperature	200 °C
TCD block temperature	200 °C
TCD filament temperature	240 °C
Reference Gas	Helium (60 ml/min)

Sample GC traces

The following is a sample GC trace from a reaction sample, showing the peak separation and identification

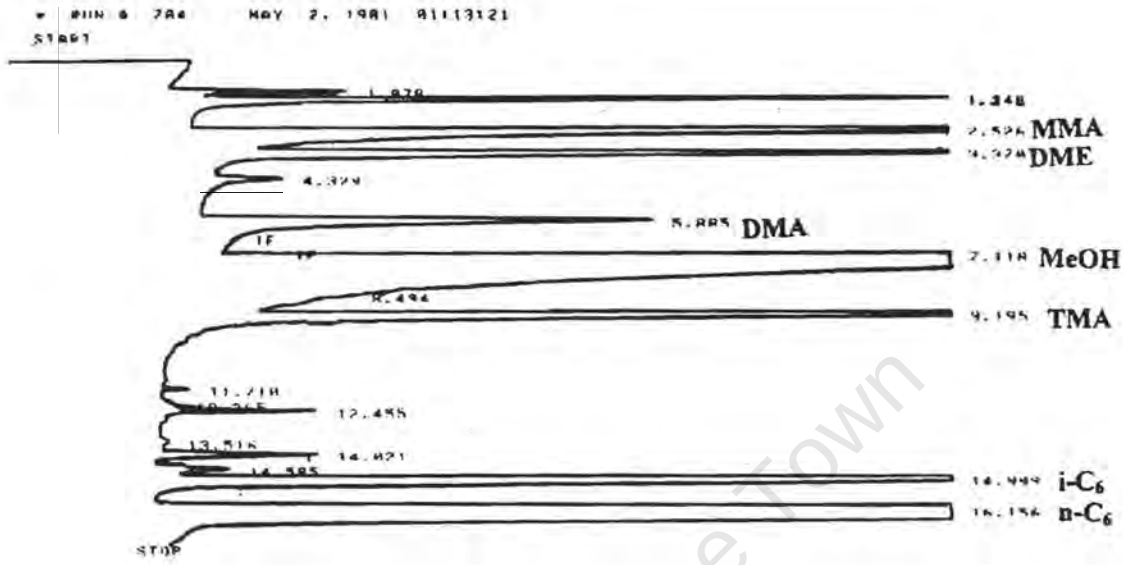

RUN# 704 MAY 2, 1981 01113121

AREA%

RT	AREA	TYPE	WIDTH	AREA%
1.479	90484	PV	.116	.09333
1.348	523727	VB	.123	.54072
2.526	1827848	PB	.175	1.88614
3.378	1049635	BB	.150	1.08359
4.329	83531	BB	.253	.08623
5.885	560154	PB	.275	.57827
7.118	4622493	SPB	.687	4.77282
8.494	1487	TBP	.827	.00154
9.195	4707133	BB	.129	4.85940
11.718	14548	VP	.184	.01511
12.265	13569	PV	.201	.01401
12.455	83286	VB	.119	.08598
13.516	17587	PV	.343	.01907
14.821	123565	VP	.156	.12756
14.585	74693	PV	.223	.07732
14.999	1927753	VB	.201	1.99011
16.156	81145792	PB	.213	83.77962

TOTAL AREA=9.6867E+07
MUL FACTOR=1.0000E+00

Calculations from GC data

A = area of a given peak

Rf = response factor

Cno. = carbon number of molecule

Carbon Balance $$C_{bal} = \frac{\left(\frac{A_{methanol}}{Rf_{methanol}} + \sum_{all\ products} \frac{A}{Rf}\right)_{reaction} / \left(\frac{A_{n-hexane}}{Rf_{n-hexane}}\right)_{reaction}}{\left(\frac{A_{methanol}}{Rf_{methanol}} / \frac{A_{n-hexane}}{Rf_{n-hexane}}\right)_{feed}}$$

Conversion of methanol $$X_m = 1 - \frac{\left(\frac{A_{methanol}}{A_{n-hexane}}\right)_{reaction}}{\left(\frac{A_{methanol}}{A_{n-hexane}}\right)_{feed}}$$

Yield of amine or ether $$Y_i = \frac{\left(\frac{A_i / Rf_i}{A_{n-hexane} / Rf_{n-hexane}}\right)_{reaction}}{\left(\frac{A_i / Rf_i}{A_{n-hexane} / Rf_{n-hexane}}\right)_{feed}} * 100 \ (C\%)$$

Product Selectivity $$S_i = \frac{Y_i}{\sum_{all\ products} Y} * 100$$

Amine fraction of total amines: $$A_{ic} = \frac{S_i}{\sum_{amines} S} * 100 \quad (C\%)$$

$$A_{im} = \frac{(A_{ic} / C_{no.})}{\sum_{amines} (A_{ic} / C_{no.})} * 100 \quad (mol\%)$$

Ammonia Conversion: $$X_a = \sum_{amines} (Y / C_{no.})$$

Response Factor determination

The response factors of the amines and dimethyl ether were determined by making up samples of varying concentrations of the amine/ether in n-hexane. These solutions were then injected into the GC. The area on the GC trace obtained from each compound is related to the amount of that compound injected by: $A = R_f * M$. Where A is the area of the GC trace, M is the amount of carbon, in the compound, injected and R_f is the response factor of that compound. For the standard solutions used, the ratio of the carbon in the two compounds fed is known, the ratio of the areas on the GC trace is determined and the response factor of n-hexane is taken as 1. Therefore, the response factor can be determined as

$$R_{f,i} = \left(\frac{A_i}{A_{n-hexane}}\right) \times R_{f\,n-hexane}\left(\frac{M_{n-hexane}}{M_i}\right)$$

The response factors of the compounds seen in this study were as follows

Compound	Response factor (Carbon basis)
Methanol	1.1
MMA	1
DMA	1
TMA	0.9
DME	1.3
n-hexane	1

APPENDIX III: X-RAY DIFFRACTION AND IR DATA

STANDARD X-RAY POWDER DIFFRACTION SPECTRA

[taken from Treacy et al., 1996]

1. Rho

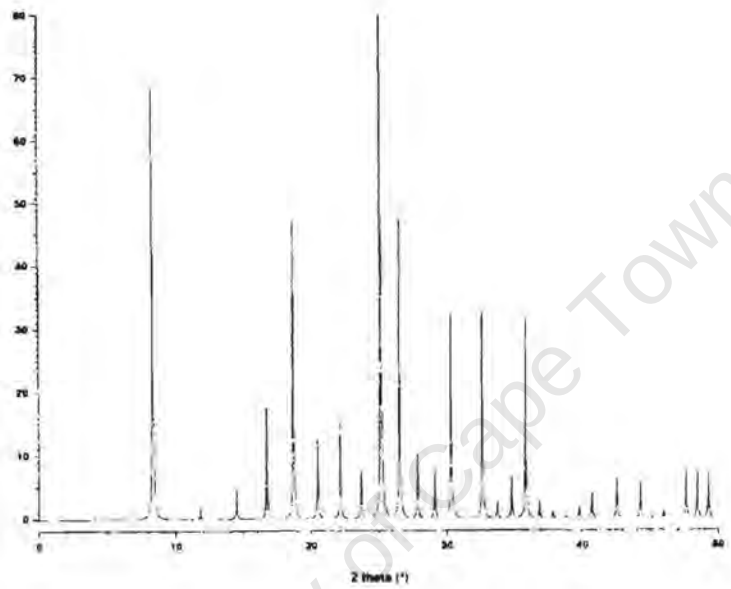

2. Chabazite

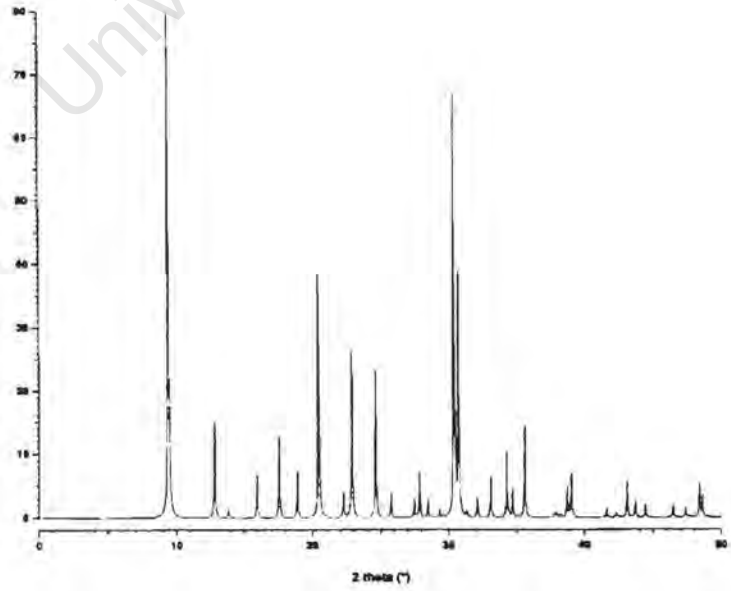

3. Analcime (Pollucite)

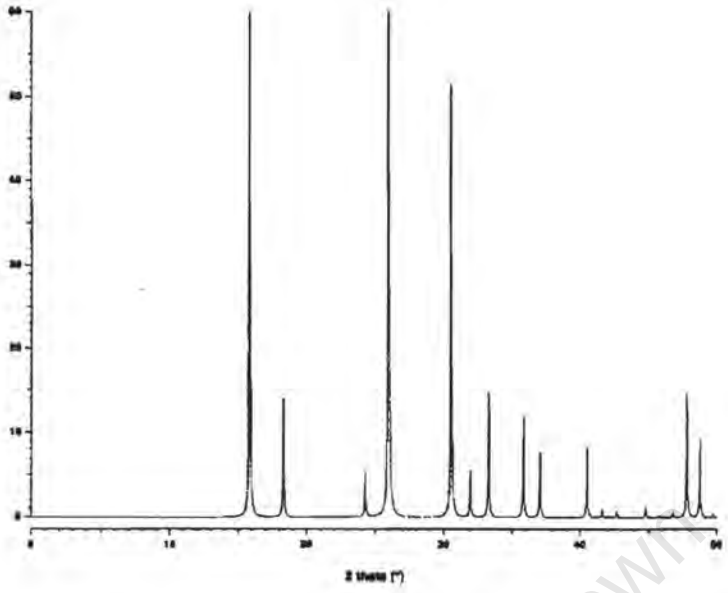

4. Mordenite

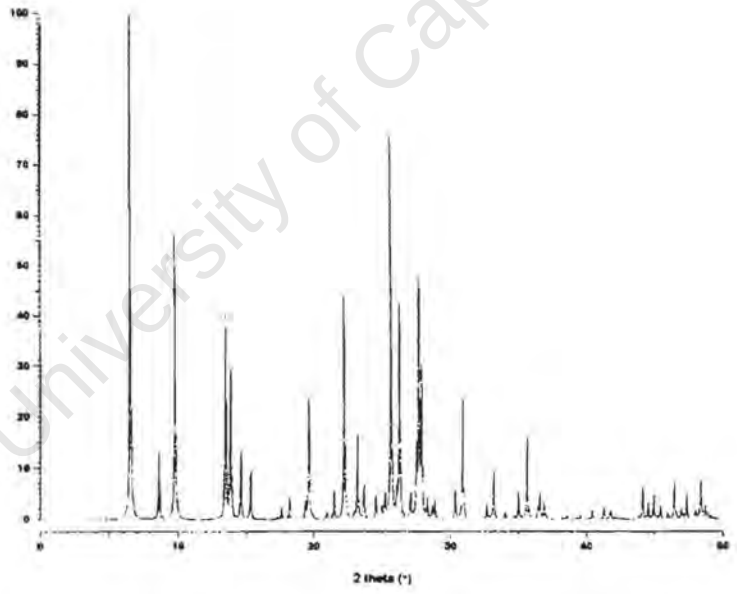

XRD RESULTS

RHO(A)

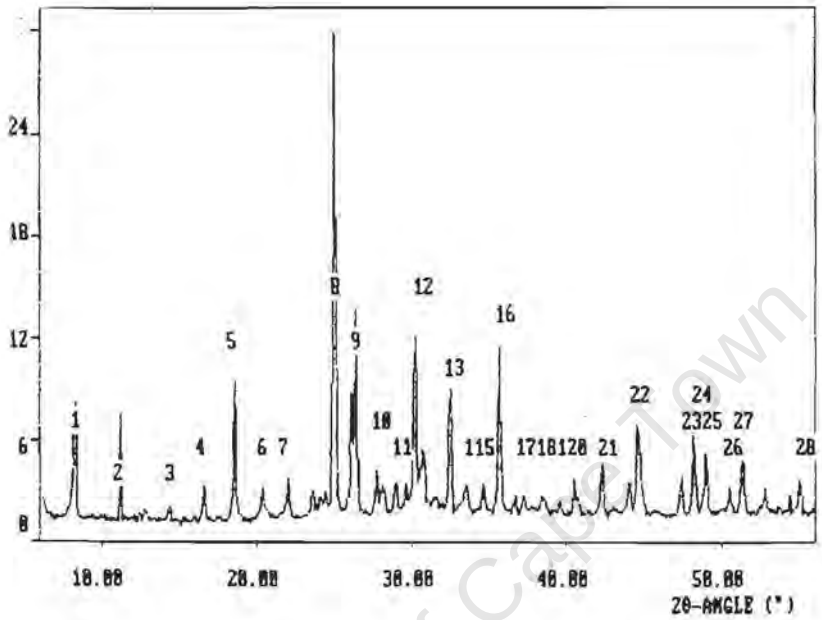

RHO (B)

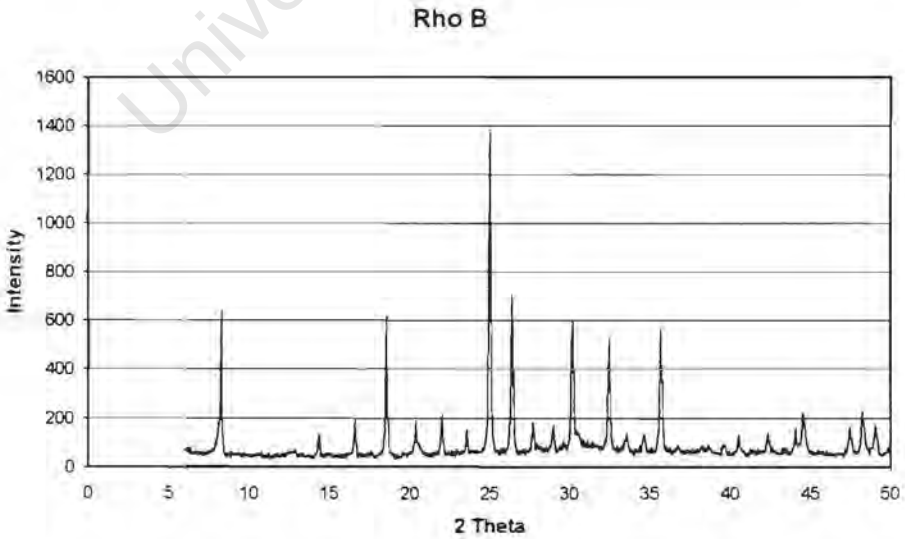

MORDENITE

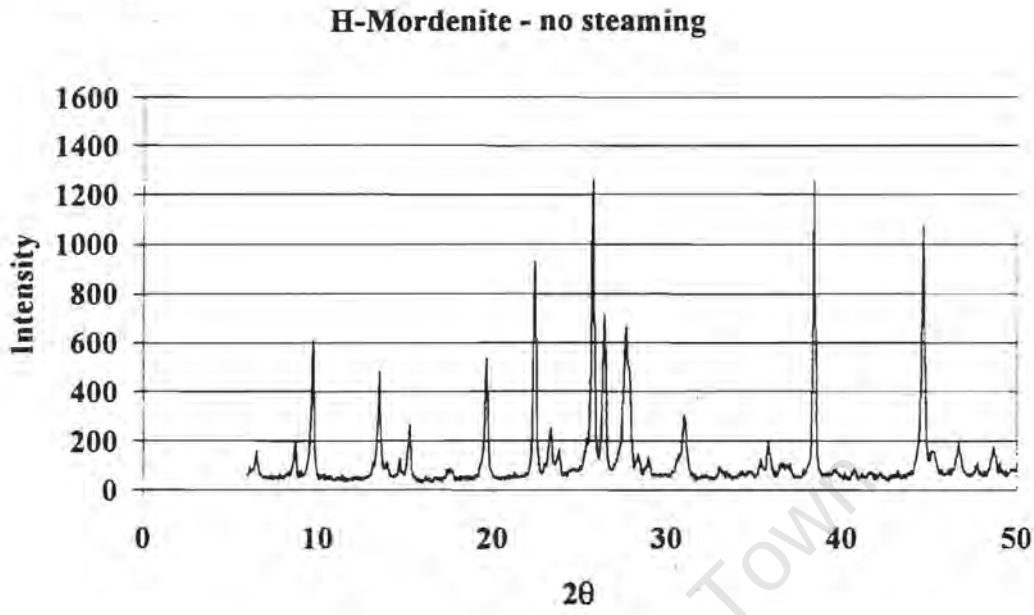

Effect of Steaming

Rho (A) – 0 and 8 hours steaming

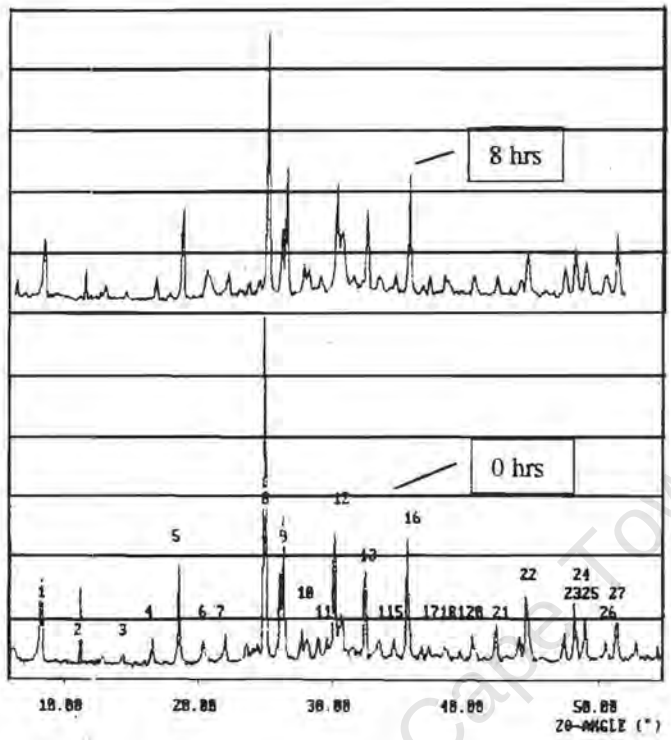

Mordenite – Comparison of Steaming Times

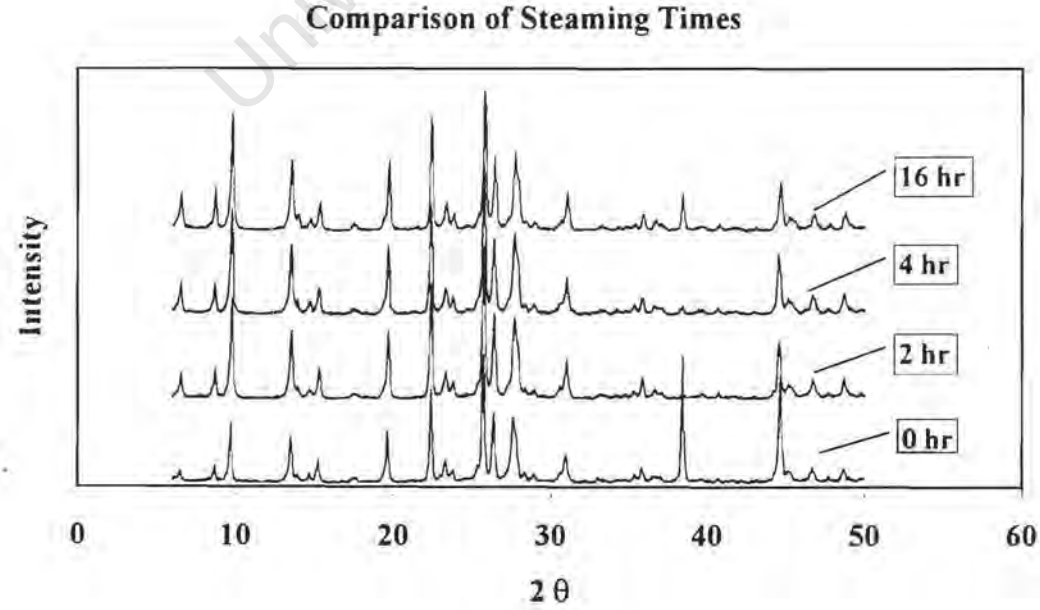

IR Spectra for calcined (protonic) and uncalcined (ammonium) Rho after ion-exchange

1. Uncalcined (Ammonium form)

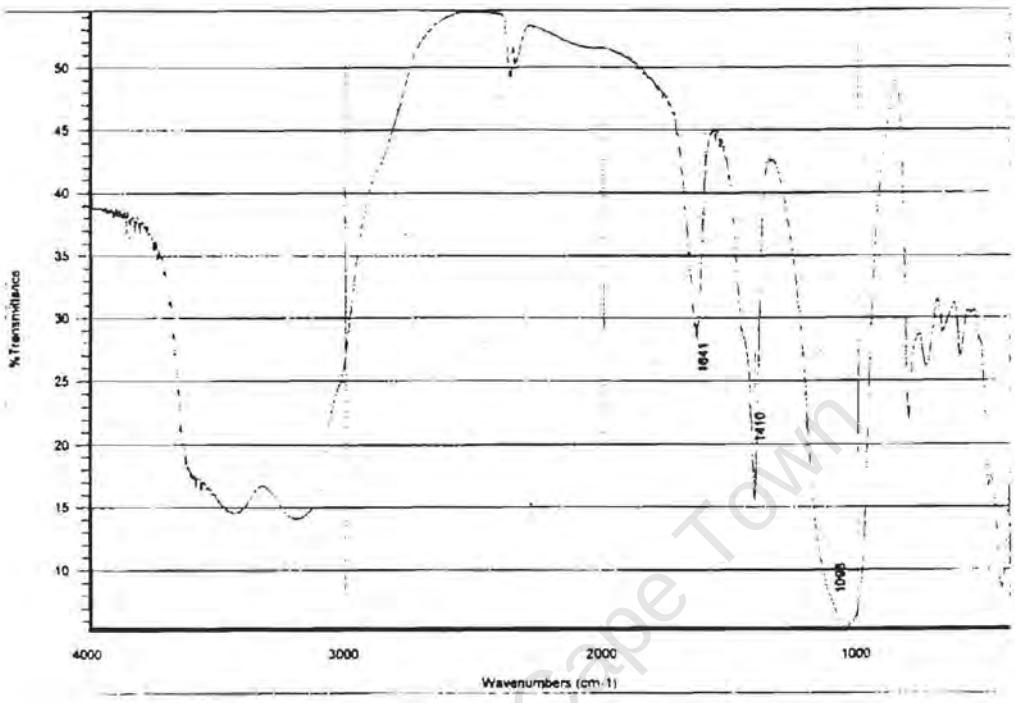

2. Calcined (Protonic form)

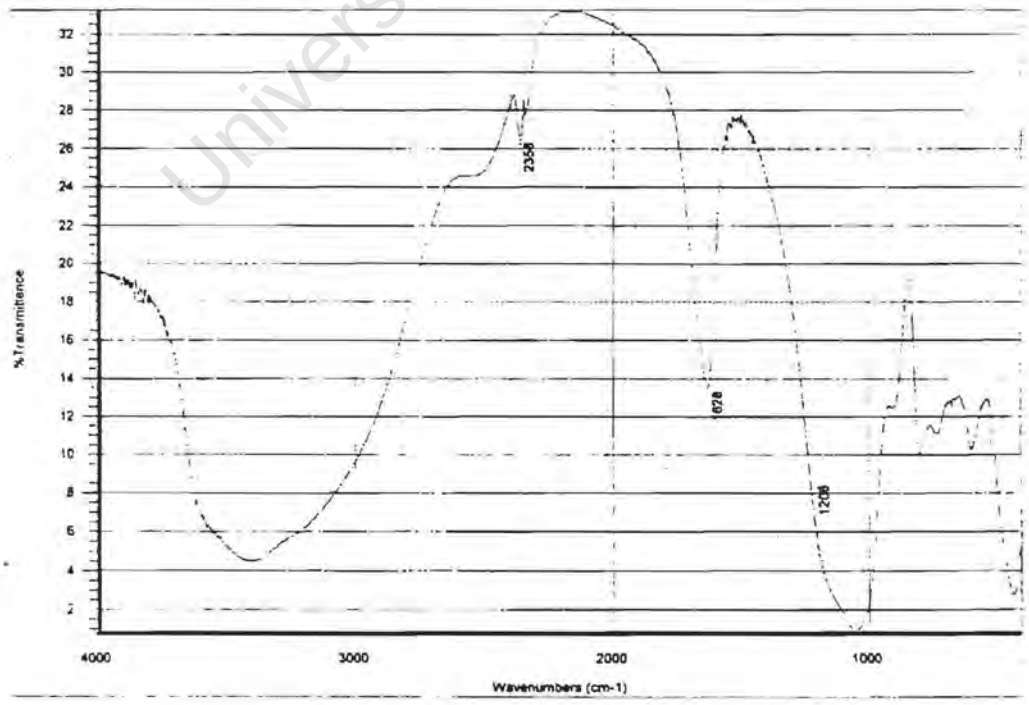

APPENDIX IV: NH_3-TEMPERATURE PROGRAMMED DESORPTION

DECONVOLUTION OF RHO(A) SPECTRA

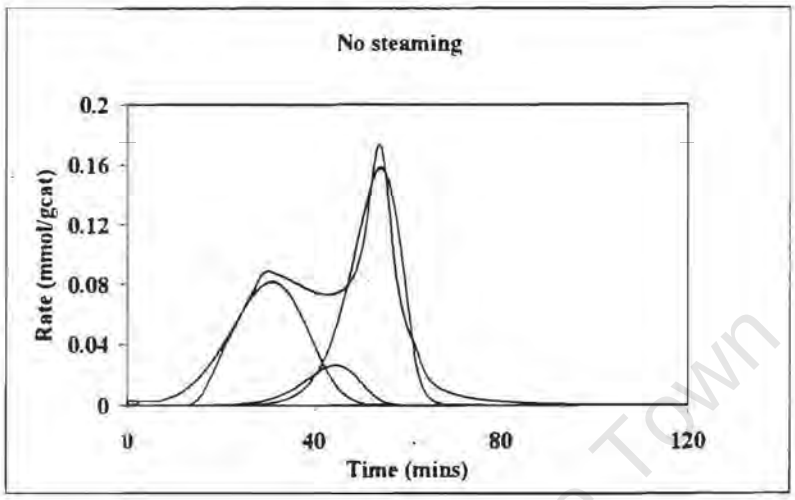

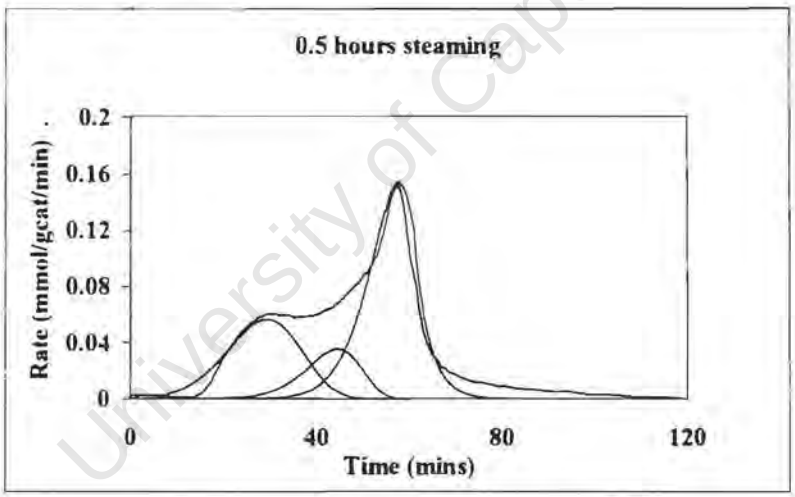

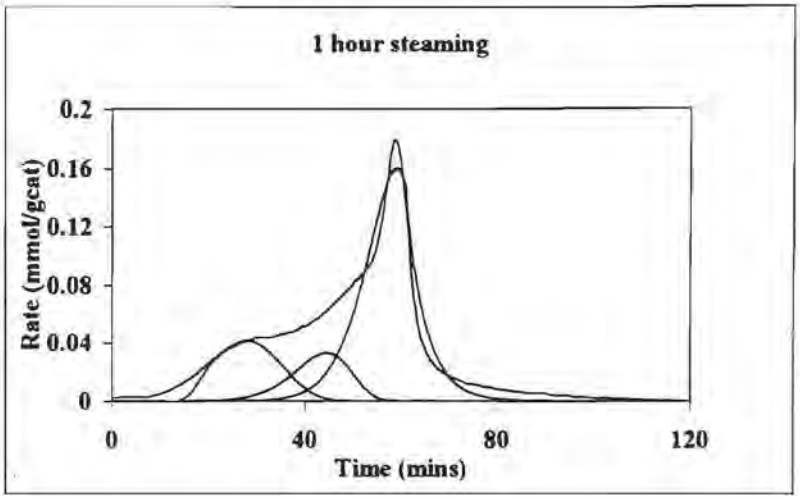

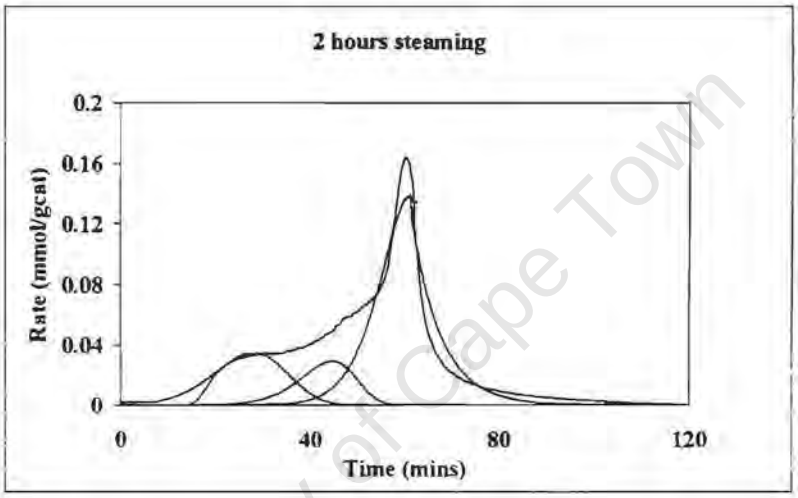

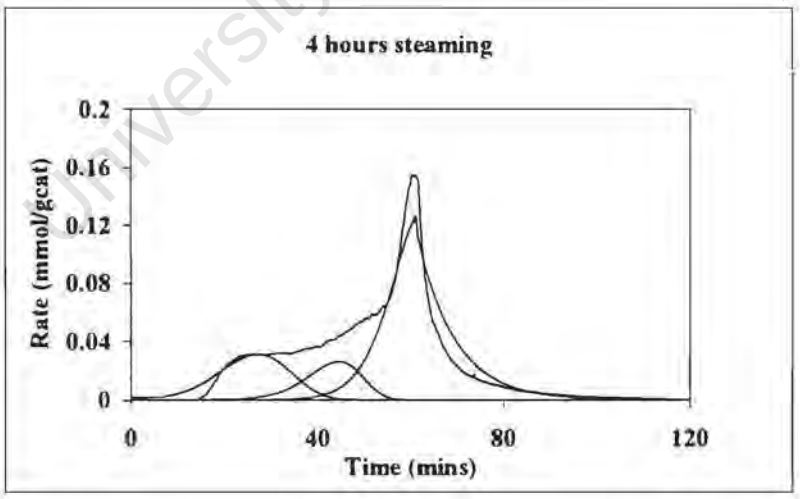

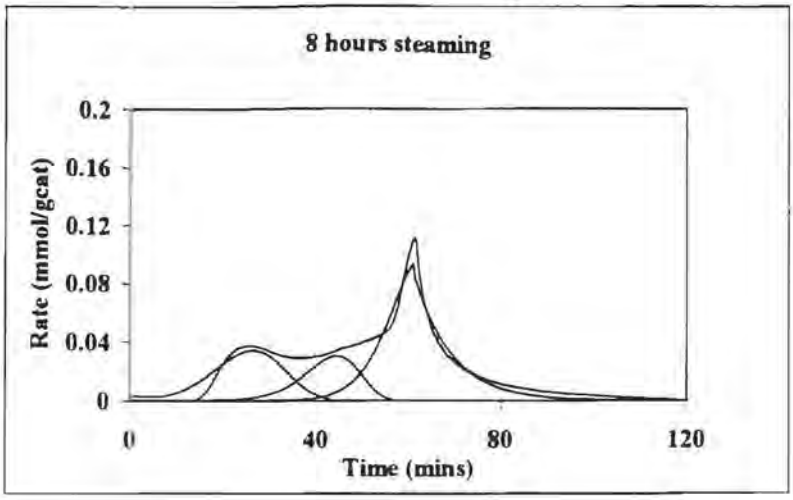

APPENDIX V: REACTION DATA

1. REACTION REGENERATION CYCLES

RHO

i) Reaction-Regeneration Series no 1:

$T_{reaction}$ = 325 °C, $t_{reaction}$=1.5 hrs/cycle, $p_{MeOH} = p_{NH3}$ = 8 kPa, p_{tot} = atmospheric, $T_{calcination}$ = 500 °C, $t_{calcination}$ = 5 hrs/cycle

Cycle no		1.00	2.00	3.00	4.00	5.00	6.00	7.00	8.00	9.00
Total Calcination time	(hours)	5.00	10.00	15.00	20.00	25.00	30.00	35.00	40.00	45.00
Total reaction time	(hours)	1.50	3.00	4.50	6.00	7.50	9.00	10.50	12.00	13.50
C-Balance		0.89	0.90	0.97	0.98	0.98	1.02	0.94	1.00	0.96
Methanol Conversion		0.28	0.36	0.39	0.49	0.54	0.55	0.62	0.59	0.60
Integral Rate of Methanol Consumption	(mmol C/ g_{cat} /hr)	28.65	36.84	40.31	50.56	55.49	56.36	64.31	60.35	61.40
Ammonia Conversion		0.05	0.09	0.15	0.20	0.23	0.24	0.26	0.27	0.26
Yields (C frac)										
MMA		0.01	0.02	0.04	0.06	0.07	0.07	0.09	0.09	0.08
DMA		0.01	0.02	0.05	0.08	0.10	0.11	0.12	0.14	0.14
TMA		0.12	0.19	0.25	0.32	0.33	0.36	0.34	0.34	0.32
DME		0.03	0.02	0.02	0.02	0.02	0.02	0.02	0.02	0.02
Absolute Selectivity (C frac)										
MMA		0.03	0.04	0.11	0.12	0.13	0.13	0.14	0.15	0.14
DMA		0.02	0.05	0.12	0.15	0.18	0.20	0.19	0.25	0.23
TMA		0.46	0.52	0.65	0.67	0.62	0.66	0.54	0.58	0.53
DME		0.10	0.07	0.06	0.03	0.03	0.04	0.03	0.03	0.03
Relative Selectivities (C frac)										
MMA		0.05	0.06	0.11	0.12	0.13	0.12	0.16	0.15	0.15
DMA		0.04	0.08	0.13	0.16	0.19	0.19	0.21	0.25	0.25
TMA		0.75	0.76	0.69	0.69	0.64	0.64	0.60	0.57	0.57
DME		0.16	0.10	0.07	0.03	0.03	0.04	0.03	0.03	0.03
Amine content in amines (C frac)										
MMA		0.06	0.07	0.12	0.12	0.14	0.13	0.16	0.16	0.15
DMA		0.04	0.08	0.14	0.17	0.20	0.20	0.22	0.25	0.26
TMA		0.90	0.85	0.74	0.71	0.67	0.67	0.62	0.59	0.59
Amine content in amines (mol frac)										
MMA		0.16	0.16	0.28	0.28	0.30	0.28	0.34	0.32	0.32
DMA		0.06	0.11	0.16	0.19	0.22	0.22	0.23	0.26	0.27
TMA		0.79	0.73	0.57	0.53	0.49	0.49	0.43	0.41	0.41

ii) Reaction-Regeneration Series no 2:

$T_{reaction}$ = 325 °C, $t_{reaction}$ =1.5 hrs/cycle, p_{MeOH} = p_{NH3} = 8 kPa, p_{tot} = atmospheric, $T_{calcination}$ = 500 °C, $t_{calcination}$ = 15 hrs/cycle

Cycle no		1.00	2.00	3.00	4.00	5.00	6.00
Total Calcination time	(hours)	15.00	30.00	45.00	60.00	75.00	90.00
Total reaction time	(hours)	1.50	3.00	4.50	6.00	7.50	9.00
C-Balance		0.90	0.89	0.93	0.96	0.93	0.96
Methanol Conversion	(fractional)	0.27	0.36	0.37	0.39	0.52	0.56
Integral Rate of Methanol Consumption	(mmolC/ g_{cat} /hr)	28.19	37.10	38.16	39.80	53.54	57.40
Yields (C frac)							
MMA		0.01	0.03	0.05	0.05	0.06	0.09
DMA		0.01	0.03	0.04	0.05	0.07	0.12
TMA		0.12	0.16	0.19	0.22	0.30	0.29
DME		0.03	0.03	0.02	0.02	0.01	0.01
Absolute Selectivity (C frac)							
MMA		0.05	0.09	0.12	0.14	0.12	0.17
DMA		0.04	0.08	0.10	0.14	0.14	0.22
TMA		0.44	0.46	0.53	0.57	0.58	0.52
DME		0.11	0.07	0.06	0.06	0.02	0.02
Relative Selectivities (C frac)							
MMA		0.07	0.12	0.15	0.15	0.14	0.18
DMA		0.07	0.11	0.13	0.15	0.17	0.24
TMA		0.69	0.66	0.65	0.63	0.67	0.55
DME		0.17	0.11	0.07	0.07	0.02	0.03
Amine content in amines (C frac)							
MMA		0.09	0.14	0.16	0.16	0.15	0.19
DMA		0.08	0.12	0.14	0.16	0.17	0.25
TMA		0.83	0.74	0.70	0.68	0.68	0.57
Amine content in amines (mol frac)							
MMA		0.21	0.31	0.35	0.34	0.32	0.37
DMA		0.10	0.13	0.15	0.17	0.18	0.25
TMA		0.69	0.56	0.50	0.48	0.49	0.38

iii) Reaction-Regeneration Series no 3:

$T_{reaction}$ = 325 °C, $t_{reaction}$=4.5 hrs/cycle, p_{MeOH} = p_{NH3} = 8 kPa, p_{tot} = atmospheric, $T_{calcination}$ = 500 °C, $t_{calcination}$ = 5 hrs/cycle

Cycle no		1.00	2.00	3.00	4.00
Total Calcination time	(hours)	5.00	10.00	15.00	20.00
Total reaction time	(hours)	4.50	9.00	13.50	18.00
C-Balance	(fractional)	0.93	0.96	0.93	0.93
Methanol Conversion	(fractional)	0.27	0.30	0.36	0.38
Integral Rate of Methanol Consumption	mmol C/ g_{cat} /hr	27.56	30.67	36.95	39.59
Yields (C%)					
MMA		0.02	0.03	0.04	0.04
DMA		0.01	0.02	0.04	0.05
TMA		0.11	0.16	0.16	0.16
DME		0.02	0.02	0.02	0.02
Absolute Selectivity (C frac)					
MMA		0.09	0.10	0.12	0.13
DMA		0.06	0.08	0.11	0.15
TMA		0.47	0.59	0.48	0.46
DME		0.10	0.09	0.06	0.06
Relative Selectivities (C frac)					
MMA		0.12	0.12	0.16	0.16
DMA		0.08	0.09	0.14	0.18
TMA		0.66	0.69	0.62	0.58
DME		0.14	0.11	0.08	0.07
Amine content in amines (C frac)					
MMA		0.14	0.13	0.17	0.17
DMA		0.10	0.10	0.16	0.20
TMA		0.76	0.77	0.67	0.63
Amine content in amines (mol frac)					
MMA		0.32	0.30	0.36	0.36
DMA		0.11	0.11	0.17	0.21
TMA		0.57	0.59	0.47	0.43

iv) Reaction-Regeneration Series no 4:

$T_{reaction}$ = 325 °C, $t_{reaction}$=21.5 hrs/cycle, p_{MeOH} = p_{NH3} = 8 kPa, p_{tot} = atmospheric, $T_{calcination}$ = 500 °C, $t_{calcination}$ = 5 hrs/cycle

Cycle no		1.00	2.00	3.00
Total Calcination time	(hours)	5.00	10.00	15.00
Total reaction time	(hours)	21.50	43.00	64.50
C-Balance	(fractional)	0.91	0.91	0.99
Methanol Conversion	(fractional)	0.26	0.38	0.44
Integral Rate of Methanol Consumption	mmol C/ g_{cat} /hr	26.46	38.86	44.90
Yields (C frac)				
MMA		0.02	0.05	0.07
DMA		0.01	0.03	0.06
TMA		0.10	0.19	0.28
DME		0.03	0.02	0.02
Absolute Selectivity (C frac)				
MMA		0.09	0.14	0.17
DMA		0.04	0.09	0.14
TMA		0.41	0.50	0.63
DME		0.10	0.04	0.04
Relative Selectivities (C frac)				
MMA		0.14	0.18	0.17
DMA		0.07	0.12	0.14
TMA		0.64	0.65	0.65
DME		0.15	0.06	0.04
Amine content in amines (C frac)				
MMA		0.16	0.19	0.18
DMA		0.08	0.13	0.14
TMA		0.76	0.68	0.68
Amine content in amines (mol frac)				
MMA		0.35	0.39	0.37
DMA		0.09	0.13	0.15
TMA		0.56	0.48	0.48

v) Reaction-Regeneration Series no 5:

$T_{reaction}$ = 325 °C, $t_{reaction}$=3 hrs/cycle, $p_{MeOH} = p_{NH3}$ = 8 kPa, p_{tot} = atmospheric, $T_{calcination}$ = 500 °C, $t_{calcination}$ = 5 hrs/cycle

Cycle no		1.00	2.00	3.00	5.00	6.00	7.00	8.00	9.00	10.00
Total Calcination time		5.00	10.00	15.00	25.00	30.00	35.00	40.00	45.00	50.00
Total reaction time		3.00	6.00	9.00	15.00	18.00	21.00	24.00	27.00	30.00
C-Balance		0.92	0.95	0.97	1.04	1.06	1.00	1.01	1.00	1.01
Methanol Conversion		0.23	0.27	0.34		0.45	0.47	0.51	0.51	0.51
Integral Rate of Methanol Consumption										
mmol C/ g_{cat} /hr		23.36	28.06	34.66		46.82	48.87	52.98	52.85	52.80
Yields (C frac)										
MMA		0.01	0.02	0.04	0.06	0.07	0.08	0.07	0.07	0.08
DMA		0.00	0.02	0.03	0.10	0.10	0.11	0.13	0.13	0.15
TMA		0.11	0.16	0.21	0.32	0.34	0.31	0.31	0.29	0.30
DME		0.03	0.03	0.03	0.01	0.02	0.02	0.01	0.02	0.02
Absolute Selectivity (C frac)										
MMA		0.03	0.07	0.11	0.14	0.15	0.15	0.13	0.13	0.14
DMA		0.00	0.07	0.09	0.21	0.22	0.21	0.25	0.25	0.29
TMA		0.47	0.60	0.62	0.71	0.72	0.61	0.60	0.57	0.56
DME		0.13	0.10	0.07	0.03	0.04	0.03	0.03	0.03	0.03
Relative Selectivities (C frac)										
MMA		0.04	0.08	0.13	0.13	0.13	0.15	0.13	0.14	0.14
DMA		0.00	0.08	0.10	0.20	0.19	0.21	0.25	0.25	0.28
TMA		0.75	0.71	0.69	0.65	0.64	0.61	0.59	0.58	0.55
DME		0.21	0.12	0.08	0.03	0.03	0.03	0.03	0.03	0.03
Amine content in amines (C frac)										
MMA		0.05	0.09	0.14	0.13	0.14	0.15	0.13	0.14	0.15
DMA		0.00	0.09	0.11	0.20	0.20	0.22	0.26	0.26	0.29
TMA		0.95	0.82	0.75	0.67	0.66	0.63	0.61	0.60	0.56
Amine content in amines (mol frac)										
MMA		0.14	0.22	0.31	0.28	0.30	0.33	0.29	0.30	0.30
DMA		0.00	0.11	0.13	0.22	0.22	0.23	0.28	0.28	0.30
TMA		0.86	0.66	0.56	0.49	0.48	0.44	0.44	0.43	0.39

MORDENITE

$T_{reaction}$ = 325 °C, $t_{reaction}$=3 hrs/cycle, p_{MeOH} = p_{NH3} = 8 kPa, p_{tot} = atmospheric, $T_{calcination}$ = 500 °C, $t_{calcination}$ = 5 hrs/cycle

Cycle no		1	2	3	4	5	6	7	8
C-Balance		0.88	0.98	0.79	0.95	0.97	0.91	0.91	0.96
Methanol Conversion		0.33	0.28	0.43	0.33	0.34	0.39	0.38	0.37
Yields (C%)									
MMA		0.04	0.06	0.04	0.06	0.08	0.07	0.07	0.08
DMA		0.02	0.03	0.01	0.03	0.04	0.03	0.03	0.03
TMA		0.09	0.09	0.08	0.09	0.10	0.10	0.10	0.11
DME		0.06	0.08	0.08	0.09	0.10	0.08	0.09	0.10
Absolute Selectivity (C frac)									
MMA		0.13	0.21	0.09	0.18	0.22	0.16	0.18	0.21
DMA		0.06	0.11	0.03	0.08	0.10	0.07	0.09	0.09
TMA		0.26	0.32	0.19	0.29	0.30	0.21	0.26	0.31
DME		0.19	0.29	0.19	0.29	0.28	0.17	0.22	0.29
Relative Selectivities (C frac)									
MMA		0.20	0.23	0.17	0.21	0.25	0.26	0.24	0.24
DMA		0.10	0.11	0.06	0.10	0.11	0.12	0.12	0.10
TMA		0.41	0.35	0.38	0.34	0.33	0.34	0.35	0.35
DME		0.29	0.31	0.38	0.35	0.31	0.28	0.29	0.32
Amine content in amines (C frac)									
MMA		0.28	0.33	0.27	0.33	0.36	0.36	0.34	0.35
DMA		0.14	0.17	0.11	0.15	0.17	0.17	0.17	0.15
TMA		0.58	0.51	0.62	0.52	0.48	0.48	0.49	0.51
Amine content in amines (mol frac)									
MMA		0.51	0.57	0.50	0.57	0.60	0.60	0.58	0.59
DMA		0.13	0.14	0.10	0.13	0.14	0.14	0.14	0.13
TMA		0.36	0.29	0.40	0.30	0.27	0.27	0.28	0.29

2. STEAMING

Rho A

Steaming Time (hours)	0	0	0.25	0.5	1	1	1.5	2	3	5	12.25	18
C-Balance	1.01	0.92	0.92	1.04	1.11	0.93	0.97	1.03	0.89	1.08	1.07	1.33
Methanol Conversion (frac)	0.27	0.27	0.43	0.48	0.60	0.38	0.79	0.66	0.86	0.72	0.56	0.41
Ammonia Conversion (frac)	0.08	0.06	0.16	0.24	0.54	0.13	0.36	0.36	0.34	0.38	0.45	0.46
Yields (C fraction)												
MMA	0.02	0.02	0.06	0.10	0.21	0.06	0.12	0.14	0.10	0.12	0.25	0.24
DMA	0.00	0.01	0.06	0.09	0.32	0.04	0.21	0.31	0.19	0.27	0.34	0.34
TMA	0.17	0.09	0.21	0.30	0.52	0.17	0.42	0.18	0.44	0.39	0.09	0.13
DME	0.09	0.07	0.03	0.03	0.02	0.04	0.02	0.05	0.02	0.03	0.03	0.02
Absolute Selectivity (C frac)												
MMA	0.12	0.08	0.14	0.20	0.22	0.16	0.15	0.22	0.12	0.17	0.38	0.60
DMA	0.00	0.05	0.14	0.20	0.34	0.10	0.26	0.47	0.22	0.37	0.51	0.84
TMA	0.60	0.33	0.48	0.63	0.54	0.46	0.53	0.28	0.51	0.53	0.14	0.33
DME	0.34	0.25	0.07	0.07	0.02	0.11	0.02	0.08	0.03	0.04	0.04	0.06
Relative Selectivities (C frac)												
MMA	0.08	0.11	0.17	0.18	0.19	0.19	0.15	0.21	0.13	0.15	0.35	0.33
DMA	0.00	0.07	0.16	0.18	0.30	0.12	0.27	0.45	0.25	0.33	0.48	0.46
TMA	0.59	0.46	0.58	0.57	0.49	0.56	0.55	0.27	0.59	0.49	0.13	0.18
DME	0.33	0.35	0.09	0.06	0.02	0.13	0.02	0.07	0.03	0.03	0.04	0.03
Amine content in amines (C frac)												
MMA	0.12	0.18	0.18	0.20	0.20	0.21	0.15	0.22	0.13	0.15	0.36	0.34
DMA	0.00	0.11	0.18	0.19	0.31	0.14	0.28	0.49	0.26	0.34	0.50	0.47
TMA	0.88	0.71	0.64	0.61	0.49	0.65	0.57	0.29	0.61	0.50	0.14	0.19
Amine content in amines (mol frac)												
MMA	0.28	0.37	0.38	0.40	0.38	0.43	0.31	0.40	0.29	0.30	0.55	0.53
DMA	0.00	0.12	0.19	0.19	0.30	0.14	0.29	0.43	0.28	0.35	0.38	0.37
TMA	0.72	0.50	0.44	0.41	0.32	0.43	0.40	0.17	0.44	0.35	0.07	0.10

Mordenite

Mild Steaming (T_{steam}=450°C, p_{H2O}=30 kPa)

Steaming Time (hours)	0	0.25	0.5	1	2	8.75
C-Balance	0.86	0.96	1.07	0.87	0.64	0.98
Methanol Conversion (frac)	0.40	0.48	0.44	0.69	0.63	0.45
Ammonia Conversion (frac)	0.15	0.09	0.15	0.16	0.07	0.12
Yields (C fraction)						
MMA	0.07	0.05	0.09	0.11	0.04	0.08
DMA	0.04	0.03	0.03	0.04	0.01	0.03
TMA	0.17	0.10	0.12	0.10	0.06	0.08
DME	0.05	0.03	0.03	0.02	0.01	0.02
Absolute Selectivity (C frac)						
MMA	0.15	0.19	0.45	0.28	0.08	0.35
DMA	0.09	0.12	0.17	0.11	0.03	0.11
TMA	0.35	0.41	0.60	0.25	0.13	0.35
DME	0.10	0.13	0.16	0.06	0.02	0.09
Relative Selectivities (C frac)						
MMA	0.22	0.20	0.33	0.41	0.32	0.39
DMA	0.13	0.13	0.12	0.15	0.11	0.13
TMA	0.51	0.52	0.44	0.36	0.49	0.39
DME	0.14	0.16	0.11	0.08	0.08	0.10
Amine content in amines (C frac)						
MMA	0.25	0.23	0.37	0.44	0.35	0.43
DMA	0.16	0.15	0.14	0.17	0.12	0.14
TMA	0.59	0.62	0.49	0.39	0.53	0.43
Amine content in amines (mol frac)						
MMA	0.48	0.42	0.61	0.67	0.59	0.67
DMA	0.15	0.14	0.12	0.13	0.10	0.11
TMA	0.37	0.44	0.27	0.20	0.31	0.22

Severe Steaming: (T_{steam}=500°C, p_{H2O}=57kPa)

Steaming Time (hours)	0	0.33	1	2	4	8	16
C-Balance	0.99	0.83	1.10	0.92	1.10	0.78	0.90
Methanol Conversion (frac)	0.69	0.95	0.83	0.91	0.59	0.73	0.59
Ammonia Conversion (frac)	0.35	0.39	0.46	0.39	0.29	0.15	0.17
Yields (C fraction)							
MMA	0.21	0.20	0.27	0.21	0.18	0.08	0.10
DMA	0.10	0.06	0.11	0.12	0.19	0.24	0.21
TMA	0.08	0.10	0.09	0.09	0.04	0.04	0.05
DME	0.29	0.42	0.45	0.42	0.28	0.14	0.13
Absolute Selectivity (C frac)							
MMA	0.31	0.21	0.33	0.23	0.31	0.12	0.17
DMA	0.15	0.07	0.14	0.13	0.32	0.33	0.36
TMA	0.12	0.10	0.10	0.10	0.07	0.05	0.08
DME	0.43	0.44	0.55	0.46	0.48	0.19	0.22
Relative Selectivities (C frac)							
MMA	0.31	0.26	0.29	0.25	0.26	0.17	0.21
DMA	0.15	0.08	0.12	0.14	0.28	0.48	0.43
TMA	0.12	0.12	0.09	0.11	0.05	0.08	0.10
DME	0.43	0.54	0.49	0.51	0.41	0.28	0.26
Amine content in amines (C frac)							
MMA	0.36	0.28	0.33	0.29	0.36	0.32	0.36
DMA	0.14	0.14	0.11	0.12	0.07	0.15	0.17
TMA	0.50	0.58	0.56	0.59	0.57	0.53	0.47
Amine content in amines (mol frac)							
MMA	0.60	0.52	0.58	0.53	0.62	0.56	0.60
DMA	0.11	0.12	0.09	0.11	0.06	0.13	0.14
TMA	0.28	0.36	0.33	0.36	0.32	0.31	0.26

APPENDIX VI: EFFECT OF PARTICLE SIZE

Please refer to section 3.3.1. The figure below shows the particle size distribution for 4 different samples of Rho (A)

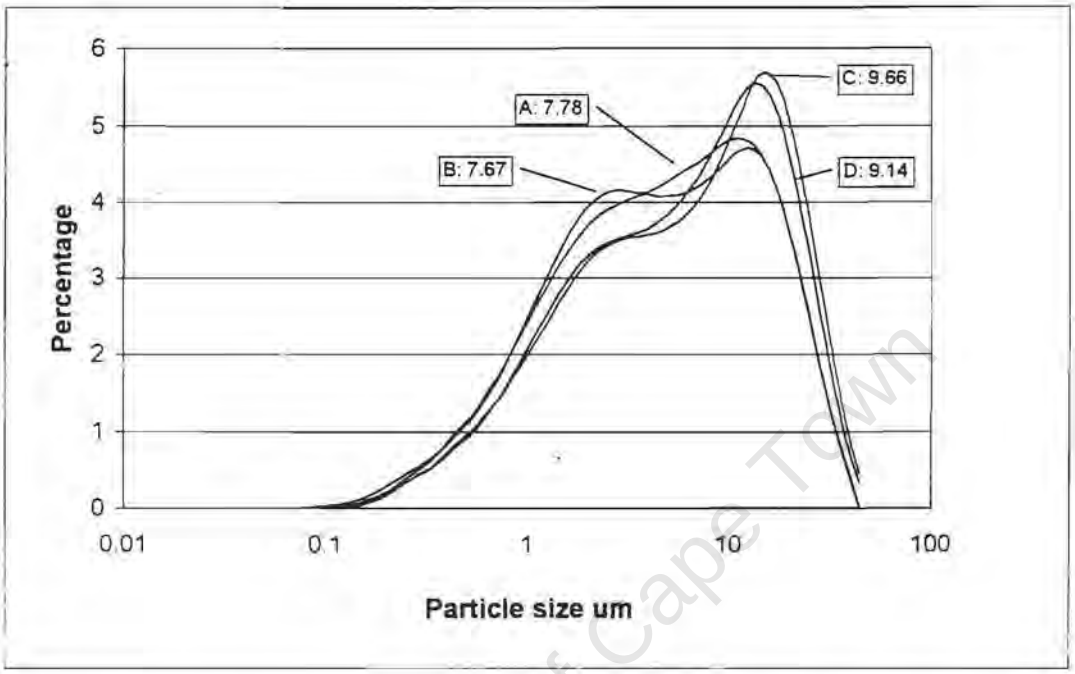

Change of catalyst particle size distribution for different cycles

(Catalysts used in the reaction/regeneration studies of Rho(A) - effect of reaction time. The reaction times in each of the cycles was as follows for the samples shown here: A=1.5 hrs, B = 4.5 hrs, C=3 hrs, D = 21.5 hrs)

The flow of any fluid through a packed bed can be described using the axial dispersed plug flow model as follows:

$$\mathcal{D}_{ax}\frac{\partial^2 C}{\partial z^2}+\frac{\partial}{\partial z}(C\nu)+\frac{\partial C}{\partial t}+\frac{(1-\epsilon)}{\epsilon}\frac{\partial \bar{q}}{\partial t}=0 \qquad (4.1)$$

[Ruthven, 1984]

Where D_{ax} is the axial dispersion coefficient and combines the contribution from molecular diffusion and turbulent mixing

and C = The gas phase concentration

z = The bed length

ϵ = Bed voidage

q = Concentration in adsorbed phase

ν = interstitial gas velocity

Now, the Diffusion Coefficient can be expressed in terms of the axial Peclet number and the Peclet number can in tern be expressed in terms of the Reynolds number as follows:

(4.2) $$Pe' = \frac{2\nu R_p}{\mathcal{D}_{ax}}$$

(4.3) $$\frac{1}{Pe'} = \frac{\gamma_1 \epsilon}{Re\,Sc} + \frac{1}{Pe'_\infty \left(1 + \frac{\beta \gamma_1 \epsilon}{Re\,Sc}\right)}$$

Where Pe_∞ is the limiting Peclet number as the Reynold's number approaches infinity, i.e., the Peclet number in a turbulent flow regime. What this means essentially is that the axial dispersion coefficient is dependent on the value of Pe as Re tends to infinity. It has been shown that while there is a maximum value for Pe_∞ of 2 at larger particle sizes, at low particle diameters the limiting Peclet number is dependent on the particle diameter. This variation is shown in figure 4.7

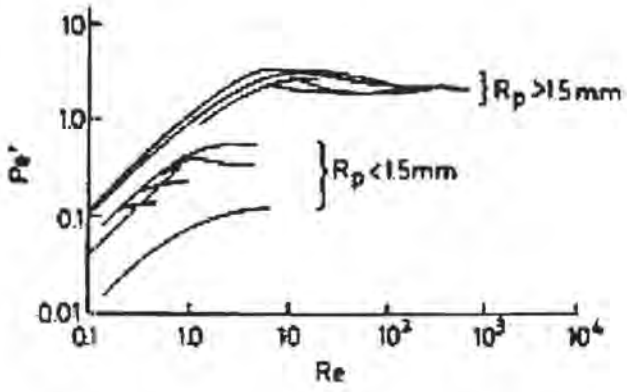

Variation of limiting Peclet number with particle diameter for flow through packed beds.

[Ruthven, 1984]

It can therefore be seen that there is a critical particle diameter of 3mm, above which the limiting Peclet number is 2 for all particle diameters. However, if R_p < 1.5mm then $Pe'_\infty \approx 3.35\ R_p$

Ruthven [1984] has stated that this means that the advantage gain from the reduced pore diffusional resistance of the very small catalyst particles can be offset by the increased axial dispersion. If there is significant axial dispersion then the reactor is no longer behaving in a true plug flow regime and the reaction rate will therefore decrease. This is born out by the results obtained in the reaction/ regeneration cycles above where the rate was seen to decrease with decreasing particle size.

In the reaction/regeneration cycles, the change in average particle diameter from 7.7 to 9.7 μm gives a change in Pe_∞ from 0.0026 to 0.0033 which in tern increases the axial dispersion coefficient from 1.403×10^{-5} to 1.413×10^{-5}. Though the change is very small, there is nonetheless an increase in the axial dispersion coefficient.

The conclusion therefore, is that the change in the catalyst seen in the reaction-regeneration cycles was not caused during the reaction phase of the process.

APPENDIX VII: IDENTIFICATION OF MASS SPECTRA PEAKS

Extract from "Eight Peak index of Mass Spectra" 4th Edition, Compiled by the Mass Spectrometry Data Centre, vol. 3 part 1, 1991, The Royal Society of Chemistry, Cambridge, U.K.

Compound	**Ion Mass/ Relative Intensity**							
DME	45	46	29	15	28	31	14	44
(relative Intensity)	100	48	36	24	7	3	2	2
TMA	58	59	30	42	44	15	18	28
(relative Intensity)	100	47	29	26	17	14	10	10
DMA	44	45	28	42	18	43	30	46
(relative Intensity)	100	56	26	15	14	13	4	3
MMA	30	31	28	29	27	15	32	17
(relative Intensity)	100	75	51	12	8	7	3	2
H_2O	18	17						
(relative Intensity)	100	21						
CO	28							
CO_2	44	28	16	12				
O_2	32	16						
N_2	28	14						

APPENDIX VIII: DEHYDROXYLATION OF ZEOLITE RHO

The figure below shows a repeat of a Thermal Desorption run of one the samples of zeolite Rho (A). It illustrates that the high temperature peak does not occur in the repeat run, which was taken to mean that this peak was due to dehydroxylation of the catalyst rather than ammonia desorption.

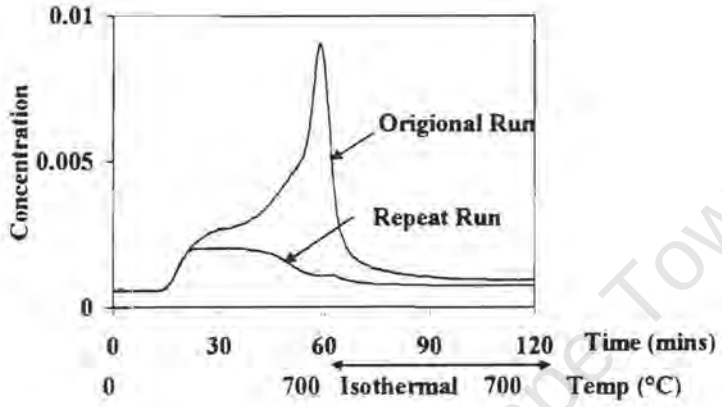

Comparison of repeated Thermal Desorption runs

Appendix IX: BET Results

SUMMARY OF RESULTS

RHO (B)

Steaming Time (hrs)	**0**	**1**	**2**	**4**	**8**
BET Surface Area (m^2/g)	463.7	443.8	634.7	623.0	662.3
Langmuir Surface Area (m^2/g)	613.6	584.6	834.1	818.5	870.9
Micro-pore Surface Area (m^2/g)	405.2	383.2	575.8	570.0	611.1
Mesopore Surface Area (m^2/g) – Ads	27.1	29.4	28.0	25.6	24.7
(17 → 3000 Å) - Des	25.7	28.4	32.5	30.6	30.1
Total Pore Volume (<1300Å ø) (cm^3/g)	0.236	0.227	0.315	0.310	0.329
Meso-pore volume (cm^3/g) – Ads	0.036	0.041	0.038	0.037	0.036
(17 → 3000 Å) - Des	0.031	0.037	0.038	0.038	0.039
Micro-pore volume (cm^3/g)	0.189	0.178	0.267	0.265	0.284
Average Pore Diameter – Langmuir	15.37	15.57	15.1	15.2	15.1
- BJH Ads	53.14	55.87	53.6	58.0	58.9
- BJH Des	48.11	52.67	46.7	50.1	51.4

MORDENITE

Steaming Time (hrs)	0	1	2	4	8	16
BET Surface Area (m^2/g)	521.5	463.3	475.2	458.9	448.4	448.8
Langmuir Surface Area (m^2/g)	586.5	613.2	627.6	607.8	595.2	592.3
Micro-pore Surface Area (m^2/g)	441.0	371.0	380.3	362.6	353.7	357.3
Mesopore Surface Area (m^2/g) – Ads	67.2	74.9	77.5	82.7	89.4	82.8
(17 → 3000 Å) - Des	77.9	86.7	94.2	98.6	105.8	99.9
Total Pore Volume (<1300Å ø) (cm^3/g)	0.288	0.297	0.303	0.303	0.313	0.307
Meso-pore volume (cm^3/g) – Ads	0.112	0.124	0.126	0.135	0.154	0.146
(17 → 3000 Å) - Des	0.118	0.131	0.135	0.144	0.164	0.153
Micro-pore volume (cm^3/g)	0.177	0.173	0.177	0.169	0.165	0.166
Average Pore Diameter – Langmuir	19.6	19.4	19.3	20.0	21.0	20.8
- BJH Ads	66.6	66.3	65.0	65.4	68.9	70.3
- BJH Des	60.3	60.5	57.4	58.4	61.9	61.4

APPENDIX X: ADSORPTION DATA

RHO

Adsorptions (mmol/ g_{cat})

Steaming Time	(hours)	0	0.5	1	2	4	8
Pure Compounds	Methanol	3.29	4.65	3.73	4.42	4.17	3.06
	Ammonia	1.82	1.83	2.39	2.5	1.8	1.57
	Water	3.91	4.73	4.18	5.73	5.52	4.69
Methanol & Water	Methanol	2.53	3.02	3.30	4.38	3.95	2.34
Mixture	Water	2.84	3.28	3.96	3.57	3.65	2.99
	Total	5.68	6.72	7.54	8.73	8.25	5.51
	Sum	5.37	6.30	7.27	7.96	7.60	5.33
Methanol & Ammonia	Methanol	1.33	2.03		2.04	1.97	1.53
Mixture	Ammonia	1.86	3.01		2	2.118	1.45
	Total	3.11	4.76		4.15	4.08	3.04
	Sum	3.20	5.05		4.04	4.08	2.99

Desorptions (mmol/gcat)

Steaming time	(hours)	0	0.5	1	2	4	8
Pure Compounds	Methanol	0.86	1.25	1.75	1.90	1.65	1.27
	Ammonia	0.43	0.39	0.60	0.67	0.58	0.45
	Water	1.24		1.92	2.42	2.19	1.72
Methanol & Water	Methanol	0.58	0.80	1.55	1.47	1.38	1.02
Mixture	Water	1.02	1.34	1.48	1.65	1.45	0.97
	Total	1.53	2.07	3.18	3.20	2.97	2.09
	Sum	1.60	2.14	3.04	3.12	2.83	1.99
Methanol & Ammonia	Methanol	0.41	0.48	0.87	0.62	1.18	1.20
Mixture	Ammonia	0.15	0.14		0.19	0.19	0.09
	Total	0.55	0.62	0.82	0.81	1.38	1.23
	Sum	0.56	0.62	0.87	0.81	1.37	1.28

MORDENITE

Adsorptions (mmol/ g_{cat})

Steaming Time	(hours)	0	1	2	4	8	16
Pure Compounds	Methanol	4.04	3.19	3.18	2.91	2.26	2.09
	Ammonia		1.42	1.42	1.25	0.92	0.84
	Water	4.82	2.71	2.81	2.98	1.92	
Methanol & Water	Methanol	3.20	3.37	2.78	2.86	2.41	2.34
	Water	1.24	0.95	0.96	0.84	0.71	0.89
	Total	5.54	5.54	5.62	5.32	3.96	4.31
	Sum	4.44	4.32	5.01	3.70	3.12	3.23
Methanol & Ammonia	Methanol	2.30	1.66	1.86	1.56	1.31	1.42
	Ammonia	1.87	1.53	1.38	1.32	1.01	0.85
	Total	3.89	3.08	2.98	2.75	2.16	2.19
	Sum	4.17	3.18	3.23	2.87	2.32	2.26

Desorptions (mmol/ g_{cat})

Steaming Time	(hours)	0	1	2	4	8	16
Pure Compounds	Methanol	1.14	1.03	1.00	1.03	0.76	0.81
	Ammonia		0.33	0.44	0.32	0.26	0.30
	Water	2.20	1.35	1.22	1.50	0.87	0.96
Methanol & Water	Methanol	0.92	0.79	0.73	0.89	0.64	0.67
	Water	1.09	0.71	0.66	0.48	0.46	0.48
	Total	2.05	1.59	1.48	1.80	1.22	1.34
	Sum	2.01	1.50	1.39	1.37	1.10	1.15
Methanol & Ammonia	Methanol	1.65	1.06	1.02	1.24	0.86	0.83
	Ammonia	0.00	0.00	0.00	0.00	0.00	0.00
	Total	1.61	1.04	1.06	1.20	0.86	0.81
	Sum	1.65	1.06	1.02	1.24	0.86	0.83

LIST OF PUBLICATIONS:

(please note that all publications are under my maiden name)

1 Callanan, L.H., van Steen, E and O'Connor, C.T. : "Methanol Amination over Solid Acid Catalysts" *Discussions on Zeolite and Microporous Materials* - Supplementary Material of the 11th IZC (H. Chon and Y.S. Uh - Eds.), (1997) 349.

2. Callanan, L.H., Sewell, G.S., van Steen, E and O'Connor, C.T.: "Selective Formation of Lower Substituted Alkylamines", *Proceedings of the 8th SAIChE conference* (1997).

3. Callanan, L.H., van Steen, E and O'Connor, C.T.: "Improved Selectivity to Lower Substituted Methylamines using Hydrothermally Treated Zeolite Rho", *Catal. Today*, **49** (1999) pp 229-235.

4 Callanan, L.H., O'Connor, C.T. and van Steen, E. "The Effect of Hydrothermal Treatment of Zeolites on the Methanol Amination Reaction", *Proceedings of 12th IZC* (1998), pp

5 Callanan, L.H., O'Connor, C.T. and van Steen, E: "The Effect of the Adsorption Properties of Steamed Zeolite Rho on its Methanol Amination Activity", *Microporous and Mesoporous Materials* (1999), in press.

CONFERENCE PRESENTATIONS:

1. Poster presentation at the *11th International Zeolite Conference*, "Methanol Amination over Solid Acid Catalysts", Seoul, Korea, 12 - 17 August, 1996

2. Oral presentation at the National Catalysis Conference:, "Methanol Ammination over Solid Acid Catalysts", Midrand, 30 October - 1 November, 1996

3. Oral presentation at the SAIChE 97 Conference, "Selective Formation of Lower Substituted Alkylamines", Cape Town, South Africa 16 - 18 April, 1997.

4. Oral presentation at IPCAT-1 (First Indo-Pacific Catalysis Conference), "Improved Selectivity to Lower Substituted Methylamines using Hydrothermally Treated Zeolite Rho", Cape Town, South Africa, 26-28 January 1998
5. Poster presentation at the 12th International Zeolite Conference, "The Effect of Hydrothermal Treatment of Zeolites on the Methanol Amination Reaction", Baltimore, U.S.A., 5 – 10 July, 1998